



The
University
Of
Sheffield.

A study of vernacular architecture in Harran, Turkey and its implications for sustainable design in a changing climate

By:
Mari Taylor

A thesis submitted in partial fulfilment of the requirements for the degree of
Master of Science in Sustainable Architecture Studies

The University of Sheffield
Faculty of Social Sciences
School of Architecture

Submission Date: 15th October 2021

Abstract

It was identified in the IPCC 5th assessment report that a significant rise in global temperature is inevitable as a result of a rise in greenhouse gas emissions (IPCC, 2014). Therefore, it is important that the building sector mitigates and adapts to this rise in temperature through the use of passive strategies, such as those found in vernacular architecture. This study looks at the vernacular architecture of Harran in a hot-dry climate, specifically its ability to maintain comfortable indoor temperatures after the effects of global warming. By using two methods of assessing the overheating risk and 2080 projected climate data on a simulation of a base model of the Harran domed houses, it is found that the overheating risk drastically increases in the future. Therefore the study focuses on strategies to reduce the overheating risk. The overheating risk assessment method includes the CIBSE TM52 and a model developed by Robinson & Haldi (2008). A sensitivity analysis of only passive strategies was used to inform the principles of an optimal building design for further simulations in a 2080 climate. These strategies include a change of construction materials, building orientation and window to wall ratios. The optimal model reduces the overheating risk significantly with the use of the best performing strategies from the sensitivity analysis. This leads to the conclusion that this style of architecture can be adapted to ensure comfortable indoor conditions in spite of global warming, without the use of applied technologies for cooling. It is clear that the architecture of Harran could be used as a sustainable model for dwellings in hot-dry climates that are resilient to climate change.

Declaration

I hereby certify that I, Mari Taylor, am the sole author of this thesis report and submit this report in partial fulfilment of the requirements for the degree of Master of Science in Sustainable Architecture Studies. I certify that, to the best of my knowledge, my thesis does not infringe upon anyone's copyright nor violate any propriety rights and that any ideas, techniques, quotations, or any other material from the work of other people included in my thesis, published or otherwise, are fully acknowledged in accordance with the standard referencing practices. I declare that this is a true copy of my thesis and that this thesis is not extensively the same as any other universities or similar institutions the work was conducted and is in accordance with all TUOS research ethic issues.

Acknowledgements

Throughout conducting of this thesis I have obtained enormous amount of support and assistance.

Firstly, I am truly grateful and thankful to my supervisor, Professor Darren Robinson for his guidance, advice and support throughout my time as a student of his.

Secondly, I am indebted to the University of Sheffield for the opportunity to conduct this research, the resources and the guidance provided by them.

I would like to thank my colleagues and friends Anupama Rao, George Ridgeway, Jaime Stone and Emily Amas, to whom I owe for their constant support and motivation upon completing this study.

I would like to express gratitude to Louis Garnham, for his knowledge, guidance, time and encouragement.

Finally, I would like to thank my parents and grandparent, Catrin Taylor, Simon Taylor and Buddug Pritchard, for their life-time support, care, motivation and financial support.

Abstract	I
Declaration	II
Acknowledgements	III
List of figures	IV
List of tables	VII
1. Introduction	11-13
1.1 Context of study	11
1.2 Choice of climate and location	12
1.3 Rationale	13
1.4 Review of studies in similar contexts and need for research	13
2. Research questions, aims and objectives	14
3. Methodology	15-21
3.1 Overall research methodology	15
3.2 Method of simulation process	17
3.3 Criteria for assessing overheating	18
3.3.1 <i>Integrated adaptive model for predicting overheating risk in offices</i>	18
3.3.2 <i>CIBSE TM52 (overheating in free-running buildings)</i>	19
3.4 Critique of methods	20
4. Literature review: Climate analysis	22-30
4.1 Geography of Harran	22
4.2 Harran's climate shifts: Present to 2080	23
4.2.1 <i>Temperature</i>	23
4.2.2 <i>Degree Days</i>	24
4.2.3 <i>Diurnal Temperature</i>	25
4.2.4 <i>Rainfall</i>	25
4.2.5 <i>Radiation</i>	26
4.2.6 <i>Psychrometric Charts</i>	27
4.2.7 <i>Relative Humidity</i>	28
4.2.8 <i>Wind</i>	28
4.2.9 <i>Earthquakes</i>	30
4.3 Climate analysis summary and key threats	30
5. Literature Review: Vernacular architecture of Harran	31-40
5.1 Urban organization	31
5.2 Nomadic society and rapid construction	32
5.3 Building form	32
5.3.1 <i>Courtyard</i>	33
5.3.2 <i>Square bases</i>	34

5.3.3 Domes	34
5.4 Openings and ventilation	34
5.5 Spatial organization and rooms	36
5.6 Materials and construction	36
5.6.1 Dome construction	37
5.6.2 Wall construction	37
5.6.3 Floor construction	38
5.6.4 Seasonal behaviour of the Harran houses	39
5.7 Summary of vernacular principles and parameters for simulation	40
6. Base model of traditional house, inputs and analysis	41-49
6.1 Traditional base model	41
6.1.1 Building form	42
6.2 Inputs in the model	42
6.2.1 Weather data	42
6.2.2 Occupancy	42
6.2.3 Construction	44
6.2.4 Openings	44
6.2.5 HVAC sensitivity analysis	45
6.3 Discussion of results of the base model	46
6.3.1 Lighting and radiation analysis	49
7. Results after change of parameters	50-64
7.1 Analysis of results after change in construction materials	50
7.2 Analysis of results after change in dome height	55
7.3 Analysis of results after change to building orientation	57
7.4 Analysis of results after change in window height	59
7.5 Analysis of results after change to WWR (window to wall ratio)	61
7.6 Analysis of results after change to ventilation parameter	63
8. Introduction of new strategies	65-73
8.1 Analysis of results after introduction of glazing systems	65
8.2 Analysis of results after introduction of shading devices	68
8.3 Analysis of results after the introduction of evaporative cooling	71
8.4 Sensitivity analysis conclusion	72
9. Optimal design results and discussion	74-75
10. Conclusion	76
11. Word count	77
12. References	78
13. Appendices	82-134

List of Figures

- Figure 1.1** Examples of indigenous and vernacular architecture (Zilliacus, 2017)
- Figure 1.2** Koppen-Geiger climate classification map (1980-2016) as taken from Beck et al., 2018.
- Figure 3.1** Framework of research methodology and steps of the study
- Figure 3.2** Methodology framework of the dynamic simulation process
- Figure 3.3** The methodologies used in the UK to assess overheating risk for different building typologies [as taken from Gorjimahlabani, 2020]
- Figure 4.1** Location of Harran in Turkey (Google Earth Web, 2020)
- Figure 4.2** Map of Harran's location on its agricultural plain, the surrounding mountains and towns (Google Earth Web, 2020)
- Figure 4.3** Map displaying the elevation and distance between Tel Abiad and Harran (Edited by author from Topographic Map, 2020)
- Figure 4.4** 1964-2011 temperature range
- Figure 4.5** 2004-2018 temperature range
- Figure 4.6** Predicted 2080 temperature range
- Figure 4.7** Month degree days 1964-2011
- Figure 4.8** Monthly degree days 2004-2018
- Figure 4.9** Monthly degree days 2080
- Figure 4.10** Diurnal temperature violin plot 2004-2018
- Figure 4.11** Diurnal temperature violin plot 2080
- Figure 4.12** Average annual rainfall in Harran – present day, data acquired from World Weather Online (2021) [Data on predicted future rainfall in 2080 is not available]
- Figure 4.13** Radiation range 1964-2011
- Figure 4.14** Radiation range 2004-2018
- Figure 4.15** Radiation range 2080
- Figure 4.16** 1964-2011 psychrometric chart with most effective design strategies
- Figure 4.17** 2004-2018 psychrometric chart with most effective design strategies
- Figure 4.18** 2080 psychrometric chart with most effective design strategies
- Figure 4.19** Psychrometric chart 2004-2018
- Figure 4.20** Psychrometric chart 2080
- Figure 4.21** Wind wheel 1964-2011
- Figure 4.22** Wind wheel 2004-2018
- Figure 4.23** Wind wheel 2080
- Figure 4.24** Wind velocity range 1964-2011
- Figure 4.25** Wind velocity range 2004-2018
- Figure 4.26** Wind velocity range 2080
- Figure 4.27** Average wind speed in Harran- based on hourly weather data from 1980 to 2016 (taken from Weather Spark, 2016)
- Figure 4.28** Map of the fault lines across Turkey and Harran's location (Turkey News, 2020)
- Figure 4.29** Location of where the Arabian and Anatolian plate meet (UC Berkeley, 2020)
- Figure 5.1** Urban plan of the ancient city of Harran
- Figure 5.2** A house at Harran (Özdeniz et al., 1998)
- Figure 5.3** General view of Harran (Özdeniz et al., 1998)
- Figure 5.4** Harran house view from the courtyard (Natural Homes, nd)
- Figure 5.5** Domed building forms found in Mesopotamia excavations belonging to 7th century BC (Özdeniz et al., 1998)
- Figure 5.6** Plans and sections of a typical Harran neighbourhood (taken from Özdeniz et al., 1998)
- Figure 5.7** Plans and sections of a typical Harran house (taken from Özdeniz et al., 1998; Sami & Özdemir, 2011)
- Figure 5.8** The plan of a vernacular Harran house (taken from Sami & Özdemir, 2011)
- Figure 5.9** A throne in the courtyard of a Harran house (Natalie, nd)
- Figure 5.10** Adobe brick material in construction (Cortesi, 2020)
- Figure 5.11** Internal view of the dome (Başaran, 2011)
- Figure 5.12** The exterior look (Padfield, 2021)
- Figure 5.13** Internal views (Padfield, 2021)

- Figure 5.14** The Harran house thermal behaviour diagrams between night and day in winter and summer
- Figure 6.1** Configuration of rooms in plan of the base model
- Figure 6.2** Halil Özyavuz Harran House from a study done by Başaran (2011)
- Figure 6.3** A sensitivity analysis of ventilation rate and potential overheating risk (P_{OH} according to Robinson & Haldi's dynamic overheating model) to inform ventilation rate for simulations. As ventilation rate increases, probability of overheating decreases.
- Figure 6.4** The highlighted rooms which were chosen for simulation
- Figure 6.5** The coloured lines show each of the rooms' indoor temperature across the year in a current climate and the black line is the outdoor dry-bulb temperature for comparison. The indoor temperatures broadly follow the outdoor temperature, but remain warmer in the winter and slightly cooler in the summer. Minimising the range of indoor temperatures across the year is desirable to ensure comfort.
- Figure 6.6** The 2080 climate results of indoor air temperature per room and the dry-bulb temperature. Temperatures have increased by around 5°C compared to the current climate (Figure 6.5). The variations are similar to those in a current climate, meaning comfort varies across the year.
- Figure 6.7** A comparison of the current and future climates accumulating probability of overheating risk, using Robinson & Haldi's dynamic model. It is ideal that the line plateaus later on the X axis and remains as low on the Y axis as possible. Therefore the current scenario in blue shows a better performance against this P_{OH} model.
- Figure 6.8** [left] The solar gains in a current climate. [right] The solar gains in a 2080 climate. It is optimal if the lines on the chart stay as low on the Y axis in the summer months
- Figure 6.9** [left] A distribution of illuminance in the base model simulated in a current climate. [right] The percentage of time the indoor illuminance is within a range of 100-400 lux. Above 100 lux is an acceptable target for indoor illuminance. The chart shows the base model performs below this for 79.5% of the time and the distribution plan shows that the only rooms receiving adequate daylight are rooms with larger openings for doorways.
- Figure 6.10** A simulation of the distribution of radiation on external surfaces of the base model across a year. The domes create shading from radiation on the courtyard and on surrounding domes. The colour bar on the left indicates the degree of incident radiation.
- Figure 6.11** The charts show annual cumulative insolation on building surfaces and the annual insolation per square metre.
- Figure 7.1** Graphics of the different building envelopes that are tested
- Figure 7.2** The effect of different construction materials on the indoor air temperature across the year in 2080, compared to the outdoor temperature. Consistent indoor temperatures across the year are desired for the purpose of thermal comfort. There are significant variations across the year with all construction materials, with type 2 performing the best.
- Figure 7.3** The indoor temperature of each construction type in a future typical winter week, compared to the dry-bulb temperature. For the purpose of comfort, consistent indoor temperatures of 20-25°C are desired. Indoor temperatures are kept consistent at 17-18°C by all construction types, varying by only a couple of degrees.
- Figure 7.4** Indoor temperatures in a typical summer week in the future climate. The indoor temperature variations are more extreme in summer than winter (Figure 7.3), showing that as outdoor nighttime temperatures drop, so do the indoor temperatures. If thermal mass materials were being adequately flushed out during nighttime ventilation, the graph would produce flat lines demonstrating more consistent indoor temperatures. However, all construction types result in large temperature variations, indicating that this is not happening.
- Figure 7.5** The indoor air temperature variations across a year in a 2080 climate for different dome heights. It is clear that the differences of each dome height on the indoor air temperature is not large, and that this has little effect on the overheating risk (Table 9). The 5m dome height provides the coolest temperatures which mirrors the overheating results in Table 9.
- Figure 7.6** The cumulative insolation of the varying dome heights on exterior surfaces. This simulation includes the courtyard in order to measure the extent to which it is shaded from radiation. It is evident that the 4m dome height results in the most radiation accumulating on the surfaces
- Figure 7.7** The radiation per square metre on the building for different dome heights. When comparing this to Figure 7.6, it is clear that 3m dome heights result in more radiation per square metre due to the smaller surface area. A dome height of 5m results in the lowest cumulative insolation and also radiation per m² due to taller domes providing more shade.

- Figure 7.8** The chart displays the effect of orientation on indoor temperatures across the year. Orientation has minimal effect on the indoor temperature throughout the year meaning the lines are almost completely superimposed. This is further supported by the results in Table 10 indicating that orientation has minimal impact on overheating risk.
- Figure 7.9** Simulation results of cumulative insolation and radiation per m² of each orientation. A 270° orientation represents the highest amount of solar radiation.
- Figure 7.10** The distribution of radiation for an orientation of 90°. Most of the shading is concentrated on the north facing walls resulting in lower overheating risk in MB1 (Table 10). South facing walls and the courtyard are completely exposed to 1829kWh/m² of radiation. It would be ideal that the domes and courtyard are more shaded as these are the spaces that residents will occupy most due to the central, inward-facing layout of the building.
- Figure 7.11** The distribution of radiation for an orientation of 180°. Most shading is hitting the north walls and domes, with very little shading in the courtyard. Radiation reaches 1856kWh/m² with this orientation which mirrors the failing of TM52 overheating criteria and higher probability of overheating in Table 10.
- Figure 7.12** The distribution of radiation for an orientation of 270°. This orientation has most shading of the courtyard of all orientation results. This is provided by the courtyard walls and the double row of domes. Shading is also provided to the inward facing walls of the courtyard which is ideal for cooling and less solar gain indoors, and outdoor activities. However, overheating risk results do not significantly decrease (Table 10), as Figure 7.9 shows a 270° orientation receives the most annual radiation.
- Figure 7.13** The indoor temperature for different window heights across the year. There is almost no variation between the different heights.
- Figure 7.14** Annual indoor air temperature after a change to the WWR. As the WWR is increased, the temperatures across the year also increase. The best performing WWR is 0.4% and the worst performing is 10%, with a significant difference.
- Figure 7.15** Indoor illuminance performance of different WWRs between a target range of 100-400 lux. A 5-10% WWR results in best indoor illuminance quality and below 0.8% results in extremely low illuminance.
- Figure 7.16** The annual indoor air temperature variations with changes to the percentage of openable windows. The impact of the change to this parameter is negligible and has almost no effect on the indoor air temperature.
- Figure 8.1** Indoor air temperature variations of different glazing systems throughout the year, and the outdoor temperature. Changing the glazing system has no discernible effect on the indoor temperature.
- Figure 8.2** Indoor air temperature across the year for different glazing systems tested on a base model with an increased WWR (2.5%). There is a clearer trend as double glazing slightly reduces temperatures across the year and single glazing increases them.
- Figure 8.3** The indoor air temperature variations with addition of different shading devices. No shading device performs better than the other in this chart for lower temperatures in the summer and higher in the winter.
- Figure 8.4** Indoor air temperature variations for the addition of different shading devices to a base model with an increased WWR to 2.5%, across the year. A 1.5m local shading device slightly reduces temperatures year round.

List of Tables

Table 1	Suggested applicability of the categories and their associated acceptable temperature range for free-running buildings and of PMV for mechanically ventilated buildings [as taken from BSI, 2007]
Table 2	CIBSE TM52 overheating criteria for free-running buildings (Sources: CIBSE 2013; Gorjimahtabani, 2020)
Table 3	Adobe as a material for vernacular construction, information sources: (Omega, nd; Costa et al., 2019; Olukoya Obafemi & Kurt, 2016; Acosta et al., 2010; Vivancos et al., 2009; Parra-Saldivar & Batty, 2006; Goodhew & Griffiths, 2005; Koenigsberger, 1975)
Table 4	Occupancy inputs for the base model
Table 5	Construction inputs for the base model
Table 6	The overheating risk of the base model in a current and future climate, compared to the outdoor dry-bulb temperature risk.
Table 7	A table detailing the different constructions that are tested
Table 8	Comparison of how construction type affects the overheating risk
Table 9	Comparison of the overheating risk for different dome heights
Table 10	Comparison of the overheating risk after changes to orientation
Table 11	Comparison of overheating risk after a change to window height
Table 12	Comparison of the overheating risk with changes to WWR
Table 13	Comparison of overheating risk with a change to percentage of openable windows
Table 14	Details of the different glazing systems tested
Table 15	Comparison of the overheating risk of different glazing systems
Table 16	Comparison of the overheating risk of different glazing systems on a base model with an increased WWR to 2.5%
Table 17	Comparison of the overheating risk for the introduction of different shading devices
Table 18	Comparison of the overheating for different shading devices on a base model with an increased WWR to 2.5%
Table 19	Comparison of the overheating risk for the addition of evaporative cooling.
Table 20	Parameters values which best reduce the overheating risk. The numbers correspond to the whole building results obtained from the sensitivity analysis.
Table 21	Parameters applied to optimal models 1 and 2, with a comparison of the base model
Table 22	Comparison of overheating risk for optimal models 1 and 2, without the addition of a PDEC
Table 23	Comparison of overheating risk for optimal models 1 and 2 with the introduction of a PDEC

1. Introduction

1.1 Context of study

The period between 1983-2012 has been recorded as having the highest temperature in the Northern Hemisphere in the last 1400 years. The Intergovernmental Panel on Climate Change (IPCC) 5th Assessment Report outlined that a significant rise in global temperature is inevitable due to greenhouse gas (GHG) emissions being the highest in history (IPCC, 2014). The UN Framework Convention on Climate Change pledges to limit global warming to 1.5°C by 2030 through reduction of GHG emissions (UNFCCC, 2015). Buildings have a huge impact on the production of GHGs, making up 18.4% of total direct and indirect transmissions. Therefore, it is imperative that changes are made to a more sustainable future in this sector.

In a pre-simulation era, design and construction techniques, such as those in vernacular architecture, emerged through trial and error and were remarkably well-adapted to their climate, delivering comfort without the use of applied energy. This study will explore vernacular architecture (Figure 1.1) as a sustainable guide for the future by understanding the extent to which energy use can be minimised to achieve comfort.

“Vernacular” derives from the Etruscan language meaning “domestic, native, indigenous” (Oxford English Dictionary, 2001). It spans an array of pre-industrial style architecture, distinguished by the use of traditional building methods, knowledge and local materials that are influenced by culture, climate and local environment (Kazimee, 2008). The use of knowledge from vernacular architecture in contemporary design can lead to more efficient, lower carbon and better-performing buildings with optimal thermal comfort for occupants (Sayigh, 2019). Effectively, by utilising and understanding vernacular principles, GHG emissions driven by the building sector in contemporary design can be reduced. Pelsmakers states that, due to buildings typically having a lifespan of 60 years, we should design for the forecasted climate (Pelsmakers, 2019). Understanding how vernacular architecture stands up against a changing climate could reveal potential mitigation and adaptation strategies, new ideas and progress in the field of sustainable design for contemporary dwellings.



Figure 1.1: Examples of indigenous and vernacular architecture (Zilliacus, 2017)

1.2 Choice of climate and location

The location of choice for this study is the ancient city of Harran, situated in the Şanlıurfa Province in the south of Turkey, just north of the Syrian border. It was established in 6200 BCE and has a rich history of trade between old Syria, Iraq and Iran (Özdeniz et al., 1998) with strong religious ties to Islam, Judaism and Christianity (Green, 1992).

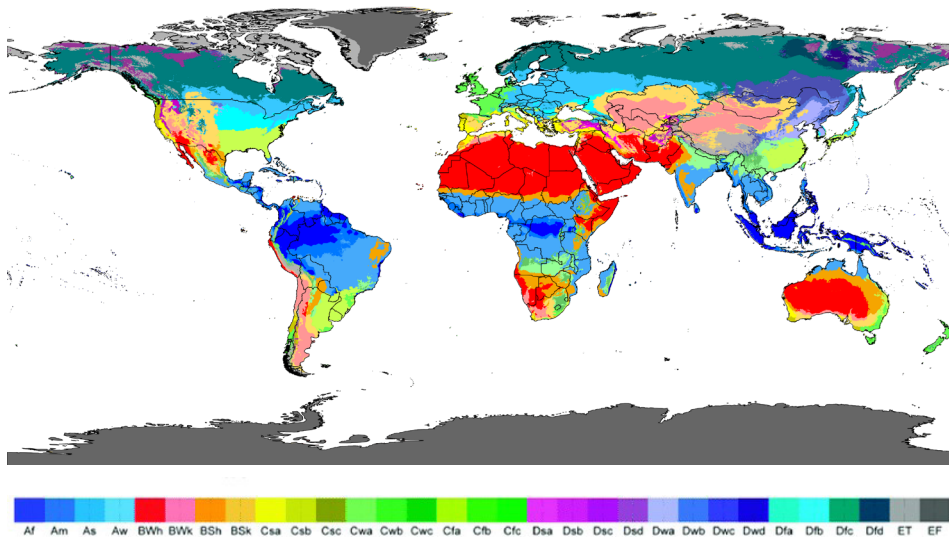


Figure 1.2: Köppen-Geiger climate classification map (1980-2016) as taken from Beck et al., 2018.

Harran is within the Csa category as defined by the Köppen climate classification system (Figure 1.2).

C (warm temperate) **s** (summer dry) **a** (hot summer)

Csa is a hot-summer Mediterranean climate which commonly experiences extremely hot and dry summers with mild and wet winters. The climate often faces summers similar to those seen in arid/semi-arid climates. All Csa climates experience winters that are wet and cold in comparison to the summer months (Kottek et al., 2006). The Csa climate has been predicted to increase to BSh (Hot semi-arid) by the year 2100 (Rubel & Kottek, 2010), and this dramatic change is a major reason for selecting Harran for this study.

1.3 Rationale

Although Turkey is a developing country, their contribution to GHG emissions has been above that of most industrialized countries, ranking 23rd globally in 2016 (Our World in Data, 2016). As Turkey's population is expected to triple by 2030 and as temperatures rise (Ministry of Environment, 2013), so will reliance on mechanical cooling systems, contributing to their already increasing energy demand (IEA, 2021). It is important to minimise this increasing energy demand through passive technologies, especially due to a lack of economic availability of mechanical technologies to the majority of Turkey's low-income populations (Norgaard, 2012).

Domed vernacular houses in Harran provide a comfortable living environment for occupants without the need for energy consumed by air-conditioning or other methods (Başaran, 2011). Studies by Özdeniz et al. (1998) and Baran & Yilmaz (2018) confirm this architecture as an energy-efficient design for sustainable habitation, making it an interesting case study to explore for future resilience to climate change. As Harran has the most common subtype of Mediterranean climate (Kottek et al., 2006), the conclusions drawn from this study could inform a vast number of other locations.

1.4 Review of studies in similar contexts and need for research

There is strong empirical evidence to show that vernacular architecture is adaptive to further climatic change. Dipasquale et al., (2014) explain that communities react in accordance to their climate. For example, in the flood-prone Gifu region of Japan, locals elevated their vernacular homes in order to protect their assets from extreme flooding as a result of climate change. However, there is a lack of quantitative data to prove that the performance of vernacular architecture in future climates is successful at creating comfortable indoor environments for occupants, without using active technologies. For example, Meir et al. (2005) quantitatively analyse the performance of vernacular architecture in a range of present-day climates, but merely speculate on future performance after the effects of global warming and more frequent extreme weather events.

Extreme weather events are predicted to have major implications for the health of a population as well as an effect on energy use in domestic buildings. The quantity of heat waves is due to increase globally (IPCC, 2014) leading to a rise in overheating in buildings that fail to mitigate the external environment, causing a rise in heat-related deaths (Hamdy et al., 2017). Din & Brotas (2016) undertake a parametric sensitivity analysis with three criteria for measuring overheating risk using projected weather files for the UK. Most studies in this area use domestic and non-domestic contemporary architecture as a base model for analysis (Heracleous & Michael, 2018). However, the application of these criteria to indigenous, passively cooled vernacular architecture has yet to be explored.

2. Research questions, aims and objectives

The aim of this study is to evaluate the most successful principles of vernacular architecture in order to inform long-lasting, contemporary building design that has a lower energy demand and carbon footprint in a changing climate. The following questions will be explored:

1. *How do the domed vernacular houses of Harran perform in their present and 2080 climates?*
2. *What strategies need to be introduced to minimise overheating risk whilst also minimising applied energy use in the 2080 climate?*

The specific objectives are:

- To understand the predicted climatic changes in Harran within the next 60 years.
- To determine the key principles in Harran's vernacular building design that have emerged to combat climatic difficulties in its region.
- To evaluate the effectiveness of individual vernacular principles through simulation analysis of the indoor environment and calculation of overheating risk.
- To draw conclusions as to the extent to which passive strategies would help to achieve comfort whilst minimising emissions.

3. Methodology

3.1 Overall research methodology

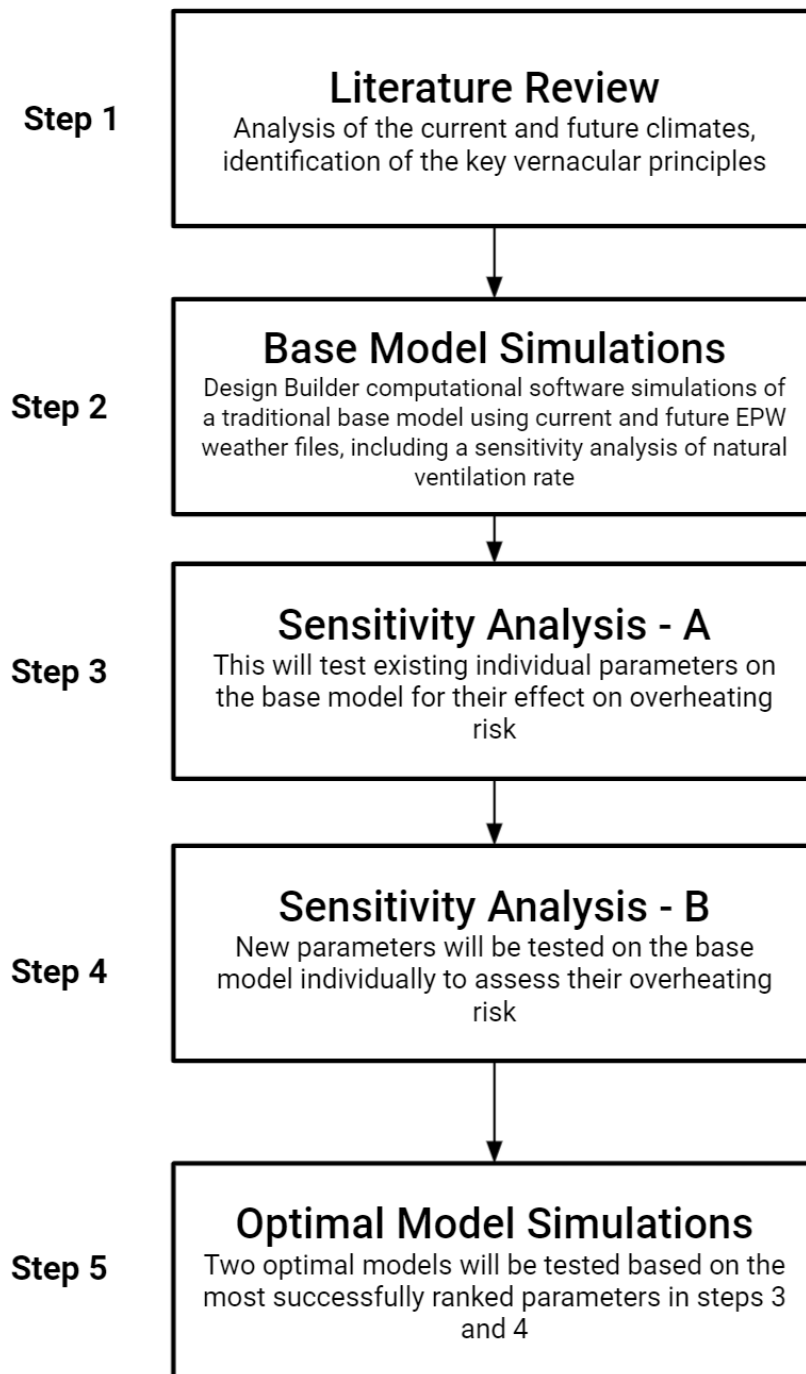


Figure 3.1:
Framework
of research
methodology and
steps of the study

[all steps refer to Figure 3.1]

Step 1:

It is important that the current and future climate of Harran is fully understood in order to identify the environmental challenges and the changes that will occur. The analysis uses Climate Consultant and PyClim software to produce charts and extract quantitative results. The closest EnergyPlus Weather (EPW) file (Tell Abiad, Syria, located 20km south of Harran) is obtained from Climate.Onebuilding (2021) for the years 1964-2011 and 2004-2018. Due to the nature of this study, it is important that the weather files are as precise as possible and not reliant on a single year weather file (EnergyPlus, nd). The 2080 EPW file is generated using the CCWorldWeatherGen tool (Jentsch et al., 2013).

Identification of the vernacular principles is done through qualitative research on the current literature and theory of the Harran domed houses. The objective is to recognize the key strategies that have been used to effectively manage the problems presented by the climate.

Step 2:

This will involve developing a base model of a traditional vernacular house devised using DesignBuilder software with inputs identified from research in step 1. Simulating this model under current and future climates will inform an evaluation of overheating risk and provide a comparison point for the sensitivity analysis.

Step 3:

Individual parameters will be adjusted to the base model, to assess how they affect overheating risk. This will be simulated in 2080 hourly weather data. These parameters are identified in step 1, with consideration to the limits of DesignBuilder inputs. This approach uses a parametric sensitivity analysis, which is chosen over other methods (such as a global sensitivity analysis or combined tree analysis) due to its simplicity and ability to enable clear evaluations to be made.

Step 4:

New, passive and bioclimatic strategies will be introduced to the base model in an extended sensitivity analysis, to be simulated as individual parameters in the 2080 climate.

Step 5:

This will involve ranking the most influential parameters by their overheating risk reduction, and testing 2 optimal models in a future climate. 2 optimals are selected according to the different methods of assessing overheating risk. Conclusions will then be drawn as to which parameters provide the least cooling demand, and if active technologies are necessary in a future climate.

3.2 Method of simulation process

DesignBuilder is chosen as the software for simulation. It is the most comprehensive user interface to EnergyPlus, which itself is the most widely used simulation engine. It is open source and has been rigorously validated (Tronchin & Fabbri, 2008). DesignBuilder simulation outputs are exported as hourly datasets of air and operative temperature, and relative humidity for overheating calculations. A main reason for choosing this method of testing is due to its ease in conducting a sensitivity analysis. Other reasons include the lack of data through qualitative analysis and lack of resources to gather occupant interviews, post-occupancy evaluation or provision of equipment to occupants to perform on-site tests. It is important to note that simulation outputs can vary significantly depending on specific inputs and so the accuracy of the results is questioned in the research approach. Therefore, it is important that representative inputs are gathered to ensure the base model is suitably calibrated. The methodology framework (Figure 3.2) details the simulation process.

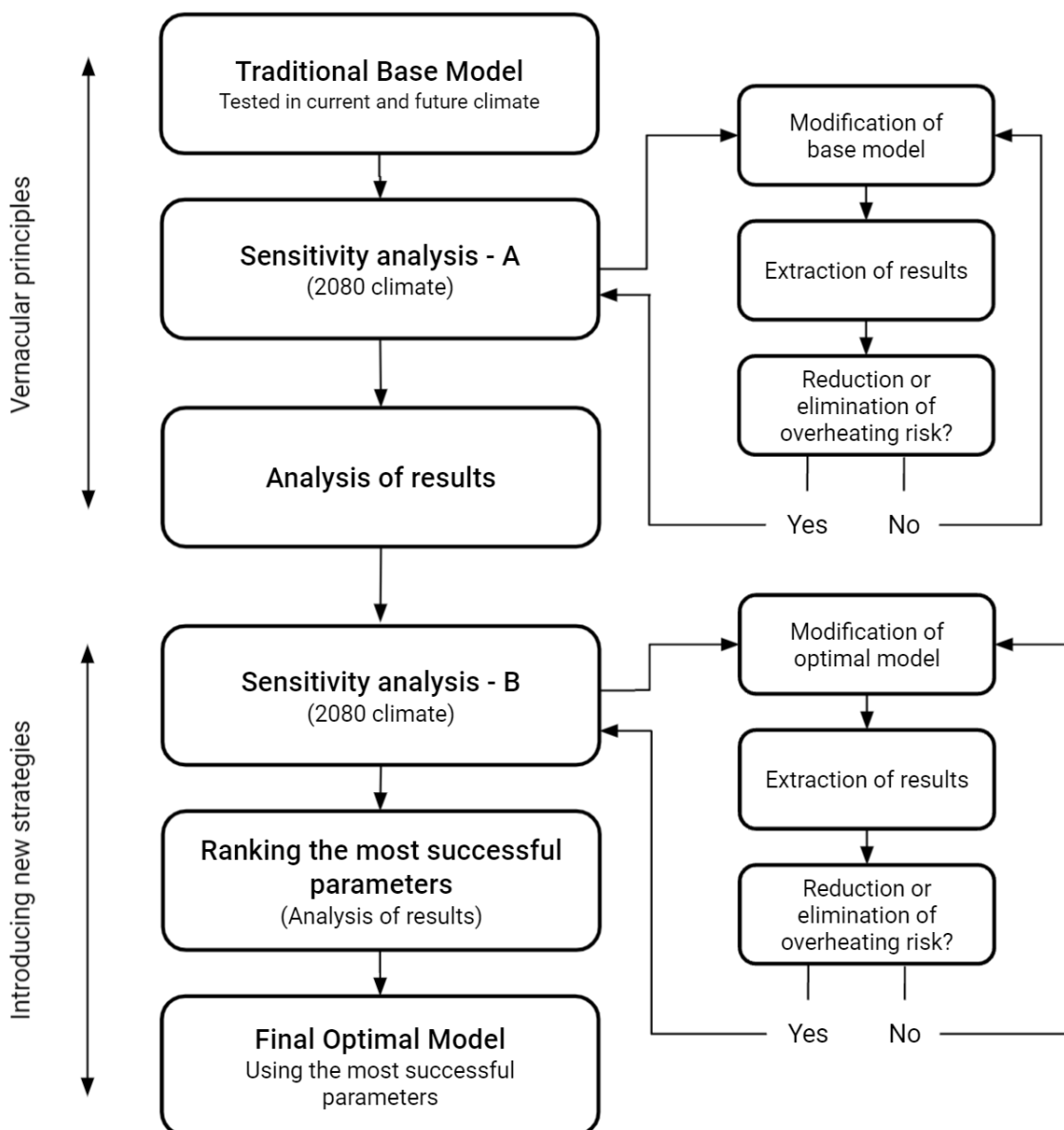


Figure 3.2: Methodology framework of the dynamic simulation process

3.3 Criteria for assessing overheating

The different overheating risk measures are listed in Figure 3.3 describing the domestic and non-domestic risk assessors (Gorjimahlabani, 2020). The CIBSE TM25 criteria and Robinson & Haldi's (2008) model are chosen to compare overheating risk for analysis.

	Domestic buildings	Domestic and Non-domestic buildings	Non-domestic buildings
Criteria	- CIBSE TM59 - SAP Appendix P	- CIBSE Guide A - CIBSE TM52 - PHPP overheating assessment (Passivhaus standard)	- BB101 (schools only) - Robinson & Haldi (2008a) (offices only) - Building regulations Part L2A Criterion 3

Figure 3.3: The methodologies used in the UK to assess overheating risk for different building typologies [as taken from Gorjimahlabani, 2020]

3.3.1 Integrated adaptive model for predicting overheating risk in offices

Robinson & Haldi (2008) produce a dynamic model to assess the potential for overheating in office buildings with consideration to human's adaptive behaviour. It proposes a mathematical model of risk based on measured environmental conditions using the following equation:

$$(1) \quad P_{OH}(t) = 1 - \exp(-\alpha' DH_{t_0,t})$$

P_{OH} : Cumulative probability of overheating

Exp (x): exponential function (exp, where $e=2.718281828$)

$\alpha' = -4.75 \times 10^{-4} [k'h^{-1}]$

DH: Degree hours

This model will be used to evaluate the risk of overheating with respect to the base point temperature of 25°C to calculate cooling degree hours.

3.3.2 CIBSE TM52 (overheating in free-running buildings)

The Chartered Institution of Building Services Engineers (CIBSE) have developed a set of 3 criteria which applies to buildings without the use of mechanical heating or cooling. This will be used to assess the base model. Categories of building types are explained in Table 1.1. They suggest the acceptable temperature range for free-running buildings, taken from CIBSE (2013).

Table 1: Suggested applicability of the categories and their associated acceptable temperature range for free-running buildings and of PMV for mechanically ventilated buildings [as taken from BSI, 2007]

Category	Explanation	Suggested acceptable range
I	High level of expectation only used for spaces occupied by very sensitive and fragile persons	±2
II	Normal expectation (for new buildings and renovations)	±3
III	A moderate expectation (used for existing buildings)	±4

In order to determine the predicted comfort temperature, the running mean of the outdoor temperature must be calculated:

$$(2) \quad T_{rm} = (1 - \alpha) (T_{od-1} + \alpha T_{od-2} + \alpha^2 T_{od-3} + \alpha^3 T_{od-4} \dots) ,$$

where α is a constant (<1), T_{rm} is the running mean of the outdoor temperature (in °C) and T_{od-1} , T_{od-2} , etc. refer to the daily mean temperatures for the previous day, the day before, etc. Then, the comfort temperature can be calculated:

$$(3) \quad T_{comf} = 0.33T_{rm} + 18.8 \text{ (}^\circ\text{C)} ,$$

where T_{comf} is the predicted comfort temperature (°C).

Therefore, with consideration to Table 1 and Equation (3), the upper limit (T_{max}) can be calculated as below:

$$(4) \quad \text{Category 1: } T_{max} = 0.33T_{rm} + 18.8 + 2$$

$$(5) \quad \text{Category 2: } T_{max} = 0.33T_{rm} + 18.8 + 3$$

$$(6) \quad \text{Category 3: } T_{max} = 0.33T_{rm} + 18.8 + 4$$

where T_{max} is the maximum acceptable temperature (°C).

ΔT must then be calculated using Equation (7):

$$(7) \quad \Delta T = T_{op} - T_{max} \text{ (}^\circ\text{C)}$$

ΔT : the difference between operative temperature in a room and maximum acceptable temperature, rounded to the nearest whole degree.

The building or room must then pass 2 of 3 criteria in Table 2 in order to be deemed not-overheated.

Table 2: CIBSE TM52 overheating criteria for free-running buildings (Sources: CIBSE 2013; Gorjimahtlabani, 2020)

Criterion	Explanation (as taken from CIBSE, 2013)	Definition (as taken from Gorjimahtlabani, 2020)
1	The first criterion sets a limit for the number of hours that the operative temperature can exceed the threshold comfort temperature (upper limit of the range of comfort temperature) by 1°C or more during the occupied hours of a typical non-heating season (1 May to 30 September).	$H_e > 3\%$ of occupied hours during non-heating season (Hours of exceedance) H_e : the number of hours during which ΔT is greater than or equal to 1°C during the occupied hours of a typical non-heating season (1 May to 30 September).
2	The second criterion deals with the severity of overheating within any one day, which can be as important as its frequency, the level of which is a function of both temperature rise and its duration. This criterion sets a daily limit for acceptability.	$W_e > 6$ degree hours (daily weighted exceedance) W_e : $W_e = \sum(H_e \times W_f) = (H_{e0} \times 0) + (H_{e1} \times 1) + (H_{e2} \times 2) + (H_{e3} \times 3) + (H_{e4} \times 4)$ (Weighting factor) $W_f = 0$ if $\Delta T \leq 0$, otherwise $W_f = \Delta T$ H_{ey} : the number of hours (h) during which $W_f = y$ Note: The equation does not continue beyond H_{e3} because criteria 3 would be met if $W_f > 4$.
3	The third criterion sets an absolute maximum daily temperature for a room, beyond which the level of overheating is unacceptable.	$(\Delta T = T_{op} - T_{max}) > 4^\circ C$ Or $T_{op} \leq (T_{upp} = T_{max} + 4^\circ C)$ (Threshold or upper limit temperature) T_{upp} : An absolute maximum daily value for indoor operative temperature (T_{op}) for a room or entire building, beyond which the level of overheating is unacceptable

3.4 Critique of methods

Firstly, Robinson & Haldi's model was developed to assess overheating in office buildings, which is inconsistent with the base model of a residential dwelling. Therefore, it is important that another overheating assessment method is also used for justification. Furthermore, TM52 is applicable to domestic and non-domestic buildings (Figure 3.3) and occupancy behaviour will vary between each. For example, occupants may be more inclined to change clothing in the comfort of their home and adapt to temperatures, making occupants in non-domestic dwellings more sensitive to temperature changes.

Gorjimahlabani (2020) details many criticisms of TM52, such as the threshold being arbitrary and not based on sufficient field data. He concludes that the model of Robinson & Haldi (2008) is more reliable for use in assessment. There is criticism that TM52 was not designed for T_{m} to exceed 30°C during the period of evaluation (Brotas & Nicol, 2017). This leaves the question of how applicable the method actually is to a study looking at higher temperatures induced by global warming.

HadCM3 A2 is a future emissions scenario published by the IPCC based on findings in their third and fourth assessment reports (Moazami et al., 2017). The CCWorldWeatherGen tool applies this to past weather files to produce projected weather data (Moazami et al., 2017). The tool uses this to superimpose relative change on the meteorological parameters stored in EPW file format. According to Jentsch (2008), the morphed weather files created using this tool are expected to overestimate the effect of climate change. When comparing the CCWorldWeatherGen to WeatherShift, it produces a more comprehensive data set as it modifies more meteorological parameters. The IPCC predicts that the degree of climate change increases for higher latitudes, as a result of Arctic amplification (IPCC, 2008). It can be concluded that the future weather file derived using this tool is the most comprehensive for production of meteorological data. Nonetheless, it cannot be considered completely accurate due to the various emissions scenarios predicted by the IPCC, leading to a wide range of climate change outcomes.

4. Literature review: Climate Analysis

4.1 Geography of Harran

Harran is a town and agricultural plain situated 44km southeast of Şanlıurfa in the southeast Antolia Region of Turkey, between the Euphrates and Tigris rivers (Figure 4.1).

Latitude: 36.86°N

Longitude: 39°E

Elevation: 369m.



**Figure 4.1: [above]
Location of Harran in
Turkey (Google Earth
Web, 2020)**



**Figure 4.2: [left] Map of
Harran's location on its
agricultural plain, the
surrounding mountains
and towns (Google Earth
Web, 2020)**

Figure 4.2 shows Harran's location, with the Tekttek mountains to the east and Falik mountains to the west. Running from the north, the Cullab river provides irrigation and means that the plain has optimal soil conditions for agriculture. The nearby mountains provide pasture for sheep, cattle and goats. Analysis of geology, pollen, lake cores and botanical remains of archeological sites suggests that the plain was seasonally swampy with wetland vegetation prior to the effects of climate change (Creekmore, 2018).

4.2 Harran's climate shifts: Present to 2080

CCWorldWeatherGen tool is used to generate a morphed 2080 EPW file. This section observes the shifts and patterns of the climate, comparing data from the past (1964-2011), current (2004-2018) and future (2080). Charts have been produced using Climate Consultant and Pyclim for analysis. The base weather file used for this is taken from Climate. Onebuilding (2021), of the closest possible location and elevation to Harran, 20km south in Tel Abiad, Syria. It is important to first note the potential discrepancies that come with using weather data taken from a slightly different location including:

- A 20m difference in elevation to 349m (Figure 4.3)
- The surrounding environment being less mountainous thus anticipating a lower wind velocity
- A probable difference in temperature due to the closer proximity to the Balikh River (Gaughan, 2017)

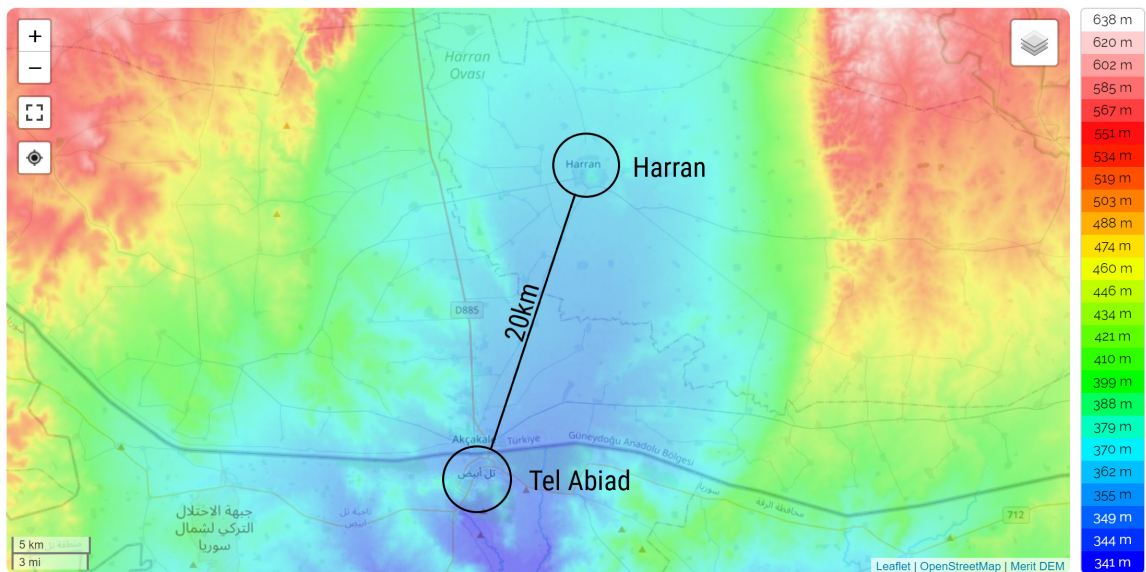
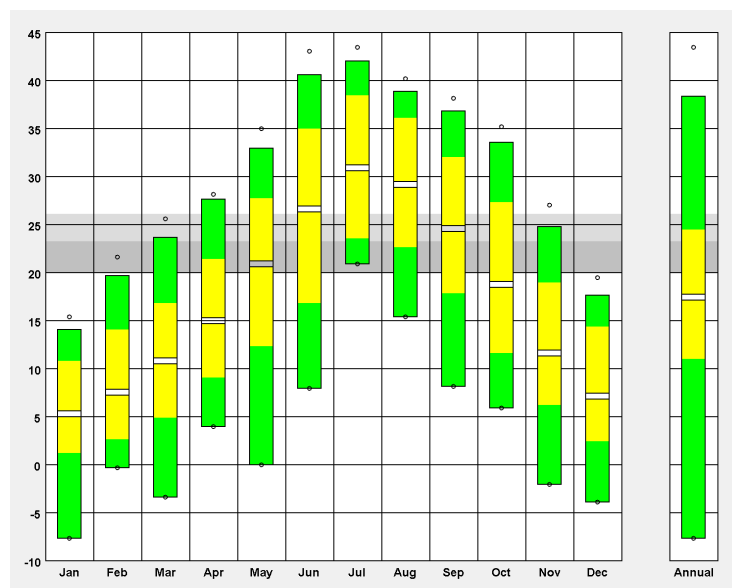
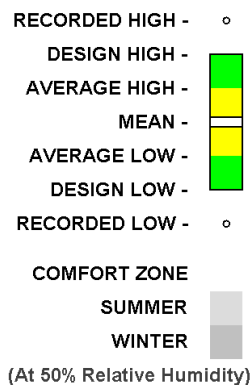


Figure 4.3: Map displaying the elevation and distance between Tel Abiad and Harran (Edited by author from Topographic Map, 2020)

4.2.1 Temperature

Figure 4.4:
[left] 1964-2011
temperature range



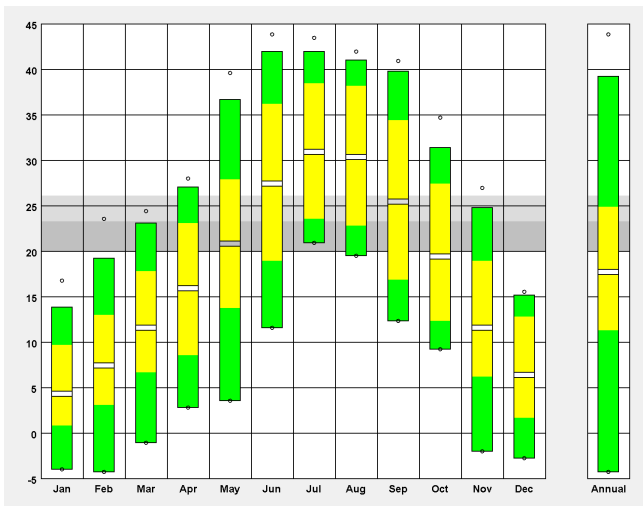


Figure 4.5: 2004-2018 temperature range

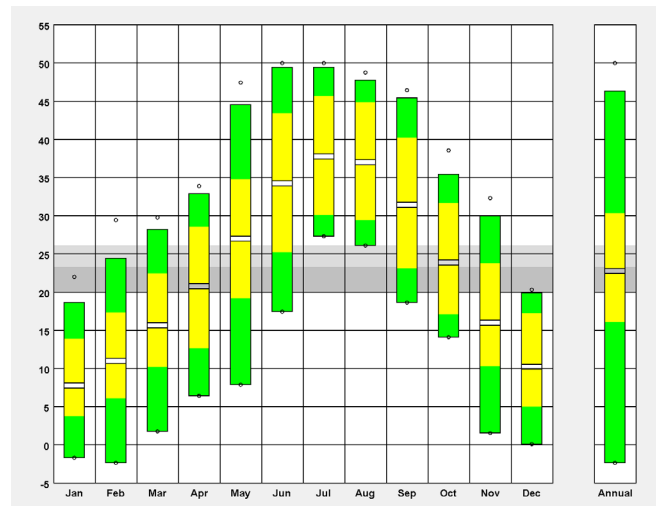


Figure 4.6: Predicted 2080 temperature range

The average annual temperature is presently 17.5°C (Figure 4.5), a slight rise from the past (Figure 4.4). The increase in average temperature by 2080 is significant, rising to 22.5°C (Figure 4.6). July's average temperatures will increase from 27.5 to 49°C, a larger increase than the past. The data indicate May and September as the average most comfortable months in terms of dry bulb temperature (ASHRAE, 2005). However, there is a predicted switch to April and October in 2080, which suggests that cooling-degree days are increasing and there will be greater demand for cooling through ventilation strategies or evaporative cooling.

4.2.2 Degree Days

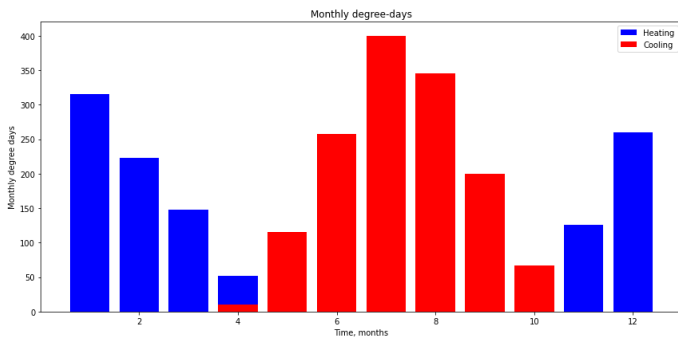
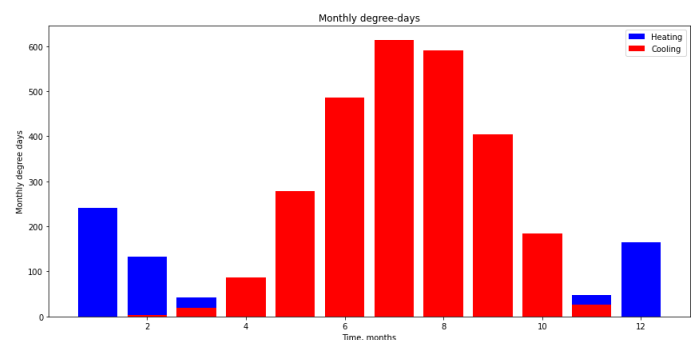
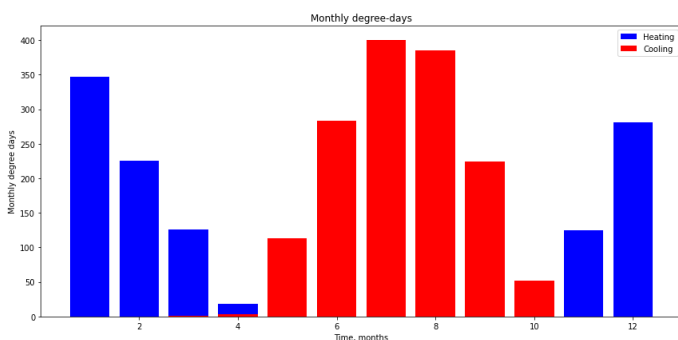


Figure 4.7: [left] Monthly degree days 1964-2011

Figure 4.8: [left below] Monthly degree days 2004-2018

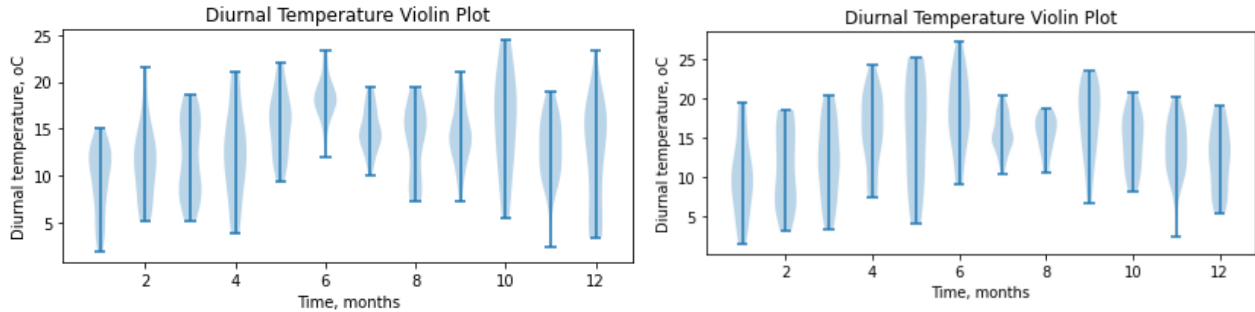
Figure 4.9: [below right] Monthly degree days 2080



It is clear from the existing climate data that cooling and heating are almost equally in demand in Harran (Figures 4.7-8). Cooling degree days have remained the same as in the past, whereas there has been a 5% increase in heating degree days. The shift in 2080 results in an 86% increase in heating degree days and a 49.5% decrease in cooling degree days, as calculated by Pyclim (Figure

4.9), which is more extreme than historical patterns, illustrating that cooling will become of elevated importance when managing the future of this climate. These data inform us that cooling degree hours and overheating risk will be the focus of the study moving forward to reduce active technology reliance.

4.2.3 Diurnal Temperature



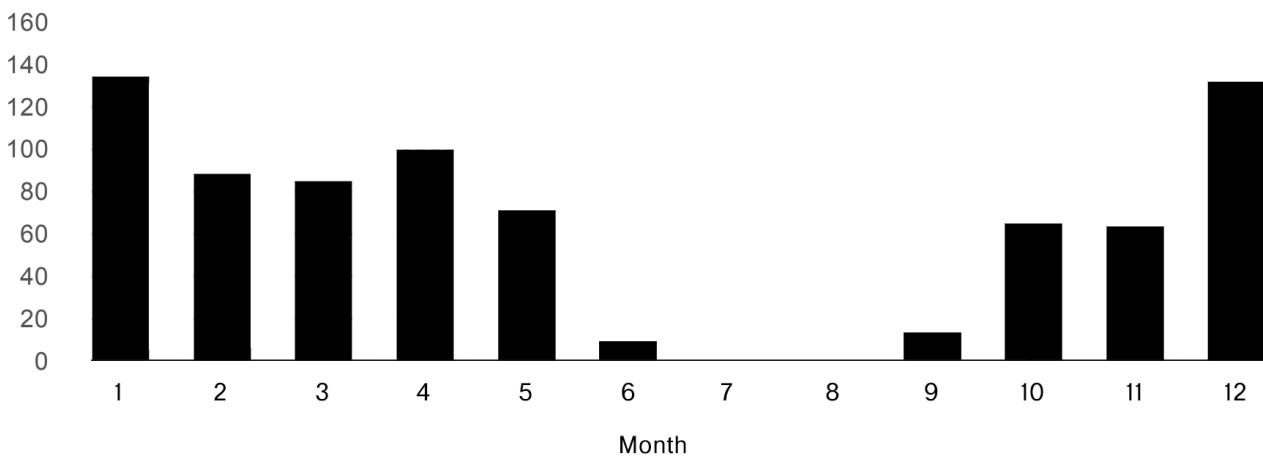
It is clear that diurnal temperature differences reduce annually in the future (Figures 4.10-11) such that temperatures at night will be more consistent with the daytime. Therefore, there will be higher demand for night-time cooling in the summer and night-time heating in the winter. Existing diurnal temperature differences are much more extreme than in the future and that temperatures at night drop significantly, allowing thermal mass materials to work more efficiently.

Figure 4.10: [left] Diurnal temperature violin plot 2004-2018

Figure 4.11: [right] Diurnal temperature violin plot 2080

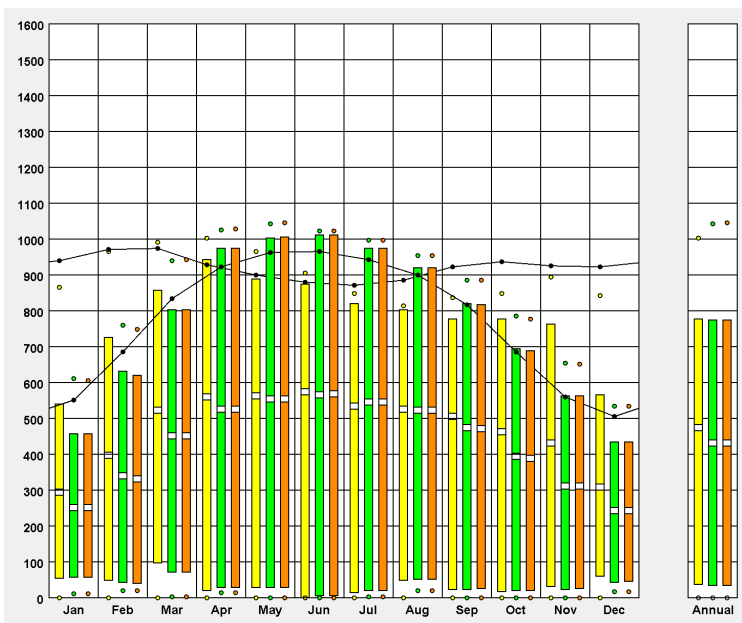
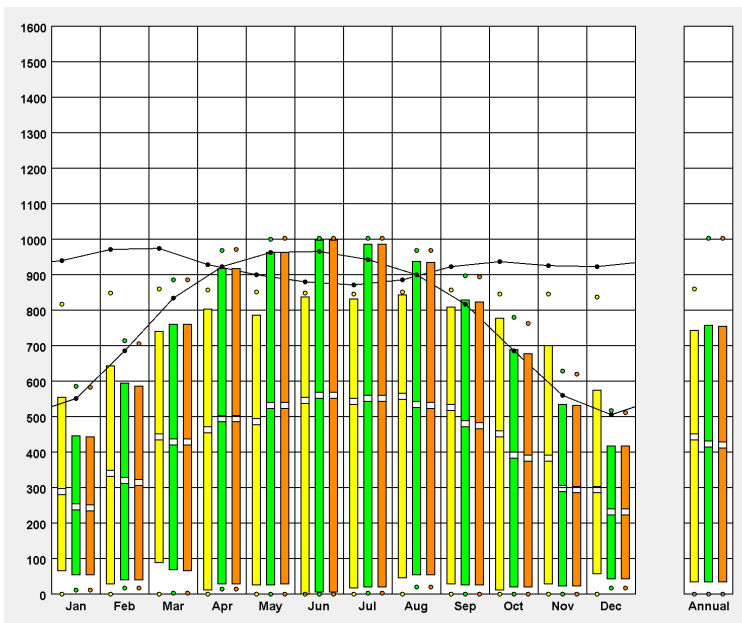
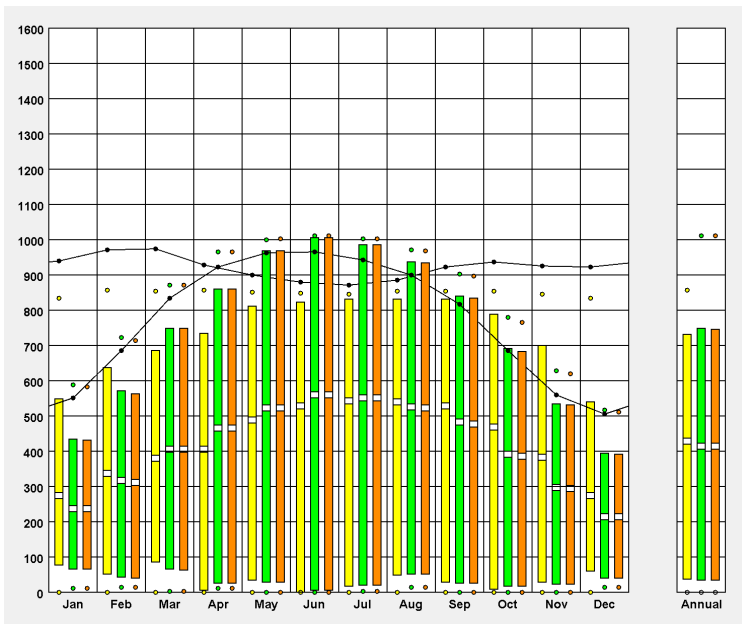
4.2.4 Rainfall

Average rainfall (mm)



In summer, there is very little rainfall which is consistent with relative humidity data (Figure 4.12). However, some rain protection must be considered in the design.

Figure 4.12: Average annual rainfall in Harran – present day, data acquired from World Weather Online (2021) [Data on predicted future rainfall in 2080 is not available]

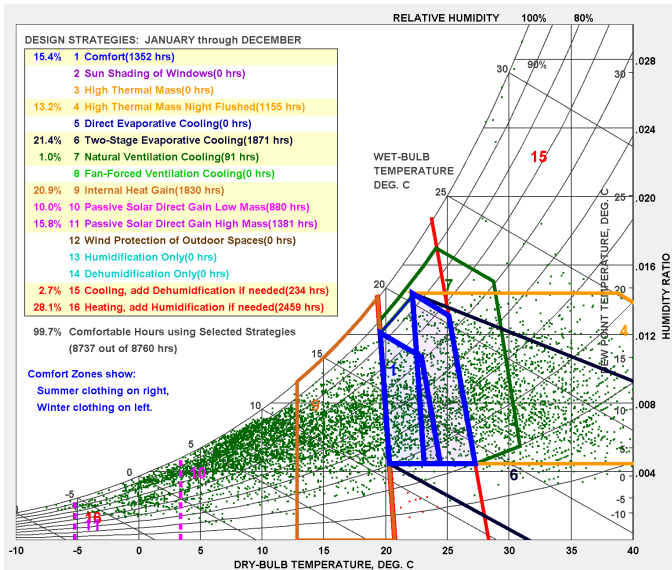


4.2.5 Radiation

The present annual average direct normal radiation (DNR) is 440Wh/m²/hr and slightly lower at 420Wh/m²/hr for the global horizontal (GH) and total surface radiation (TSR) (Figure 4.14). Radiation levels have risen since the past and there are indications of a rise in the future (Figure 4.13). In 2080, DNR is predicted to rise while only a slight increase in GH and TSR is expected (Figure 4.15). An increase in diffuse fraction would be expected, as absolute humidity and temperatures increase. Therefore, shading to reduce cumulative radiation on surfaces is extremely important, as this results in rises to indoor temperatures and could have damaging impacts on human health (USEPA, 2015).

[right: in vertical order]
Figure 4.13: Radiation range 1964-2011
Figure 4.14: [above] Radiation range 2004-2018
Figure 4.15: [below] Radiation range 2080

4.2.6 Psychrometric Charts



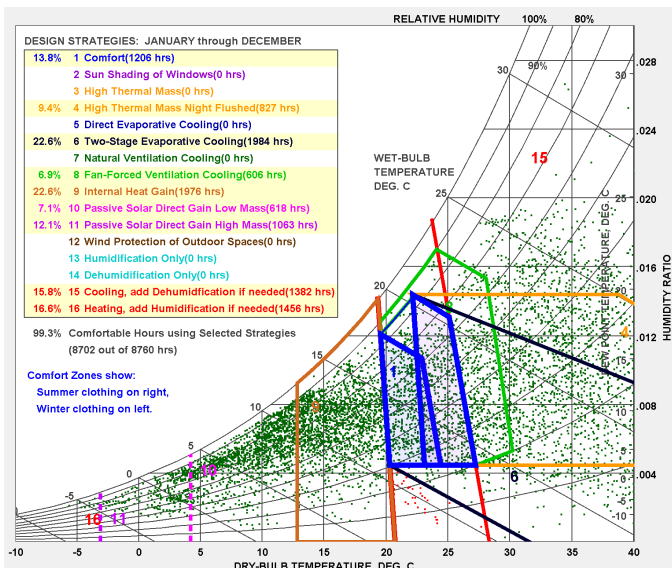
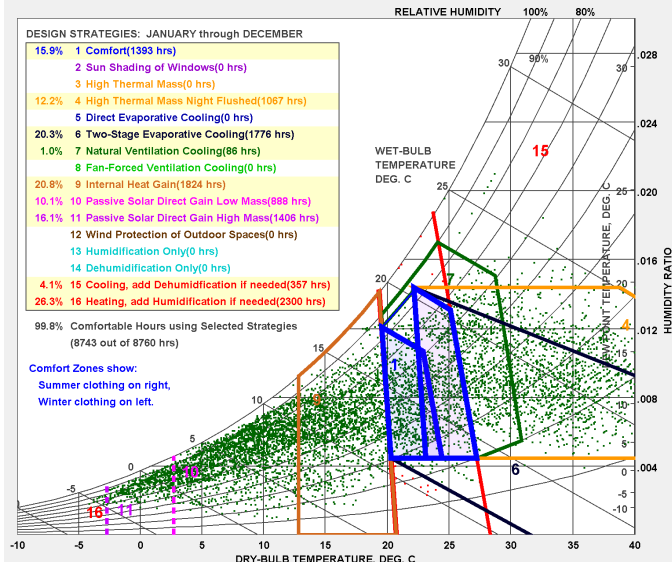
[in vertical order]

Figure 4.16: 1964-2011 psychrometric chart with most effective design strategies

Figure 4.17: 2004-2018

psychrometric chart with most effective design strategies

Figure 4.18: 2080 psychrometric chart with most effective design strategies



The past and present weather data suggest that heating around 60% of the time and cooling for 24.2% of the time could help to achieve 100% comfortable hours indoors (Figures 4.16-18), including the use of mechanical systems. In order to achieve maximum comfortable hours, design strategies such as two-stage evaporative cooling during the dry months, internal heat gains in winter, high thermal mass with night flush, passive solar direct gain and natural ventilation for cooling could help to decrease the heating and cooling loads.

The future climate weather data suggest that heating for 46% of the time and cooling for 38.9% of the time is necessary to achieve 100% comfortable hours. Strategies to reduce these loads could include:

- two-stage evaporative cooling
- high thermal mass with night flush
- passive solar direct gain (thermal mass)
- fan-forced ventilation.

4.2.7 Relative Humidity

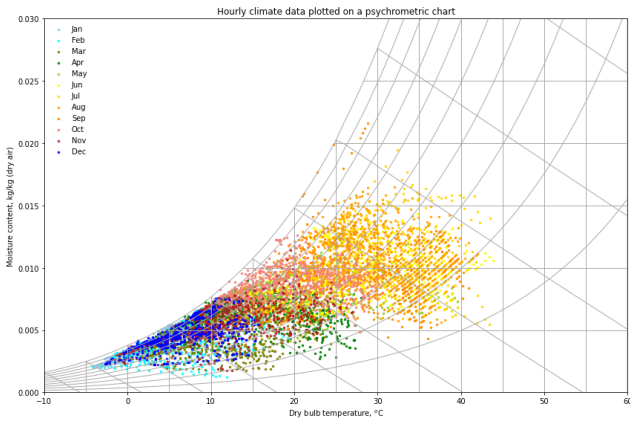


Figure 4.19: [left] Psychrometric chart 2004-2018

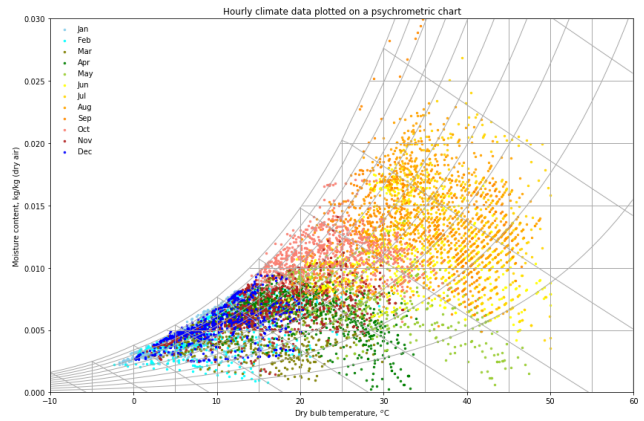


Figure 4.20: [right] Psychrometric chart 2080

Relative humidity is higher in the winter months (concentrated around 80-90%) and lower in the summer months (concentrated around 30-50%). In 2080, the predicted annual humidity range will drop and, with temperatures rising, there is an increasing potential for evaporative cooling (Figures 4.19-20).

4.2.8 Wind

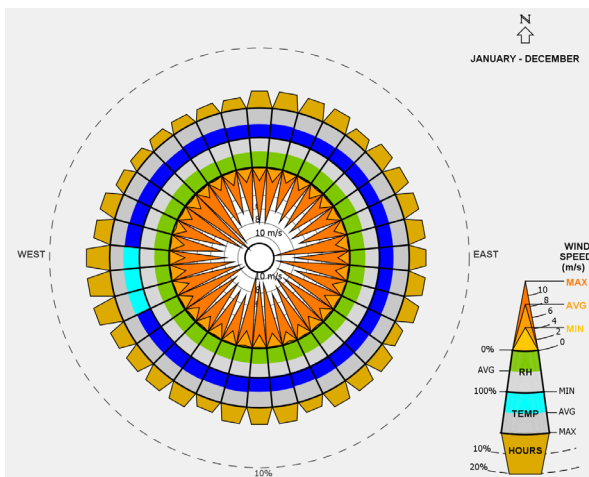
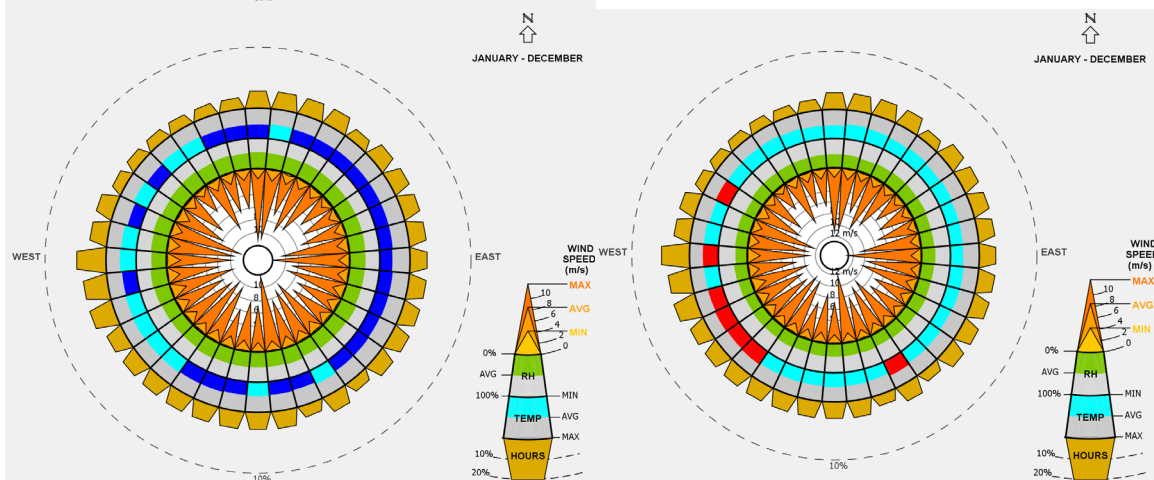


Figure 4.21: [above] Wind wheel 1964-2011

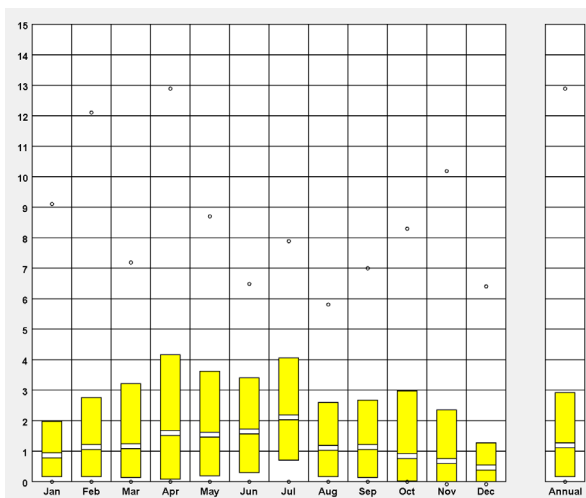
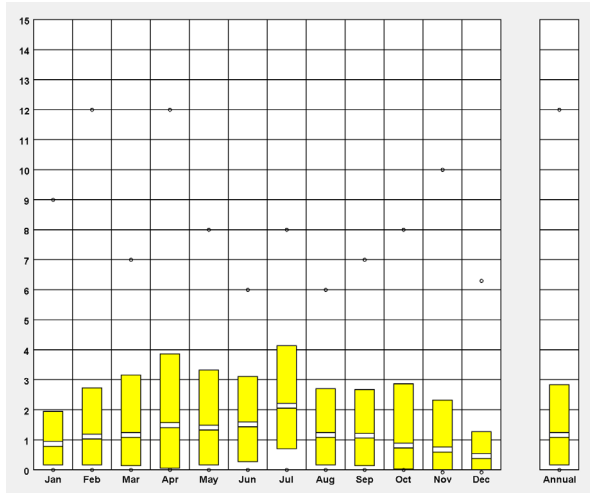
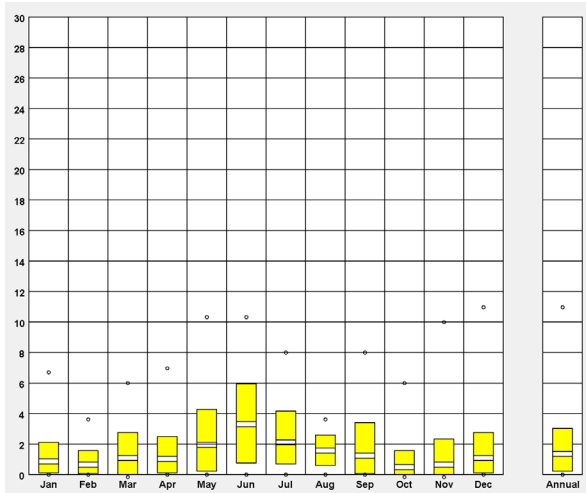
Figure 4.22: [below left] Wind wheel 2004-2018

Figure 4.23: [below right] Wind wheel 2080



Wind velocity ranges are predicted to slightly increase (Figures 4.24-26). Wind is multi-directional, reaching speeds of 10m/s in all weather scenarios (Figures 4.21-23). Therefore, orientation for wind-driven ventilation systems does not need consideration, and there is an opportunity for a passive wind-catcher system.

Research shows that it is particularly windy along the Harran plain due to its proximity to mountainous areas (Creekmore, 2018). Recent data on wind speed show it can reach 18.4km/h in summer (Figure 4.27). Therefore, managing multi-directional, hot and dusty winds will have design implications.



[left to right]
Figure 4.24: Wind velocity range 1964-2011
Figure 4.25: Wind velocity range 2004-2018
 [below]
Figure 4.26: Wind velocity range 2080

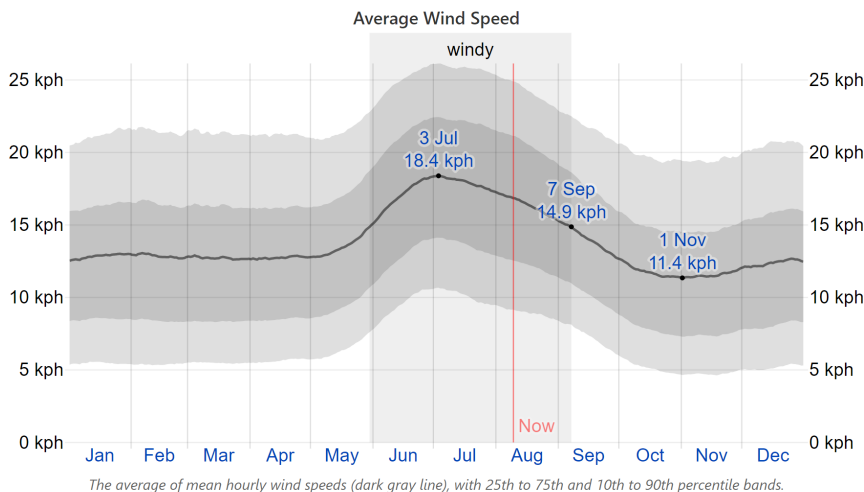


Figure 4.27: Average wind speed in Harran- based on hourly weather data from 1980 to 2016 (taken from Weather Spark, 2016)

4.2.9 Earthquakes

Harran sits in close proximity to the East Anatolian Fault line (Figure 4.28-29), where the Arabian plate meets the Anatolian Plate. The fault line runs through two regions bordering west Sanliurfa. Research shows that it is prone to small-scale, frequent earthquakes with larger ones occurring north-west of Harran (Volcano Discovery, 2021). Therefore, robustness and strength of materials should be considered in the design of the dwellings.

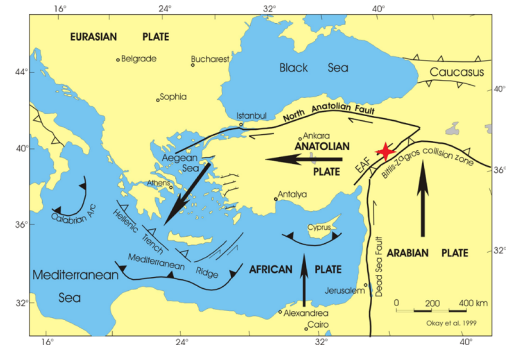
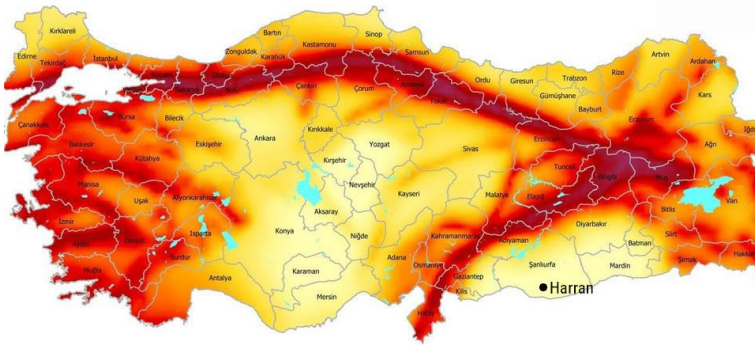


Figure 4.28: [left] Map of the fault lines across Turkey and Harran's location (Turkey News, 2020)

Figure 4.29: [right] Location of where the Arabian and Anatolian plate meet (UC Berkeley, 2020)

4.3 Climate analysis summary and the key threats

The main major threats of the current climate are as follows:

- Temperatures are not comfortable for the majority of summer and winter, with very few months being in the ASHRAE thermal comfort range (ASHRAE, 2005), resulting in excessive thermal loading
- Radiation is extreme in summer
- High winds exist along the plain, which could blow hot, dusty wind into the dwellings
- Small, frequent earthquakes causing stress on the structure

The projected trends in weather patterns are more extreme than past trends. It can be concluded from the analysis that cooling demand will be much higher and heating much lower. The decreasing relative humidity offers an opportunity for evaporation as a mechanism for cooling.

- The key threats of the future climate include:
 - Increasing temperatures
 - Increase in radiation and illumination

5. Literature Review: Vernacular architecture of Harran

5.1 Urban organization

The structure of Harran's ancient city consists of a 5m high castle wall surrounding the city, roads for trade transport, farming land and residential vernacular houses (Figure 5.1). The northeast and southwest are sparsely populated, as these corners have varied terrain and poorer agricultural soils (Creekmore, 2018). The street layout mirrors Harran's social condition, as tribes and families liked to live close-by to each other.

The Ancient City of Harran

- 1 Residential area
- 2 Farming and agricultural land
- 3 Inner castle
- 4 City wall
- 5 Mound
- 6 Grand mosque
- 7 Rakka gate
- 8 Aleppo gate
- 9 Road

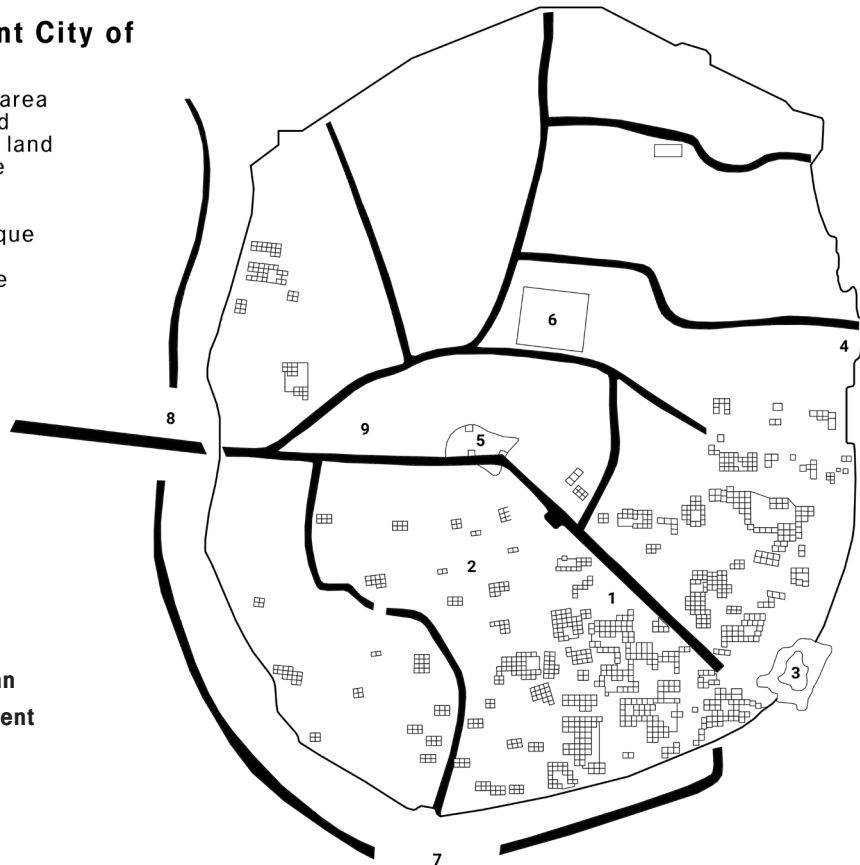


Figure 5.1: Urban plan of the ancient city of Harran





Figure 5.2: [previous page left] A house at Harran (Özdeniz et al., 1998)

Figure 5.3: [previous page right] General view of Harran (Özdeniz et al., 1998)

Figure 5.4: [left] Harran house view from the courtyard (Natural Homes, nd)

5.2 Nomadic society and rapid construction

The houses (Figures 5.2-4) were originally part of nomadic societies in the Mesopotamian civilizations, in 7th century BC. It is hypothesised that they were adopted from the “trullo” design of South Italy, as they were easily built with local materials (Ozdeniz et al., 1998). The rapid construction of the architecture reflects the itinerant lifestyle, with evidence suggesting they were easily erected and dismantled without advanced technology. This speed of construction enabled easy extension, with flexibility to add or remove rooms for new family members, thus reflecting social conditions. However, due to the use of weak rendering materials and sometimes poor construction, they needed repairing every 1-3 years; research shows the lifespan is limited to 70-150 years before rebuilding. Ozdeniz et al. (1998) indicate they are a quick and cost-effective solution for housing shortages in underdeveloped countries.

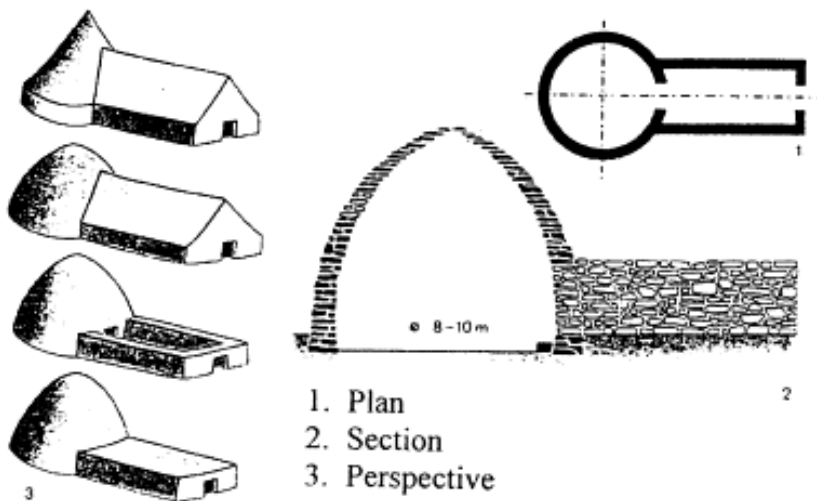


Figure 5.5: Domed building forms found in Mesopotamia excavations belonging to 7th century BC (Özdeniz et al., 1998)

5.3 Building form

The form of the Harran house has adapted over time. Photographs from the 19th century (Figure 5.5) show a random organisation of the forms compared to 20th century square-planned bases (Ozdeniz et al., 1998). Harran houses are typically adjacent to each other in small cells, allowing for easy access to livestock and agricultural activities (Figure 5.6).

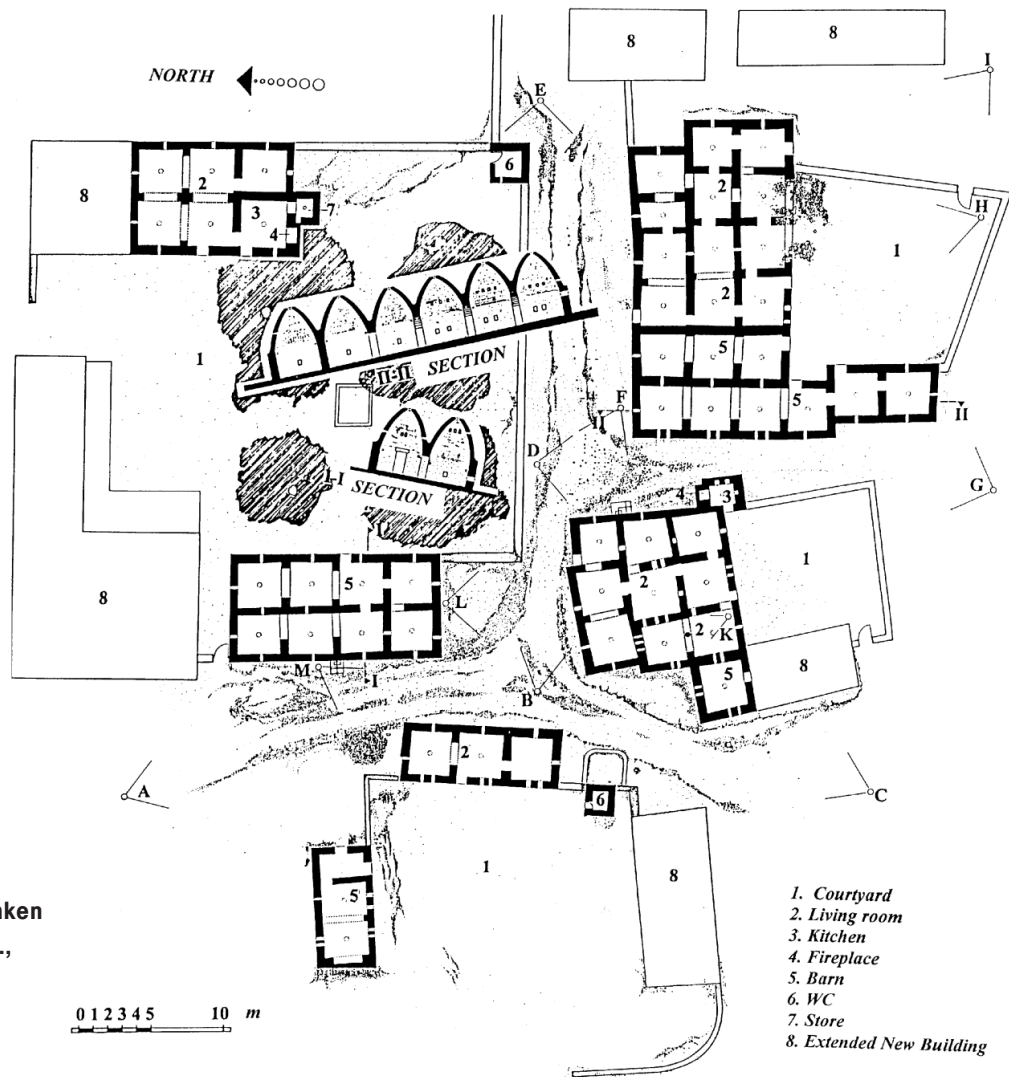


Figure 5.6: Plans and sections of a typical Harran neighbourhood (taken from Özdeniz et al., 1998)

5.3.1 Courtyard

A central courtyard is enclosed with a high wall at the front (Baran & Yilmaz, 2018), providing a shaded area to keep cool from sunlight and radiation. It is also a communal area for occupants to cook, do laundry, and for children to play (Figure 5.7).

Breezes in hot-dry climates cannot be used to ventilate indoor environments unless the air is cooled and dust is filtered (Koenigsberger, 1975). As natural ventilation is the main form of cooling, the courtyard can facilitate cooler, filtered air due to shading by the building and courtyard walls. This creates a gentle microclimate, whilst providing protection from winds picked up along the Harran plain (Ozorhon, 2014). This bioclimatic strategy is similar to those in other parts of southeast Turkey, such as Mardin, where the climate is also hot-dry (Ozorhon, 2014). It is common to use evaporative cooling in courtyards in these climates to reduce temperatures (Koenigsberger, 1975); this could be an appropriate strategy to introduce inside the Harran houses as humidity decreases and temperatures rise.

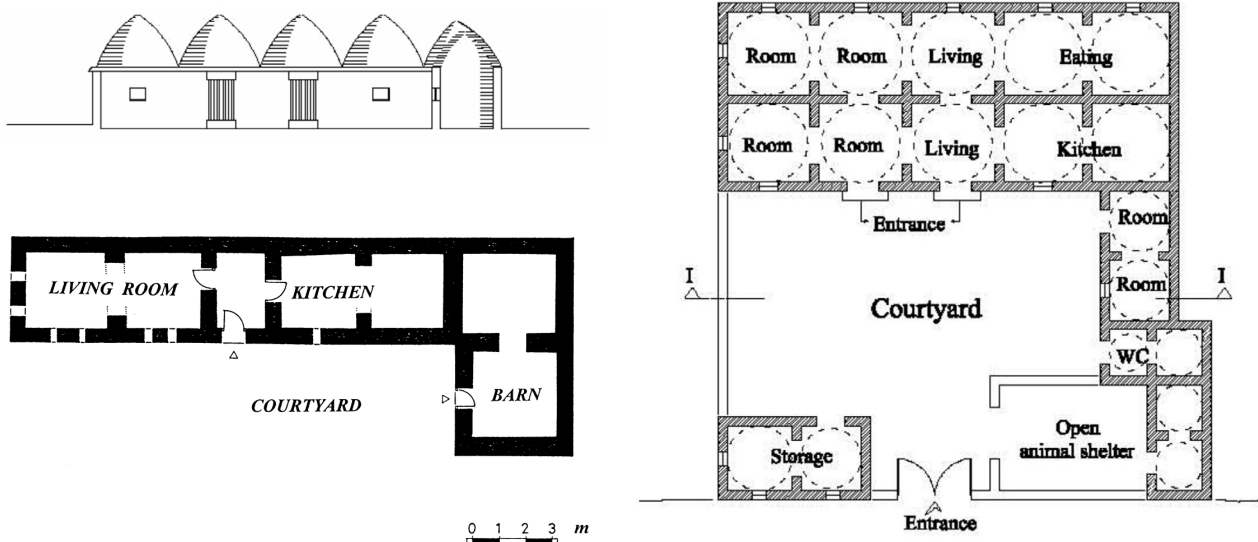


Figure 5.7: Plans and sections of a typical Harran house (taken from Özdeniz et al., 1998; Sami & Özdemir, 2011)

5.3.2 Square bases

Each unit consists of a square base to provide strength to the building against lateral forces and the domes above. These are typically 3x3-4x4m² in plan with walls 1.5-2.5m high (Sami & Özdemir, 2011).

5.3.3 Domes

Above each base sits a parabolic cone. These provide cooling via ventilation indoors, and shading in the courtyard to limit radiation on exterior surfaces and living spaces. During the summer, 40% of the domed roofs are shaded from solar radiation due to the beehive formations. The domes are typically located on the east-west axis of the courtyard to ensure shading in the courtyard from south and west during daytime (Özdeniz et al., 1998). The courtyard is exposed to the sky during night-time, allowing radiant heat emission to be conducted from the thermal mass building fabric to the ground and released externally (Koenigsberger, 1975).

It is thought that the use of conical roofs allow the dwellings to withstand strong winds (Vefik Alp, 1991). This provides structural robustness and smooth, aerodynamic surfaces, whilst facilitating better and more consistent indoor air circulation (Laila et al., 2018). These shapes also have a strong ability to reflect radiation back into the clear sky, convecting heat from the surfaces during the night (Koenigsberger, 1975).

The domes are typically 3.5-5m in height from the base. This has been deemed an optimal height for sufficient shading and stack ventilation.

5.4 Openings and ventilation

Natural cross and stack ventilation is commonly used as a method of cooling in hot/semi-arid climates (Koenigsberger, 1975). Doors of Harran houses are occasionally situated into the courtyard so that an in-flow of cool air and a basic source of natural light is provided (Sami & Özdemir, 2011). Openings are

closed by bricks during winter for minimal heat loss, and only open during summer night-time to flush out stored heat from high thermal mass materials (Baran & Yilmaz, 2018). Each dome has a 20cm diameter hole at the top, which acts as an escape for hot air and smoke from cooking, and entrance for light. A small brick roof is used above as protection from occasional rainfall. Small, 40x30cm windows open into the courtyard and street, to facilitate cross ventilation, minimising the chance of dusty air entering. These do not need to be large to provide reasonable indoor illuminance due to the clear skies. Cross-ventilation is provided in part by pairs of holes located opposite each other in the domes. The openings act like a vacuum in that they create a negative pressure and extract internal air (Baran & Yilmaz, 2018). Arches between each room allow for cool air to circulate.

Natural ventilation flushes out stored heat in the walls from the day: a method that is common in hot-dry climates as a strategy to cool indoor air at night (Fathy et al., 1986), although sometimes residents prefer to sleep outdoors in summer (Başaran, 2011).

Openings are covered using mesh wire to protect the interior space from insects and birds. They are closed during winter with brick and stone (Özdeniz et al., 1998).

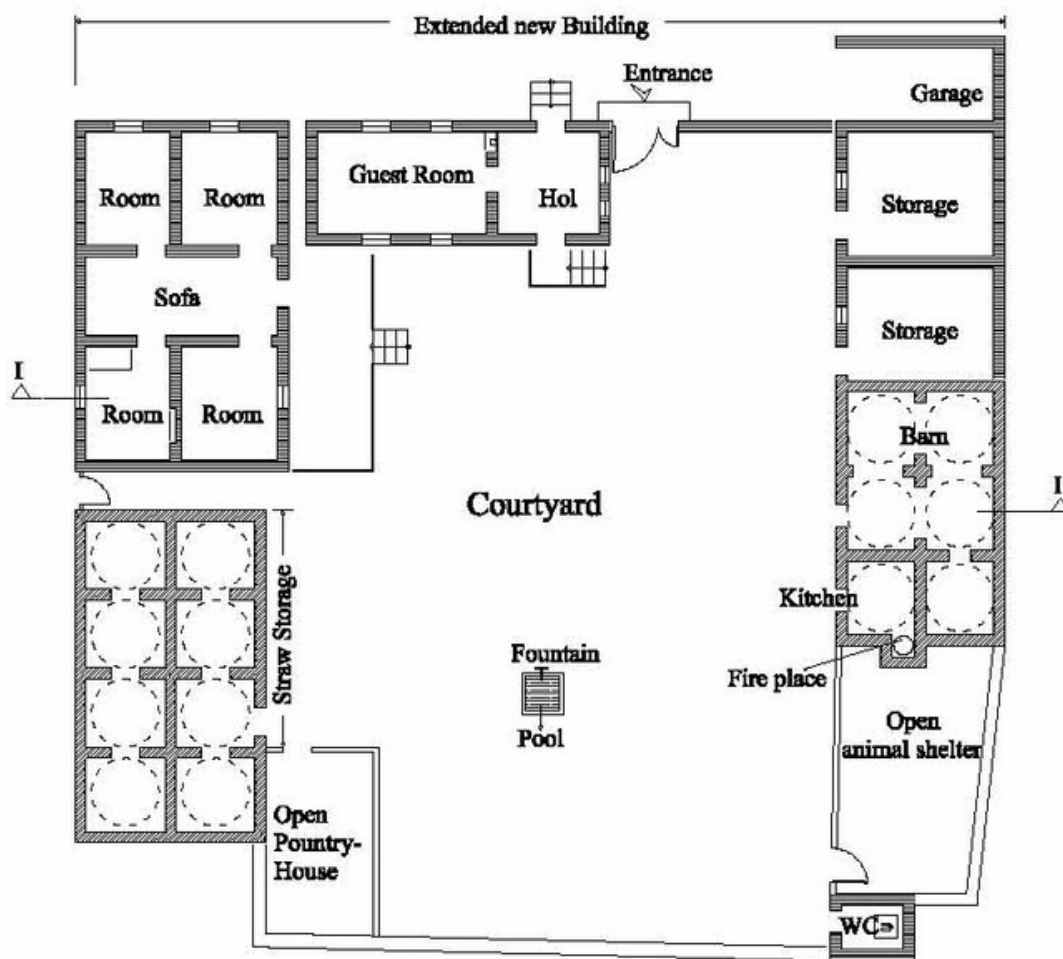


Figure 5.8: The plan of a vernacular Harran house (taken from Sami & Özdemir, 2011)

5.5 Spatial organization and rooms

The layout sits compact, inward to the courtyard, on the ground floor (Figure 5.8), with rooms under one structure in order to: minimise thermal loading from the sun and hot air; and also lessen physical fatigue for residents during the hot summer months (Koenigsberger, 1975).

Spatial arrangement is important to the residents' social structure and work (Sami & Özdemir, 2011). The layout consists of multiple rooms: a kitchen with a bathing area, living room, cellar, storage space or barn, stable, and units for storing agricultural products. The single storey layout is compact and inward-facing to the courtyard (Figure 5.9), with rooms under one structure to minimise thermal loading from the sun and lessen physical fatigue for residents during hot summers (Koenigsberger, 1975). During the winter months, the kitchen is used as a living room as it tends to be a warmer space due to heat gains from fire pits for cooking. Toilets are typically located in a corner of the courtyard (Özdeniz et al., 1998). A 1m deep fire pit in the kitchen provides a natural floor heating system in winter. Cooking is done in the courtyard during the summer to avoid unwanted heat gains.



Figure 5.9:
[right] A
throne in the
courtyard of a
Harran house
(Natalie, nd)

5.6 Materials and construction

Costa et al., (2019) explains that adobe buildings can last hundreds of years, without need for regular maintenance, making it a sustainable material in low humidity climates. Table 3 displays properties of adobe as a material (see Figure 10) and its application to Harran's climate.



Figure 5.10: [left]
Adobe brick
material in
construction
(Cortesi,
2020)

Property		Value	Comments specific to site
Strength (MPa)		Between 0.3 and 3.5	Ability to withstand frequent earthquakes Strength for load-bearing walls to take the weight of domes
Emissivity		0.9	Ability to reflect 90% of radiation on its surface back into the atmosphere Good material to avoid extreme radiation absorption in the summer months
Absorption		0.1	
Capillary water absorption (kg/m ² /h ^{1/2})		Between 3 and 21	Rain and relative humidity can cause changes in its thermal behaviour
Thermal conductivity (kW/(m-K))	<i>Fired adobe</i>	0.244	Good insulating properties
	<i>Concrete block</i>	0.627	
	<i>Adobe with straw</i>	0.180	
	<i>Adobe</i>	0.240	
Specific heat capacity (J/kg-K)		1260	Good thermal mass properties to make use of diurnal temperature extremes and for the prevailing solar heat gain to be stored in the walls
Density (kg/m ³)		1540	

Table 3: Adobe as a material for vernacular construction, information sources: (Omega, nd; Costa et al., 2019; Olukoya Obafemi & Kurt, 2016; Acosta et al., 2010; Vivancos et al., 2009; Parra-Saldivar & Batty, 2006; Goodhew & Griffiths, 2005; Koenigsberger, 1975)

5.6.1 Dome construction

Materials used for the dome are important, as the roof is exposed to the sky for longer than any other surface (Koenigsberger, 1975). They must bear the ability to manage the extreme radiation and thermal loading of the climate. The domes appear in a light earth colour (Figure 5.12) which means they are more likely to reflect radiation than absorb it (Koenigsberger, 1975). Uniquely square and flat shaped clay tiles and sun-dried adobe bricks were used for construction (Figure 5.11) with the corbelling technique of overlapping bricks.

The corbelling technique involves a cantilever effect and requires thick walls to provide structural support for the domes (Todisco et al. 2017). Cardinale et al., (2011) argue that this method interrupts thermal flow passage by creating frequent voids in the masonry and this could then impact indoor temperatures during months of extreme weather. However the conical roof form and thickness are proven to be effective at creating comfortable indoor environments through their facilitation of stack ventilation in conjunction with thermal mass materials. This is also proven to be the case with the Italian “trulli” houses in a thermal analysis study by Cardinale et al. (2013).

The use of adobe brick is thought to distinguish the Harran houses from similar types in the region (Sami & Özdemir, 2011; Özdeniz et al., 1998). Rendering consists of mud, and straw

for strength in binding. It is applied to the whole exterior of the dome and 2.5m up on the interior walls (Figure 5.13) (Özdeniz et al., 1998). This process is repeated annually in June, when the weather is driest. The walls are 30-35cm thick (Baran & Yilmaz, 2018).

5.6.2 Wall construction

The exterior and interior walls are constructed in the same way (both 50-70cm), with sun-dried adobe brick and, occasionally, local stone that is rendered and joined in mud mortar mixed with straw. In any climate, adobe walls should be thick, to make use of its successful mechanical and thermal properties (Costa et al., 2019).

Brick sizes are typically 24x24x4.5cm or 13x24x4.5cm, and a thickness of 2-3 bricks is used for dome support. The top corners of the base are filled with stone, acting also as a platform to render the exterior of the dome. The exterior rendering is often washed in white soil/paint due to its reflective quality, limiting daylight from entering inside (Başaran, 2011).



Figure 5.11: [above left] Internal view of the dome (Başaran, 2011)

Figure 5.12: [above right] The exterior look (Padfield, 2021)

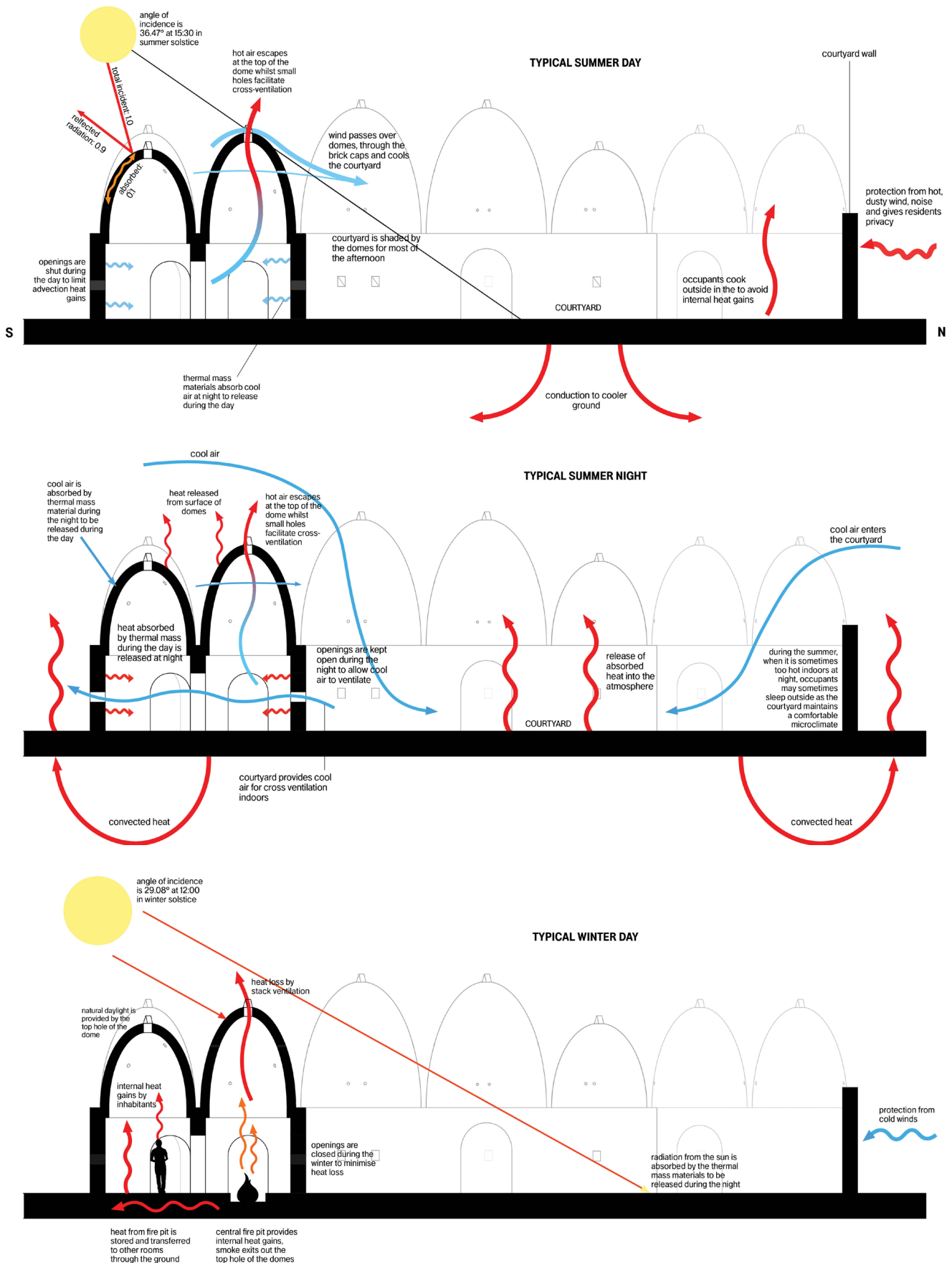
Figure 5.13: [below left and right] Internal views (Padfield, 2021)

5.6.3 Floor construction

The houses are supported by a 1-1.5m deep foundation made up of random-sized rubble, overlaid with a clay and mud and straw rendering flooring (Başaran, 2011).

5.6. Seasonal behaviour of the Harran houses

The diagrams (Figure 5.14) show the house's thermal behaviour, during the day, night, winter and summer.



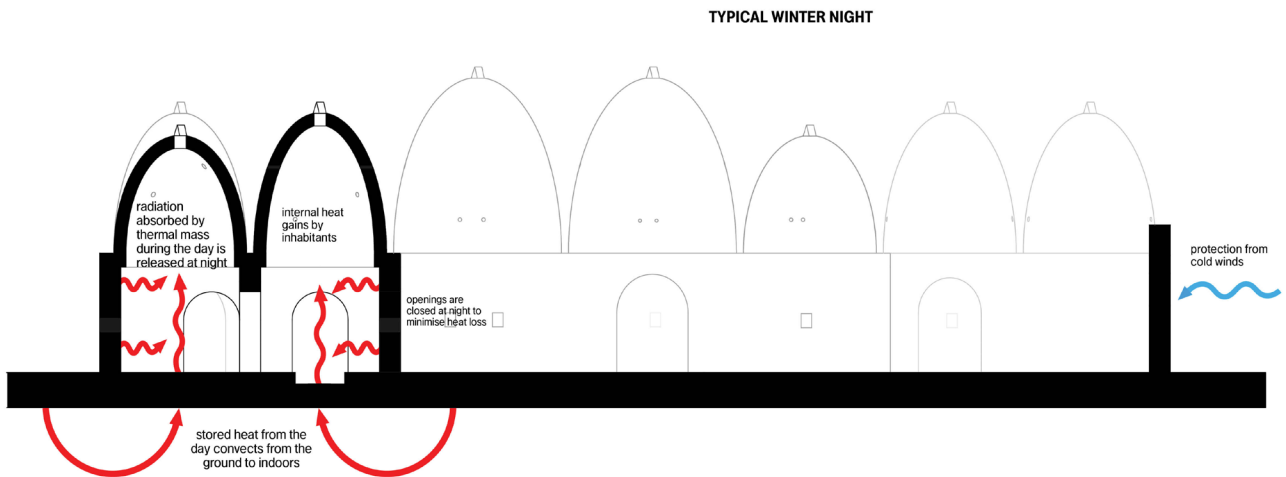


Figure 5.14: The Harran house thermal behaviour diagrams between night and day in winter and summer

5.7 Summary of vernacular principles and parameters for simulation

It is clear that Harran houses rely on the use of locally sourced, thermal mass materials, cross and stack ventilation and building form to facilitate cooling in summer. Thermal mass materials, occupancy and closing of openings in winter are predominant strategies used to assist heating. Therefore, it is important that the following principles are looked at individually for assessment of their effect on internal temperature:

- Thermal mass materials
- Passive ventilation via openings
- Occupancy
- Building form

These strategies will be tested by making adjustments to the model. The parameters that will inform these strategies through simulation are as follows:

- Construction materials
- Window to wall ratio
- Window height
- Orientation
- Dome height

6. Base model of traditional house, inputs and analysis

An initial simulation of the base model in DesignBuilder is first completed and evaluated in order to inform the probability of overheating, and as a comparison point for further simulations. The details of the model and inputs were predominantly based on research and certain assumptions.

6.1 Traditional Base Model

The base model is developed in DesignBuilder, situated in the southeast residential area of Harran (Figure 5.1). Figure 6.1 shows the configuration of the rooms on the ground floor:

- | | |
|-------|---|
| 1 | Courtyard: surrounding walls are high and are adobe construction |
| 2 | Main entrance: here there is a central firepit |
| 3-4 | Living room: used only during the summer |
| 5-6 | Bedroom |
| 7 | Storage room |
| 8-9 | Dining room: used only during the winter |
| 10-11 | Kitchen: Only used during the winter (cooking is done in the courtyard during the summer) |
| 12-13 | Main bedroom |
| 14-15 | W.C. |
| 16-17 | Livestock, with an open animal shelter in front in the courtyard |
| 18-19 | Storage for agricultural products |

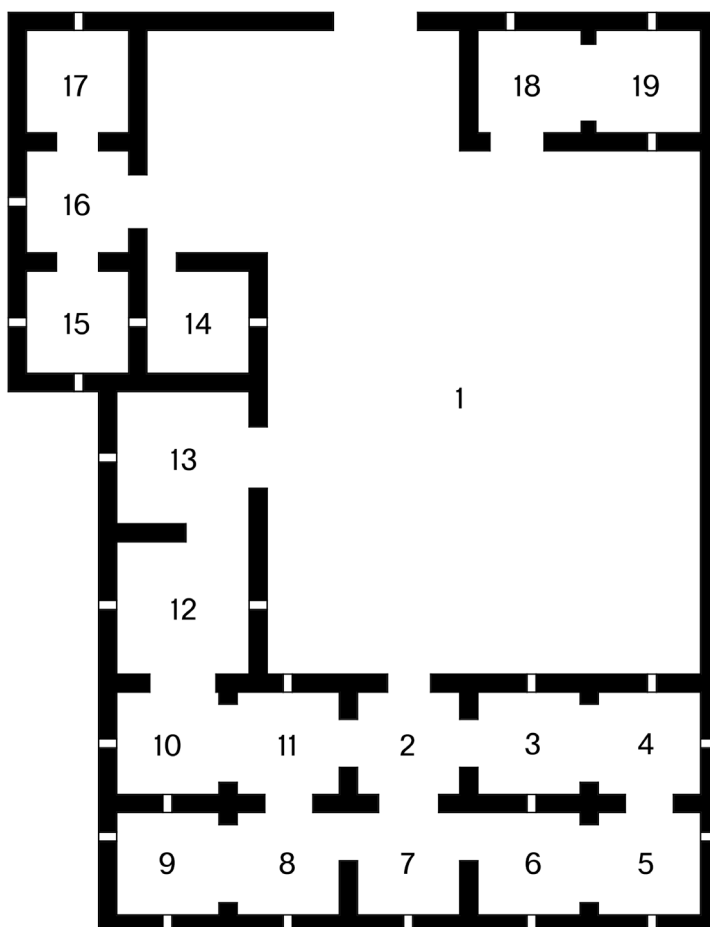


Figure 6.1: Configuration of rooms in plan of the base model

6.1.1 Building Form

All rooms sizes are 4x4m, except for main bedrooms which are 5x5m. The base room walls are all 3m high under the domes. In the model, dome height varies (between 3-5), most being 4m. Each dome has a maximum 35cm diameter holes to facilitate cross ventilation and a 20cm opening at the top. The orientation of the dwelling means the entrance is from the north and there is a row of domes along the east-west axis. The dwelling is centred around a courtyard. Openings between rooms are either arches or small windows to allow adequate air flow and circulation.

Visual assumptions were based on images and descriptions of an existing dwelling called “Halil Özyavuz Harran House”, included in a thermal analysis case study by Başaran (2011). The house in Figure 6.2 is approximately 210 years old, and was restored for touristic purposes.



Figure 6.2: Halil Özyavuz Harran House from a study done by Başaran (2011)

6.2 Inputs in the model

6.2.1 Weather data

Hourly weather data of Tel Abiad, Syria was imported into the software of the current and 2080 climate scenario.

6.2.2 Occupancy

Table 4 indicates the occupancy schedule inputs that replicate the use of the residential dwelling as it is currently and traditionally used.

Sources: Özdeniz et al., 1998; Sami & Özdemir, 2011; Baran & Yilmaz, 2018.

Occupancy of the domes was set to “<None>”.

Table 4: Occupancy inputs for the base model

Room	Description	Power Density (W/m ²)	Metabolic rate per person (W/person)	Occupation density (people/m ²)	Occupancy latent fraction	Occupancy	Days per week	Target Illuminance	DHW rate (l/m ² -day)	Heating set point temperature (°C)	Cooling set point temperature (°C)	Minimum fresh air (l/s-person)	Natural ventilation set point temperature (°C)
1	Main entrance	8.00	180 (light manual work)	0.0155	0.5	7am-11pm	7	100	Off	18	25	10	24
2	Living room	1.5	108 (resting)	0.188	0.5	4pm-11pm	7	150	Off	18	25	10	24
3	Living room	1.5	108 (resting)	0.188	0.5	4pm-11pm	7	150	Off	18	25	10	24
4	Bedroom	3.5	90 (resting)	0.0229	0.5	24hrs	7	100	Off	18	25	10	24
5	Bedroom	3.5	90 (resting)	0.0229	0.5	24hrs	7	100	Off	18	25	10	24
6	Storage room	0.0	140 (standing/walking)	0.1037	0.5	8am-6pm	7	50	Off	18	25	10	24
7	Dining room	3.0	110 (eating/drinking)	0.0169	0.5	7am-10pm	7	150	Off	18	25	10	24
8	Dining room	3.0	110 (eating/drinking)	0.0169	0.5	7am-10pm	7	150	Off	18	25	10	24
9	Kitchen	15.0	160 (work involving walking)	0.0237	0.5	7am-11pm	7	300	1.050	18	25	10	24
10	Kitchen	15.0	160 (work involving walking)	0.0237	0.5	7am-11pm	7	300	1.050	18	25	10	24
11	Main Bedroom	3.5	90 (resting)	0.0229	0.5	24hrs	7	100	Off	18	25	10	24
12	Main bedroom	3.5	90 (resting)	0.0229	0.5	24hrs	7	100	Off	18	25	10	24
13	W.C	1.61	140 (standing/walking)	0.0243	0.5	6am-10pm	7	100	4.350	18	25	10	24
14	W.C	1.61	140 (standing/walking)	0.0243	0.5	6am-10pm	7	100	4.850	18	25	10	24
15	Livestock	0.0	-	-	0.5	-	7	-	-	10	30	10	24
16	Livestock	0.0	-	-	0.5	-	7	-	-	10	30	10	24
17	Storage	0.0	140 (standing/walking)	0.1037	0.5	8am-6pm	7	Off	Off	18	25	10	24
18	Storage	0.0	140 (standing/walking)	0.1037	0.5	8am-6pm	7	Off	Off	18	25	10	24

6.2.3 Construction

Table 5 shows inputted construction templates of the dwelling.

Table 5: Construction inputs for the base model

Material	Thickness	Thermal Conductivity	Density	Specific heat capacity	U-Value	Thermal mass
	mm	W/(m·K)	Kg/m ³	J/(kg·K)	W/(m ² ·K)	Kj/(m ² ·K)
External walls and internal walls	700				0.255	465
Mud mortar with straw	50	0.24	440	750		16.5
Sun-dried adobe brick	600	0.18	800	900		432
Mud mortar with straw	50	0.24	440	750		16.5
Dome walls	400				0.444	249
Mud mortar with straw	50	0.24	440	750		16.5
Sun-dried adobe brick	300	0.18	800	900		216
Mud mortar with straw	50	0.24	440	750		16.5
Floor	1900				0.328	3032.4
Mud mortar with straw	200	0.24	440	750		66
Sun-dried adobe brick	200	0.18	800	900		144
Random rubble (aggregate)	1500	1.80	2240	840		2822.4
Roof corners of square bases	50				0.686	46.02
Mud mortar with straw	30	0.24	440	750		9.9
Stone	20	3.00	2150	840		36.12

6.2.4 Openings

A limitation of DesignBuilder is that natural ventilation cannot be modelled as it is used in real life. This is because it does not allow for the modelling of empty windows that are opened and closed daily with brick as identified in the research (Baran & Yilmaz, 2018). Therefore, these empty windows are modelled as thin as possible with 3mm single glazing. This may produce inaccurate simulation outputs and result in over-estimated solar gain via windows, which is important to remember when discussing results. However, the opening of windows is scheduled when indoor temperatures exceed 25°C and external air is cooler, meaning natural ventilation will still occur in the model. Without glazing, hot air entering from outside may also result in hotter indoor temperatures, as well as radiation entering the building through openings directly and indirectly via elements like reflection. Therefore, there is likely to be some error in the modelled air temperatures.

The doors are modelled as a simple fabric curtain. No shading devices were inputted on the base model. Arches range from 0.5-2m in width between rooms and are 1m as entrances to the building. All windows are 0.3x0.4m, located 1m from the ground (Baran & Yilmaz, 2018).

6.2.5 HVAC Sensitivity Analysis

Natural ventilation (no heating or cooling) is selected as the HVAC system input. A sensitivity analysis (Figure 6.3) is undertaken with a ventilation rate from 5-25ac/h. It is important that natural ventilation rate input is correct in order to accurately model the assumed night-time ventilation that works with thermal mass materials. By measuring the sensitivity of ac/h against probability of overheating (Robinson & Haldi, 2008), it is found that the trendline does not plateau due to the outside air temperature already being at overheating risk limit. It would be ideal in further studies, to complete a more thorough calculation of ventilation rate to accurately model natural ventilation. However, for the purposes of this study, it has been assumed that the most appropriate natural ventilation rate to input is 10ac/h.

The schedule for natural ventilation to be used was set as 'always on'. However, in the future, a system that determines when openings are open would be a more accurate way to model the natural ventilation in the dwelling.

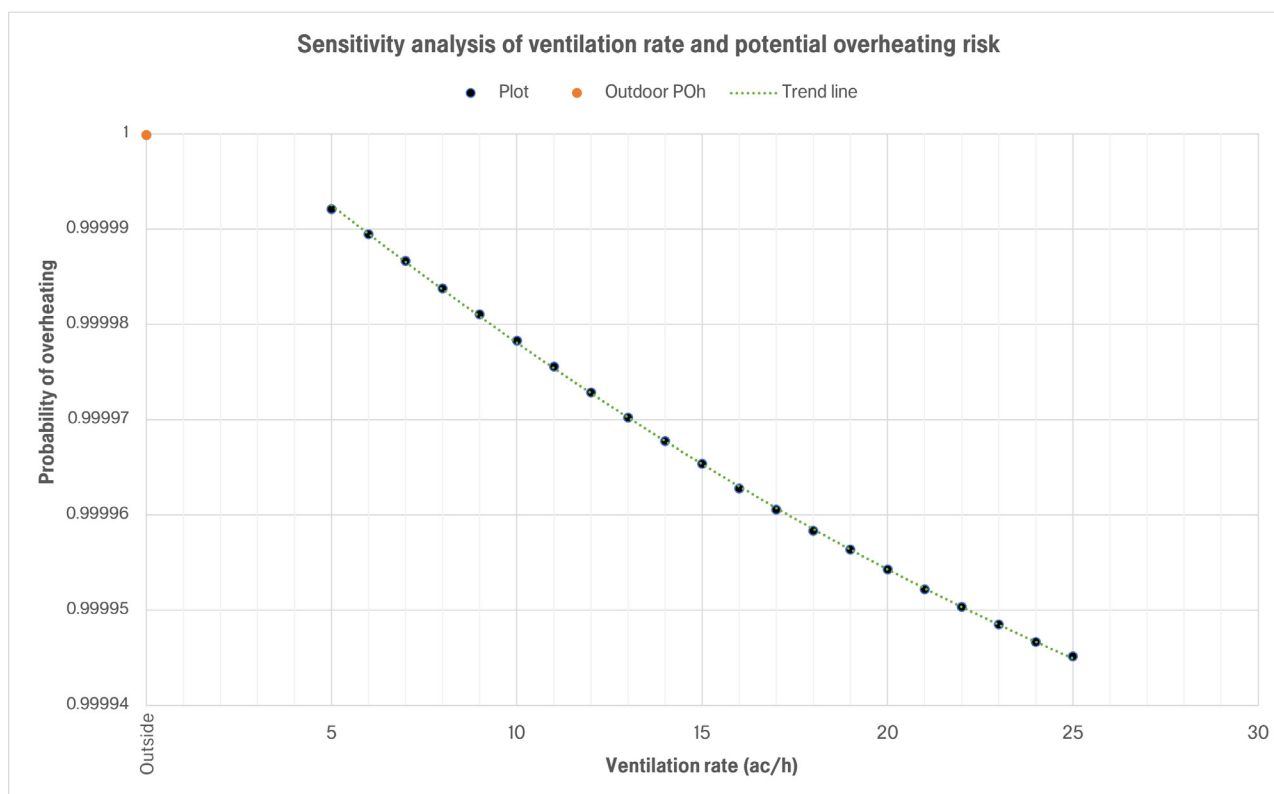


Table 6.3: A sensitivity analysis of ventilation rate and potential overheating risk (P_{OH} according to Robinson & Haldi's dynamic overheating model) to inform ventilation rate for simulations. As ventilation rate increases, probability of overheating decreases.

6.3 Discussion of results of the base model

4 rooms were simulated (Figure 6.4), these were chosen to understand the the performance of zones that are most commonly used in different locations of the house. These consist of the kitchen, living room, main bedroom and bedroom 3.



This section compares the results of the base model simulated in a current and future climate. Table 6 shows the results of each room (as described in Figure 6.4) and the building as a whole. Figures 6.5-6 show indoor air temperature variations compared to the dry-bulb temperature across the year, in the current and 2080 climate. The overheating risk at present is much lower than in 2080. The base model in a 2080 scenario fails to pass any TM52 criteria and exceeds 20% overheating risk around a month earlier than at present (Figure 6.7). This means that the building will become reliant on cooling technologies earlier in the year in order to avoid discomfort for occupants, resulting in more carbon emissions.

In both scenarios, rooms B3 and K2 have the lowest overheating risk and fewest cooling degree hours (CDD), and LR2 and MB1 are at greatest risk of overheating. This is due to B3 and K2 both sitting below smaller domes (3m) with just 1 exterior wall, meaning there is less surface area exposure to solar radiation and solar gain. These 3m domes are also neighbored by taller domes (4-5m), resulting in further shading from radiation.

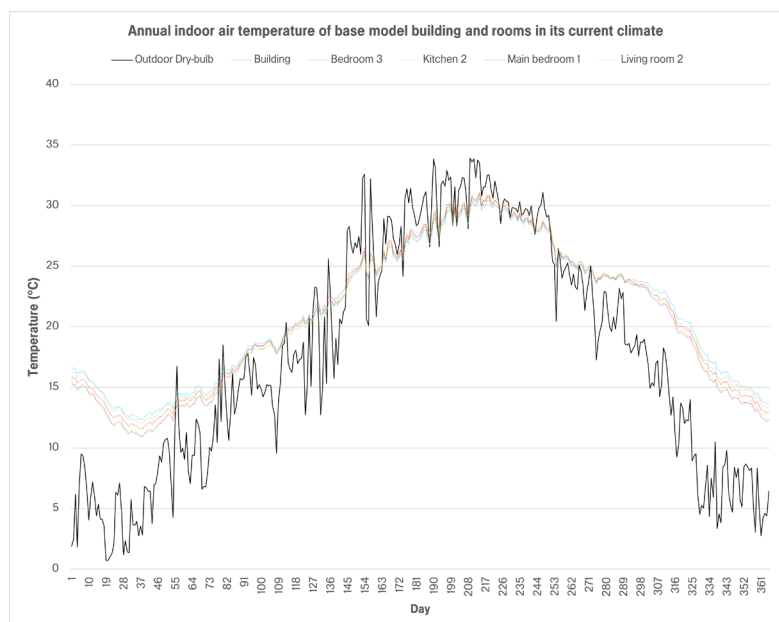
LR2 sits below a 4m dome, whilst MB1 has a 5m dome. These larger sizes lead to better cross and stack ventilation, and a higher flow rate, which results in more heat loss in these rooms through external ventilation (Appendix 2.2). However, both rooms result in a higher probability of overheating compared to the others. This is due to these rooms having a significantly higher solar gain than B3 and K2, as shown in Figure 6.8. This leads to the conclusion that the effect of building fabric and solar radiation on external surface area has a greater effect on overheating risk than ventilation. This is likely due to the small window to wall ratio (WWR) resulting in ventilation having a lesser impact.

Table 6: The overheating risk of the base model in a current and future climate, compared to the outdoor dry-bulb temperature risk.

Simulation Description	CIBSE TM52				Robindon and Haldi (2008)		
	TM52: Criteria 1	TM52: Criteria 2	TM52: Criteria 3	Pass/Fail	Degree Hours (>25°C)	P _{OH} (25°C)	P _{OH} Exceeds 20% (Date)
Base Model: Current Climate							
Building	0	0	0	Pass	8,465.61	0.982068	6/21/2002 16:00
B3	0	0	0	Pass	7,832.01	0.975771	6/25/2002 10:00
K2	0	0	0	Pass	7,780.54	0.975171	6/24/2002 14:00
LR2	0	0	0	Pass	9,082.49	0.986623	6/18/2002 21:00
MB1	0	0	0	Pass	8,553.54	0.982801	6/18/2002 21:00
Base Model: 2080 Climate							
Building	14.46	57.39	0	Fail	22,602.56	0.999978	5/26/2002 18:00
B3	13.03	46.31	0	Fail	21,701.97	0.999967	5/28/2002 10:00
K2	12.68	49.59	0	Fail	21,704.72	0.999967	5/27/2002 22:00
LR2	15.55	63.57	1	Fail	23,356.2	0.999985	5/26/2002 11:00
MB1	14.60	64.19	0	Fail	22,771.06	0.999980	5/25/2002 17:00
Current Climate Results (using hourly weather data)							
Outdoor Dry-Bulb Temperature	8.76	68.49	224	Fail	15,406.22	0.999336	5/26/2002 15:00
2080 Climate Results (using hourly weather data)							
Outdoor Dry-Bulb Temperature	21.06	178.52	1	Fail	33,599.11	1	4/22/2002 16:00

Research indicates that the kitchen is typically not utilised during the summer, and cooking is rather undertaken in the courtyard, thereby avoiding unwanted high indoor temperatures and internal heat gain. In the future, the extremely high indoor temperatures during the summer (see Figure 6.5-6) might lead the occupants to spend even more time outside in the courtyard, where there is shade or breeze. However, due to the increase in radiation in the future, this could have adverse health impacts (USEPA, 2015). This means that Harran’s vernacular architecture does not perform particularly well in 2080, highlighting the importance of finding effective passive cooling strategies to achieve indoor thermal comfort.

Figure 6.5: The coloured lines show each of the rooms’ indoor temperature across the year in a current climate and the black line is the outdoor dry-bulb temperature for comparison. The indoor temperatures broadly follow the outdoor temperature, but remain warmer in the winter and slightly cooler in the summer. Minimising the range of indoor temperatures across the year is desirable to ensure comfort.



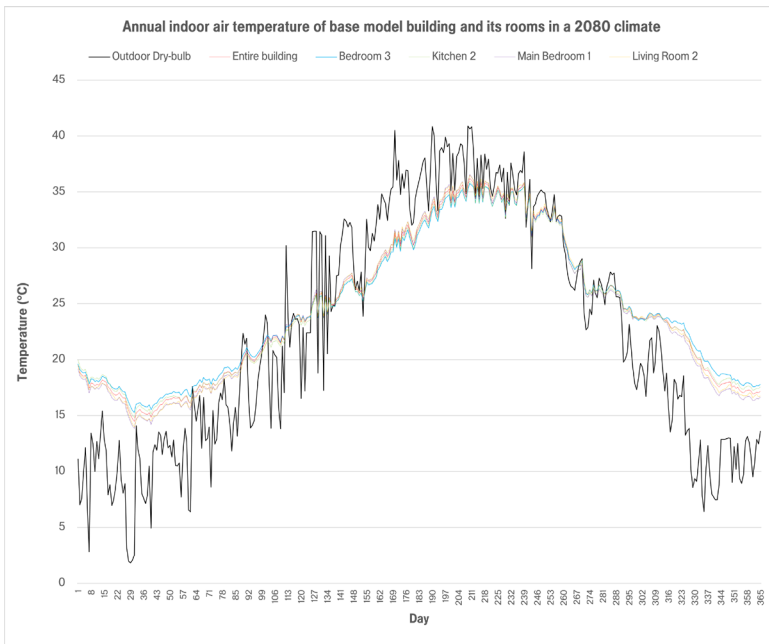


Figure 6.6: The 2080 climate results of indoor air temperature per room and the dry-bulb temperature. Temperatures have increased by around 5°C compared to the current climate (Figure 6.5). The variations are similar to those in a current climate, meaning comfort varies across the year.

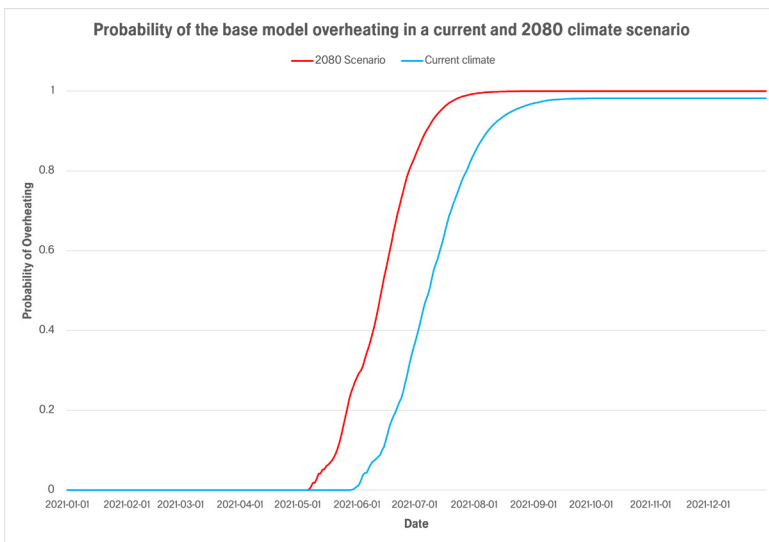


Figure 6.7: A comparison of the current and future climates accumulating probability of overheating risk, using Robinson & Haldi's dynamic model. It is ideal that the line plateaus later on the X axis and remains as low on the Y axis as possible. Therefore the current scenario in blue shows a better performance against this P_{OH} model.

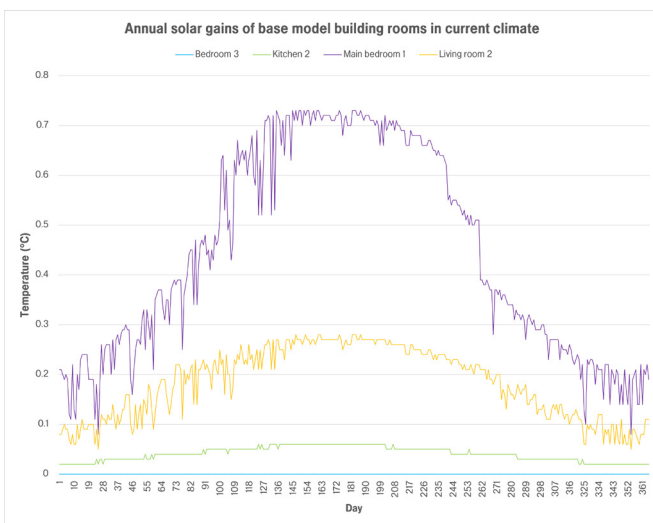


Figure 6.8: [left] The solar gains in a current climate. [right] The solar gains in a 2080 climate. It is optimal if the lines on the chart stay as low on the Y axis in the summer months to avoid unwanted solar gain. Therefore bedroom 3 performs the best and main bedroom 1 performs the worst.

6.3.1 Lighting and radiation analysis

As well as thermal comfort, it is also important that visual comfort is addressed when creating indoor environments. This involves maximising natural daylight inside and minimising dependence on artificial lighting, without compromising thermal comfort. To assess the visual comfort of the base model, an annual simulation of the present-climate indoor illuminance is undertaken using Revit. It is not possible to input a future 2080 weather file to simulate illuminance and radiation in Revit as the software does not allow for the input of custom weather files. A software like IESVE may be useful to achieve this for further studies, but using it is beyond the scope of this work. When adjusting parameters for radiation and illuminance, the current Tel Abiad weather file is used. This may not give an accurate depiction of the performance of the dwelling in its future climate, however, it can determine the effect these adjustments have on visual comfort and shading when moving into a future of increasing radiation and illumination.

The simulation of indoor illuminance was undertaken using a clear sky, as this reflects the typical conditions in Harran. For visual comfort, the indoor illuminance should exceed 100 lux (EFA, 2014). As shown in Figure 6.9, all rooms without an external doorway fail to achieve this as a result of a low WWR.

However, the research here shows that residents have adapted to a semi-outdoor lifestyle, making use of the natural daylight in the courtyard that is not otherwise provided indoors. Although this outdoor lifestyle is not ideal for residents in the future due to an increase of radiation causing adverse health impacts (USEPA, 2015). Therefore, the vernacular architecture will not perform well in a 2080 scenario and there is space for improvement to visual and thermal comfort.

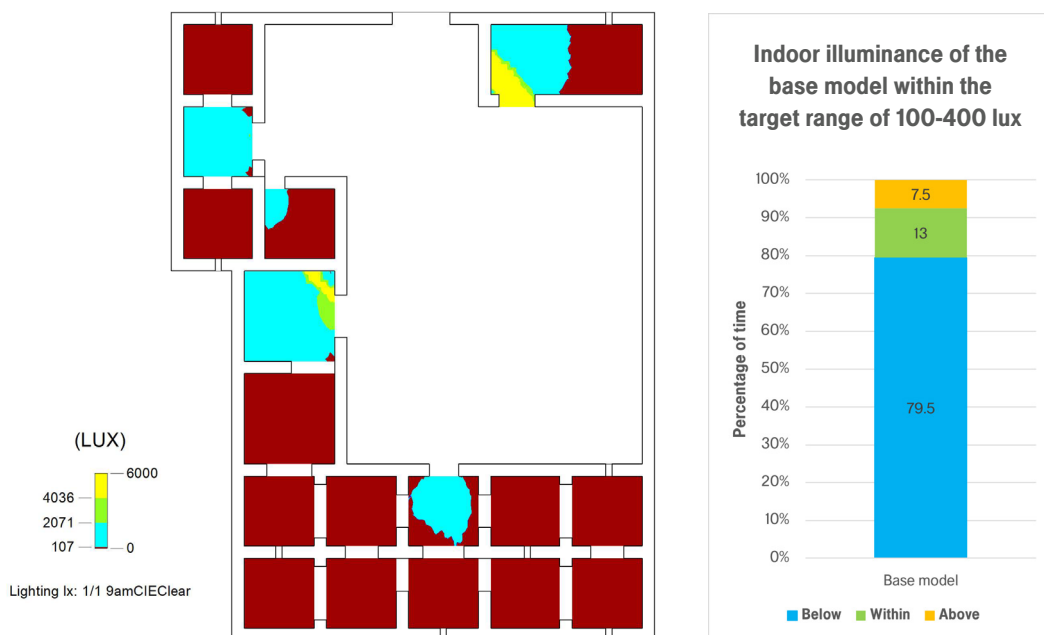


Figure 6.9: [left] A distribution of illuminance in the base model simulated in a current climate. [right] The percentage of time the indoor illuminance is within a range of 100-400 lux. Above 100 lux is an acceptable target for indoor illuminance. The chart shows the base model performs below this for 79.5% of the time and the distribution plan shows that the only rooms receiving adequate daylight are rooms with larger openings for doorways.

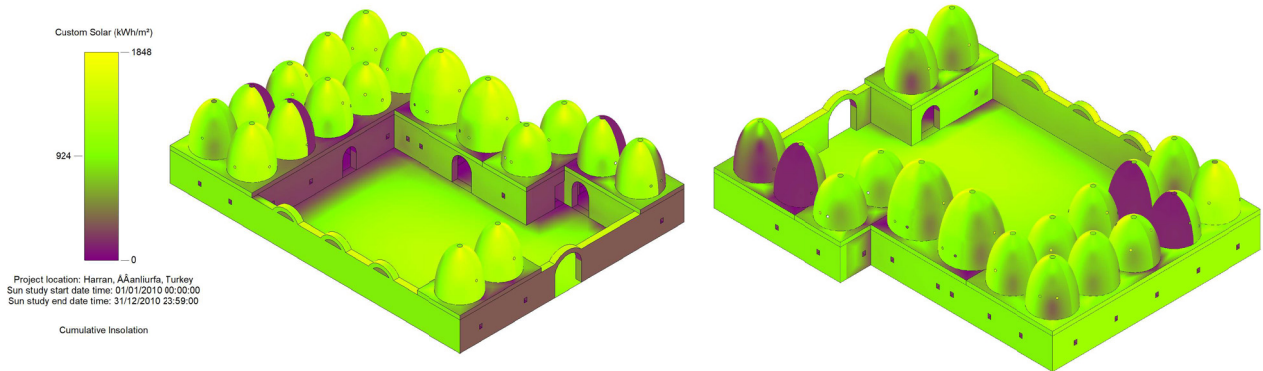


Figure 6.10: [above] A simulation of the distribution of radiation on external surfaces of the base model across a year. The domes create shading from radiation on the courtyard and on surrounding domes. The colour bar on the left indicates the degree of incident radiation.

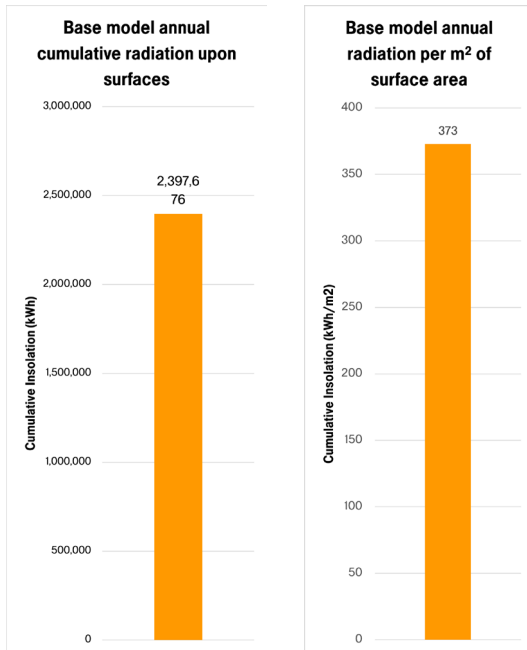


Figure 6.11: [left] The charts show annual cumulative insolation on building surfaces and the annual insolation per square metre.

Figure 6.10 shows the distribution of radiation on the base model. In the current climate, the overall cumulative insolation annually is high at 2,397,676kWh (Figure 6.11). However, the large surface area introduced by the domes and the courtyard means that the radiation per unit area is low, at 373kWh/m². As with the illuminance analysis, a simulation using the 2080 weather data is not possible. Nonetheless, it has been identified that radiation is due to increase in the future, which means that the radiation per unit area will be higher in 2080.

B3's dome is shaded almost entirely on the west side, which is the reason for it having the lowest overheating risk of the rooms. MB1's 5m dome receives little shading from radiation, contributing to its high overheating risk. The courtyard receives little shading, which means that occupants may have a high demand for comfortable temperatures indoors when this space becomes too hot, especially when considering the rising temperatures that a 2080 climate presents. Therefore, in order to maximise comfort for occupants in the future, orientations and shading devices should be explored to further optimise sheltering from radiation.

7. Results after change of parameters

This section explores the effect that a change to construction materials, window placement, window to wall ratio (WWR), building orientation, dome height and percentage of windows open have on the indoor temperature of the building. The simulations are performed using 2080 hourly weather data in order to effectively adapt the building to a future climate and reduce overheating risk.

7.1 Analysis of results after change in construction materials

This subsection will explore how the construction materials affect the performance of the dwelling. A mixture of traditional and contemporary assemblies are tested (Turkish Standard, 2008). The building is modelled as being built entirely of each construction type, with the exception of the floor, which remains unchanged.

Table 7 and Figure 7.1 detail the different construction types that are tested.

Table 7: A table detailing the different constructions that are tested

Parameters Alteration (change in materials)			
Material	Thickness	U-Value	Thermal Mass
	mm	W/(m ² ·K)	kJ/(m ² ·K)
Base model (vernacular construction)			
External Walls	700	0.255	465
1. Turkish Standard Construction			
Plaster	20		12
Concrete Blocks	200		400
Insulation	60		8.064
Plaster	20		12
	300	0.442	432.064
2. Addition of insulation			
Mud rendering	50		16.5
Adobe bricks	500		360
Insulation	100		60
Mud rendering	50		16.5
	700	0.167	453
3. Addition of reflective external rendering			
White paint	5		6.5
Mud rendering	50		16.5
Adobe bricks	600		432
Mud rendering	50		16.5
	705	0.254	471.5
4. Concrete as thermal mass			
Mud rendering	50		16.5
Concrete blocks	600		360
Mud rendering	50		16.5
	700	0.218	393
5. Stone as thermal mass			
Mud rendering	50		16.5
Stone	600		1728
Mud rendering	50		16.5
	700	1.087	1761
6. 300mm envelope with insulation			
Mud rendering	50		16.5
Adobe bricks	100		72
Insulation	100		60
Mud rendering	50		16.5
	300	0.265	165

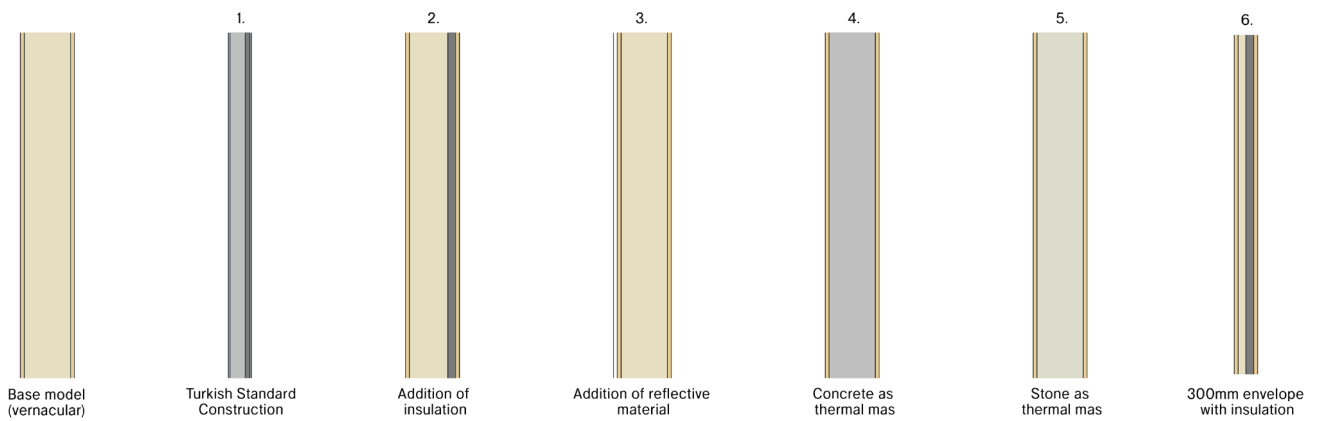


Figure 7.1: Graphics of the different building envelopes that are tested

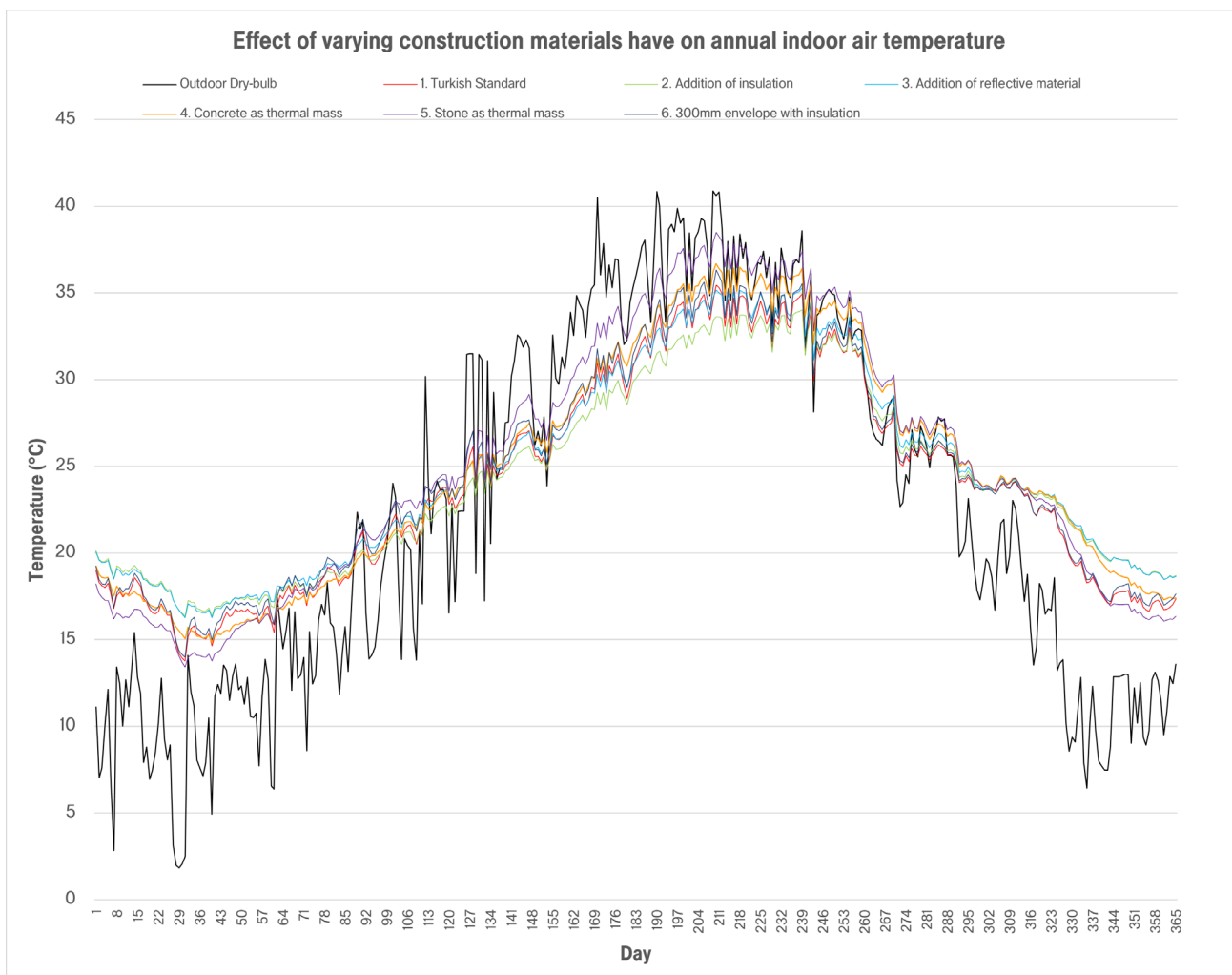


Figure 7.2: The effect of different construction materials on the indoor air temperature across the year in 2080, compared to the outdoor temperature. Consistent indoor temperatures across the year are desired for the purpose of thermal comfort. There are significant variations across the year with all construction materials, with type 2 performing the best.

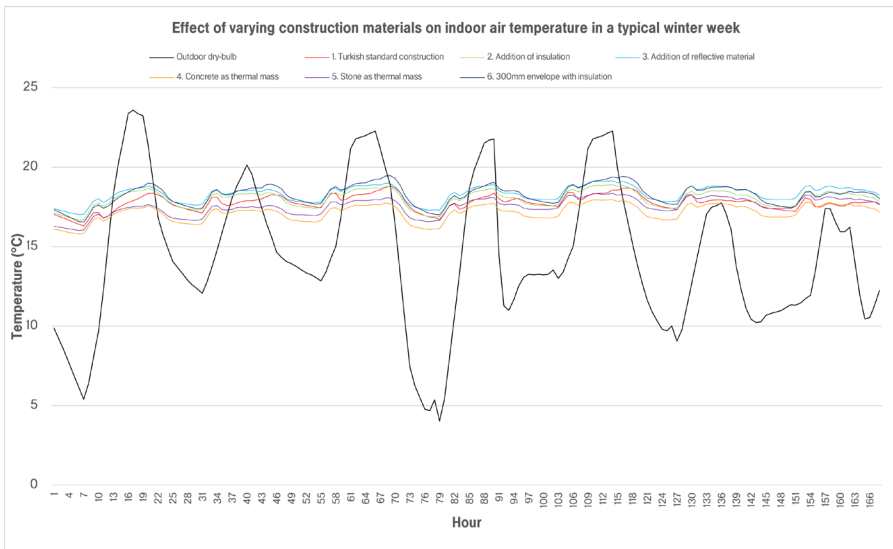


Figure 7.3: The indoor temperature of each construction type in a future typical winter week, compared to the dry-bulb temperature. For the purpose of comfort, consistent indoor temperatures of 20-25°C are desired. Indoor temperatures are kept consistent at 17-18°C by all construction types, varying by only a couple of degrees.

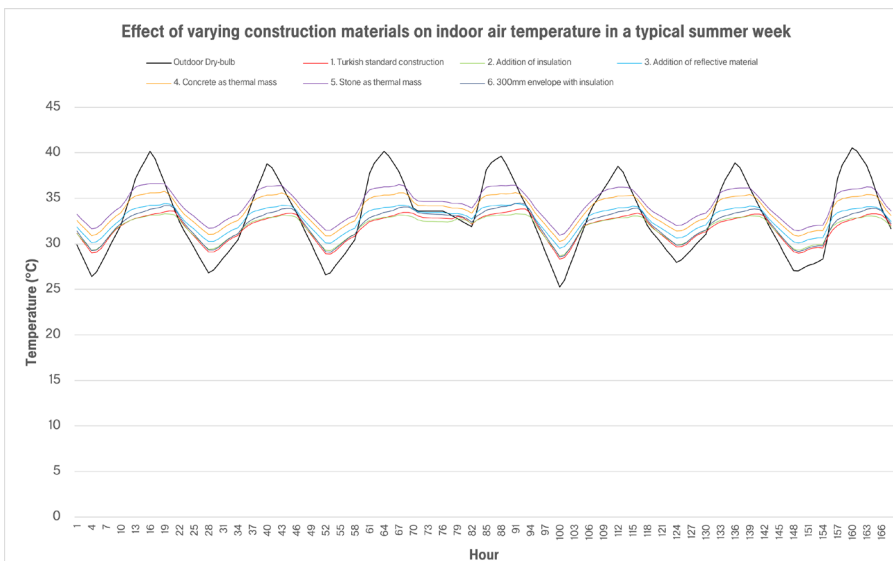


Figure 7.4: Indoor temperatures in a typical summer week in the future climate. The indoor temperature variations are more extreme in summer than winter (Figure 7.3), showing that as outdoor nighttime temperatures drop, so do the indoor temperatures. If thermal mass materials were being adequately flushed out during night-time ventilation, the graph would produce flat lines demonstrating more consistent indoor temperatures. However, all construction types result in large temperature variations, indicating that this is not happening.

Table 8: Comparison of how construction type affects the overheating risk

Simulation Description	CIBSE TM52				Robindon and Haldi (2008)		
	TM52: Criteria 1	TM52: Criteria 2	TM52: Criteria 3	Pass/Fail	Degree Hours (>25°C)	P _{OH} (25°C)	P _{OH} Exceeds 20% (Date)
1. Turkish Standard Construction							
Building	10.86	47.05	0	Fail	20,780.06	0.999948	5/26/2002 17:00
B3	9.21	36.46	0	Fail	19,843.00	0.999919	5/28/2002 19:00
K2	9.81	41.03	0	Fail	20,245.03	0.999933	5/27/2002 15:00
LR2	12.07	55.68	12	Fail	21,625.03	0.999965	5/25/2002 21:00
MB1	11.05	51.45	0	Fail	20,865.88	0.999950	5/26/2002 07:00
2. Addition of Insulation							
Building	2.91	1.97	0	Pass	17,712.63	0.999778	06/09/2002 13:00
B3	0	0	0	Pass	15,822.31	0.999455	6/14/2002 08:00
K2	0.41	0	0	Pass	16,468.66	0.999599	06/12/2002 16:00
LR2	2.61	2.31	0	Pass	17,728.02	0.999780	06/10/2002 01:00
MB1	7.02	14.97	0	Fail	19,164.22	0.999889	06/03/2002 19:00

3. Addition of Reflective Material							
Building	11.60	30.39	0	Fail	21,113.16	0.999956	5/29/2002 16:00
B3	7.80	11.18	0	Fail	19,282.05	0.999895	06/06/2002 13:00
K2	7.69	14.77	0	Fail	19,271.15	0.999894	06/05/2002 21:00
LR2	11.80	30.62	0	Fail	21,294.84	0.999960	5/31/2002 07:00
MB1	14.41	49.66	0	Fail	22,672.84	0.999979	5/25/2002 22:00
4. Concrete as thermal mass							
Building	17.07	66.89	1	Fail	24,644.45	0.999992	5/27/2002 04:00
B3	15.06	46.85	0	Fail	22,971.72	0.999982	5/31/2002 11:00
K2	14.17	45.33	0	Fail	22,249.06	0.999974	06/02/2002 18:00
LR2	17.41	69.61	49	Fail	24,963.33	0.999993	5/27/2002 14:00
MB1	18.84	86.96	186	Fail	26,182.01	0.999996	5/23/2002 20:00
5. Stone as thermal mass							
Building	22.48	117.34	464	Fail	29,068.76	0.999999	5/20/2002 09:00
B3	20.32	98.69	279	Fail	27,610.62	0.999998	5/22/2002 20:00
K2	18.94	90.63	155	Fail	25,987.47	0.999996	5/24/2002 19:00
LR2	22.63	120.19	497	Fail	29,361.34	0.999999	5/20/2002 17:00
MB1	23.72	138.66	608	Fail	30,679.73	1	5/15/2002 14:00
6. 300mm envelope with insulation							
Building	12.20	55.54	0	Fail	21,761.70	0.999968	5/24/2002 12:00
B3	10.88	44.56	0	Fail	20,845.55	0.999950	5/25/2002 18:00
K2	11.18	47.79	0	Fail	21,052.26	0.999955	5/25/2002 12:00
LR2	13.46	64.83	0	Fail	22,678.96	0.999979	5/23/2002 16:00
MB1	12.36	59.83	0	Fail	21,784.99	0.999968	5/23/2002 22:00

It was deduced in Section 6.3 that the building fabric has a larger impact on the overheating risk than the ventilation. Table 8 shows how each construction type affects the overheating risk and Figure 7.2 shows a graph of the indoor temperature variations throughout the year. The addition of insulation to the vernacular construction materials (adobe brick) results in the lowest overheating risk according to both criteria, and the smallest number of CDH. It is the only envelope that passes the majority of TM52 criteria and also exceeds 20% probability of overheating latest in the year. The reason for it performing the best is that insulation slows conductive and convective heat flow, meaning that less heat is transferred between the external and internal environments. Again, the rooms LR2 and MB1 are at the greatest risk of overheating.

The main characteristics of MB1 are the 5m dome above, 2 external walls and 4 windows. The other rooms have smaller domes, fewer external walls and fewer windows, which means that MB1 has the greatest exposure to radiation. MB1 is at the highest risk of overheating, unless a thinner wall is applied (construction types 1 and 6, see Table 8). This indicates that the lower thermal mass of a thinner wall might aid in keeping the indoor temperatures low for rooms that have a large surface area exposed to radiation. This could be due to the heat not being trapped in the walls, and rather being flushed out of the room quicker through natural ventilation as a result of the bigger stack effect of a 5m dome.

Concrete and stone are tested and perform the worst of all construction types. These high thermal mass materials provide the highest temperatures during summer suggesting that stored heat is being inadequately discharged through night ventilation (Figures 7.3-4). It is possible that this inadequacy is due to small opening sizes which leads to little air flow, trapped heat and subsequently less air pressure to drive stack ventilation.

This is an example of the limitations of a sensitivity analysis, as two parameters could reduce the overheating risk together, yet not separately. For example, a larger WWR with a higher thermal mass materials like stone, could lead to higher heat storage with more efficient night-time ventilation resulting in a lower risk of overheating. However, adjusting these parameters individually may subsequently increase the overheating risk. Therefore a global sensitivity analysis would be more efficient here to understand combined principle behaviour.

7.2 Analysis of results after change in dome height

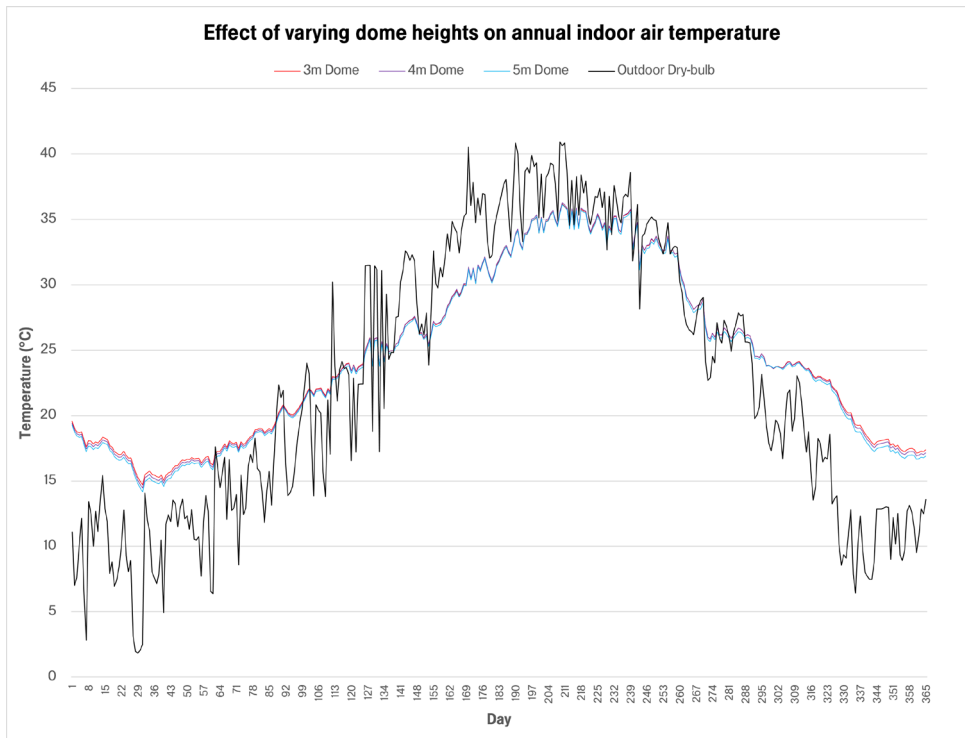


Figure 7.5: The indoor air temperature variations across a year in a 2080 climate for different dome heights. It is clear that the differences of each dome height on the indoor air temperature is not large, and that this has little effect on the overheating risk (Table 9). The 5m dome height provides the coolest temperatures which mirrors the overheating results in Table 9.

Table 9: Comparison of the overheating risk for different dome heights

Simulation Description	CIBSE TM52				Robindon and Haldi (2008)		
	TM52: Criteria 1	TM52: Criteria 2	TM52: Criteria 3	Pass/Fail	Degree Hours (>25°C)	P _{OH} (25°C)	P _{OH} Exceeds 20% (Date)
3m dome height							
Building	14.46	55.92	0	Fail	22,601.41	0.999978	5/26/2002 15:00
B3	12.99	46.15	0	Fail	21,680.87	0.999966	5/28/2002 09:00
K2	12.87	50.06	0	Fail	21,805.33	0.999968	5/27/2002 14:00
LR2	15.14	60.56	0	Fail	23,135.20	0.999983	5/26/2002 13:00
MB1	15.34	64.02	0	Fail	23,189.42	0.999984	5/25/2002 01:00
4m dome height							
Building	14.86	59.07	0	Fail	22,798.96	0.999980	5/26/2002 15:00
B3	13.57	49.53	0	Fail	21,945.91	0.999970	5/28/2002 06:00
K2	13.23	53.05	0	Fail	21,968.67	0.999971	5/27/2002 16:00
LR2	15.50	63.74	4	Fail	23,336.43	0.999985	5/26/2002 13:00
MB1	15.56	67.07	0	Fail	23,313.10	0.999984	5/25/2002 06:00

5m dome height							
Building	13.64	55.26	0	Fail	22,103.46	0.999972	5/27/2002 17:00
B3	12.19	45.45	0	Fail	21,219.03	0.999958	5/30/2002 11:00
K2	11.89	48.18	0	Fail	21,183.20	0.999957	5/29/2002 13:00
LR2	14.36	59.86	0	Fail	22,642.33	0.999979	5/27/2002 14:00
MB1	14.25	63.13	0	Fail	22,573.53	0.999978	5/26/2002 07:00

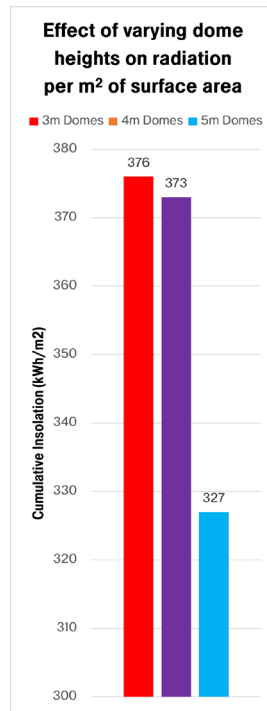
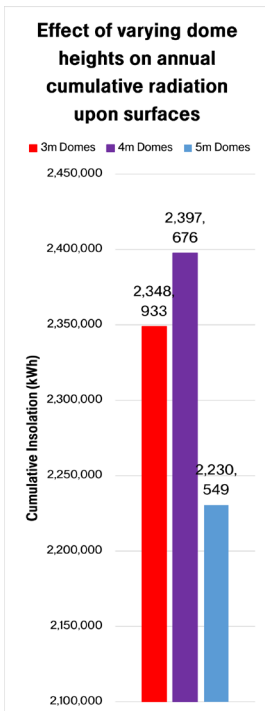


Figure 7.6 [left] The cumulative insolation of the varying dome heights on exterior surfaces. This simulation includes the courtyard in order to measure the extent to which it is shaded from radiation. It is evident that the 4m dome height results in the most radiation accumulating on the surfaces

Figure 7.7: [right] The radiation per square metre on the building for different dome heights. When comparing this to Figure 7.6, it is clear that 3m dome heights result in more radiation per square metre due to the smaller surface area. A dome height of 5m results in the lowest cumulative insolation and also radiation per m² due to taller domes providing more shade.

Table 9 details the overheating risk when adjusting dome height between 3m, 4m and 5m. Individual rooms show similar patterns as with the base model, where B3 and K2 have the lowest overheating risk. The overheating risk is marginally lowest with a dome height of 5m and annual temperatures are reduced (Figure 7.5). In principle, it may be that this is due to a larger dome creating a bigger stack effect which helps to drive airflow rates. However, DesignBuilder limits an understanding that this is actually the case, as it only allows for a scheduling of natural ventilation and not a calculation of airflow rate. It can be presumed that the lower overheating risk of 5m domes is also a result of less cumulative radiation on the surface area of the building (Figures 7.6-7). The higher the dome, the more shadowing that occurs on neighbouring domes, and the larger surface area they provide, the more heat transfer occurs from inside to outside when night-time temperatures drop.

7.3 Analysis of results after change to building orientation

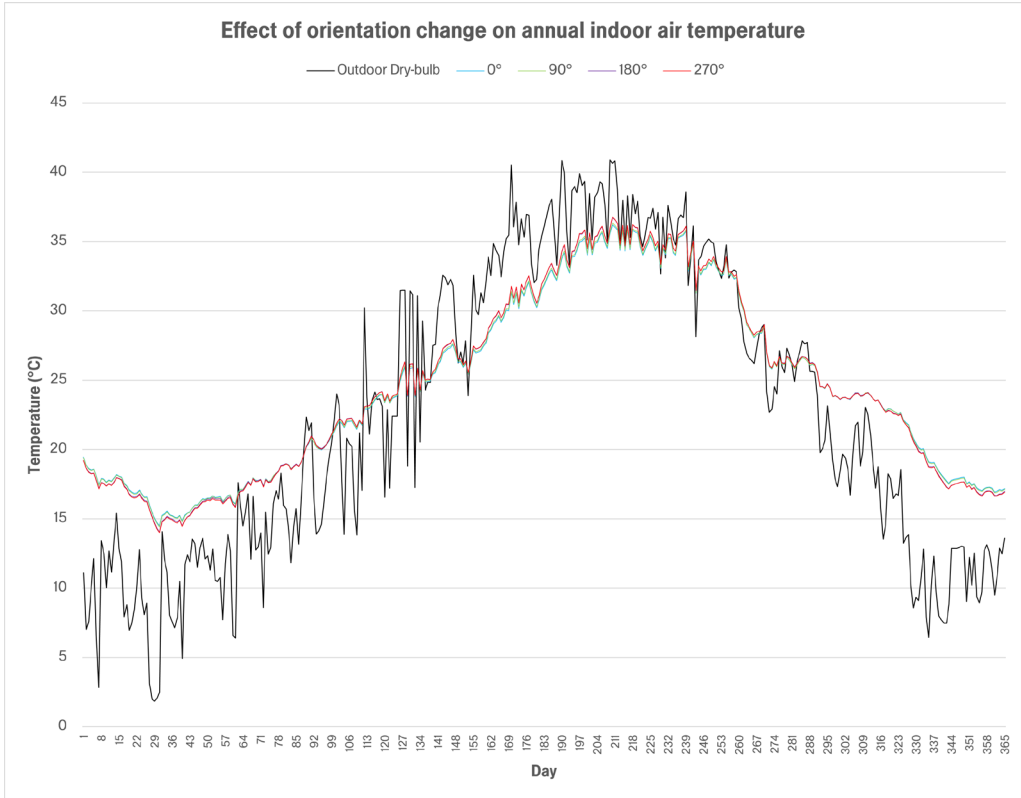


Figure 7.8: The chart displays the effect of orientation on indoor temperatures across the year. Orientation has minimal effect on the indoor temperature throughout the year meaning the lines are almost completely superimposed. This is further supported by the results in Table 10 indicating that orientation has minimal impact on overheating risk.

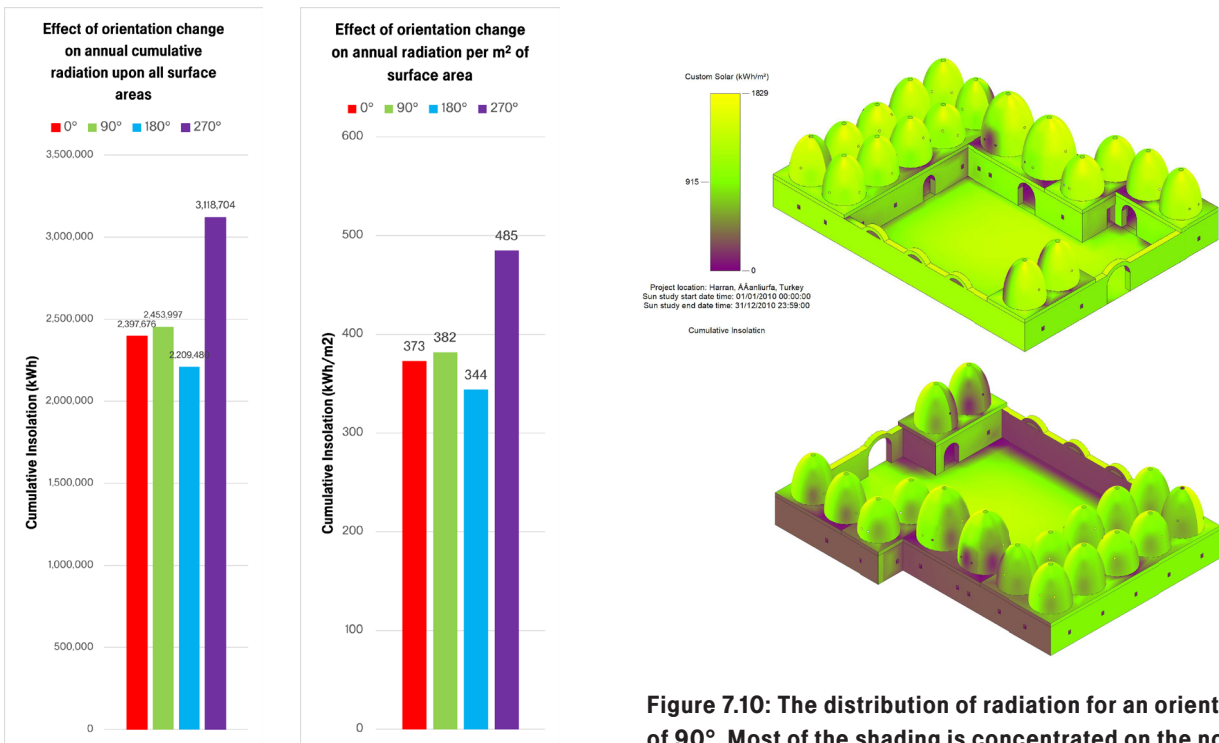


Figure 7.9: Simulation results of cumulative insolation and radiation per m² of each orientation. A 270° orientation represents the highest amount of solar radiation.

Figure 7.10: The distribution of radiation for an orientation of 90°. Most of the shading is concentrated on the north facing walls resulting in lower overheating risk in MB1 (Table 10). South facing walls and the courtyard are completely exposed to 1829kWh/m² of radiation. It would be ideal that the domes and courtyard are more shaded as these are the spaces that residents will occupy most due to the central, inward-facing layout of the building.

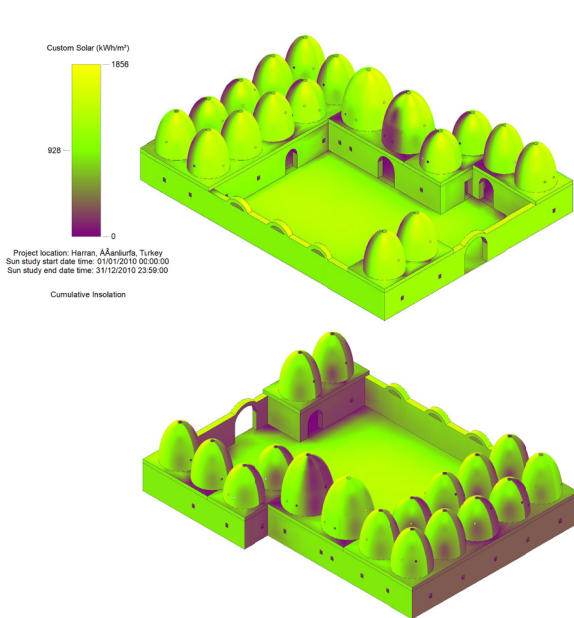


Figure 7.11: The distribution of radiation for an orientation of 180°. Most shading is hitting the north walls and domes, with very little shading in the courtyard. Radiation reaches 1856kWh/m² with this orientation which mirrors the failing of TM52 overheating criteria and higher probability of overheating in Table 10.

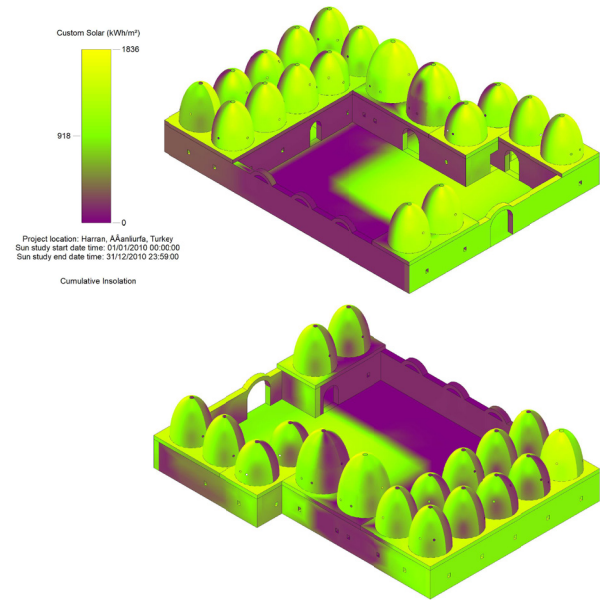


Figure 7.12: The distribution of radiation for an orientation of 270°. This orientation has most shading of the courtyard of all orientation results. This is provided by the courtyard walls and the double row of domes. Shading is also provided to the inward facing walls of the courtyard which is ideal for cooling and less solar gain indoors, and outdoor activities. However, overheating risk results do not significantly decrease (Table 10), as Figure 7.9 shows a 270° orientation receives the most annual radiation.

Table 10: Comparison of the overheating risk after changes to orientation

Simulation Description	CIBSE TM52				Robinson and Haldi (2008)		
	TM52: Criteria 1	TM52: Criteria 2	TM52: Criteria 3	Pass/Fail	Degree Hours (>25°C)	P _{OH} (25°C)	P _{OH} Exceeds 20% (Date)
0° orientation							
Building	14.46	57.39	0	Fail	22,602.56	0.999978	5/26/2002 18:00
B3	13.03	46.31	0	Fail	21,701.97	0.999967	5/28/2002 10:00
K2	12.68	49.59	0	Fail	21,704.72	0.999967	5/27/2002 22:00
LR2	15.55	63.57	2	Fail	23,356.20	0.999985	5/26/2002 11:00
MB1	14.60	64.19	0	Fail	22,771.06	0.999980	5/25/2002 17:00
90° orientation							
Building	14.85	60.47	0	Fail	22,909.60	0.999981	5/26/2002 07:00
B3	13.85	54.56	0	Fail	22,213.57	0.999974	5/27/2002 08:00
K2	13.96	56.28	0	Fail	22,437.82	0.999976	5/26/2002 14:00
LR2	16.66	70.98	18	Fail	24,426.65	0.999991	5/24/2002 13:00
MB1	11.97	45.99	0	Fail	21,110.40	0.999956	5/29/2002 18:00
180° orientation							
Building	16.15	69.85	3	Fail	23,742.31	0.999987	5/25/2002 08:00
B3	12.92	51.65	0	Fail	21,671.12	0.999966	5/29/2002 09:00
K2	15.16	63.41	7	Fail	23,204.28	0.999984	5/25/2002 19:00
LR2	17.34	81.54	55	Fail	25,224.97	0.999994	5/23/2002 13:00
MB1	16.45	76.95	23	Fail	24,006.92	0.999989	5/24/2002 07:00

270° orientation							
Building	16.18	70.67	11	Fail	23,799.09	0.999988	5/25/2002 07:00
B3	15.24	64.24	0	Fail	23,087.84	0.999983	5/26/2002 07:00
K2	11.60	30.39	0	Fail	21,113.16	0.999956	5/29/2002 16:00
LR2	16.96	80.26	41	Fail	24,680.52	0.999992	5/24/2002 17:00
MB1	13.84	57.88	0	Fail	22,222.13	0.999974	5/27/2002 11:00

The orientation of the building is varied to understand the effect it has on overheating in individual rooms (Figure 7.8). The results are displayed in Table 10. Orientation affects the solar gain experienced by each room, and therefore the overheating risk. For example, the pattern seen in previous subsections of rooms B3 and K2 having the lowest overheating risk, changes with an orientation of 180° and 270°, where they become more at risk. This is due to them gaining radiation exposure from the south and east respectively without neighbouring domes for shading. LR2 is still at highest risk of overheating in all orientation scenarios. This is due to its location meaning that, apart from at a 0° orientation (base model), the room always has external walls exposed to either south or west, and little neighbouring domes for shadowing. This accumulates more surface radiation and results in higher indoor temperatures.

Cumulative insolation is most reduced when the orientation is at 180° (Figure 7.9). This may show a quantitative reduction, however, a 180° orientation change results in very little shading in the courtyard. It would be ideal for the courtyard to be heavily shaded to create a more comfortable outdoor space for the occupants. Therefore a 270° orientation change would be the most effective here (Figures 7.10-12). It is interesting that a 180° orientation change actually increases the overheating risk due to a larger exposure of external walls to the south. Either a 0° change for lower indoor temperatures, or a 270° change for courtyard shading, is concluded to be most ideal.

7.4 Analysis of results after change to window height

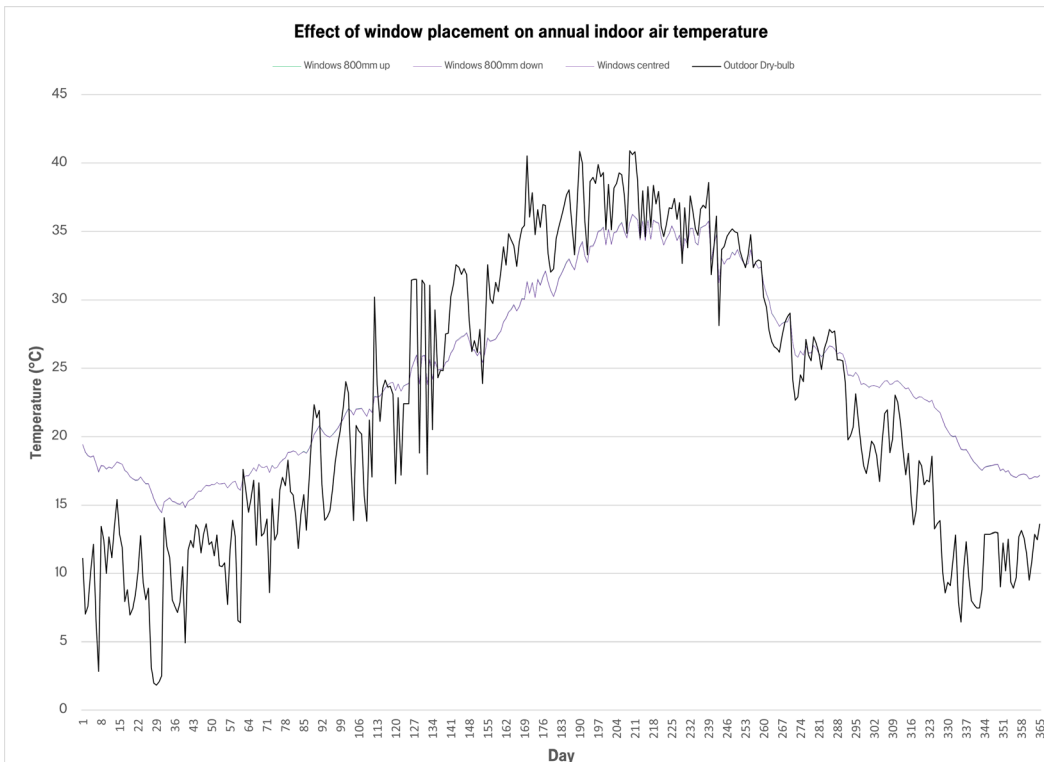


Figure 7.13: The indoor temperature for different window heights across the year. There is almost no variation between the different heights.

Table 11: Comparison of overheating risk after a change to window height

Simulation Description	CIBSE TM52				Robinson and Haldi (2008)		
	TM52: Criteria 1	TM52: Criteria 2	TM52: Criteria 3	Pass/Fail	Degree Hours (>25°C)	P _{OH} (25°C)	P _{OH} Exceeds 20% (Date)
Windows 800mm up							
Building	14.46	57.39	0	Fail	22,602.56	0.999980	5/26/2002 18:00
B3	13.03	46.31	0	Fail	21,701.97	0.999967	5/28/2002 10:00
K2	12.68	49.59	0	Fail	21,704.72	0.999967	5/27/2002 22:00
LR2	15.55	63.57	2	Fail	23,356.20	0.999985	5/26/2002 11:00
MB1	14.60	64.19	0	Fail	22,771.06	0.999981	5/25/2002 17:00
Windows centred							
Building	14.85	60.47	0	Fail	22,909.60	0.999978	5/26/2002 07:00
B3	13.85	54.56	0	Fail	22,213.57	0.999967	5/27/2002 08:00
K2	13.96	56.28	0	Fail	22,437.82	0.999967	5/26/2002 14:00
LR2	16.66	70.98	18	Fail	24,426.65	0.999985	5/24/2002 13:00
MB1	11.97	45.99	0	Fail	21,110.40	0.999980	5/29/2002 18:00
Windows 800mm down							
Building	16.15	69.85	3	Fail	23,742.31	0.999980	5/25/2002 08:00
B3	12.92	51.65	0	Fail	21,671.12	0.999967	5/29/2002 09:00
K2	15.16	63.41	7	Fail	23,204.28	0.999967	5/25/2002 19:00
LR2	17.34	81.54	55	Fail	25,224.97	0.999985	5/23/2002 13:00
MB1	16.45	76.95	23	Fail	24,006.92	0.999982	5/24/2002 07:00

Manioğlu & Yılmaz (2008) state that the construction of windows at a high level helps to block reflected radiation from the ground outside. Therefore, a change in window placement is simulated in order to understand if this bioclimatic strategy has an effect on the indoor temperature. Results in Table 11 and Figure 7.13 indicate that the overheating risk does not change and that the strategy has no effect on the cooling of rooms. This implies that this is due to the small WWR, meaning that there is only a small quantity of radiation entering the building through openings and that changes to WWR would have a larger impact on the ventilation. Due to the negligible results, this parameter will not be considered in the optimal model.

7.5 Analysis of results after change to WWR (window to wall ratio)

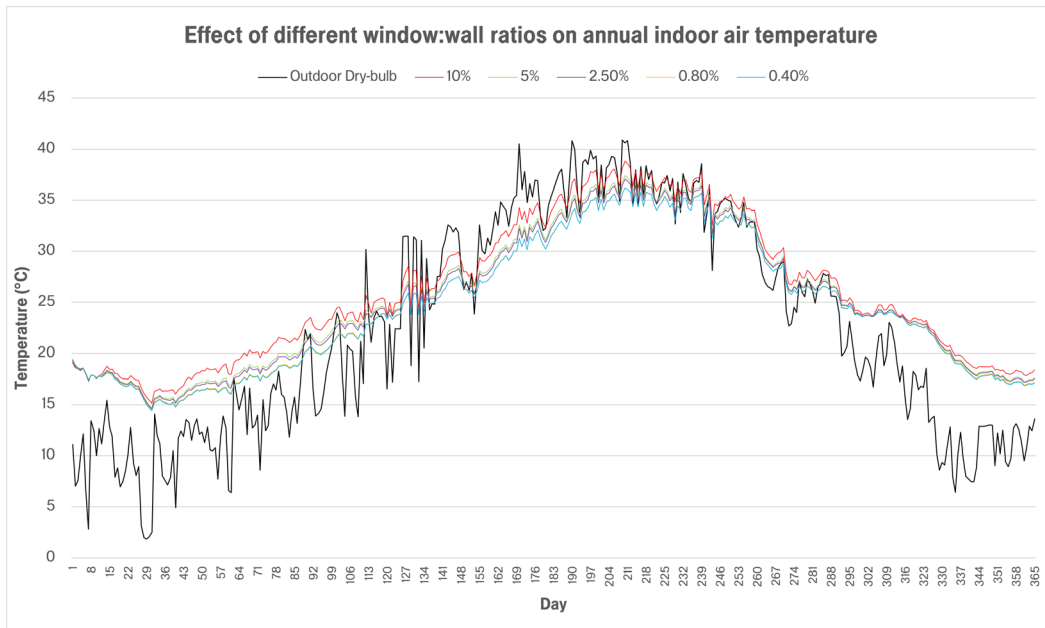


Figure 7.14: Annual indoor air temperature after a change to the WWR. As the WWR is increased, the temperatures across the year also increase. The best performing WWR is 0.4% and the worst performing is 10%, with a significant difference.

Table 12: Comparison of the overheating risk with changes to WWR

Simulation Description	CIBSE TM52				Robindon and Haldi (2008)		
	TM52: Criteria 1	TM52: Criteria 2	TM52: Criteria 3	Pass/Fail	Degree Hours (>25°C)	P _{OH} (25°C)	P _{OH} Exceeds 20% (Date)
0.4% WWR							
Building	14.29	57.05	0	Fail	22,537.63	0.999978	5/26/2002 19:00
B3	12.32	43.21	0	Fail	21,294.36	0.999960	5/29/2002 16:00
K2	12.59	49.04	0	Fail	21,634.12	0.999966	5/28/2002 08:00
LR2	15.29	61.75	0	Fail	23,154.70	0.999983	5/26/2002 17:00
MB1	14.50	64.22	0	Fail	22,737.06	0.999980	5/25/2002 19:00
0.8% WWR							
Building	14.46	57.39	0	Fail	22,602.56	0.999978	5/26/2002 18:00
B3	13.03	46.31	0	Fail	21,701.97	0.999967	5/28/2002 10:00
K2	12.68	49.59	0	Fail	21,704.72	0.999967	5/27/2002 22:00
LR2	15.55	63.57	2	Fail	23,356.2	0.999985	5/26/2002 11:00
MB1	14.60	64.19	0	Fail	22,771.06	0.999980	5/25/2002 17:00
2.5% WWR							
Building	17.16	78.54	27	Fail	24,995.48	0.999993	5/22/2002 17:00
B3	15.94	64.76	0	Fail	23,933.84	0.999988	5/24/2002 08:00
K2	14.68	63.16	7	Fail	23,099.81	0.999983	5/25/2002 12:00
LR2	18.16	86.48	115	Fail	25,880.30	0.999995	5/21/2002 22:00
MB1	19.93	101.07	286	Fail	26,904.25	0.999997	5/17/2002 10:00
5% WWR							
Building	18.12	86.74	93	Fail	25,941.04	0.999996	5/20/2002 19:00
B3	16.83	72.67	14	Fail	24,934.68	0.999993	5/22/2002 11:00
K2	15.64	68.84	14	Fail	23,703.95	0.999987	5/24/2002 13:00
LR2	19.65	95.97	240	Fail	26,968.97	0.999997	5/19/2002 14:00
MB1	21.27	115.83	463	Fail	28,489.19	0.999999	5/13/2002 08:00

10% WWR							
Building	22.49	124.12	547	Fail	30,493.59	0.999999	05/10/2002 10:00
B3	21.52	108.21	451	Fail	29,663.46	0.999999	05/09/2002 12:00
K2	19.10	94.30	189	Fail	26,496.85	0.999997	5/19/2002 16:00
LR2	23.80	138.34	673	Fail	31,959.32	1	05/08/2002 22:00
MB1	26.45	174.88	1,012	Fail	35,578.40	1	05/03/2002 13:00

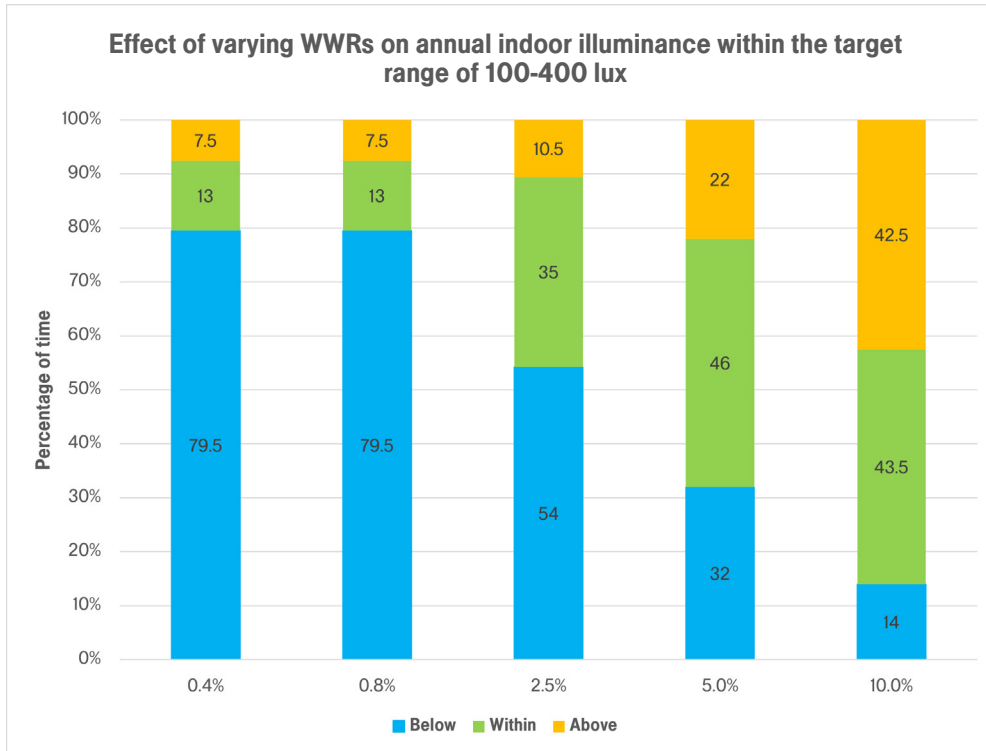


Figure 7.15: Indoor illuminance performance of different WWRs between a target range of 100-400 lux. A 5-10% WWR results in best indoor illuminance quality and below 0.8% results in extremely low illuminance.

The base model has a WWR of 0.8% due its few windows and their small size (0.3x0.4m). It is observed in Table 12 and Figure 7.14 that any increase to the WWR increases the overheating risk due to the larger exposure to solar radiation and entrance for hot outside air. This suggests that the use of external shading may be useful to allow for solar gain during winter and block it during summer due to the varying angle of incidence between seasons. However, a global sensitivity analysis would provide more accuracy to understand how WWR and shading would work together to reduce overheating risk whilst also improving indoor illuminance.

Figure 7.15 shows how varying the WWR affects the annual indoor illuminance, assessed by the fraction of time spent within a target range of 100-400 lux. It is clear that below a ratio of 0.8%, the illuminance is not affected and the overheating risk is neither substantially reduced (Table 12). Using a ratio of 2.5% results in very minimal rise in temperatures during the summer, but large benefits of indoor illuminance to create visual comfort indoors. This is a strategy that could be looked at in conjunction with shading to reduce unwanted solar gains.

7.6 Analysis of results after change to ventilation parameter

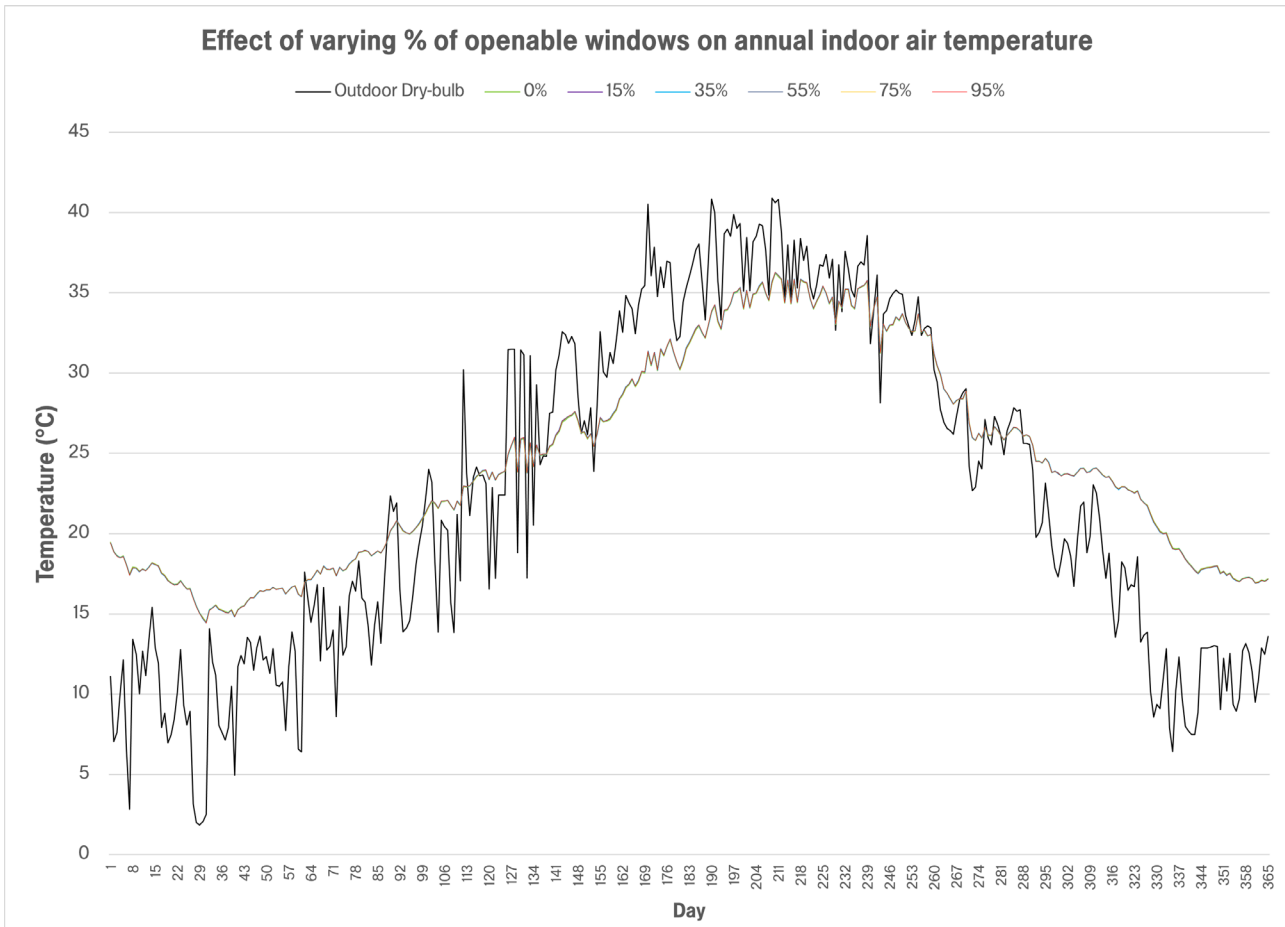


Figure 7.16: The annual indoor air temperature variations with changes to the percentage of openable windows. The impact of the change to this parameter is negligible and has almost no effect on the indoor air temperature.

Table 13: Comparison of overheating risk with a change to percentage of openable windows

Simulation Description	CIBSE TM52				Robinson and Haldi (2008)		
	TM52: Criteria 1	TM52: Criteria 2	TM52: Criteria 3	Pass/Fail	Degree Hours (>25°C)	P _{OH} (25°C)	P _{OH} Exceeds 20% (Date)
5% openable windows							
Building	14.46	57.39	0	Fail	22,602.56	0.999978	5/26/2002 18:00
B3	13.03	46.31	0	Fail	21,701.97	0.999967	5/28/2002 10:00
K2	12.68	49.59	0	Fail	21,704.72	0.999967	5/27/2002 22:00
LR2	15.55	63.57	2	Fail	23,356.2	0.999985	5/26/2002 11:00
MB1	14.60	64.19	0	Fail	22,771.06	0.999980	5/25/2002 17:00
15% openable windows							
Building	14.65	58.82	0	Fail	22,752.91	0.999980	5/26/2002 12:00
B3	13.03	46.35	0	Fail	21,704.93	0.999967	5/28/2002 09:00
K2	12.68	49.77	0	Fail	21,714.52	0.999967	5/27/2002 23:00
LR2	15.55	63.59	2	Fail	23,353.64	0.999985	5/26/2002 12:00
MB1	14.84	66.06	0	Fail	22,948.61	0.999982	5/25/2002 12:00

35% openable windows							
Building	14.65	58.82	0	Fail	22,747.44	0.999980	5/26/2002 13:00
B3	13.03	46.35	0	Fail	21,701.47	0.999967	5/28/2002 11:00
K2	12.68	49.76	0	Fail	21,711.49	0.999967	5/28/2002 06:00
LR2	15.55	63.58	2	Fail	23,350.79	0.999985	5/26/2002 12:00
MB1	14.84	66.06	0	Fail	22,940.18	0.999981	5/25/2002 14:00
55% openable windows							
Building	14.65	58.82	0	Fail	22,751.60	0.999980	5/26/2002 12:00
B3	13.03	46.35	0	Fail	21,705.37	0.999967	5/28/2002 09:00
K2	12.68	49.77	0	Fail	21,715.34	0.999967	5/27/2002 22:00
LR2	15.55	63.59	2	Fail	23,354.64	0.999985	5/26/2002 11:00
MB1	14.84	66.06	0	Fail	22,944.59	0.999982	5/25/2002 12:00
75% openable windows							
Building	14.65	58.82	0	Fail	22,751.60	0.999980	5/26/2002 12:00
B3	13.03	46.35	0	Fail	21,705.37	0.999967	5/28/2002 09:00
K2	12.68	49.77	0	Fail	21,715.34	0.999967	5/27/2002 22:00
LR2	15.55	63.59	2	Fail	23,354.64	0.999985	5/26/2002 11:00
MB1	14.84	66.06	0	Fail	22,944.59	0.999982	5/25/2002 12:00
95% openable windows							
Building	14.65	58.82	0	Fail	22,751.60	0.999980	5/26/2002 12:00
B3	13.03	46.35	0	Fail	21,705.37	0.999967	5/28/2002 09:00
K2	12.68	49.77	0	Fail	21,715.34	0.999967	5/27/2002 22:00
LR2	15.55	63.59	2	Fail	23,354.64	0.999985	5/26/2002 11:00
MB1	14.84	66.06	0	Fail	22,944.59	0.999982	5/25/2002 12:00

The base model's openable area of windows is set at 5%. This is increased from 15% in increments of 20%, to explore whether this would increase air flow and result in a reduction of overheating risk. The overheating risk does not change beyond 55%, probably as a result of a small WWR, indicating that the maximum inflow of air is reached at this percentage. The probability of overheating increases by 0.000002 when increasing the openable window percentage from 5% to 55% (Table 13): clearly this parameter has very little effect on the overheating risk. No percentage of openable windows results in drastic overheating risk increase (Figure 7.16), and none meet the criteria of TM52.

8. Introduction of new strategies

This section explores the effects of introducing new bioclimatic and contemporary passive strategies that may reduce the overheating risk of the Harran houses when moving into a future climate. Again, simulations were undertaken using 2080 hourly weather data.

8.1 Analysis of results after introduction of glazing systems

The work of Singh, Garg, & Jha (2008) suggests that different glazing systems in a hot-dry climate can result in varying thermal comfort results. In the present study, three different glazing types are tested on the base model for their performance in Table 14.

Table 14: Details of the different glazing systems tested

Glazing Type	U-Value (W/m ² •K)	G-Value
Single glazing, clear, 6mm	5.778	0.819
Double glazing, clear, electrochromic, reflective	2.429	0.636
Double glazing, clear, reflective	2.761	0.154
Triple glazing, clear, Low-e, argon filled	0.780	0.474

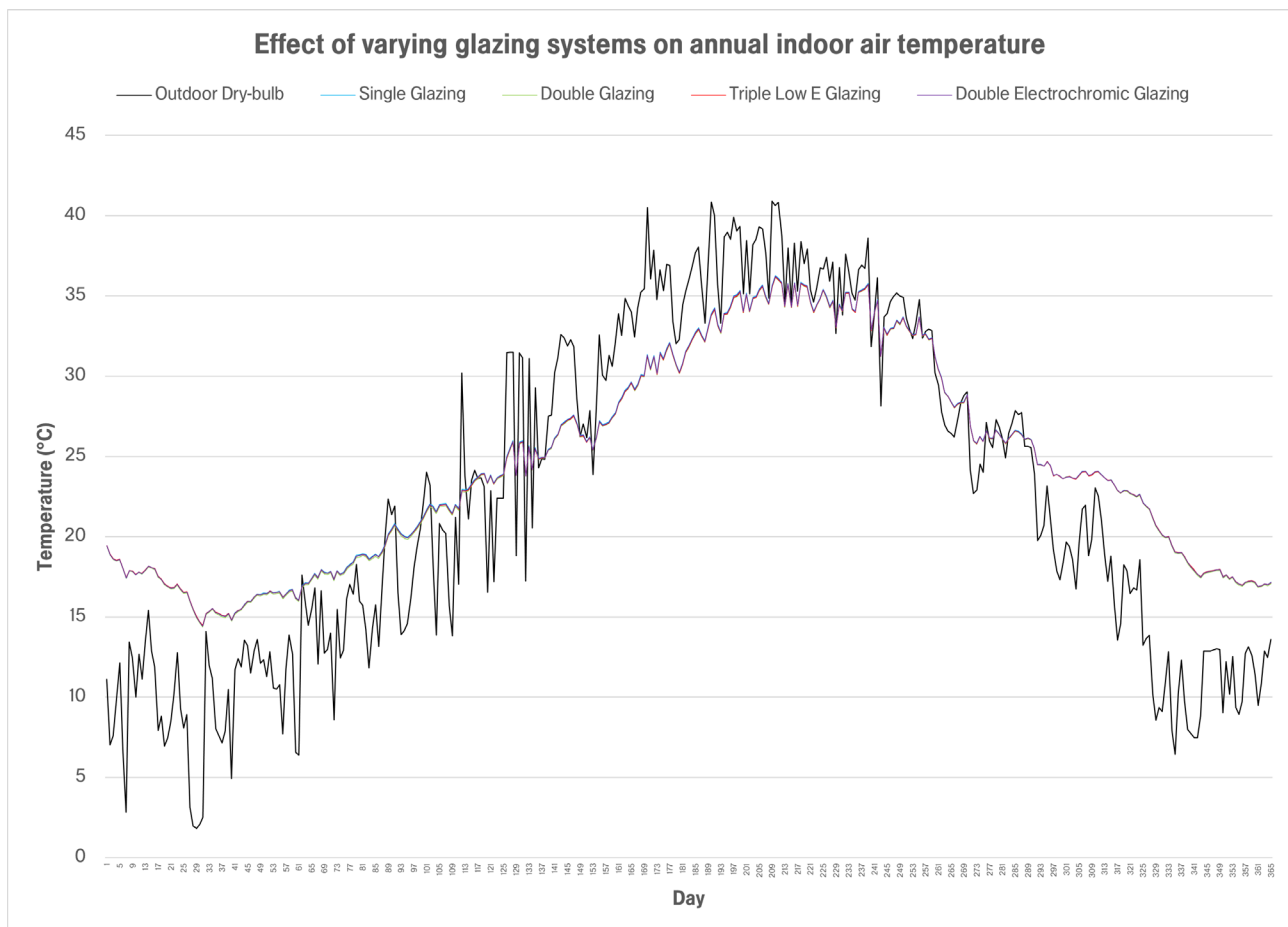


Figure 8.1: Indoor air temperature variations of different glazing systems throughout the year, and the outdoor temperature. Changing the glazing system has no discernible effect on the indoor temperature.

Table 15: Comparison of the overheating risk of different glazing systems

Simulation Description	CIBSE TM52				Robinson and Haldi (2008)		
	TM52: Criteria 1	TM52: Criteria 2	TM52: Criteria 3	Pass/Fail	Degree Hours (>25°C)	P _{OH} (25°C)	P _{OH} Exceeds 20% (Date)
Single glazing							
Building	14.62	58.73	0	Fail	22,738.95	0.999980	5/26/2002 13:00
B3	12.99	46.16	0	Fail	21,683.29	0.999966	5/28/2002 11:00
K2	12.68	49.60	0	Fail	21,703.79	0.999967	5/28/2002 06:00
LR2	15.55	63.41	1	Fail	23,332.21	0.999985	5/26/2002 13:00
MB1	14.83	65.83	0	Fail	22,924.79	0.999981	5/25/2002 13:00
Double glazing, electrochromic							
Building	14.42	57.55	0	Fail	22,602.40	0.999978	5/26/2002 17:00
B3	12.68	44.61	0	Fail	21,497.65	0.999963	5/29/2002 07:00
K2	12.52	48.79	0	Fail	21,612.33	0.999965	5/28/2002 08:00
LR2	15.32	61.83	0	Fail	23,173.42	0.999983	5/26/2002 17:00
MB1	14.75	65.56	0	Fail	22,890.41	0.999981	5/25/2002 14:00
Double glazing, reflective							
Building	14.08	55.62	0	Fail	22,388.22	0.999976	5/27/2002 07:00
B3	12.31	43.11	0	Fail	21,308.93	0.999960	5/29/2002 14:00
K2	12.26	47.46	0	Fail	21,476.22	0.999963	5/28/2002 13:00
LR2	14.83	59.56	0	Fail	22,909.96	0.999981	5/27/2002 08:00
MB1	13.85	60.12	0	Fail	22,312.25	0.999975	5/26/2002 15:00
Triple low-e glazing							
Building	14.20	56.31	0	Fail	22,491.51	0.999977	5/26/2002 20:00
B3	12.44	43.50	0	Fail	21,384.50	0.999961	5/29/2002 10:00
K2	12.36	47.75	0	Fail	21,523.09	0.999964	5/28/2002 10:00
LR2	15.07	60.54	0	Fail	23,044.93	0.999982	5/26/2002 20:00
MB1	14.13	61.40	0	Fail	22,476.76	0.999977	5/26/2002 09:00

All glazing systems fail TM52 criteria (Table 15). Using double reflective glazing results in a slightly reduced overheating risk than the other glazing types, when using Robinson & Haldi’s model. This is most likely due to a low G-value letting in a lower percentage of solar heat due to its reflective coating. However, these differences are minute, only exceeding a 20% overheating risk a day or two later than other glazing systems because of the small WWR.

Therefore, the glazing systems were then tested on a model with a higher WWR of 2.5%, in order to gain a better understanding of the glazing systems’ relationship with overheating risk. The results in Table 16 show that, again, the use of reflective double glazing performs best to minimize overheating risk because more rooms pass criterion 3 of TM52, and has a lower probability of overheating. Triple low-e glazing performs nearly as well. This is a marginal difference showing more clearly which glazing system performs best. This is further supported by Figure 8.2, where the difference in indoor temperature when using different glazing types is more apparent than in Figure 8.1, with a lower WWR.

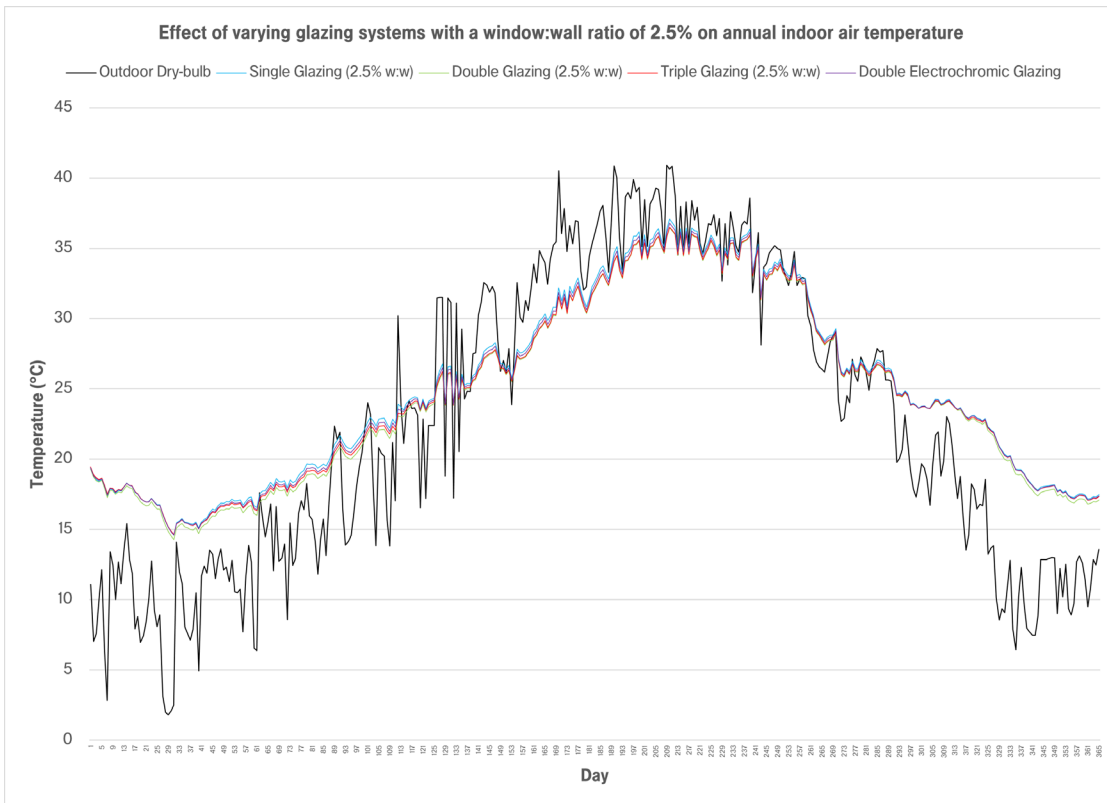


Figure 8.2: Indoor air temperature across the year for different glazing systems tested on a base model with an increased WWR (2.5%). There is a clearer trend as double glazing slightly reduces temperatures across the year and single glazing increases them.

Table 16: Comparison of the overheating risk of different glazing systems on a base model with an increased WWR to 2.5%

Simulation Description	CIBSE TM52				Robinson and Haldi (2008)		
	TM52: Criteria 1	TM52: Criteria 2	TM52: Criteria 3	Pass/Fail	Degree Hours (>25°C)	P _{OH} (25°C)	P _{OH} Exceeds 20% (Date)
2.5% WWR: Single glazing							
Building	17.04	77.85	26	Fail	24,917.86	0.999993	5/22/2002 20:00
B3	15.82	64.08	0	Fail	23,844.76	0.999988	5/24/2002 10:00
K2	14.62	62.60	7	Fail	23,040.64	0.999982	5/25/2002 13:00
LR2	15.79	66.77	12	Fail	23,634.83	0.999987	5/25/2002 18:00
MB1	15.46	71.17	14	Fail	23,531.47	0.999986	5/24/2002 09:00
2.5% WWR: Double glazing, electrochromic							
Building	15.11	62.46	9	Fail	24,113.99	0.999983	5/24/2002 06:00
B3	13.42	48.79	0	Fail	23,001.83	0.999970	5/25/2002 16:00
K2	12.98	51.73	0	Fail	22,551.19	0.999969	5/26/2002 11:00
LR2	15.79	66.77	12	Fail	23,634.83	0.999987	5/25/2002 18:00
MB1	15.46	71.17	99	Fail	25,360.53	0.999986	5/21/2002 08:00
2.5% WWR: Double glazing, reflective							
Building	15.11	62.46	0	Fail	23,123.26	0.999989	5/25/2002 18:00
B3	13.42	48.79	0	Fail	21,939.73	0.999982	5/27/2002 20:00
K2	12.98	51.73	0	Fail	21,876.74	0.999978	5/27/2002 17:00
LR2	15.79	66.77	12	Fail	23,634.83	0.999987	5/25/2002 18:00
MB1	15.46	71.17	14	Fail	23,531.47	0.999994	5/24/2002 09:00

2.5% WWR: Triple low-e glazing							
Building	15.51	63.80	0	Fail	23,373.17	0.999985	5/25/2002 09:00
B3	14.12	50.57	0	Fail	22,318.80	0.999975	5/26/2002 23:00
K2	13.41	53.32	0	Fail	22,108.07	0.999973	5/27/2002 08:00
LR2	16.54	71.13	16	Fail	24,240.48	0.999990	5/24/2002 17:00
MB1	15.58	70.11	10	Fail	23,481.95	0.999986	5/24/2002 11:00

8.2 Analysis of results after introduction of shading devices

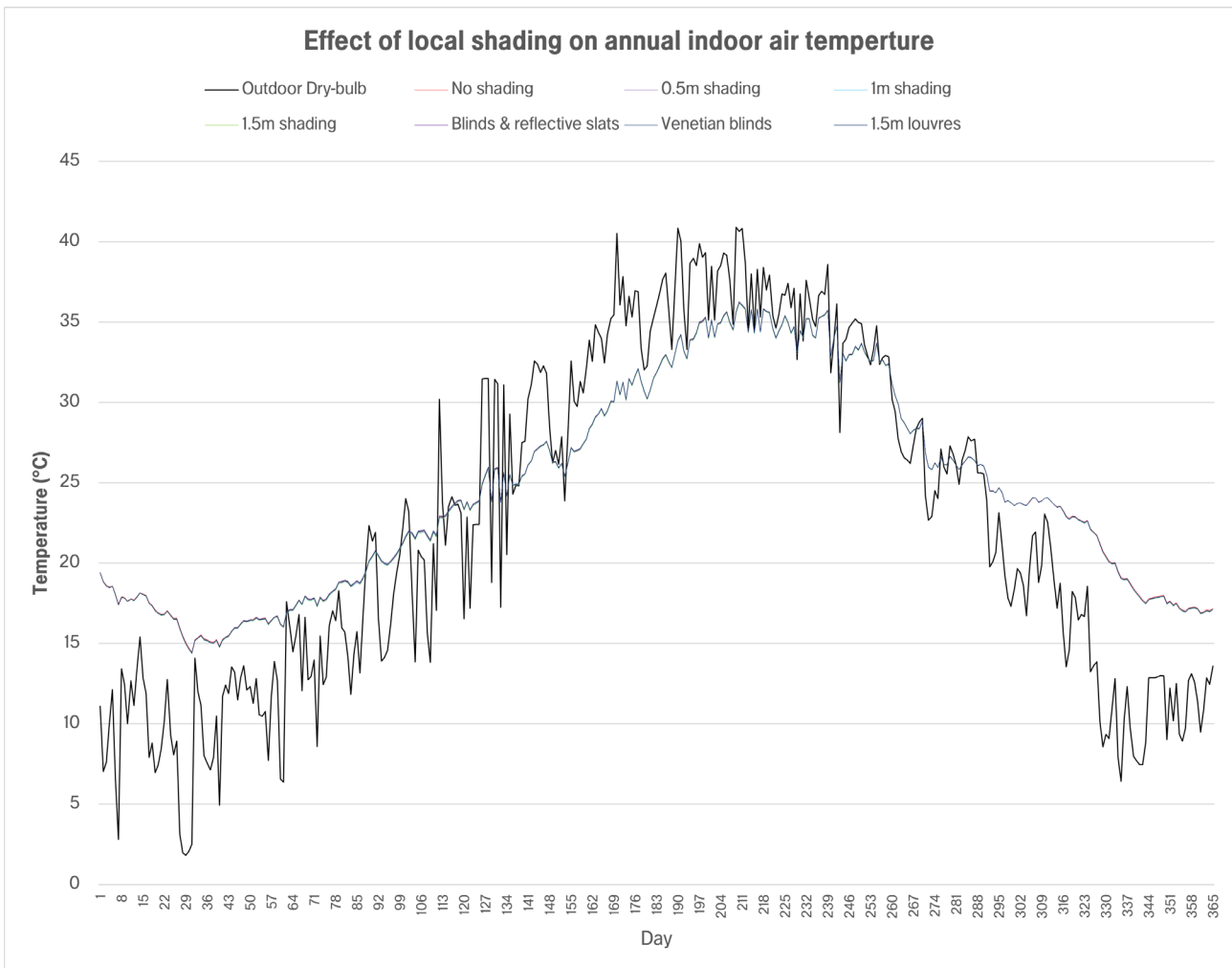


Figure 8.3: The indoor air temperature variations with addition of different shading devices. No shading device performs better than the other in this chart for lower temperatures in the summer and higher in the winter.

The base model inputs include single 3mm glazing, resulting in potentially inaccurate results due to an overestimation of solar gain (see Section 6.2.4). Introducing shading on windows can block summer sun from entering the internal environment whilst allowing in low winter sun. This is a common bioclimatic strategy in hot climates (Hyde, 2000). Shading devices on windows are introduced to the model. Six different types are simulated:

- 0.5m local shading
- 1m local shading
- 1.5m local shading
- Blinds with highly reflective slats
- Venetian Blinds
- 1.5m louvres

Table 17: Comparison of the overheating risk for the introduction of different shading devices

Simulation Description	CIBSE TM52				Robindon and Haldi (2008)		
	TM52: Criteria 1	TM52: Criteria 2	TM52: Criteria 3	Pass/Fail	Degree Hours (>25°C)	P _{OH} (25°C)	P _{OH} Exceeds 20% (Date)
0.5m shades							
Building	14.19	56.61	0	Fail	22,499.61	0.999977	5/26/2002 20:00
B3	12.50	44.16	0	Fail	21,422.08	0.999962	5/29/2002 09:00
K2	12.45	48.28	0	Fail	21,562.95	0.999964	5/28/2002 11:00
LR2	15.22	61.26	0	Fail	23,108.71	0.999983	5/26/2002 19:00
MB1	14.13	61.35	0	Fail	22,466.64	0.999977	5/26/2002 11:00
1m shades							
Building	14.11	56.16	0	Fail	22,458.59	0.999977	5/26/2002 23:00
B3	12.40	43.66	0	Fail	21,372.11	0.999961	5/29/2002 10:00
K2	12.41	48.02	0	Fail	21,543.42	0.999964	5/28/2002 10:00
LR2	15.09	60.81	0	Fail	23,054.05	0.999982	5/26/2002 21:00
MB1	14.00	60.45	0	Fail	22,381.84	0.999976	5/26/2002 13:00
1.5m shades							
Building	14.11	55.95	0	Fail	22,435.71	0.999976	5/27/2002 05:00
B3	12.34	43.33	0	Fail	21,343.89	0.999960	5/29/2002 13:00
K2	12.36	47.83	0	Fail	21,520.99	0.999964	5/28/2002 13:00
LR2	15.02	60.65	0	Fail	23,039.59	0.999982	5/26/2002 23:00
MB1	13.90	60.12	0	Fail	22,342.44	0.999975	5/26/2002 15:00
Blinds with highly reflective slats							
Building	14.54	58.34	0	Fail	22,697.54	0.999979	5/26/2002 14:00
B3	12.91	45.88	0	Fail	21,649.01	0.999966	5/28/2002 12:00
K2	12.68	49.55	0	Fail	21,693.24	0.999967	5/28/2002 04:00
LR2	15.54	63.37	1	Fail	23,327.41	0.999985	5/26/2002 13:00
MB1	14.73	65.12	0	Fail	22,850.52	0.999981	5/25/2002 15:00
Venetian blinds							
Building	14.63	58.71	0	Fail	22,740.02	0.999980	5/26/2002 13:00
B3	12.99	46.17	0	Fail	21,688.42	0.999966	5/28/2002 11:00
K2	12.68	49.70	0	Fail	21,710.41	0.999967	5/27/2002 23:00
LR2	15.54	63.53	2	Fail	23,348.17	0.999985	5/26/2002 12:00
MB1	14.84	65.74	0	Fail	22,926.13	0.999981	5/25/2002 13:00
1.5m louvres							
Building	14.39	57.55	0	Fail	22,614.65	0.999978	5/26/2002 17:00
B3	12.77	45.03	0	Fail	21,564.39	0.999964	5/28/2002 17:00
K2	12.52	48.84	0	Fail	21,625.45	0.999965	5/28/2002 08:00
LR2	15.33	62.37	0	Fail	23,214.92	0.999984	5/26/2002 17:00
MB1	14.37	63.39	0	Fail	22,663.48	0.999979	5/25/2002 23:00

Figure 8.3 shows the effect of shading devices on the indoor temperature. Using different shading types has virtually no effect on the indoor temperature, nor on the overheating risk (Table 17). However, the overheating risk is slightly reduced with 1.5m local shading as it blocks more solar gain in summer and allows it during winter. These minor effects are due to a small WWR. Therefore, simulations are run again using a WWR of 2.5% to enhance the effect of changing the shading type.

Figure 8.4 shows a clearer difference between the effect of various shading devices on indoor air temperature using a larger WWR. The results in Table 18 show that the overheating risk reduces

with 1.5m local shading. However, this device does not significantly reduce the overheating risk of B3 and K2, due to these rooms having fewer windows that also face north. The most significant reduction occurs in MB2 due to this room having 2 more windows than the other rooms, which also face east and west. Blinds with reflective slats and venetian blinds have a much smaller effect on lowering the overheating risk. 1.5m louvres perform worse than 1.5m local shading, likely because they reflect solar radiation into the building.

Table 18: Comparison of the overheating for different shading devices on a base model with an increased WWR to 2.5%

Simulation Description	CIBSE TM52				Robindon and Haldi (2008)		
	TM52: Criteria 1	TM52: Criteria 2	TM52: Criteria 3	Pass/Fail	Degree Hours (>25°C)	P _{OH} (25°C)	P _{OH} Exceeds 20% (Date)
2.5% WWR: 0.5m shades							
Building	16.39	71.57	12	Fail	24,157.82	0.999990	5/24/2002 07:00
B3	14.85	57.30	0	Fail	22,929.78	0.999981	5/25/2002 22:00
K2	14.18	59.37	1	Fail	22,693.70	0.999979	5/26/2002 07:00
LR2	17.28	79.04	50	Fail	25,038.56	0.999993	5/23/2002 14:00
MB1	17.63	86.71	86	Fail	25,316.94	0.999994	5/21/2002 12:00
2.5% WWR: 1m shades							
Building	16.06	69.02	4	Fail	23,881.31	0.999988	5/24/2002 15:00
B3	14.71	56.14	0	Fail	22,765.96	0.999980	5/26/2002 10:00
K2	13.96	57.70	0	Fail	22,533.72	0.999978	5/26/2002 12:00
LR2	17.00	76.79	41	Fail	24,775.59	0.999992	5/24/2002 06:00
MB1	16.78	79.57	34	Fail	24,581.14	0.999992	5/22/2002 19:00
2.5% WWR: 1.5m shades							
Building	15.92	68.13	1	Fail	23,776.66	0.999988	5/24/2002 19:00
B3	14.61	55.54	0	Fail	22,694.02	0.999979	5/26/2002 13:00
K2	13.89	57.21	0	Fail	22,475.71	0.999977	5/26/2002 15:00
LR2	16.84	75.61	38	Fail	24,645.77	0.999992	5/24/2002 11:00
MB1	16.42	77.20	25	Fail	24,298.77	0.999990	5/23/2002 10:00
2.5% WWR: Blinds with highly reflective slats							
Building	15.64	62.48	0	Fail	23,654.09	0.999987	5/24/2002 18:00
B3	16.92	76.33	23	Fail	24,722.91	0.999992	5/23/2002 09:00
K2	14.55	62.36	6	Fail	22,993.55	0.999982	5/25/2002 17:00
LR2	18.07	85.46	100	Fail	25,784.52	0.999995	5/22/2002 08:00
MB1	19.26	96.75	228	Fail	26,434.12	0.999996	5/18/2002 18:00
2.5% WWR: Venetian blinds							
Building	17.09	77.88	26	Fail	24,943.03	0.999993	5/22/2002 19:00
B3	15.86	64.11	0	Fail	23,886.61	0.999988	5/24/2002 08:00
K2	14.66	62.87	7	Fail	23,072.95	0.999983	5/25/2002 13:00
LR2	18.13	86.05	112	Fail	25,856.34	0.999995	5/21/2002 21:00
MB1	19.86	99.86	268	Fail	26,818.40	0.999997	5/17/2002 13:00
2.5% WWR: 1.5m louvres							
Building	16.48	71.97	13	Fail	24,215.86	0.999990	5/24/2002 05:00
B3	15.31	60.75	0	Fail	23,356.71	0.999985	5/25/2002 08:00
K2	14.19	59.25	2	Fail	22,697.77	0.999979	5/26/2002 06:00
LR2	17.24	79.00	50	Fail	25,022.67	0.999993	5/23/2002 18:00
MB1	19.86	83.53	67	Fail	24,932.76	0.999993	5/22/2002 11:00

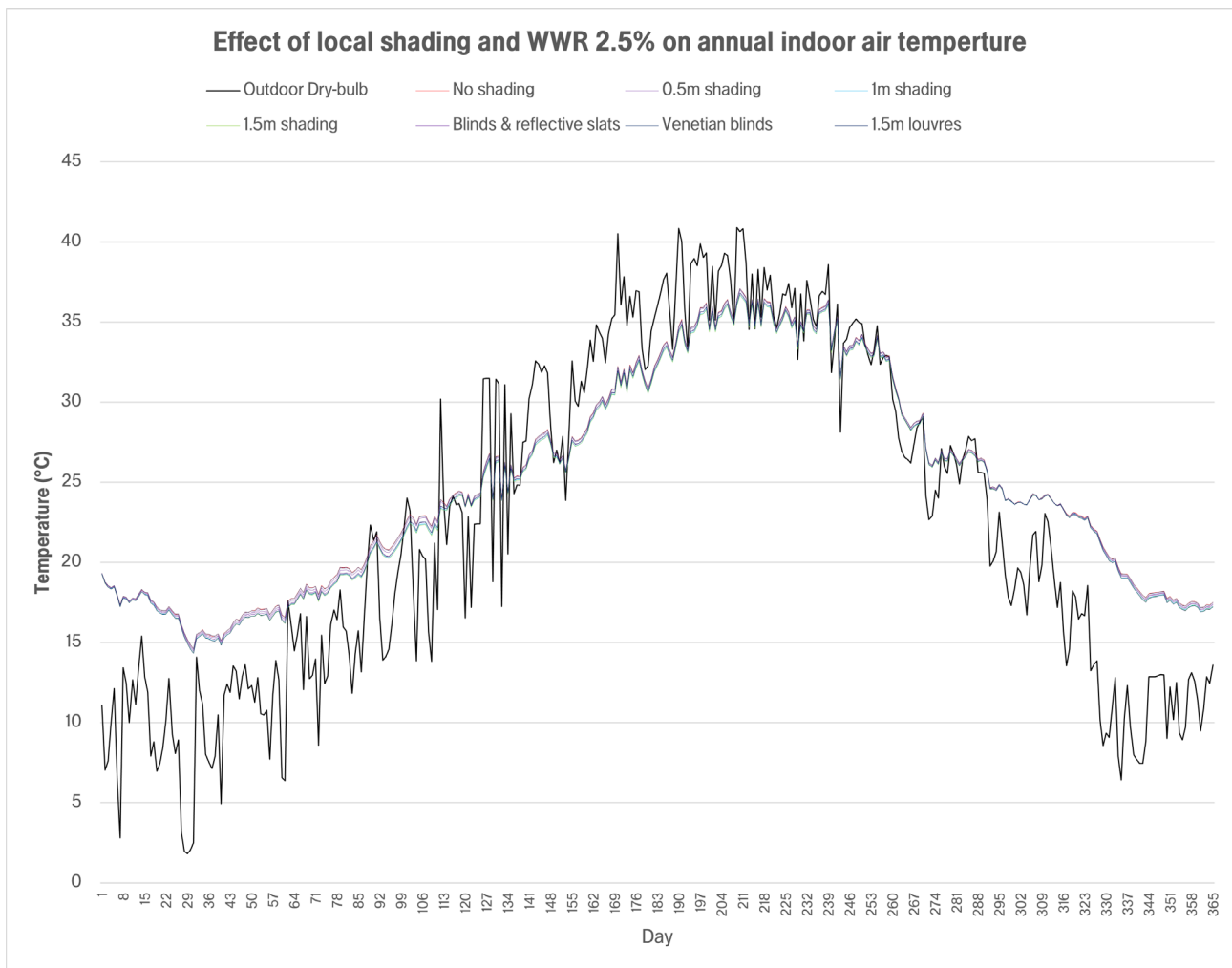


Figure 8.4: Indoor air temperature variations for the addition of different shading devices to a base model with an increased WWR to 2.5%, across the year. A 1.5m local shading device slightly reduces temperatures year round.

8.3 Analysis of results after the introduction of evaporative cooling

Evaporative cooling is a common bioclimatic, passive method of cooling in hot-dry climates (Hyde, 2000). It works to remove latent heat from the air and replace it with water vapour. An evaporative cooling system is not able to be successfully implemented in DesignBuilder for this study. Therefore, literature has been used to determine the result of this input to the building. Ideally, no mechanical system is used to reduce overheating risk, paralleling the ideals and principles of vernacular architecture. A study by Robinson (2000) finds that a passive downdraught evaporative cooling system (PDEC) cools dry-bulb temperature points to 70% of the wet-bulb temperature depression. Therefore, temperatures after the implementation of a PDEC are manually calculated to produce a set of results in Table 19.

Wet-bulb temperature was calculated using the following equation:

$$(8) \quad T_w = T \arctan(0.151977(RH\% + 8.313659)^{1/2}) + \arctan(T + RH\%) - \arctan(RH\% - 1.676331) + 0.00391838(RH\%)^{3/2} \arctan(0.023101 RH\%) - 4.686035,$$

where T_w = Wet-bulb temperature, T = Indoor dry-bulb temperature and $RH\%$ = relative humidity as a percentage.

This is a heat index calculation using relative humidity and dry-bulb temperature, not a wet-bulb globe temperature which accounts for wind speed, sun angle and cloud cover (Stull, 2011).

Note that this method will not produce accurate results, as the effect of the PDEC in a different climate and with different ventilation systems (as in this study) may be different to its effect in Robinson's study. Nevertheless, it can provide an estimate of the resulting indoor temperatures to help understand the potential effect of introducing evaporative cooling.

Table 19: Comparison of the overheating risk for the addition of evaporative cooling.

Simulation Description	CIBSE TM52				Robinson and Haldi (2008)		
	TM52: Criteria 1	TM52: Criteria 2	TM52: Criteria 3	Pass/Fail	Degree Hours (>25°C)	P _{OH} (25°C)	P _{OH} Exceeds 20% (Date)
No evaporative cooling							
Building	14.46	57.39	0	Fail	22,602.56	0.999978	5/26/2002 18:00
B3	13.03	46.31	0	Fail	2,1701.97	0.999967	5/28/2002 10:00
K2	12.68	49.59	0	Fail	21,704.72	0.999967	5/27/2002 22:00
LR2	15.55	63.57	2	Fail	23,356.2	0.999985	5/26/2002 11:00
MB1	14.60	64.19	0	Fail	22,771.06	0.999980	5/25/2002 17:00
Evaporative cooling by PDEC							
Building	0.16	0	0	Pass	3,723.15	0.829411	7/17/2002 10:00
B3	0.16	0	0	Pass	3,311.26	0.792547	7/20/2002 05:00
K2	0.17	0	0	Pass	3,358.82	0.797181	7/18/2002 08:00
LR2	0.16	0	0	Pass	4,092.32	0.856849	7/16/2002 08:00
MB1	0.17	0	0	Pass	3,882.11	0.841817	7/16/2002 08:00

The reduction in temperature is calculated for all hours where cooling is in demand (temperatures exceeding 25°C). Therefore, no fixed schedule has been set, and in reality, occupants might only utilise this method during hot summer months. The results show a significant reduction to cooling degree hours and the overheating risk; as shown in Table 19, the probability of overheating (P_{OH}) is below 0.85 in all rooms, whilst no other parameter has yielded a P_{OH} below 0.99. This is because the low humidity of a 2080 climate allows for more water vapour to evaporate, rendering evaporative cooling a very efficient passive cooling mechanism that could replace the use of a mechanically driven one.

8.4 Sensitivity analysis conclusion and optimal model design

A sensitivity analysis has been conducted to assess the effect of various properties of Harran vernacular houses on the indoor temperatures and the risk of overheating in a 2080 climate. These parameters include existing properties and the introduction of passive cooling strategies. Optimal values for these parameters (those which most reduce the overheating risk) are listed in Table 20, and are used to inform two optimal models.

The results occasionally differ for each method of assessing the overheating risk, i.e. a room will pass the TM52 criteria but result in a high probability of overheating (P_{OH}) according to Robinson & Haldi's model. The two instances of this are the addition of insulation to the vernacular construction and the introduction of a PDEC, which both pass all TM52 criteria yet result in a POH exceeding 0.8. This disagreement suggests that the models of assessing overheating are somewhat unreliable. This might simply be because they are models being applied to a new situation; whilst Robinson & Haldi's model is based on empirical evidence, no model is perfect and thus it is not 100% accurate when used in a different scenario. Similarly, simulations cannot be considered a totally accurate

representation of reality.

There are three parameters for which two parameter values perform similarly well. These are the construction type, dome height, and glazing type. Because of this, as well as the unpredictable way in which different parameters can work together to reduce the overheating risk, two optimal models with different parameter values are tested and compared. Note that a combined tree analysis was undertaken for a small number of parameters (altering WWR with glazing and shading types, see Sections 8.1-2) to assess how they work together. This is used to inform the optimal models.

Table 20: Parameters values which best reduce the overheating risk. The numbers correspond to the whole building results obtained from the sensitivity analysis.

Simulation Description	CIBSE TM52				Robindon and Haldi (2008)		
	TM52: Criteria 1	TM52: Criteria 2	TM52: Criteria 3	Pass/Fail	Degree Hours (>25°C)	P _{OH} (25°C)	P _{OH} Exceeds 20% (Date)
Base model							
Building	14.46	57.39	0	Fail	22,602.56	0.999978	5/26/2002 18:00
Construction							
Addition of insulation	2.91	1.97	0	Pass	17,712.63	0.999778	06/09/2002 13:00
Addition of reflective material	11.60	30.39	0	Fail	21,113.16	0.999956	5/29/2002 16:00
Dome height							
3m	14.46	55.92	0	Fail	22,601.41	0.999978	5/26/2002 15:00
5m	13.64	55.26	0	Fail	22,103.46	0.999972	5/27/2002 17:00
Orientation							
No change (0°)	14.46	57.39	0	Fail	22,602.56	0.999978	5/26/2002 18:00
WWR							
2.5%	17.16	78.54	27	Fail	24,995.48	0.999993	5/22/2002 17:00
Openable windows							
55%	14.65	58.82	0	Fail	22,751.60	0.999980	5/26/2002 12:00
Glazing							
Double reflective	14.08	55.62	0	Fail	22,388.22	0.999976	5/27/2002 07:00
Triple Low-E	14.20	56.31	0	Fail	22,491.51	0.999977	5/26/2002 20:00
Shading							
1.5m local shading	14.11	55.95	0	Fail	22,435.71	0.999976	5/27/2002 05:00
Evaporative cooling							
PDEC	0.16	0	0	Pass	3,723.15	0.829411	7/17/2002 10:00

The details of the optimal models are listed in Table 21. The first uses all the optimal parameter values, while the second uses the second best values for the three aforementioned parameters (where the second best value yields results nearly as good as the optimal value). A WWR of 2.5% is applied to both models. A larger WWR was identified as slightly increasing the overheating risk, however larger windows allow more light in and increase visual comfort. This is equally important to reduce reliance on electrical lighting and the time spent outdoors in hot temperatures, which is a likely outcome of the very low illuminance in the base model with a WWR of 0.8%.

Table 21: Parameters applied to optimal models 1 and 2, with a comparison of the base model

	Construction	Dome height	Orientation	WWR	Openable windows	Glazing	Shading	Evaporative cooling
Base model	Vernacular construction (adobe brick)	3m-5m range	0°	0.8%	5%	Single 3mm	No shading	No evaporative cooling
Optimal model 1	Insulation addition	5m domes	0°	2.5%	5%	Triple Low-E	1.5m local shading	Yes (PDEC)
Optimal model 2	Reflective coating	3m domes	0°	2.5%	5%	Double reflective	1.5m local shading	Yes (PDEC)

9. Optimal design results and discussion

Table 22 shows the results of a simulation of the optimal models conducted without the introduction of a PDEC, to see the overheating risk without implementing the less-precise modelling of evaporative cooling. The results indicate that Model 2 performs best to reduce the overheating risk according to both criteria. The fact that the best-performing model does not use every optimal parameter confirms the limitations of the sensitivity analysis (where optimal values were identified using individual variables); non-'optimal' parameter values can work together to yield a lower risk of overheating. For example, a reflective construction type and 3m dome height were not ranked as providing the least overheating risk. However, the global use of these parameters in Model 2 demonstrates them working together to reduce overheating risk. The use of a reflective coating on the building and openings performs better in Model 2 than insulation addition and triple low e glazing. This may be due to its ability to reflect radiation on a lower surface area provided by the 3m domes. Also, whilst both models pass TM52 criteria, the P_{OH} is still very high (exceeding 0.995).

Table 22: Comparison of overheating risk for optimal models 1 and 2, without the addition of a PDEC

Simulation Description	CIBSE TM52				Robindon and Haldi (2008)		
	TM52: Criteria 1	TM52: Criteria 2	TM52: Criteria 3	Pass/Fail	Degree Hours (>25°C)	P_{OH} (25°C)	P_{OH} Exceeds 20% (Date)
Optimal model 1 without PDEC							
Building	0.03	0	0	Pass	16,549.78	0.999615	6/13/2002 08:00
B3	0	0	0	Pass	13,825.17	0.998594	6/19/2002 22:00
K2	0	0	0	Pass	14,620.62	0.999036	6/17/2002 18:00
LR2	0	0	0	Pass	15,366.31	0.999324	6/16/2002 13:00
MB1	0.1	0	0	Pass	16,515.96	0.999608	06/12/2002 13:00
Optimal model 2 without PDEC							
Building	0	0	0	Pass	13,220.26	0.998126	6/23/2002 09:00
B3	0	0	0	Pass	11,253.16	0.995229	6/28/2002 21:00
K2	0	0	0	Pass	12,008.54	0.996668	6/25/2002 21:00
LR2	0	0	0	Pass	12,468.56	0.997322	6/24/2002 21:00
MB1	0	0	0	Pass	13,027.43	0.997946	6/22/2002 22:00

Table 23 gives results for the simulation with the inclusion of a PDEC system. It is clear that the overheating risk is vastly reduced, and with this the demand of applied energy for cooling. Both models pass all TM52 criteria, and P_{OH} is reduced to 0.4 for Model 1 and 0.2 for Model 2. Note that a P_{OH} below 0.85 has not been achieved in any of the sensitivity analysis overheating results previously in this study, demonstrating that the combined use of these parameter values promote

cooler temperatures. Model 2 performs best with the lowest P_{OH} , where some rooms do not at all exceed a 20% risk of overheating. MB1 has the highest risk in both models, which is most likely due to its lack of neighbouring domes, more external walls, more windows and therefore larger exposure to radiation and solar gain.

Due to the way PDEC is calculated (see Section 8.3), the results may not be totally accurate as it is impossible to know exactly how much this system would reduce the overheating risk without precise computer modelling or empirical experiments. A PDEC is applied at every hour where temperatures exceed 25°C, and is not scheduled for a specific time period. However even if the results are overestimated, it is evident that evaporative cooling would still reduce the cooling demand.

Table 23: Comparison of overheating risk for optimal models 1 and 2 with the introduction of a PDEC

Simulation Description	CIBSE TM52				Robindon and Haldi (2008)		
	TM52: Criteria 1	TM52: Criteria 2	TM52: Criteria 3	Pass/Fail	Degree Hours (>25°C)	P_{OH} (25°C)	P_{OH} Exceeds 20% (Date)
Optimal model 1 with PDEC							
Building	0	0	0	Pass	1,194.00	0.432862	8/16/2002 08:00
B3	0	0	0	Pass	592.89	0.245443	8/30/2002 10:00
K2	0	0	0	Pass	756.63	0.301906	8/22/2002 01:00
LR2	0	0	0	Pass	909.41	0.350770	8/20/2002 14:00
MB1	0.07	0	0	Pass	1,243.05	0.445921	08/07/2002 13:00
Optimal model 2 with PDEC							
Building	0	0	0	Pass	529.12	0.222236	09/07/2002 09:00
B3	0	0	0	Pass	271.18	0.120858	-
K2	0	0	0	Pass	353.98	0.154764	-
LR2	0	0	0	Pass	426.18	0.183259	-
MB1	0	0	0	Pass	508.11	0.214434	09/08/2002 08:00

10. Conclusion

The vernacular architecture of Harran is well adapted to coping with high temperatures presented by its climate, to enable thermal comfort indoors. In this study, a typical Harran house was tested to assess its resilience to overheating in a 2080 climate, experiencing higher temperatures and radiation levels as a result of global warming. A sensitivity analysis was conducted by testing the key vernacular principles of these houses and introducing new strategies by simulation to a base model, to understand how they reduce the overheating risk.

Two methods were used to assess the overheating risk: CIBSE TM52 criteria and Robinson & Haldi's (2008) integrated adaptive model. The base model was far more prone to overheating in a future climate than at present. Hence the focus of this study was on adapting the architecture to perform better in the face of climate change.

The sensitivity analysis revealed that passive strategies such as evaporative cooling, addition of insulation to the building fabric, and a taller dome height had the greatest reduction of overheating risk in 2080. This was used to inform two optimal model designs which would ensure comfortable indoor temperatures in the future. Interestingly, the optimal model which utilised the non-optimal parameter values (as identified by the sensitivity analysis), resulted in a significantly lower overheating risk than the model which used all the optimal values. This highlights the limitations of the sensitivity analysis which assumes that parameters act independently of each other. In fact, parameters work together to impact performance, therefore it is suggested that further studies use a global or combined tree analysis for refined accuracy.

Passive strategies were utilised in this study to inform whether it is possible to reduce overheating risk without reliance on mechanical systems, mirroring vernacular principles. It was notable that a calculation of evaporative cooling was inputted manually without running a simulation, therefore the effect of this as a parameter is deemed less precise. Nonetheless, it appears to have a significant impact on indoor temperatures. A future study may expand on this through more precise modelling of evaporative cooling, and testing it against mechanical cooling systems, which were not assessed here.

There are two factors which may have led to an overestimated overheating risk. Firstly, the projected climate data potentially overestimates the effects of global warming, which would have a similar effect on the overheating results. Secondly, one of the methods for assessing the overheating risk is designed for office buildings, where occupants are predicted to be more sensitive to temperature increases than in domestic settings. This increased sensitivity could lead to the risk being overestimated. However, this does not significantly affect the conclusions of the study; the strategies identified as providing the coolest temperatures would not change. Another limitation was the lack of accuracy in the modelling of natural ventilation. A future study could improve on this by modelling actual wind and buoyancy forces to determine ventilation rates, and incorporating realistic scheduling of when windows are opened.

In conclusion, it is possible to passively reduce the overheating risk in these dwellings to provide a comfortable indoor environment in a hotter future, meaning the reliance on applied energy and carbon emissions are also reduced. Therefore, the architecture of Harran could be used as a sustainable model for dwellings in hot-dry climates after global warming, if adapted with the appropriate strategies as identified in this work. It is clear that looking back to historical architecture can inform a future path towards healthier and longer lasting buildings, which are resilient to climate change.

11. Word Count

[without tables and captions for figures and tables]

1. Introduction	947
2. Research questions, aims and objectives	159
3. Methodology	1,292
4. Literature Review: Climate analysis	1,144
5. Literature Review: Vernacular architecture of Harran	1,752
6. Base model of traditional house, inputs and analysis	1,717
7. Results after change of parameters	1,412
8. Introduction of new strategies	1,355
9. Optimal design results and discussion	511
10. Conclusion	585
Total	10,874

12. References

- Acosta, J. D. R., Diaz, A. G., Zarazua, G. M. S.- & Garcia, E. R.-. (2010). Adobe as a Sustainable Material: A Thermal Performance. *Journal of Applied Sciences*, 10(19), 2211–2216.
- ASHRAE. (2005). *2005 ASHRAE Handbook: Fundamentals*. Atlanta, GA.: ASHRAE ;
- Baran, M. & Yilmaz, A. (2018). A Study of Local Environment of Harran Historical Domed Houses in Terms of Environmental Sustainability. *Journal of Asian Scientific Research*, 8(6), 211–220.
- Başaran, T. (2011). Thermal Analysis of the Domed Vernacular Houses of Harran, Turkey. *Indoor and Built Environment*, 20(5), 543–554.
- Beck, H. E., Zimmermann, N. E., McVicar, T. R., Vergopolan, N., Berg, A. & Wood, E. F. (2018). Present and Future Köppen-Geiger Climate Classification Maps at 1-Km Resolution. *Scientific Data*, 5(1), 180214.
- Brotas, L. & Nicol, F. (2017). Estimating Overheating in European Dwellings. *Architectural Science Review*, 60(3), 180–191.
- BSI. (2012). *Indoor Environmental Input Parameters for Design and Assessment of Energy Performance of Buildings Addressing Indoor Air Quality, Thermal Environment, Lighting and Acoustics*. European Committee for Standardization, Technical Committee CEN/TC 156 'Ventilation for Buildings'.
- Cardinale, N., Rospi, G. & Stefanizzi, P. (2013). Energy and Microclimatic Performance of Mediterranean Vernacular Buildings: The Sassi District of Matera and the Trulli District of Alberobello. *Building and Environment*, 59, 590–598.
- Cardinale, N., Rospi, G., Stefanizzi, P. & Augenti, V. (2011). Thermal Properties of the Vernacular Buildings Envelopes: The Case of the 'Sassi Di Matera' and 'Trulli Di Alberobello'. *International Journal of Energy and Environment (IJEE)*, 2(4), 605–614.
- CIBSE. (2013). *CIBSE TM52: The Limits of Thermal Comfort: Avoiding Overheating in European Buildings*. London : The Chartered Institution of Building Services Engineers.
- Climate.Onebuilding. (2021). Climate.Onebuilding.Org. *Climate.onebuildng.org*. Retrieved April 16, 2021, from <http://climate.onebuilding.org/>
- Cortesi, M. (2020). Harran Beehive Houses. *Atlas Obscura*. Retrieved July 16, 2021, from <http://www.atlasobscura.com/places/harran-beehive-houses>
- Costa, C., Cerqueira, Â., Rocha, F. & Velosa, A. (2019). The Sustainability of Adobe Construction: Past to Future. *International Journal of Architectural Heritage*, 13(5), 639–647.
- Creekmore, A. T. (2018). Landscape and Settlement in the Harran Plain, Turkey: The Context of Third-Millennium Urbanization. *American Journal of Archaeology*, 122(2), 177.
- Din, A. & Brotas, L. (2016). The Evaluation of the Variables of Domestic Overheating in the UK under TM52 Using a Future Climate Model- Guidance for Designers. *9th Windsor Conference: Making Comfort Relevant*. Retrieved from <http://repository.londonmet.ac.uk/1048/>
- Dipasquale, L., Kisa Ovali, P., Mecca, S. & Özel, B. (2014). Resilience of Vernacular Architecture. *Versus: Heritage for Tomorrow; Firenze University Press: Florence, Italy*, 65–73.
- EFA. (2014). EFA Daylight Design Guide. Retrieved from https://assets.publishing.service.gov.uk/government/uploads/system/uploads/attachment_data/file/388373/EFA_Daylight_design_guide.pdf
- EnergyPlus. (nd). Weather Data for Simulation. *EnergyPlus*. Retrieved April 20, 2021, from <https://energyplus.net/weather/simulation>

- Fathy, H., Shearer, W. & Sultān, 'Abd al-Rahmān. (1986). *Natural Energy and Vernacular Architecture: Principles and Examples with Reference to Hot Arid Climates*. Chicago: Published for the United Nations University by the University of Chicago Press.
- Gaughan, R. (2017). How Solar Energy Affects the Earth's Atmosphere. *Sciencing*. Retrieved August 2, 2021, from <https://sciencing.com/solar-energy-affects-earths-atmosphere-22463.html>
- Goodhew, S. & Griffiths, R. (2005). Sustainable Earth Walls to Meet the Building Regulations. *Energy and Buildings*, 37(5), 451–459.
- Google Earth Web. (2020). Harran, Turkey. Retrieved from <https://earth.google.com/web/@36.86711589,39.02952278,371.59076457a,965.419791d,30.00000472y,0h,0t,0r>
- Gorjimahlabani, S. (2020). Evaluation of Overheating Risk in Homes.
- Green, T. M. (1992). *The City of the Moon God: Religious Traditions of Harran*. Leiden ; New York: E.J. Brill.
- Hamdy, M., Carlucci, S., Hoes, P.-J. & Hensen, J. L. M. (2017). The Impact of Climate Change on the Overheating Risk in Dwellings—A Dutch Case Study. *Building and Environment*, 122, 307–323.
- Heracleous, C. & Michael, A. (2018). Assessment of Overheating Risk and the Impact of Natural Ventilation in Educational Buildings of Southern Europe under Current and Future Climatic Conditions. *Energy*, 165, 1228–1239.
- Hyde, R. (2000). *Climate Responsive Architecture*. London: E & F Spon, imprint of Chapman & Hall.
- IEA. (2021). *Turkey 2021 Energy Policy Review*. Paris: International Energy Agency. Retrieved from https://iea.blob.core.windows.net/assets/cc499a7b-b72a-466c-88de-d792a9daff44/Turkey_2021_Energy_Policy_Review.pdf
- IPCC, Field, C. B. & Barros, V. R. (Eds.). (2014). *Climate Change 2014: Impacts, Adaptation, and Vulnerability: Working Group II Contribution to the Fifth Assessment Report of the Intergovernmental Panel on Climate Change*. New York, NY: Cambridge University Press.
- Jentsch, M. F., Bahaj, A. S. & James, P. A. B. (2008). Climate Change Future Proofing of Buildings—Generation and Assessment of Building Simulation Weather Files. *Energy and Buildings*, 40(12), 2148–2168.
- Jentsch, M. F., James, P. A. B., Bourikas, L. & Bahaj, A. S. (2013). Transforming Existing Weather Data for Worldwide Locations to Enable Energy and Building Performance Simulation under Future Climates. *Renewable Energy*, 55, 514–524.
- Kazimee, B. A. (2008). Learning from Vernacular Architecture: Sustainability and Cultural Conformity, in: *Eco-Architecture II*, (pp. 3–13). Algarve, Portugal: WIT Press. Retrieved March 4, 2021, from <http://library.witpress.com/viewpaper.asp?pcode=ARC08-001-1>
- Koenigsberger, O. H. (1975). *Manual of Tropical Housing and Building: Climatic Design*. Chennai: Orient Longman.
- Kottek, M., Grieser, J., Beck, C., Rudolf, B. & Rubel, F. (2006). World Map of the Köppen-Geiger Climate Classification Updated. *Meteorologische Zeitschrift*, 15(3), 259–263.
- Laila, T., Arruda, A., Barbosa, J. & Moura, E. (2018). The Constructive Advantages of Buckminster Fuller's Geodesic Domes and Their Relationship to the Built Environment Ergonomics, in: Rebelo, F. and Soares, M. (Eds.), *Advances in Ergonomics in Design*, (pp. 357–368). Advances in Intelligent Systems and Computing. Cham: Springer International Publishing. Retrieved August 2, 2021, from http://link.springer.com/10.1007/978-3-319-60582-1_36
- Manioğlu, G. & Yılmaz, Z. (2008). Energy Efficient Design Strategies in the Hot Dry Area of Turkey. *Building and Environment*, 43(7), 1301–1309.

Meir, I. & Roaf, S. (2005). The Future of the Vernacular. Towards New Methodologies for the Understanding and Optimization of the Performance of Vernacular Buildings., in: *Vernacular Architecture in the Twentyfirst Century: Theory, Education and Practice*, (pp. 215–230).

Ministry of Environment. (2013). *Turkey's Fifth National Communication Under the UNFCCC*. Turkey: The United Nations Development Programme (UNDP), Turkey. Retrieved July 3, 2021, from https://unfccc.int/files/national_reports/annex_i_natcom/submitted_natcom/application/pdf/nc5_turkey%5B1%5D.pdf

Moazami, A., Carlucci, S. & Geving, S. (2017). Critical Analysis of Software Tools Aimed at Generating Future Weather Files with a View to Their Use in Building Performance Simulation. *Energy Procedia*, 132, 640–645.

Natalie. (nd). Beehive Houses of Harran : Southeast Turkey : Turkish Travel Blog. Retrieved July 16, 2021, from <https://turkishtravelblog.com/the-beehive-houses-of-harran-turkey/>

Natural Homes. (nd). Adobe Beehive Homes, Turkey. Retrieved July 9, 2021, from <http://naturalhomes.org/beehive-harran-turkey.htm>

Norgaard, K. M. (2012). Climate Denial and the Construction of Innocence: Reproducing Transnational Environmental Privilege in the Face of Climate Change. *Race, Gender & Class*, 19(1/2), 80–103.

Olukoya Obafemi, A. P. & Kurt, S. (2016). Environmental Impacts of Adobe as a Building Material: The North Cyprus Traditional Building Case. *Case Studies in Construction Materials*, 4, 32–41.

Omega. (nd). Emissivity of Common Materials. *Omega*. Retrieved August 4, 2021, from <https://www.omega.co.uk/literature/transactions/volume1/emissivityb.html>

Our World in Data. (2016). Greenhouse Gas Emissions. *Our World in Data*. Retrieved July 3, 2021, from <https://ourworldindata.org/greenhouse-gas-emissions>

Oxford English Dictionary. Oxford English Dictionary. Retrieved from <http://www.oed.com/viewdictionaryentry/Entry/11125>

Özdeniz, M. B., Bekleyen, A., Gönül, I. A., Gönül, H., Sarigül, H., Ilter, T., Dalkılıç, N. & Yildirim, M. (1998). Vernacular Domed Houses of Harran, Turkey. *Habitat International*, 22(4), 477–485.

Ozorhon, G. (2014). Learning from Mardin and Cumalıkızık: Turkish Vernacular Architecture in the Context of Sustainability. *Arts*, 3(1), 175–189.

Padfield, D. (2021). Harran Turkey, Carrhae, Abraham, Terah, Lot. Retrieved July 16, 2021, from <https://www.padfield.com/turkey/harran/index.html>

Parra-Saldivar, M. L. & Batty, W. (2006). Thermal Behaviour of Adobe Constructions. *Building and Environment*, 41(12), 1892–1904.

Pelsmakers, S. (2019). *The Environmental Design Pocketbook*. London, S.L.: Riba.

Robinson, D. (2000). Passive Dwindraught Evaporative Cooling (PDEC) Applied to an Office in Botswana. *BDSP Partnership*, 9(6), 325–334.

Robinson, D. & Haldi, F. (2008a). An Integrated Adaptive Model for Overheating Risk Prediction. *Journal of Building Performance Simulation*, 1(1), 43–55.

Robinson, D. & Haldi, F. (2008b). Model to Predict Overheating Risk Based on an Electrical Capacitor Analogy. *Energy and Buildings*, 40(7), 1240–1245.

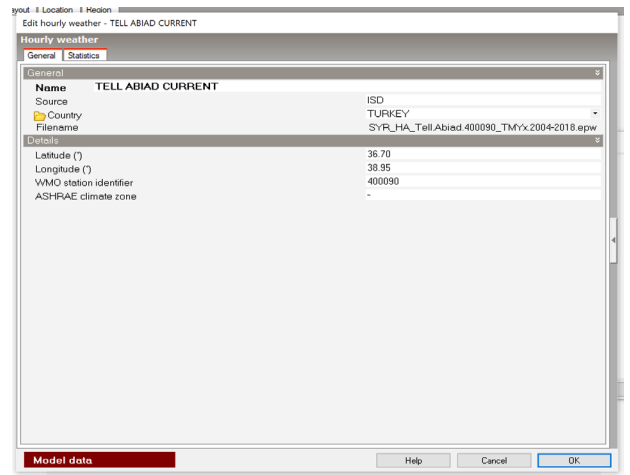
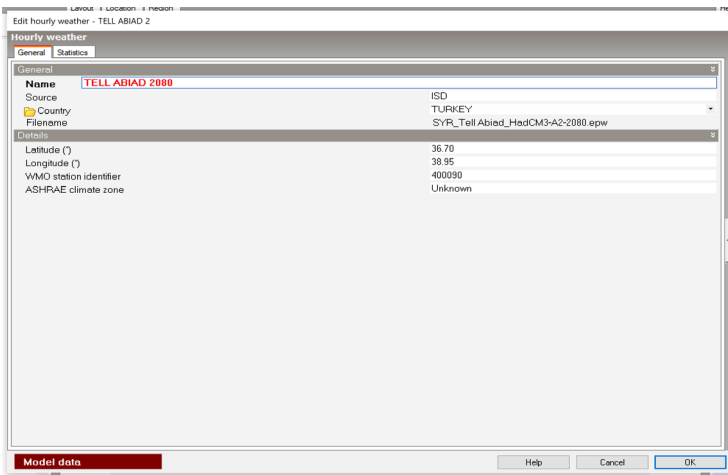
Rubel, F. & Kotteck, M. (2010). Observed and Projected Climate Shifts 1901-2100 Depicted by World Maps

- of the Köppen-Geiger Climate Classification. *Meteorologische Zeitschrift*, 19(2), 135–141.
- Sami, K. & Özdemir, İ. (2011). The Vernacular Houses of Harran and Cultural Heritage - Turkey. *International Journal of Academic Research*, 3(3). Retrieved from https://www.researchgate.net/profile/Kamuran-Sami/publication/310983319_KAMURAN_SAMI_1/links/583c06ab08ae3a74b4a1824a/KAMURAN-SAMI-1.pdf
- Sayigh, A. (2019). *Sustainable Vernacular Architecture: How the Past Can Enrich the Future*. Retrieved February 26, 2021, from <https://doi.org/10.1007/978-3-030-06185-2>
- Singh, M. C., Garg, S. N. & Jha, R. (2008). Different Glazing Systems and Their Impact on Human Thermal Comfort—Indian Scenario. *Building and Environment*, 43(10), 1596–1602.
- Stull, R. (2011). Wet-Bulb Temperature from Relative Humidity and Air Temperature. *Journal of Applied Meteorology and Climatology*, 50(11), 2267–2269.
- Todisco, L., Sanitate, G. & Lacorte, G. (2017). Geometry and Proportions of the Traditional Trulli of Alberobello. *Nexus Network Journal*, 19(3), 701–721.
- Topographic Map. (2020). Şanlıurfa Topographic Map, Elevation, Relief. *topographic-map.com*. Retrieved August 2, 2021, from <https://en-gb.topographic-map.com/maps/5hff/%C5%9Eanl%C4%B1urfa/>
- Tronchin, L. & Fabbri, K. (2008). Energy Performance Building Evaluation in Mediterranean Countries: Comparison between Software Simulations and Operating Rating Simulation. *Energy and Buildings*, 40(7), 1176–1187.
- Turkey News. (2020). Timeline: Major Earthquakes in Turkey. *Hürriyet Daily News*. Retrieved August 9, 2021, from <https://www.hurriyetdailynews.com/timeline-major-earthquakes-in-turkey-151401>
- Turkish Standard. (2008). Thermal Insulation Requirements for Buildings.
- UC Berkeley. (2020). Quake in Turkey Highlights the Hazard in the East Bay. Retrieved August 9, 2021, from <https://seismo.berkeley.edu/blog/2020/01/26/quake-in-turkey-highlights-the-hazard-in-the-east-bay.html>
- UNFCCC. (2015). The Paris Agreement. . Retrieved June 29, 2021, from <https://unfccc.int/process-and-meetings/the-paris-agreement/the-paris-agreement>
- USEPA, O. (2015). Health Effects of UV Radiation. Retrieved August 9, 2021, from <https://www.epa.gov/sunsafety/health-effects-uv-radiation>
- Vefik Alp, A. (1991). Vernacular Climate Control in Desert Architecture. *Energy and Buildings*, 16(3–4), 809–815.
- Vivancos, J.-L., Soto, J., Perez, I., Ros-Lis, J. V. & Martínez-Mañez, R. (2009). A New Model Based on Experimental Results for the Thermal Characterization of Bricks. *Building and Environment*, 44(5), 1047–1052.
- Volcano Discovery. (2021). Earthquake Monitor: Look up Quakes by Place. Retrieved August 9, 2021, from <https://www.volcanodiscovery.com/place/5187/earthquakes/sanliurfa/largest.html>
- Weather Spark. (2016). Average Weather in Harran, Turkey, Year Round. Retrieved August 9, 2021, from <https://weatherspark.com/y/101186/Average-Weather-in-Harran-Turkey-Year-Round>
- World Weather Online. (2021). Harran Monthly Climate Averages. *WorldWeatherOnline.com*. Retrieved April 20, 2021, from <https://www.worldweatheronline.com/harran-weather/sanliurfa/tr.aspx>
- Zilliacus, A. (2017). 11 Vernacular Building Techniques That Are Disappearing. *ArchDaily*. Retrieved October 13, 2021, from <https://www.archdaily.com/805415/11-vernacular-building-techniques-that-are-disappearing>

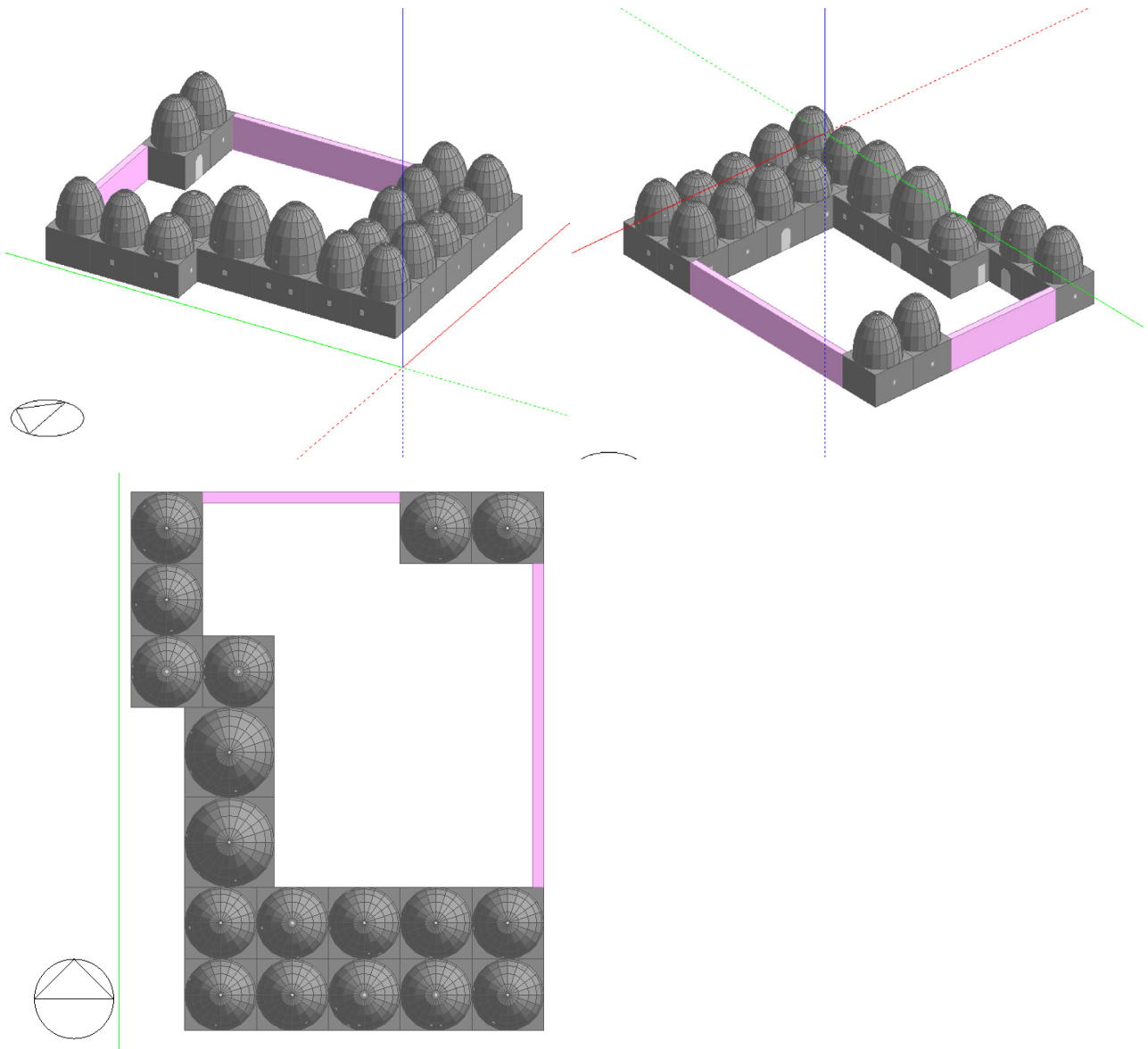
13. Appendices

Appendix 1: Base model inputs

1.1 Weather data inputs



1.2 The model



1.3 Occupancy inputs

Activity Template

Template Harran Bedroom

Sector Residential spaces

Zone type 1-Standard

Zone multiplier 1

Include zone in thermal calculations

Include zone in Radiance daylighting calculations

Occupancy

Occupied?

Occupancy density (people/m2) 0.0229

Schedule Dwell_DomBed_Occ

Metabolic

Clothing

Comfort Radiant Temperature Weighting

Contaminant Generation and Removal

DHW

Environmental Control

Heating Setpoint Temperatures

Heating (°C) 18.0

Heating set back (°C) 12.0

Cooling Setpoint Temperatures

Cooling (°C) 25.0

Cooling set back (°C) 28.0

Humidity Control

Ventilation Setpoint Temperatures

Minimum Fresh Air

Lighting

Computers

On

Office Equipment

On

Power density (W/m2) 3.58

Schedule Dwell_DomBed_Equip

Radiant fraction 0.200

Miscellaneous

On

Catering

Process

Data Report (Not Editable)

General

Harran Bedroom

An area primarily used for sleep.

Source UK NCT

Category Residential spaces

Region General

Sector Residential spaces

Holidays

Holidays No

Colour Shading in Model

Floor shade colour

All Gains

Power density (W/m2) 3.50

Occupancy details

Occupancy density (people/m2) 0.0229

Number of people 0.00

Metabolic Heat

Metabolic rate Bedroom (dwelling) 0.90

Metabolic factor (0.85 for women, 0.75 children) 0.0000000382

CO2 generation rate (m3/s-W) 0.5000

Latent fraction

Clothing

Clothing schedule definition 1-Generic summer and wint

Winter clothing (clo) 1.00

Summer clothing (clo) 0.50

Clothing schedule Default clothing schedule (N

Workday profile

Occupancy From 0 to 24

Days / week 5

Schedules

Schedule Dwell_DomBed_Occ

Computers

On No

Office Equipment

On Yes

Power density (W/m2) 3.58

Absolute zone power (W) 0.00

Radiant fraction 0.200

Workday profile

General Lighting

On No

Workday profile

Equipment From 7 to 23

Schedules

Schedule Dwell_DomBed_Light

DHW

On Yes

Consumption rate (l/m2-day) 0.530

Workday profile

Operation From 0 to 24

Schedules

Schedule Dwell_DomBed_Occ

Heating

Set point temperature (°C) 18.000

Set back temperature (°C) 12.000

Workday profile

Operation From 0 to 24

Schedules

Schedule Dwell_DomBed_Heat

Cooling

Set point temperature (°C) 25.000

Cooling set back (°C) 28.000

Workday profile

Operation From 0 to 24

Schedules

Schedule Dwell_DomBed_Cool

Ventilation Set Point Temperatures

Natural Ventilation

Nat. vent set point (°C) 24.000

Schedule Dwell_DomBed_Occ

Mechanical Ventilation

Mech. vent set point (°C) 10.000

Schedule Dwell_DomBed_Occ

Lighting

Target illuminance (lux) 100

Default display lighting density (W/m2) 0.000

Ventilation Fresh Air

Min fresh air (l/s-person) 10.000

Mech vent per area (l/s-m2) 0.000

Activity Template

Template Harran Dining Room

Sector Residential spaces

Zone type 1-Standard

Zone multiplier 1

Include zone in thermal calculations

Include zone in Radiance daylighting calculations

Occupancy

Occupied?

Occupancy density (people/m2) 0.0169

Schedule Dwell_DomDining_Occ

Metabolic

Clothing

Comfort Radiant Temperature Weighting

Air Velocity

Contaminant Generation and Removal

DHW

Environmental Control

Heating Setpoint Temperatures

Heating (°C) 18.0

Heating set back (°C) 12.0

Cooling Setpoint Temperatures

Cooling (°C) 25.0

Cooling set back (°C) 28.0

Humidity Control

Ventilation Setpoint Temperatures

Minimum Fresh Air

Lighting

Computers

On

Office Equipment

On

Miscellaneous

On

Catering

Process

General

Harran Dining Room

An area which is primarily used for eating meals.

Source UK NCT

Category Residential spaces

Region General

Sector Residential spaces

Holidays

Holidays No

Colour Shading in Model

Floor shade colour

All Gains

Power density (W/m2) 3.00

Occupancy details

Occupancy density (people/m2) 0.0169

Number of people 0.00

Metabolic Heat

Metabolic rate Eating/drinking 0.90

Metabolic factor (0.85 for women, 0.75 child... 0.0000000382

CO2 generation rate (m3/s-W) 0.5000

Latent fraction

Clothing

Clothing schedule definition 1-Generic summer an

Winter clothing (clo) 1.00

Summer clothing (clo) 0.50

Clothing schedule Default clothing sched

Workday profile

Occupancy From 7 to 22

Days / week 5

Schedules

Schedule Dwell_DomDining_Oc

Computers

On No

Office Equipment

On No

Miscellaneous

On No

Catering

On No

Miscellaneous

On No

Catering

On No

Process

On No

General Lighting

On Yes

Workday profile

Equipment From 6 to 22

Schedules

Schedule Dwell_DomDining_Lig

DHW

On No

Heating

Set point temperature (°C) 18.000

Set back temperature (°C) 12.000

Workday profile

Operation From 4 to 22

Schedules

Schedule Dwell_DomDining_He

Cooling

Set point temperature (°C) 25.000

Cooling set back (°C) 28.000

Workday profile

Operation From 4 to 22

Schedules

Schedule Dwell_DomDining_Co

Ventilation Set Point Temperatures

Natural Ventilation

Nat. vent set point (°C) 24.000

Schedule Dwell_DomDining_Oc

Mechanical Ventilation

Mech. vent set point (°C) 10.000

Schedule O# 247

Lighting

Target illuminance (lux) 150

Default display lighting density (W/m2) 0.000

Ventilation Fresh Air

Min fresh air (l/s-person) 10.000

Mech vent per area (l/s-m2) 0.000

Activity Template

Template Harran Kitchen

Sector Residential spaces

Zone type 1-Standard

Zone multiplier 1

Include zone in thermal calculations

Include zone in Radiance daylighting calculations

Occupancy

Occupied?

Occupancy density (people/m2) 0.0237

Schedule Winter on Summer off Kitchen

Metabolic

Clothing

Comfort Radiant Temperature Weighting

Air Velocity

Contaminant Generation and Removal

DHW

Environmental Control

Heating Setpoint Temperatures

Heating (°C) 18.0

Heating set back (°C) 12.0

Cooling Setpoint Temperatures

Cooling (°C) 25.0

Cooling set back (°C) 28.0

Humidity Control

Ventilation Setpoint Temperatures

Minimum Fresh Air

Lighting

Computers

On

Office Equipment

On

Miscellaneous

On

Catering

Process

General

Harran Kitchen

The area within the dwelling where food is prepared

Source UK NCT

Category Residential spaces

Region General

Sector Residential spaces

Holidays

Holidays Yes

Colour Shading in Model

Floor shade colour

All Gains

Power density (W/m2) 15.00

Occupancy details

Occupancy density (people/m2) 0.0237

Number of people 0.00

Metabolic Heat

Metabolic rate Work involving walkin 0.90

Metabolic factor (0.85 for women, 0.75 child... 0.0000000382

CO2 generation rate (m3/s-W) 0.5000

Latent fraction

Clothing

Clothing schedule definition 1-Generic summer an

Winter clothing (clo) 1.00

Summer clothing (clo) 0.50

Clothing schedule Default clothing sched

Workday profile

Occupancy From 7 to 23

Days / week 7

Schedules

Schedule Winter on Summer off

Computers

On No

Office Equipment

On No

Miscellaneous

On No

Catering

On No

Miscellaneous

On No

Catering

On No

Process

On No

General Lighting

On Yes

Workday profile

Equipment From 7 to 23

Schedules

Schedule Dwell_DomKitchen_Li

DHW

On Yes

Consumption rate (l/m2-day) 1.050

Workday profile

Operation From 7 to 23

Schedules

Schedule Dwell_DomKitchen_O

Heating

Set point temperature (°C) 18.000

Set back temperature (°C) 12.000

Workday profile

Operation From 5 to 23

Schedules

Schedule Dwell_DomKitchen_H

Cooling

Set point temperature (°C) 25.000

Cooling set back (°C) 28.000

Workday profile

Operation From 5 to 24

Schedules

Schedule Dwell_DomKitchen_C

Ventilation Set Point Temperatures

Natural Ventilation

Nat. vent set point (°C) 24.000

Schedule Dwell_DomKitchen_O

Mechanical Ventilation

Mech. vent set point (°C) 10.000

Schedule Dwell_DomKitchen_O

Lighting

Activity Template

Template <None>

Sector: General

Zone type: 1-Standard

Zone multiplier: 1

Include zone in thermal calculations

Include zone in Radiance daylighting calculations

Occupancy

Occupancy density (people/m2): 0.0000

Schedule: Off 24/7

Metabolic

Clothing

Comfort Radiant Temperature Weighting

Contaminant Generation and Removal

DHW

Environmental Control

Heating Setpoint Temperatures

Heating (°C): 0.0

Heating set back (°C): -50.0

Cooling Setpoint Temperatures

Cooling (°C): 30.0

Cooling set back (°C): 30.0

Humidity Control

Ventilation Setpoint Temperatures

Minimum Fresh Air

Lighting

Computers

On

Office Equipment

On

Miscellaneous

On

Catering

Process

General

<None>

Source: DesignBuilder

Category: <General>

Region: General

Sector: General

Holidays: Yes

Colour Shading in Model

Floor shade colour

All Gains

Power density (W/m2): 0.00

Occupancy details

Occupancy density (people/m2): 0.0000

Number of people: 0.00

Metabolic Heat

Metabolic rate: Typing

Metabolic factor (0.85 for women, 0.75 children): 1.00

CO2 generation rate (m3/s-W): 0.000000382

Latent fraction: 0.5000

Clothing

Clothing schedule definition: 1-Generic summer and wint

Winter clothing (clo): 1.00

Summer clothing (clo): 0.50

Clothing schedule: Default clothing schedule (N)

Workday profile

Occupancy: From 0 to 0

Days / week: 5

Schedules

Schedule: Off 24/7

Computers

On: No

Office Equipment

On: No

Miscellaneous

On: No

Catering

On: No

Process

On: No

Activity Template

Template Copy of Harran Circulation

Sector: Residential spaces

Zone type: 1-Standard

Zone multiplier: 1

Include zone in thermal calculations

Include zone in Radiance daylighting calculations

Occupancy

Occupied?

Occupancy density (people/m2): 0.0155

Schedule: Winter on Summer off Kitchen

Metabolic

Clothing

Comfort Radiant Temperature Weighting

Air Velocity

Contaminant Generation and Removal

DHW

Environmental Control

Heating Setpoint Temperatures

Heating (°C): 18.0

Heating set back (°C): 12.0

Cooling Setpoint Temperatures

Cooling (°C): 25.0

Cooling set back (°C): 28.0

Humidity Control

Ventilation Setpoint Temperatures

Minimum Fresh Air

Lighting

Computers

On

Office Equipment

On

Miscellaneous

Catering

Process

Activity templates

Data Report (Not Editable)

General

Copy of Harran Circulation

For all circulation areas within the dwelling.

Source: UK NCT

Category: Residential spaces

Region: General

Sector: Residential spaces

Holidays: No

Colour Shading in Model

Floor shade colour

All Gains

Power density (W/m2): 1.57

Occupancy details

Occupancy density (people/m2): 0.0155

Number of people: 0.00

Metabolic Heat

Metabolic rate: Light manual work

Metabolic factor (0.85 for women, 0.75 child): 0.90

CO2 generation rate (m3/s-W): 0.000000382

Latent fraction: 0.5000

Clothing

Clothing schedule definition: 1-Generic summer an

Winter clothing (clo): 1.00

Summer clothing (clo): 0.50

Clothing schedule: Default clothing sched

Workday profile

Occupancy: From 7 to 23

Days / week: 5

Schedules

Schedule: Winter on Summer off

Computers

On: No

Office Equipment

On: No

Miscellaneous

On: Yes

Power density (W/m2): 0.00

Absolute zone power (W): 0.00

Schedules

Schedule: Dwell_DomCirculation

Catering

On: No

Process

On: No

General Lighting

On: Yes

Workday profile

Equipment: From 7 to 23

Schedules

Schedule: Dwell_DomCirculation

DHW

On: No

Heating

Set point temperature (°C): 18.000

Set back temperature (°C): 12.000

Workday profile

Operation: From 5 to 23

Schedules

Schedule: Dwell_DomCirculation

Cooling

Set point temperature (°C): 25.000

Cooling set back (°C): 28.000

Workday profile

Operation: From 5 to 23

Schedules

Schedule: Dwell_DomCirculation

Ventilation Set Point Temperatures

Natural Ventilation

Nat. vent. set point (°C): 24.000

Mechanical Ventilation

Mech. vent. set point (°C): 10.000

Schedule: Off 24/7

Lighting

Target illuminance (lux): 100

Default display lighting density (W/m2): 0.000

Ventilation Fresh Air

Min fresh air (l/s-person): 10.000

Mech vent per area (l/s-m2): 0.000

Activity Template

Template Harran Lounge

Sector: Residential spaces

Zone type: 1-Standard

Zone multiplier: 1

Include zone in thermal calculations

Include zone in Radiance daylighting calculations

Occupancy

Occupied?

Occupancy density (people/m2): 0.0188

Schedule: Summer on Winter off Lounge

Metabolic

Clothing

Comfort Radiant Temperature Weighting

Air Velocity

Contaminant Generation and Removal

DHW

Environmental Control

Heating Setpoint Temperatures

Heating (°C): 21.0

Heating set back (°C): 12.0

Cooling Setpoint Temperatures

Cooling (°C): 25.0

Cooling set back (°C): 28.0

Humidity Control

Ventilation Setpoint Temperatures

Minimum Fresh Air

Lighting

Computers

On

Office Equipment

On

Power density (W/m2): 3.90

Schedule: Dwell_DomLounge_Equip

Radiant fraction: 0.200

Miscellaneous

On

Catering

Process

Activity templates

Data Report (Not Editable)

General

Harran Lounge

The main reception room of the home.

Source: UK NCT

Category: Residential spaces

Region: General

Sector: Residential spaces

Holidays: No

Colour Shading in Model

Floor shade colour

All Gains

Power density (W/m2): 1.50

Occupancy details

Occupancy density (people/m2): 0.0188

Number of people: 0.00

Metabolic Heat

Metabolic rate: Seated quiet

Metabolic factor (0.85 for women, 0.75 child): 0.90

CO2 generation rate (m3/s-W): 0.000000382

Latent fraction: 0.5000

Clothing

Clothing schedule definition: 1-Generic summer an

Winter clothing (clo): 1.00

Summer clothing (clo): 0.50

Clothing schedule: Default clothing sched

Workday profile

Occupancy: From 16 to 23

Days / week: 7

Schedules

Schedule: Summer on Winter off

Computers

On: No

Office Equipment

On: No

Miscellaneous

On: No

Catering

On: No

Miscellaneous

On: No

Catering

On: No

Process

On: No

General Lighting

On: Yes

Workday profile

Equipment: From 16 to 23

Schedules

Schedule: Dwell_DomLounge_Li

DHW

On: No

Heating

Set point temperature (°C): 21.000

Set back temperature (°C): 12.000

Workday profile

Operation: From 14 to 23

Schedules

Schedule: Dwell_DomLounge_H

Cooling

Set point temperature (°C): 25.000

Cooling set back (°C): 28.000

Workday profile

Operation: From 14 to 23

Schedules

Schedule: Dwell_DomLounge_C

Ventilation Set Point Temperatures

Natural Ventilation

Nat. vent. set point (°C): 24.000

Mechanical Ventilation

Mech. vent. set point (°C): 10.000

Schedule: Off 24/7

Lighting

Target illuminance (lux): 150

Default display lighting density (W/m2): 0.000

Ventilation Fresh Air

Min fresh air (l/s-person): 10.000

Mech vent per area (l/s-m2): 0.000

Activity Template
Template Copy of Harran Circulation
 Sector Residential spaces
 Zone type 1-Standard
 Zone multiplier 1
 Include zone in thermal calculations
 Include zone in Radiance daylighting calculations

Occupancy
 Occupied?
 Occupancy density (people/m2) 0.0155
 Schedule Winter on Summer off Kitchen

Metabolic
 Clothing
 Comfort Radiant Temperature Weighting
 Air Velocity
 Contaminant Generation and Removal
 DHW
 Environmental Control
 Heating Setpoint Temperatures
 Heating (°C) 18.0
 Heating set back (°C) 12.0
 Cooling Setpoint Temperatures
 Cooling (°C) 25.0
 Cooling set back (°C) 28.0
 Humidity Control
 Ventilation Setpoint Temperatures
 Minimum Fresh Air
 Lighting
 Computers
 On
 Office Equipment
 On
 Miscellaneous
 Catering
 Process

File Visualise Heating design Cooling design Simulation CFD Daylighting Cost and Carbon

Activity templates
 Data Report (Not Editable)

General
 Copy of Harran Circulation
 For all circulation areas within the dwelling.
 Source UK NCT
 Category Residential spaces
 Region General
 Sector Residential spaces
 Holidays No

Colour Shading in Model
 Floor shade colour

All Gains
 Power density (W/m2) 1.57

Occupancy details
 Occupancy density (people/m2) 0.0155
 Number of people 0.00

Metabolic Heat
 Metabolic rate Light manual work
 Metabolic factor (0.85 for women, 0.75 child) 0.90
 CO2 generation rate (m3/s-W) 0.000000382
 Latent fraction 0.5000

Clothing
 Clothing schedule definition 1-Generic summer an
 Winter clothing (clo) 1.00
 Summer clothing (clo) 0.50
 Clothing schedule Default clothing sched

Workday profile
 Occupancy From 7 to 23
 Days / week 5

Schedules
 Schedule Winter on Summer off

Computers
 On No

Office Equipment
 On No

Miscellaneous
 On Yes
 Power density (W/m2) 0.00
 Absolute zone power (W) 0.00

Schedules
 Schedule Dwell_DomCirculation

Catering
 On No

Process
 On No

General Lighting
 On Yes
 Workday profile From 7 to 23
 Equipment Schedules
 Schedule Dwell_DomCirculation

DHW
 On No

Heating
 Set point temperature (°C) 18.000
 Set back temperature (°C) 12.000
 Workday profile From 5 to 23
 Operation Schedules
 Schedule Dwell_DomCirculation

Cooling
 Set point temperature (°C) 25.000
 Cooling set back (°C) 28.000
 Workday profile From 5 to 23
 Operation Schedules
 Schedule Dwell_DomCirculation

Ventilation Set Point Temperatures
 Natural Ventilation Nat. vent set point (°C) 24.000
 Schedule Dwell_DomCirculation
 Mechanical Ventilation Mech. vent set point (°C) 10.000
 Off 24/7
 Schedule Dwell_DomCirculation

Lighting
 Target illuminance (lux) 100
 Default display lighting density (W/m2) 0.000

Ventilation Fresh Air
 Min fresh air (l/s-person) 10.000
 Mech vent per area (l/s-m2) 0.000

Activity Template
Template Copy of Harran Store Room
 Sector B8 Storage or Distribution
 Zone type 1-Standard
 Zone multiplier 1
 Include zone in thermal calculations
 Include zone in Radiance daylighting calculations

Occupancy
 Occupied?
 Occupancy density (people/m2) 0.1037
 Schedule Ware_Store_Occ

Metabolic
 Clothing
 Comfort Radiant Temperature Weighting
 Air Velocity
 Contaminant Generation and Removal
 DHW
 Environmental Control
 Heating Setpoint Temperatures
 Heating (°C) 18.0
 Heating set back (°C) 12.0
 Cooling Setpoint Temperatures
 Cooling (°C) 25.0
 Cooling set back (°C) 28.0
 Humidity Control
 Ventilation Setpoint Temperatures
 Minimum Fresh Air
 Lighting
 Computers
 On
 Office Equipment
 On
 Miscellaneous
 Catering
 Process

File Visualise Heating design Cooling design Simulation CFD Daylighting Cost and Carbon

Activity templates
 Data Report (Not Editable)

General
 Copy of Harran Store Room
 Areas for un-chilled goods storage with low transient occupancy.
 Source UK NCT
 Category Storage or Distribution
 Region General
 Sector B8 Storage or Distribut
 Holidays No

Colour Shading in Model
 Floor shade colour

All Gains
 Power density (W/m2) 0.00

Occupancy details
 Occupancy density (people/m2) 0.1037
 Number of people 0.00

Metabolic Heat
 Metabolic rate Standing/walking
 Metabolic factor (0.85 for women, 0.75 child) 0.90
 CO2 generation rate (m3/s-W) 0.000000382
 Latent fraction 0.5000

Clothing
 Clothing schedule definition 1-Generic summer an
 Winter clothing (clo) 1.00
 Summer clothing (clo) 0.50
 Clothing schedule Default clothing sched

Workday profile
 Occupancy From 8 to 18
 Days / week 7

Schedules
 Schedule Ware_Store_Occ

Computers
 On No

Office Equipment
 On No

Miscellaneous
 On No

Catering
 On No

Computers
 On No

Office Equipment
 On No

Miscellaneous
 On No

Catering
 On No

Process
 On No

General Lighting
 On No

DHW
 On No

Heating
 Set point temperature (°C) 18.000
 Set back temperature (°C) 12.000
 Workday profile From 6 to 18
 Operation Schedules
 Schedule Ware_Store_Heat

Cooling
 Set point temperature (°C) 25.000
 Cooling set back (°C) 28.000
 Workday profile From 6 to 18
 Operation Schedules
 Schedule Ware_Store_Cool

Ventilation Set Point Temperatures
 Natural Ventilation Nat. vent set point (°C) 24.000
 Schedule Ware_Store_Occ
 Mechanical Ventilation Mech. vent set point (°C) 10.000
 Ware_Store_Occ
 Schedule Ware_Store_Occ

Lighting
 Target illuminance (lux) 50
 Default display lighting density (W/m2) 0.100

Ventilation Fresh Air
 Min fresh air (l/s-person) 10.000
 Mech vent per area (l/s-m2) 0.000

Activity Template
Template Harran WC
 Sector Residential spaces
 Zone type 1-Standard
 Zone multiplier 1
 Include zone in thermal calculations
 Include zone in Radiance daylighting calculations

Occupancy
 Occupied?
 Occupancy density (people/m2) 0.0243
 Schedule Dwell_DomToilet_Occ

Metabolic
 Clothing
 Comfort Radiant Temperature Weighting
 Air Velocity
 Contaminant Generation and Removal
 DHW
 Environmental Control
 Heating Setpoint Temperatures
 Heating (°C) 18.0
 Heating set back (°C) 12.0
 Cooling Setpoint Temperatures
 Cooling (°C) 25.0
 Cooling set back (°C) 28.0
 Humidity Control
 Ventilation Setpoint Temperatures
 Minimum Fresh Air
 Lighting
 Computers
 On
 Office Equipment
 On
 Miscellaneous
 Catering
 Process

File Visualise Heating design Cooling design Simulation CFD Daylighting Cost and Carbon

Activity templates
 Data Report (Not Editable)

General
 Harran WC
 An area containing a toilet and basin which is separate from the main
 Source UK NCT
 Category Residential spaces
 Region General
 Sector Residential spaces
 Holidays No

Colour Shading in Model
 Floor shade colour

All Gains
 Power density (W/m2) 1.61

Occupancy details
 Occupancy density (people/m2) 0.0243
 Number of people 0.00

Metabolic Heat
 Metabolic rate Standing/walking
 Metabolic factor (0.85 for women, 0.75 child) 0.90
 CO2 generation rate (m3/s-W) 0.000000382
 Latent fraction 0.5000

Clothing
 Clothing schedule definition 1-Generic summer an
 Winter clothing (clo) 1.00
 Summer clothing (clo) 0.50
 Clothing schedule Default clothing sched

Workday profile
 Occupancy From 6 to 22
 Days / week 7

Schedules
 Schedule Dwell_DomToilet_Oc

Computers
 On No

Office Equipment
 On No

Miscellaneous
 On No

Catering
 On No

General Lighting
 On Yes
 Workday profile From 6 to 22
 Equipment Schedules
 Schedule Dwell_DomToilet_Lig

DHW
 On Yes
 Consumption rate (l/m2-day) 4.850
 Workday profile From 6 to 22
 Operation Schedules
 Schedule Dwell_DomToilet_Oc

Heating
 Set point temperature (°C) 18.000
 Set back temperature (°C) 12.000
 Workday profile From 4 to 22
 Operation Schedules
 Schedule Dwell_DomToilet_He

Cooling
 Set point temperature (°C) 25.000
 Cooling set back (°C) 28.000
 Workday profile From 4 to 22
 Operation Schedules
 Schedule Dwell_DomToilet_Co

Ventilation Set Point Temperatures
 Natural Ventilation Nat. vent set point (°C) 24.000
 Schedule Dwell_DomToilet_Oc
 Mechanical Ventilation Mech. vent set point (°C) 10.000
 Off 24/7
 Schedule Dwell_DomToilet_Oc

Lighting
 Target illuminance (lux) 100
 Default display lighting density (W/m2) 0.000

Ventilation Fresh Air
 Min fresh air (l/s-person) 12.000
 Mech vent per area (l/s-m2) 0.000

1.4 Construction inputs

Data Report (Not Editable)

General

Base corners

Source: DesignBuilder
Roofs: TURKEY
Region: TURKEY
Colour:

Definition

Definition method: 1-Layers

Calculation Settings

Simulation solution algorithm: 1-Default
Involves metal cladding: No

Layers

Number of layers: 2

Outermost layer

Mud Mortar with Straw
Thickness (m): 0.3000
Bridged?: No

Innermost layer

Stone - sandstone
Thickness (m): 0.2000
Bridged?: No

Outside Surface

Fix convective heat transfer coefficient: No

Inside Surface

Fix convective heat transfer coefficient: No

Cross Section

Inner surface

Convective heat transfer coefficient (W/m ² K)	4.460
Radiative heat transfer coefficient (W/m ² K)	5.540
Surface resistance (m ² K/W)	0.100

Outer surface

Convective heat transfer coefficient (W/m ² K)	19.870
Radiative heat transfer coefficient (W/m ² K)	5.130
Surface resistance (m ² K/W)	0.040

No Bridging

U-Value surface to surface (W/m ² K)	0.759
R-Value (m ² K/W)	1.457
U-Value (W/m ² K)	0.686

With Bridging (BS EN ISO 6946)

Thickness (m)	0.5000
Upper resistance limit (m ² K/W)	1.457
Lower resistance limit (m ² K/W)	1.457
U-Value surface to surface (W/m ² K)	0.759
R-Value (m ² K/W)	1.457
U-Value (W/m ² K)	0.686

Cost

Cost type: 1-Auto-calculate

Data Report (Not Editable)

General

Vernacular Harran Floor

Source: Internal/External Slabs
Category: Slabs
Region: TURKEY
Colour:

Definition

Definition method: 1-Layers

Calculation Settings

Simulation solution algorithm: 1-Default
Involves metal cladding: No

Layers

Number of layers: 3

Outermost layer

Mud Mortar with Straw
Thickness (m): 0.2000
Bridged?: No

Layer 2

Sun Dried Adobe Brick
Thickness (m): 0.2000
Bridged?: No

Innermost layer

Miscellaneous materials - aggregate Undred
Thickness (m): 1.5000
Bridged?: No

Outside Surface

Fix convective heat transfer coefficient: No

Inside Surface

Fix convective heat transfer coefficient: No

Cross Section

Inner surface

Convective heat transfer coefficient (W/m ² K)	4.460
Radiative heat transfer coefficient (W/m ² K)	5.540
Surface resistance (m ² K/W)	0.100

Outer surface

Convective heat transfer coefficient (W/m ² K)	0.342
Radiative heat transfer coefficient (W/m ² K)	5.540
Surface resistance (m ² K/W)	0.170

No Bridging

U-Value surface to surface (W/m ² K)	0.368
R-Value (m ² K/W)	3.048
U-Value (W/m ² K)	0.328

With Bridging (BS EN ISO 6946)

Thickness (m)	1.9000
Upper resistance limit (m ² K/W)	3.048
Lower resistance limit (m ² K/W)	3.048
U-Value surface to surface (W/m ² K)	0.368
R-Value (m ² K/W)	3.048
U-Value (W/m ² K)	0.328

Cost

Cost type: 1-Auto-calculate

Data Report (Not Editable)

General

Vernacular External Walls

Source: Walls
Category: Walls
Region: TURKEY
Colour:

Definition

Definition method: 1-Layers

Calculation Settings

Simulation solution algorithm: 1-Default
Involves metal cladding: No

Layers

Number of layers: 3

Outermost layer

Mud Mortar with Straw
Thickness (m): 0.0500
Bridged?: No

Layer 2

Sun Dried Adobe Brick
Thickness (m): 0.6000
Bridged?: No

Innermost layer

Mud Mortar with Straw
Thickness (m): 0.0500
Bridged?: No

Outside Surface

Fix convective heat transfer coefficient: No

Inside Surface

Fix convective heat transfer coefficient: No

Cross Section

Inner surface

Convective heat transfer coefficient (W/m ² K)	2.152
Radiative heat transfer coefficient (W/m ² K)	5.540
Surface resistance (m ² K/W)	0.130

Outer surface

Convective heat transfer coefficient (W/m ² K)	19.870
Radiative heat transfer coefficient (W/m ² K)	5.130
Surface resistance (m ² K/W)	0.040

No Bridging

U-Value surface to surface (W/m ² K)	0.267
R-Value (m ² K/W)	3.920
U-Value (W/m ² K)	0.255

With Bridging (BS EN ISO 6946)

Thickness (m)	0.7000
Upper resistance limit (m ² K/W)	3.920
Lower resistance limit (m ² K/W)	3.920
U-Value surface to surface (W/m ² K)	0.267
R-Value (m ² K/W)	3.920
U-Value (W/m ² K)	0.255

Cost

Cost type: 1-Auto-calculate

Data Report (Not Editable)

General

Dome Walls

Source: Walls
Category: Walls
Region: TURKEY
Colour:

Definition

Definition method: 1-Layers

Calculation Settings

Simulation solution algorithm: 1-Default
Involves metal cladding: No

Layers

Number of layers: 3

Outermost layer

Mud Mortar with Straw
Thickness (m): 0.0500
Bridged?: No

Layer 2

Sun Dried Adobe Brick
Thickness (m): 0.3000
Bridged?: No

Innermost layer

Mud Mortar with Straw
Thickness (m): 0.0500
Bridged?: No

Outside Surface

Fix convective heat transfer coefficient: No

Inside Surface

Fix convective heat transfer coefficient: No

Cross Section

Inner surface

Convective heat transfer coefficient (W/m ² K)	2.152
Radiative heat transfer coefficient (W/m ² K)	5.540
Surface resistance (m ² K/W)	0.130

Outer surface

Convective heat transfer coefficient (W/m ² K)	19.870
Radiative heat transfer coefficient (W/m ² K)	5.130
Surface resistance (m ² K/W)	0.040

No Bridging

U-Value surface to surface (W/m ² K)	0.480
R-Value (m ² K/W)	2.253
U-Value (W/m ² K)	0.444

With Bridging (BS EN ISO 6946)

Thickness (m)	0.4000
Upper resistance limit (m ² K/W)	2.253
Lower resistance limit (m ² K/W)	2.253
U-Value surface to surface (W/m ² K)	0.480
R-Value (m ² K/W)	2.253
U-Value (W/m ² K)	0.444

Cost

Cost type: 1-Auto-calculate

Construction Template

Template Vernacular Construction

Construction

- External walls: Vernacular External Walls
- Below grade walls: Vernacular External Walls
- Flat roof: Base corners
- Pitched roof (occupied): Pitched roof - Energy code standard - Medium weight
- Pitched roof (unoccupied): Clay tiles (25mm) on air gap (20mm) on roofing felt (5mm)
- Internal partitions: Vernacular External Walls

Semi-Exposed

- Semi-exposed walls: Vernacular External Walls
- Semi-exposed ceiling: Base corners
- Semi-exposed floor: Vernacular Harran Floor

Floors

- Ground floor: Vernacular Harran Floor
- External floor: Vernacular Harran Floor
- Internal floor: Vernacular Harran Floor

Sub-Surfaces

- Internal Thermal Mass
- Component Block
- Geometry, Areas and Volumes
- Surface Convection
- Linear Thermal Bridging at Junctions

Airtightness

- Model infiltration
 - Constant rate (ac/h): 0.500
 - Schedule: On 24/7
- Delta T and Wind Speed Coefficients

Cost

Construction Template

Template Vernacular Construction Domes

Construction

- External walls: Dome Walls
- Below grade walls: Dome Walls
- Flat roof: Dome Walls
- Pitched roof (occupied): Dome Walls
- Pitched roof (unoccupied): Dome Walls
- Internal partitions: Dome Walls

Semi-Exposed

- Semi-exposed walls: Dome Walls
- Semi-exposed ceiling: Dome Walls
- Semi-exposed floor: Dome Walls

Floors

- Ground floor: Vernacular Harran Floor
- External floor: Vernacular Harran Floor
- Internal floor: Vernacular Harran Floor

Sub-Surfaces

- Internal Thermal Mass
- Geometry, Areas and Volumes
- Surface Convection
- Linear Thermal Bridging at Junctions

Airtightness

- Model infiltration
 - Constant rate (ac/h): 0.500
 - Schedule: On 24/7
- Delta T and Wind Speed Coefficients

Cost

1.5 Lighting

Lighting Template

Template <None>

General Lighting

- On

Task and Display Lighting

- On

Exterior Lighting

- On

Cost

1.6 Openings inputs

Glazing Template

Template No windows

External Windows

Glazing type Sgl Clr 3mm

Layout Preferred height 1.5m, 30% glazed

Dimensions

Type	3-Preferred height
Window to wall %	30.00
Window height (m)	1.50
Window spacing (m)	5.00
Sill height (m)	0.80
Outside reveal depth (m)	0.000

Frame and Dividers

Shading

Window shading

Local shading

Airflow Control Windows

Airflow control

Free Aperture

Opening position	1-Top
% Glazing area opens	5

Internal Windows

Sloped Roof Windows/Skylights

Doors

Vents

1.7 HVAC inputs

HVAC Template

Template Natural ventilation - No Heating/Cooling

Mechanical Ventilation

On

Auxiliary Energy

Pump etc energy (W/m²) 0.0000

Schedule Residential Occ

Heating

Heated

Cooling

Cooled

Humidity Control

DHW

On

Natural Ventilation

On

Outside air definition method 1-By zone

Outside air (ac/h) 10.000

Operation

Schedule On always

Outdoor Temperature Limits

Delta T Limits

Delta T and Wind Speed Coefficients

Mixed Mode Zone Equipment

Mixed mode on

Earth Tube

Air Temperature Distribution

Cost

HVAC templates

Data Report (Not Editable)

General

Natural ventilation - No Heating/Cooling

Source DB

Category Generic

Region General

Simple

Auxiliary energy (kWh/m²) 0.00

Colour Shading in Model

Floor shade colour

Natural Ventilation

On Yes

Rate (ac/h) 5.00

Design flow rate (m³/s) 0.10000000

Mixed mode on No

Mechanical Ventilation

On No

Heating

On No

Cooling

Cooling On No

Humidification

Humidification No

Dehumidification

Dehumidification No

Air Temperature Distribution

Distribution mode 1-Mixed

Interpolation mode 3-Inside-outside Delta

Upper Conditions

Temperature (°C) 10.00

Heat rate (W) 1000.00

Temperature gradient (°C/m) 1.00

Lower Conditions

Temperature (°C) 0.00

Heat rate (W) 0.00

Temperature gradient (°C/m) 0.00

Heights

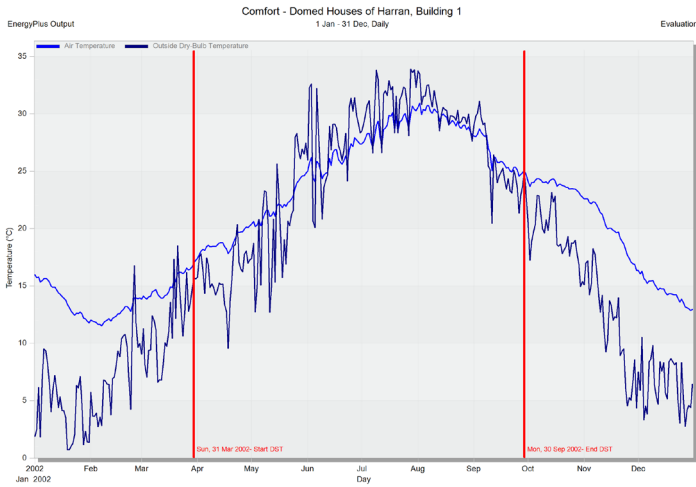
Thermostat height (m) 1.50

Return air height (m) 3.50

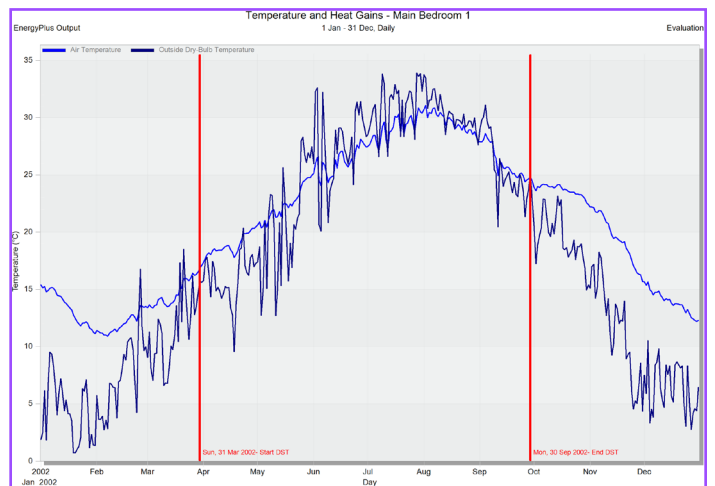
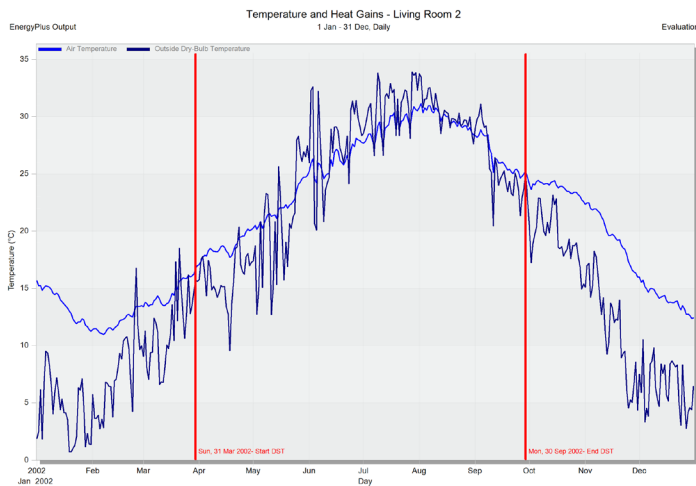
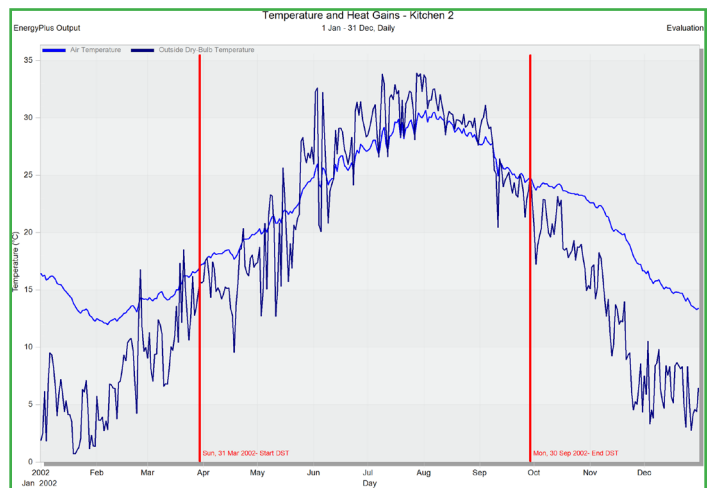
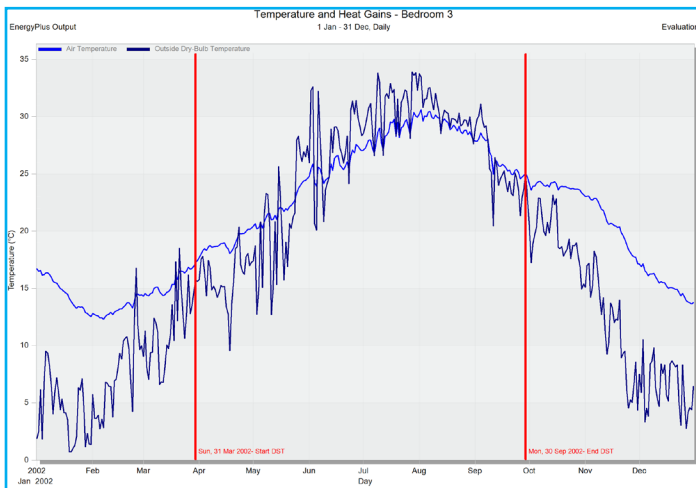
Edt Visualise Heating design Cooling design Simulation CFD Daylighting Cost and Carbon

Appendix 2: Base model outputs

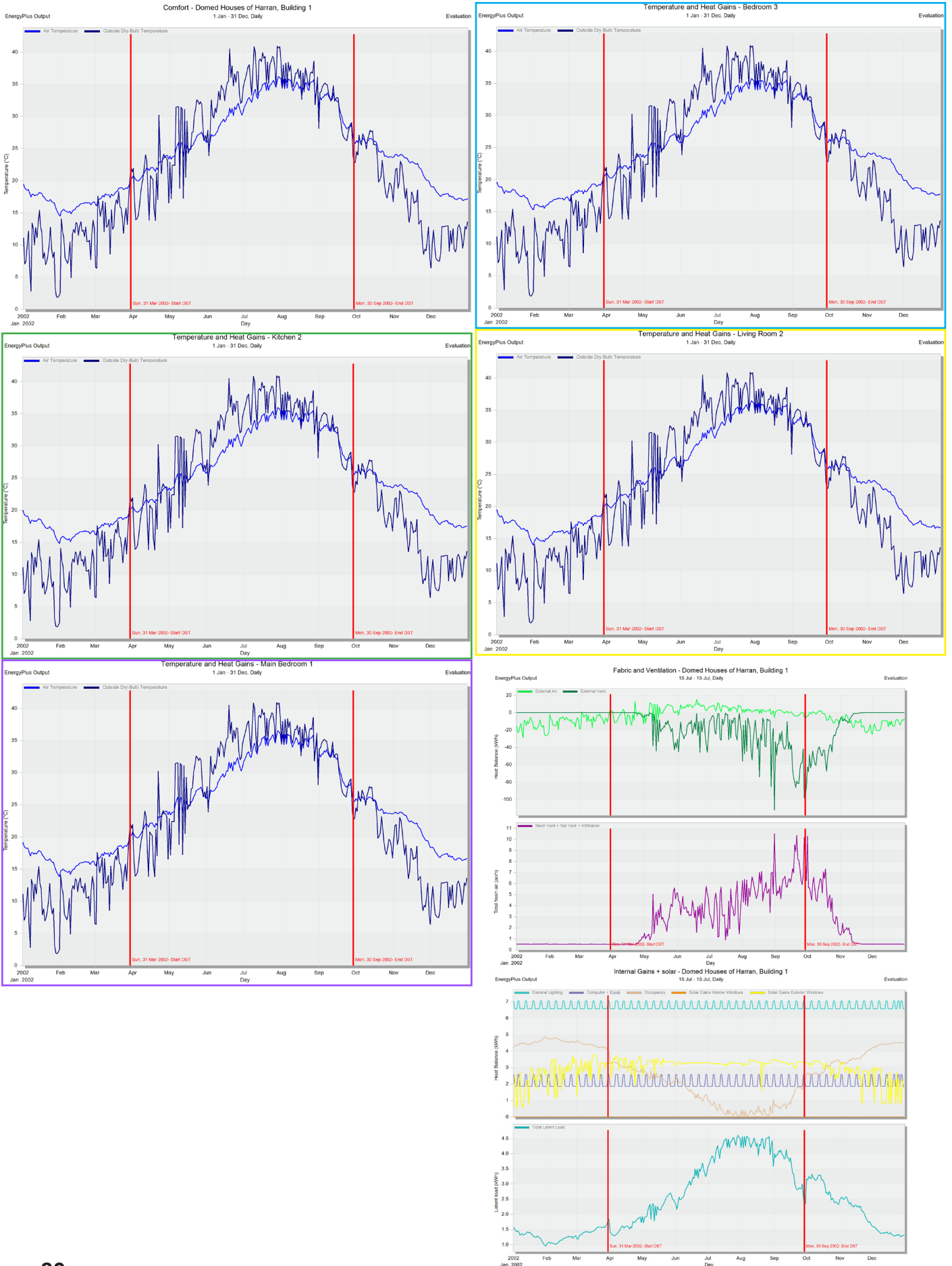
2.1 Current climate



- █ = Living room 2 (LR2)
- █ = Bedroom 3 (B3)
- █ = Kitchen 2 (K2)
- █ = Main Bedroom 1 (MB1)



2.2 2080 climate

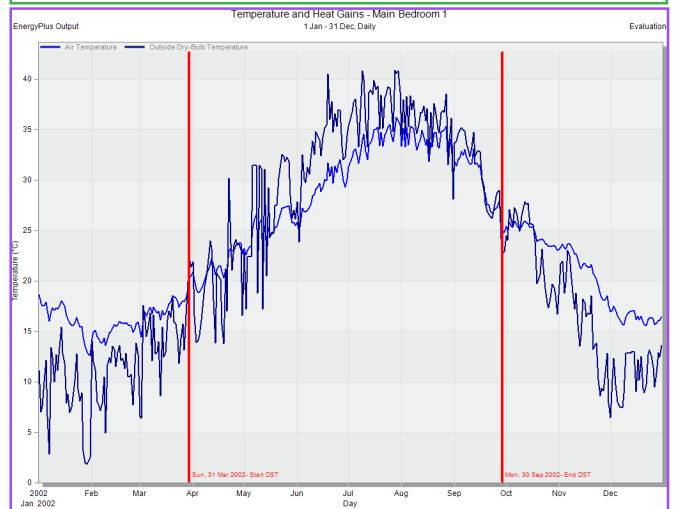
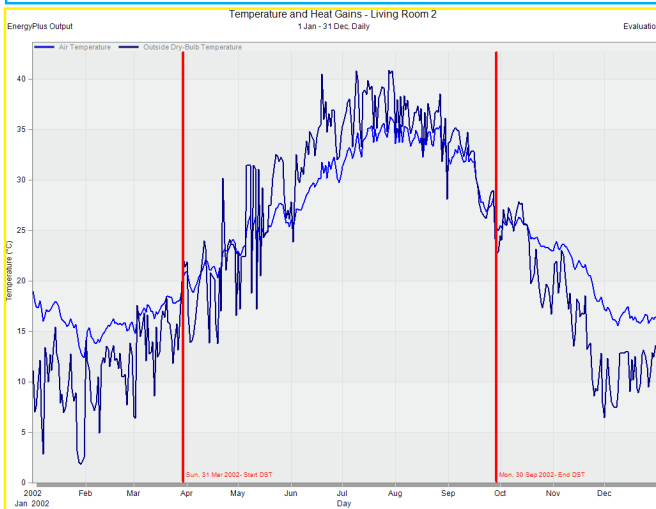
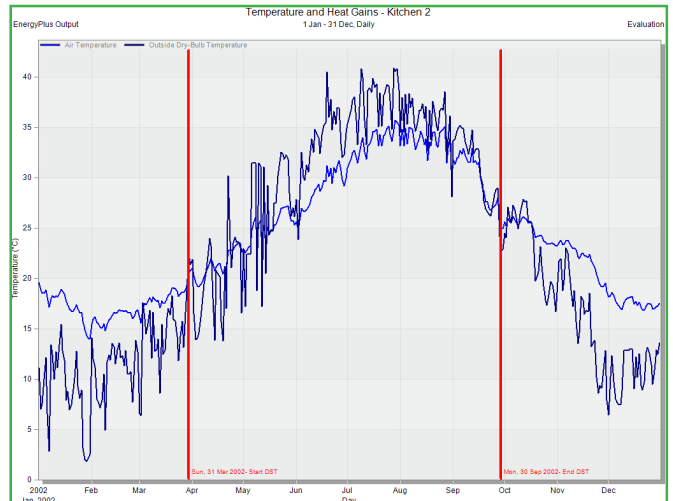
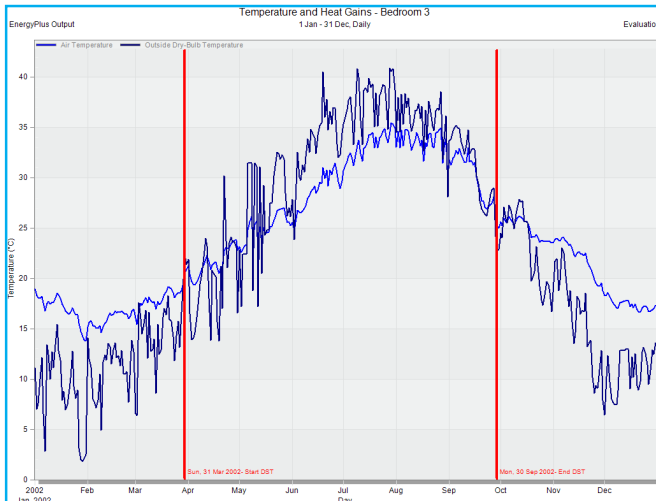
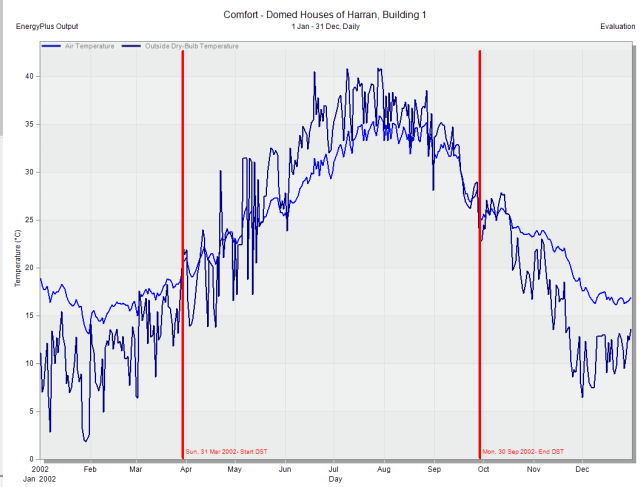




Appendix 3: Construction changes

3.1 Turkish Standard Construction inputs and outputs

General		Cross Section	
Turkish Standard			
Source		Walls	
Category		TURKEY	
Region			
Colour			
Definition			
Definition method	1-Layers		
Calculation Settings			
Simulation solution algorithm	1-Default		
Involves metal cladding	No		
Layers			
Number of layers	4		
Outermost layer			
Plaster (Lightweight)		Inner surface	
Thickness (m)	0.0200	Convective heat transfer coefficient (W/m ² -K)	2.152
Bridged?	No	Radiative heat transfer coefficient (W/m ² -K)	5.540
Layer 2			
Aerated Concrete Slab		Surface resistance (m ² -K/W)	0.130
Thickness (m)	0.2000	Outer surface	
Bridged?	No	Convective heat transfer coefficient (W/m ² -K)	19.870
Layer 3			
Mineral fibre/wool - wool		Radiative heat transfer coefficient (W/m ² -K)	5.130
Thickness (m)	0.0600	Surface resistance (m ² -K/W)	0.040
Bridged?	No	No Bridging	
Innermost layer			
Plaster (Lightweight)		U-Value surface to surface (W/m ² -K)	0.325
Thickness (m)	0.0200	R-Value (m ² -K/W)	3.249
Bridged?	No	U-Value (W/m ² -K)	0.308
Outside Surface			
Fix convective heat transfer coefficient	No	With Bridging (BS EN ISO 6946)	
Inside Surface			
Fix convective heat transfer coefficient	No	Thickness (m)	0.3000
		Upper resistance limit (m ² -K/W)	3.249
		Lower resistance limit (m ² -K/W)	3.249
		U-Value surface to surface (W/m ² -K)	0.325
		R-Value (m ² -K/W)	3.249
		U-Value (W/m²-K)	0.308
Cost			
Cost type	1-Auto-calculate		



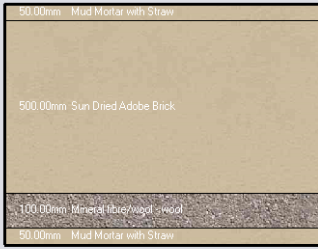
3.2 Addition of insulation inputs and outputs

Outside Surface
Fix convective heat transfer coefficient No

Inside Surface
Fix convective heat transfer coefficient No

Cross Section

Outer surface



Inner surface

Inner surface

Convective heat transfer coefficient (...) 2.152
Radiative heat transfer coefficient (W/m²·K) 5.540
Surface resistance (m²·K/W) 0.130

Outer surface

Convective heat transfer coefficient (...) 19.870
Radiative heat transfer coefficient (W/m²·K) 5.130
Surface resistance (m²·K/W) 0.040

No Bridging

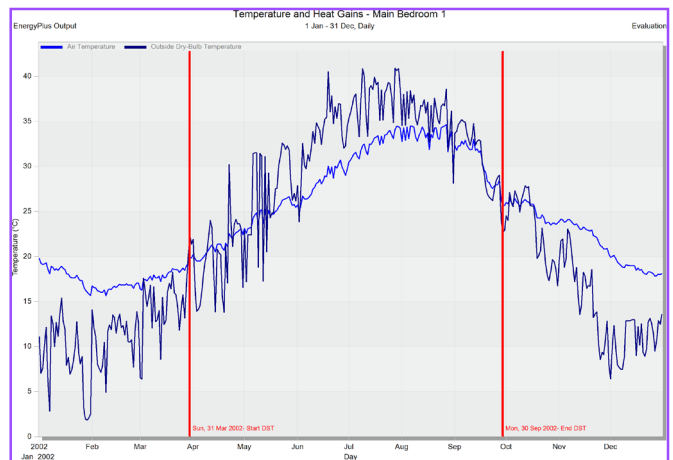
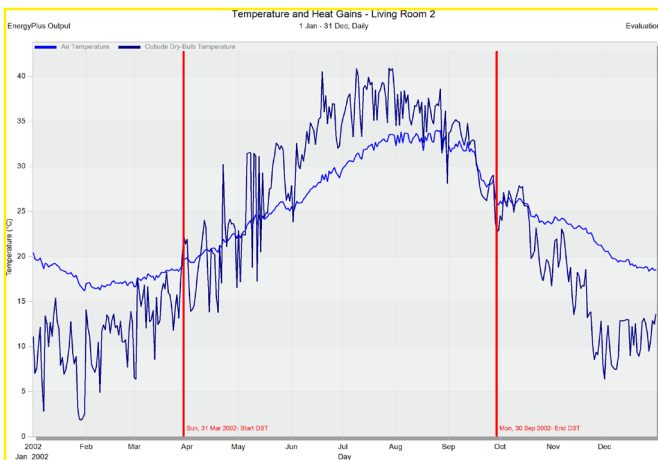
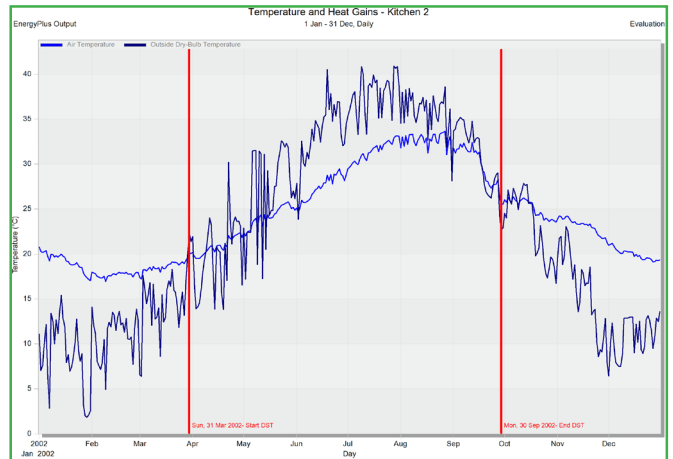
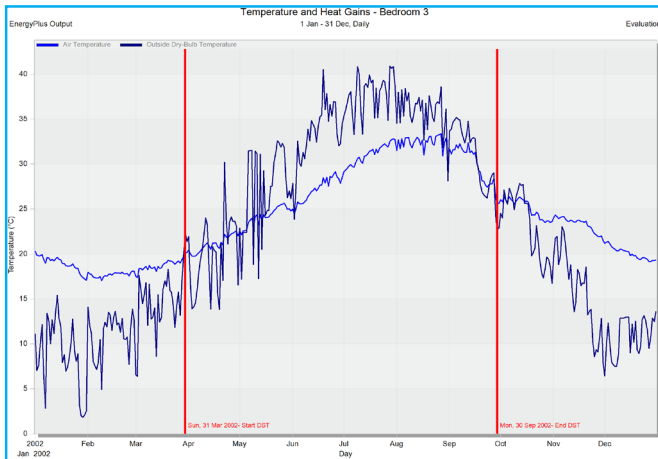
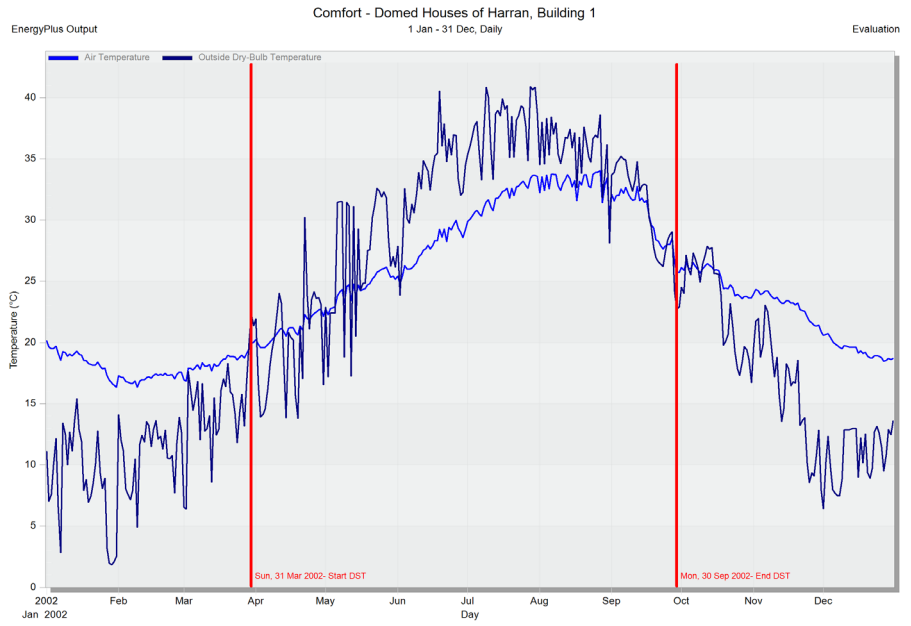
U-Value surface to surface (W/m²·K) 0.172
R-Value (m²·K/W) 5.996
U-Value (W/m²·K) 0.167

With Bridging (BS EN ISO 6946)

Thickness (m) 0.7000
Upper resistance limit (m²·K/W) 5.996
Lower resistance limit (m²·K/W) 5.996
U-Value surface to surface (W/m²·K) 0.172
R-Value (m²·K/W) 5.996
U-Value (W/m²·K) 0.167

Cost

Cost type 1-Auto-calculate



3.3 Addition of reflective material inputs and outputs

Outside Surface
 Fix convective heat transfer coefficient No

Inside Surface
 Fix convective heat transfer coefficient No

Cross Section
 Outer surface
 20.00mm Copy of Stone - white calcareous stone Firm, dry(not to scale)
 50.00mm Mud Mortar with Straw(not to scale)
 600.00mm Sun Dried Adobe Brick
 50.00mm Mud Mortar with Straw(not to scale)
 Inner surface

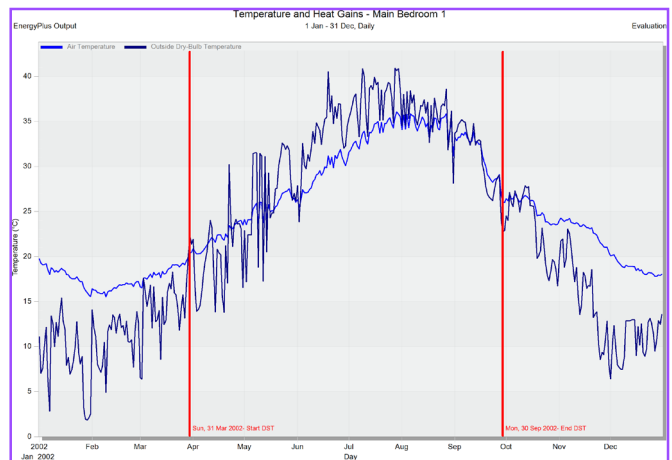
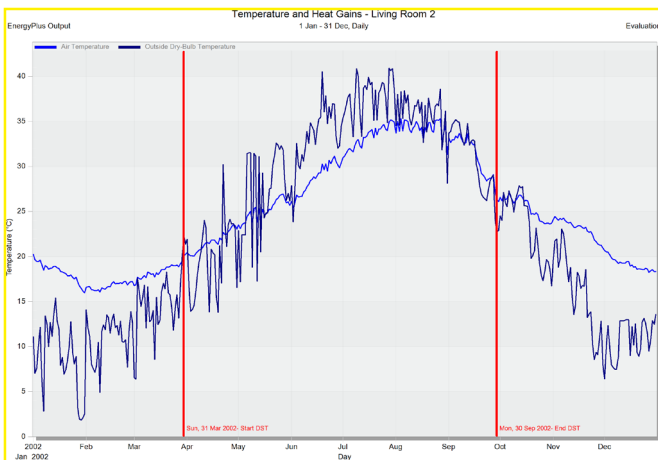
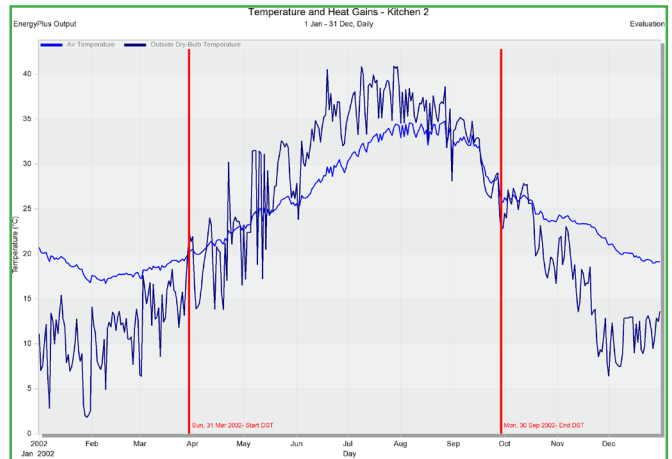
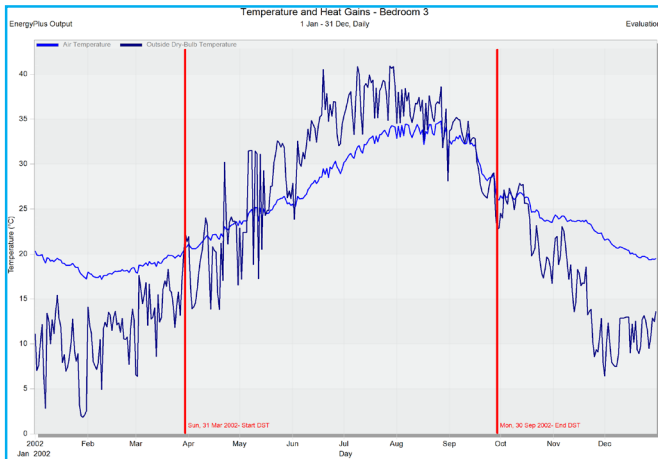
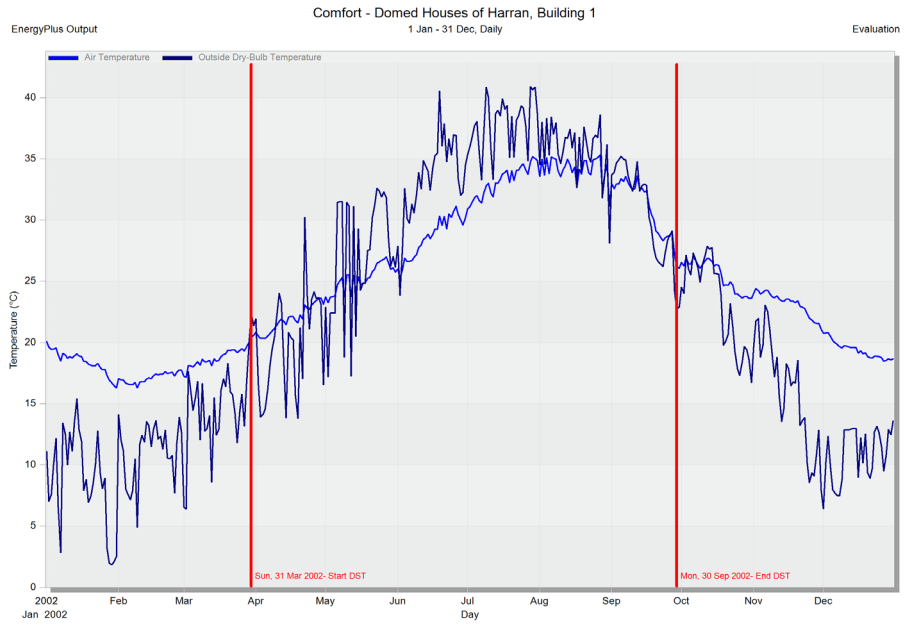
Inner surface
 Convective heat transfer coefficient (...) 2.152
 Radiative heat transfer coefficient (W/m²K) 5.540
 Surface resistance (m²K/W) 0.130

Outer surface
 Convective heat transfer coefficient (...) 19.357
 Radiative heat transfer coefficient (W/m²K) 5.643
 Surface resistance (m²K/W) 0.040

No Bridging
 U-Value surface to surface (W/m²K) 0.266
 R-Value (m²K/W) 3.931
 U-Value (W/m²K) 0.254

With Bridging (BS EN ISO 6946)
 Thickness (m) 0.7200
 Upper resistance limit (m²K/W) 3.931
 Lower resistance limit (m²K/W) 3.931
 U-Value surface to surface (W/m²K) 0.266
 R-Value (m²K/W) 3.931
U-Value (W/m²K) 0.254

Cost
 Cost type 1-Auto-calculate




3.4 Concrete as thermal mass inputs and outputs

Outside Surface
 Fix convective heat transfer coefficient No

Inside Surface
 Fix convective heat transfer coefficient No

Cross Section



Outer surface

50.00mm Mud Mortar with Straw

600.00mm Concrete

50.00mm Mud Mortar with Straw

Inner surface

Inner surface

Convective heat transfer coefficient (...) 2.152
 Radiative heat transfer coefficient (W/m²K) 5.540
 Surface resistance (m²K/W) 0.130

Outer surface

Convective heat transfer coefficient (...) 19.870
 Radiative heat transfer coefficient (W/m²K) 5.130
 Surface resistance (m²K/W) 0.040

No Bridging

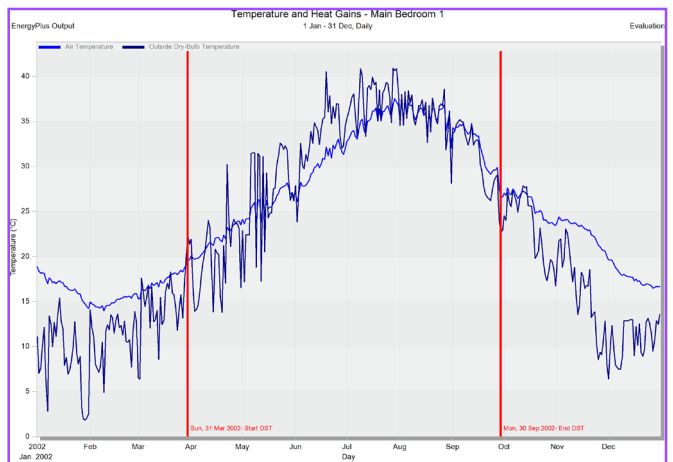
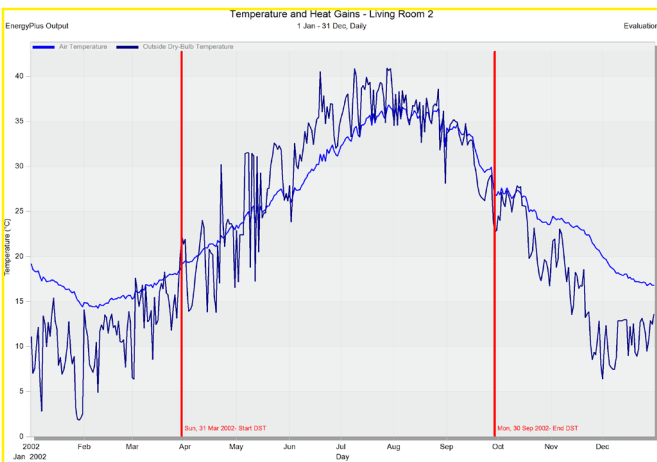
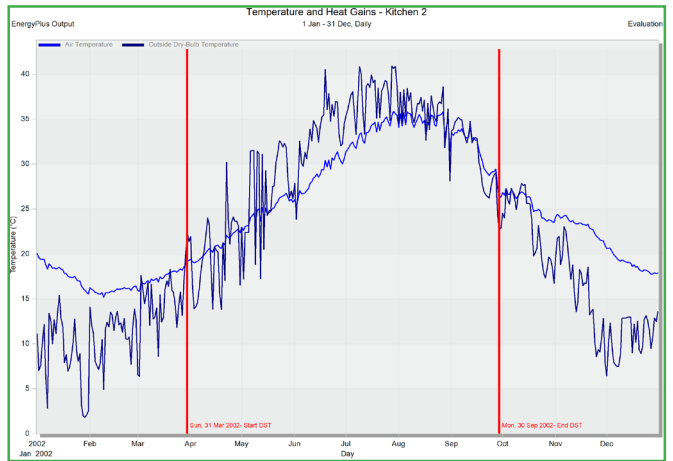
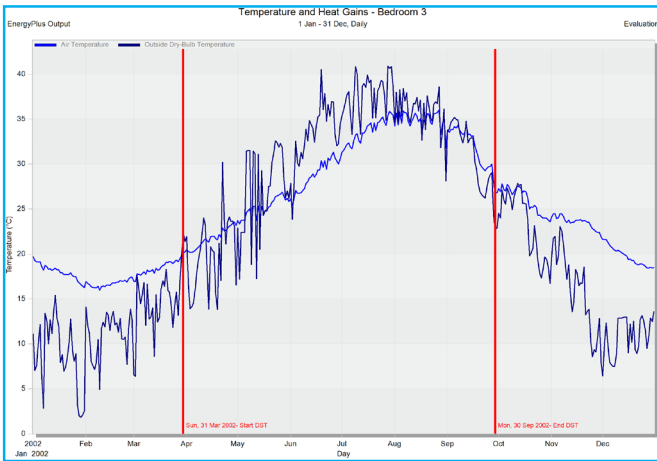
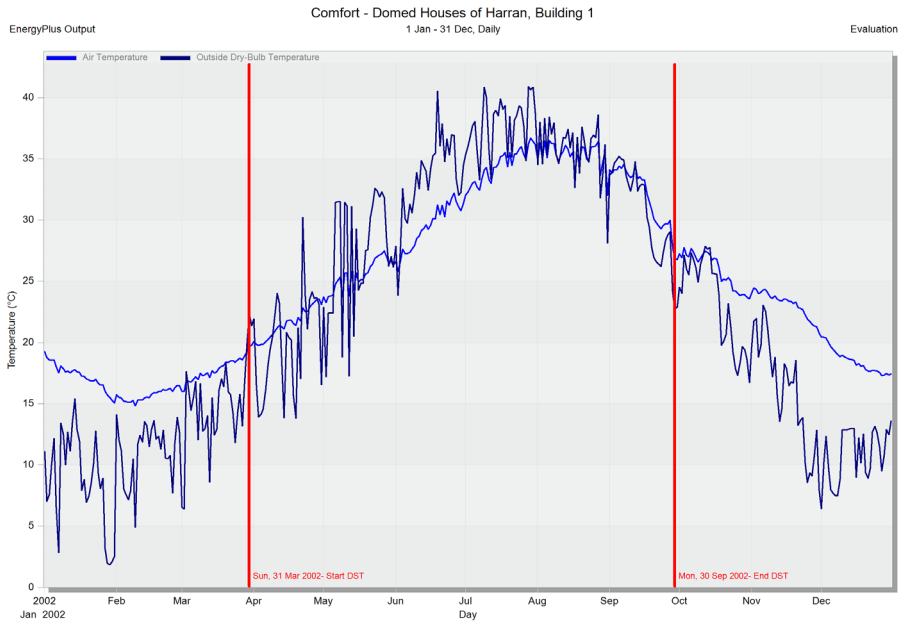
U-Value surface to surface (W/m²K) 0.730
 R-Value (m²K/W) 1.539
 U-Value (W/m²K) 0.650

With Bridging (BS EN ISO 6946)

Thickness (m) 0.7000
 Upper resistance limit (m²K/W) 1.539
 Lower resistance limit (m²K/W) 1.539
 U-Value surface to surface (W/m²K) 0.730
 R-Value (m²K/W) 1.539
U-Value (W/m²K) 0.650

Cost

Cost type 1-Auto-calculate




3.5 Stone as thermal mass inputs and outputs

Outside Surface
Fix convective heat transfer coefficient No

Inside Surface
Fix convective heat transfer coefficient No

Cross Section

Outer surface



Inner surface

Inner surface

- Convective heat transfer coefficient (...) 2.152
- Radiative heat transfer coefficient (W/m2-K) 5.540
- Surface resistance (m2-K/W) 0.130

Outer surface

- Convective heat transfer coefficient (...) 19.870
- Radiative heat transfer coefficient (W/m2-K) 5.130
- Surface resistance (m2-K/W) 0.040

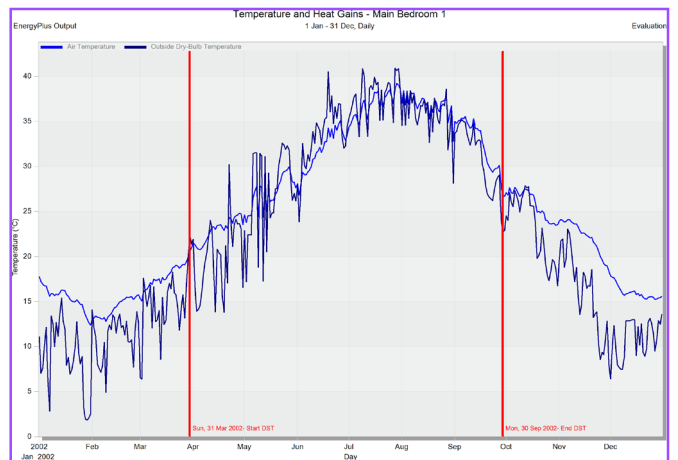
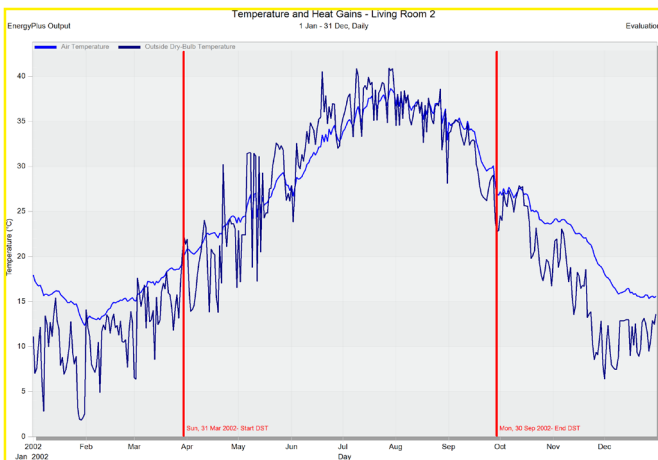
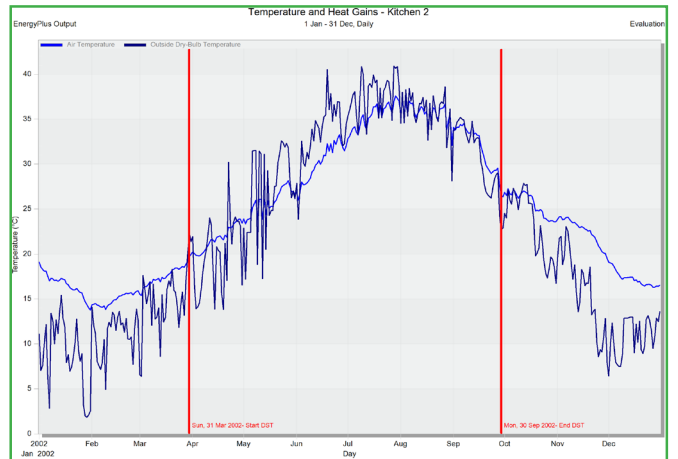
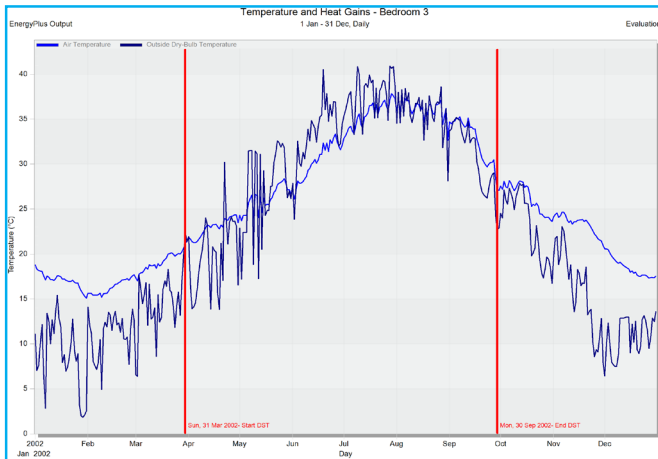
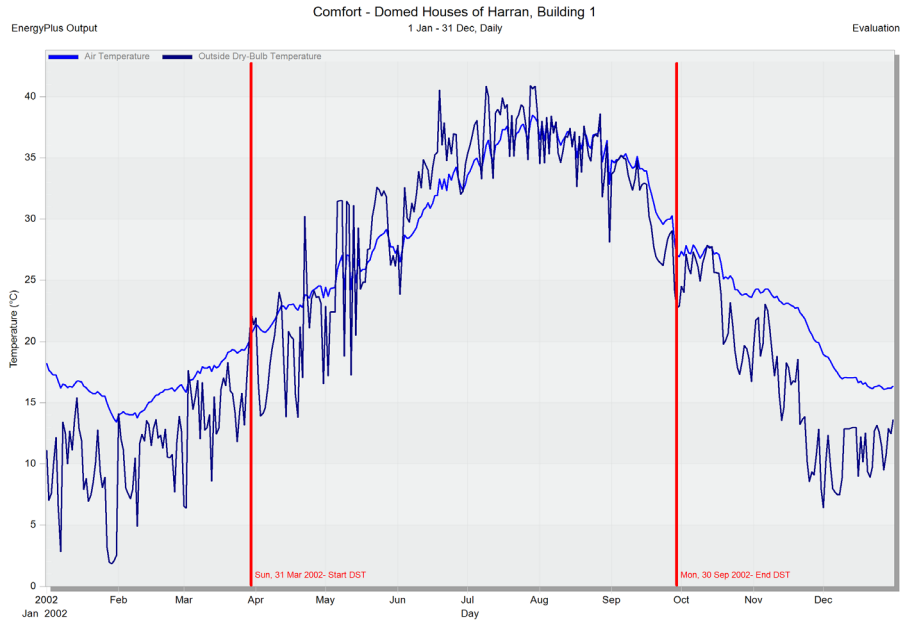
No Bridging

- U-Value surface to surface (W/m2-K) 1.699
- R-Value (m2-K/W) 0.759
- U-Value (W/m2-K) 1.318

With Bridging (BS EN ISO 6946)

- Thickness (m) 0.7000
- Upper resistance limit (m2-K/W) 0.759
- Lower resistance limit (m2-K/W) 0.759
- U-Value surface to surface (W/m2-K) 1.699
- R-Value (m2-K/W) 0.759
- U-Value (W/m2-K) 1.318

Cost
Cost type 1-Auto-calculate




3.6 300mm envelope with insulation inputs and outputs

Outside Surface
Fix convective heat transfer coefficient No

Inside Surface
Fix convective heat transfer coefficient No

Cross Section

Outer surface



Inner surface

Inner surface

- Convective heat transfer coefficient (...) 2.152
- Radiative heat transfer coefficient (W/m²K) 5.540
- Surface resistance (m²K/W) 0.130

Outer surface

- Convective heat transfer coefficient (...) 19.870
- Radiative heat transfer coefficient (W/m²K) 5.130
- Surface resistance (m²K/W) 0.040

No Bridging

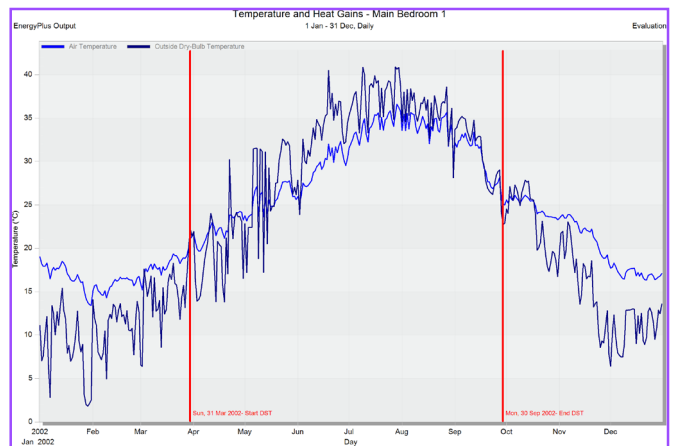
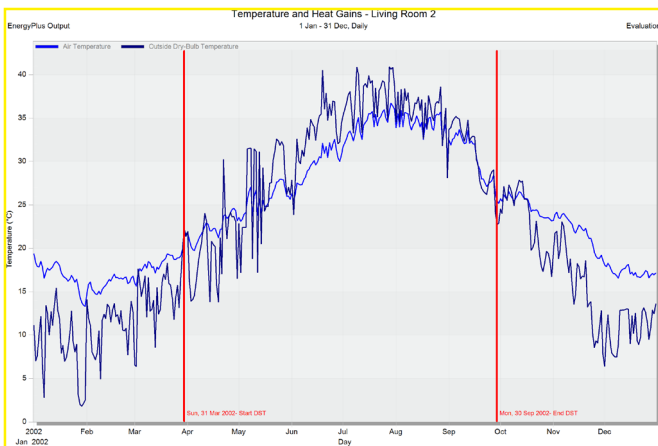
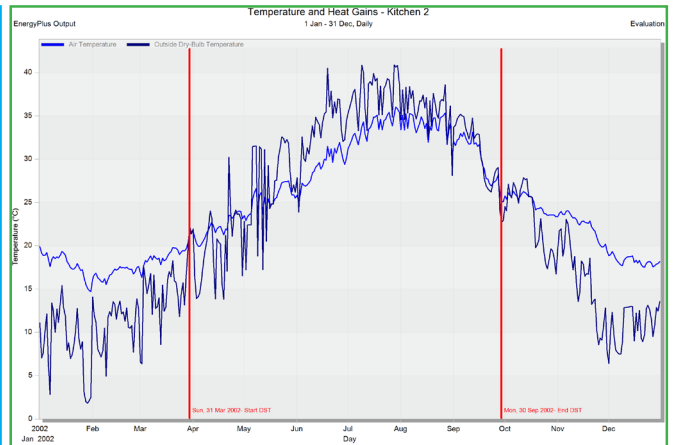
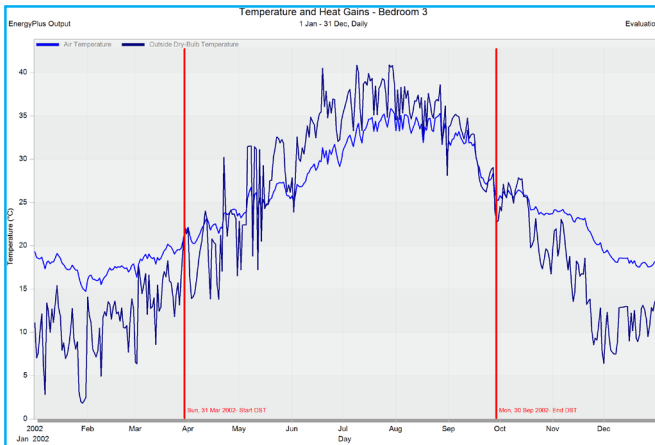
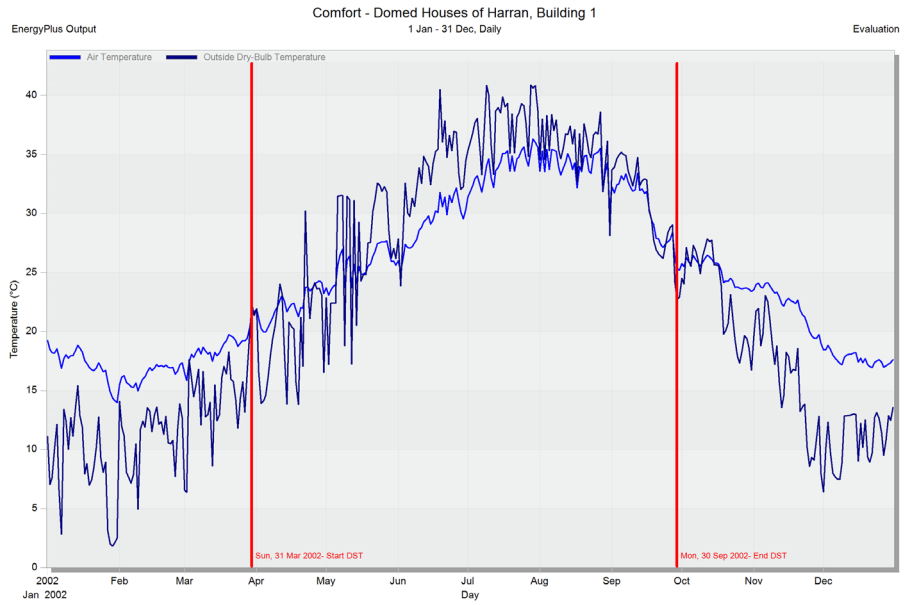
- U-Value surface to surface (W/m²K) 0.277
- R-Value (m²K/W) 3.774
- U-Value (W/m²K) 0.265

With Bridging (BS EN ISO 6946)

- Thickness (m) 0.3000
- Upper resistance limit (m²K/W) 3.774
- Lower resistance limit (m²K/W) 3.774
- U-Value surface to surface (W/m²K) 0.277
- R-Value (m²K/W) 3.774
- U-Value (W/m²K) 0.265**

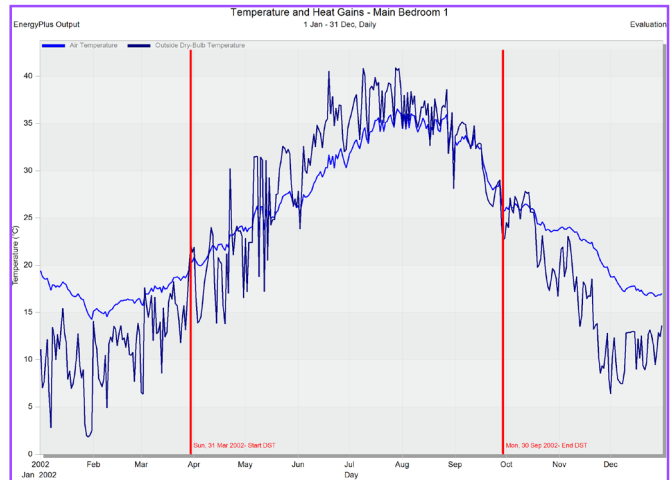
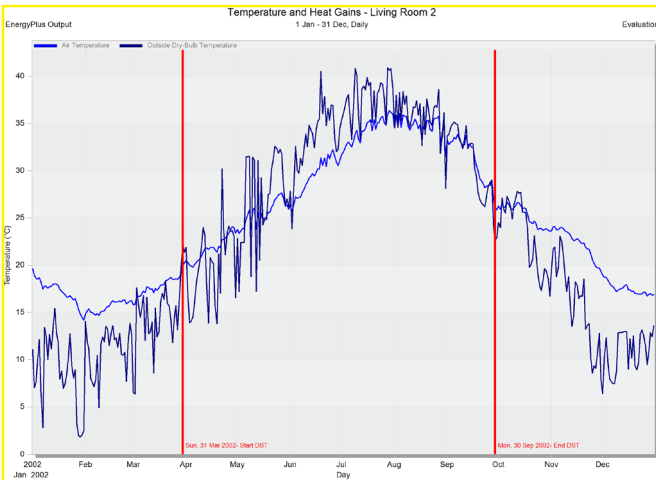
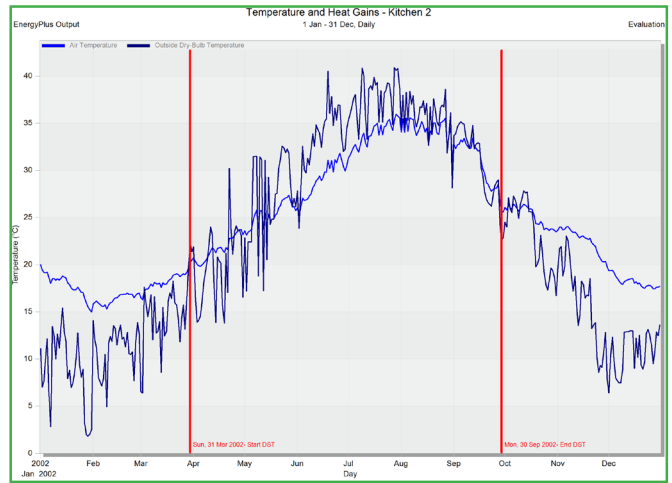
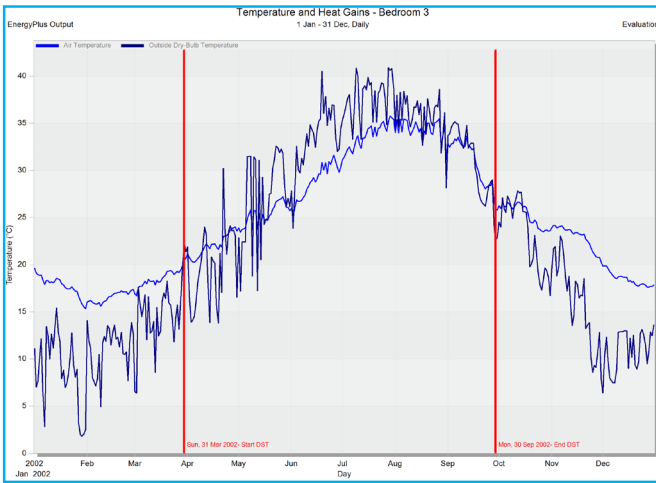
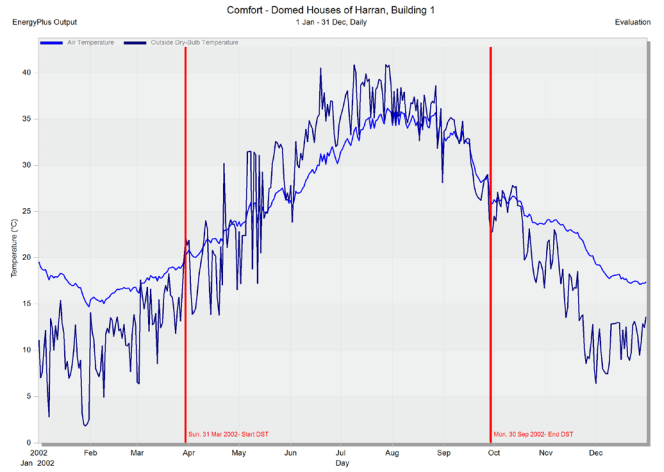
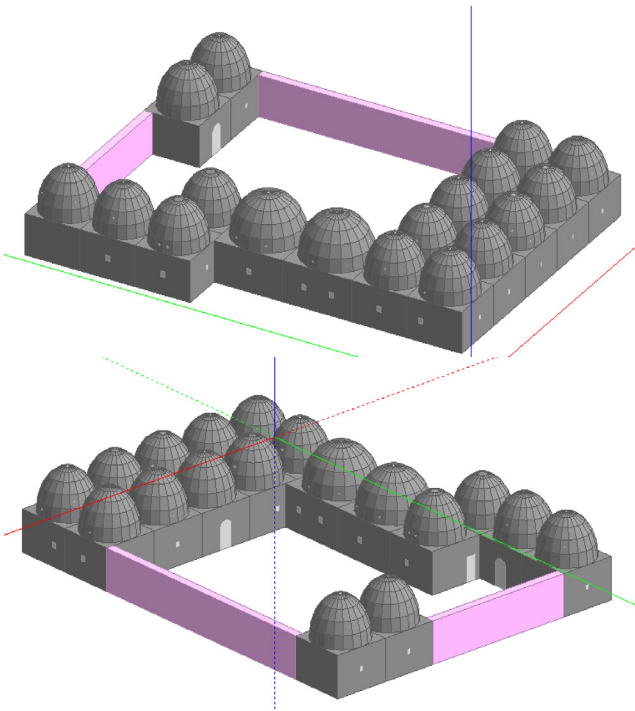
Cost

Cost type 1-Auto-calculate

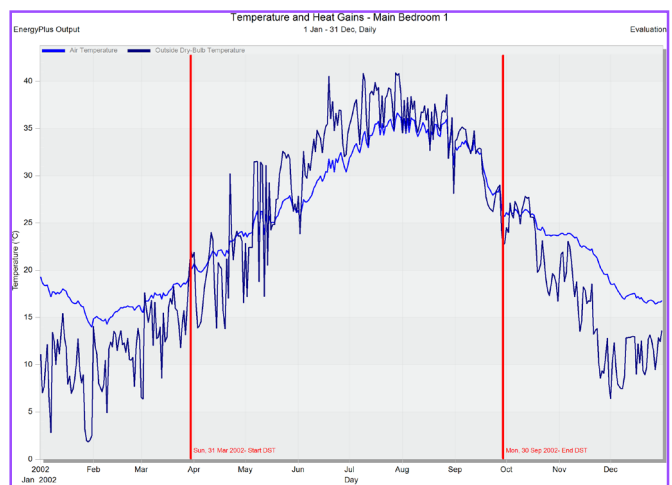
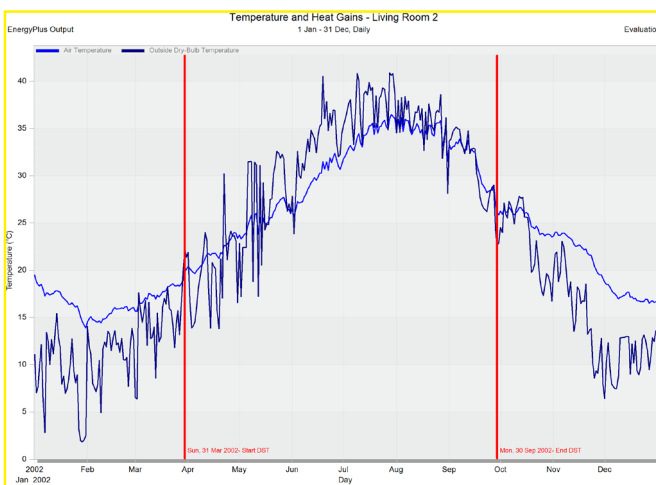
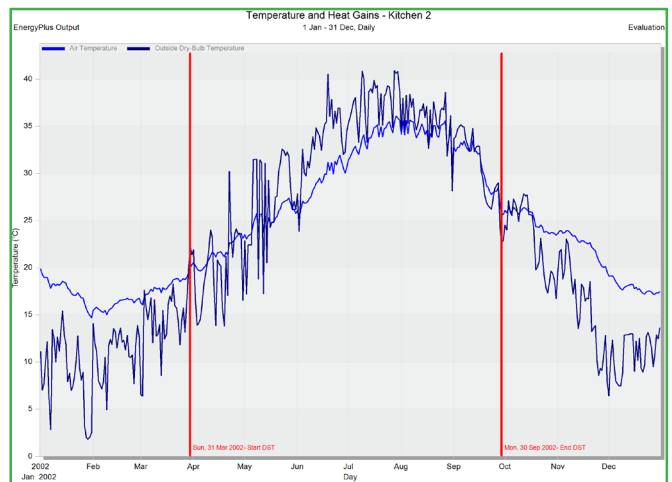
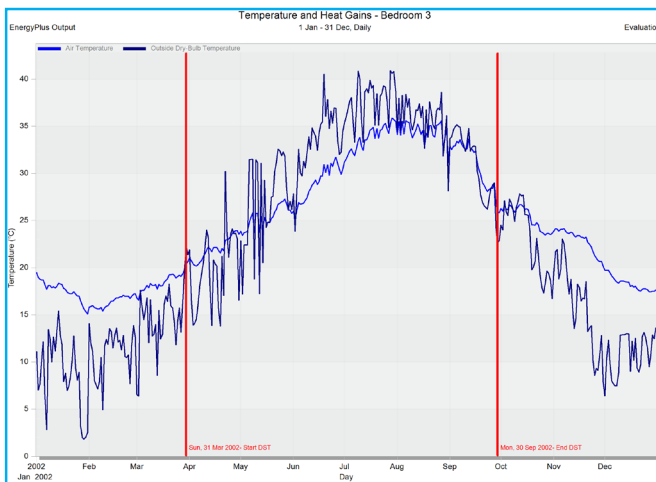
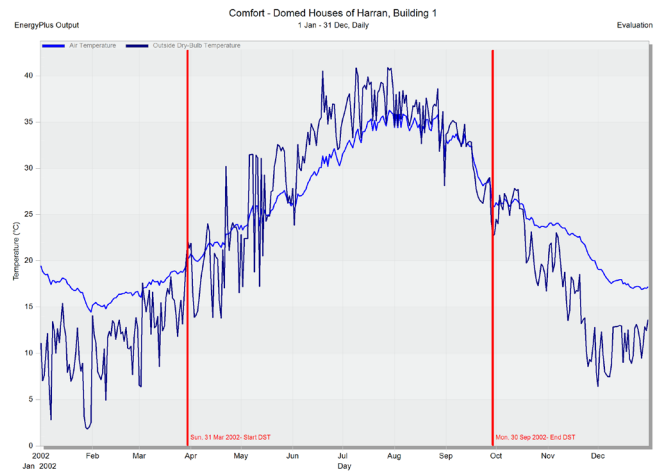
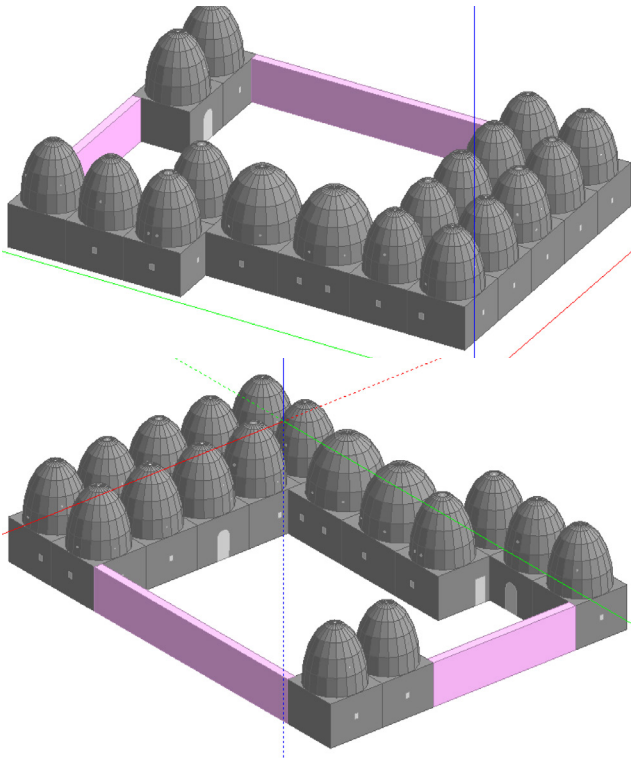


Appendix 4: Dome height changes

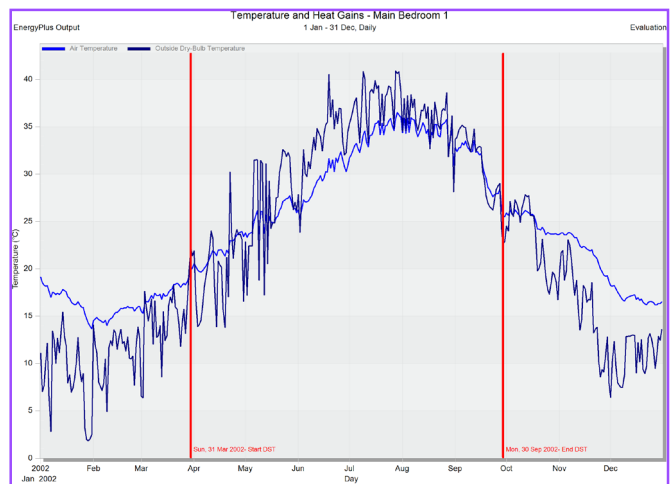
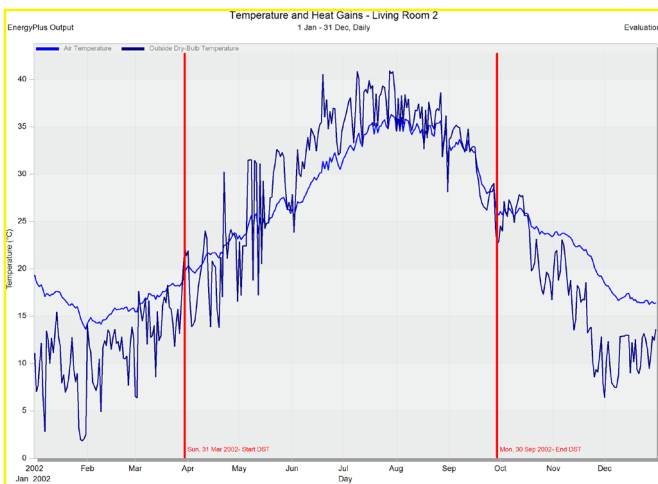
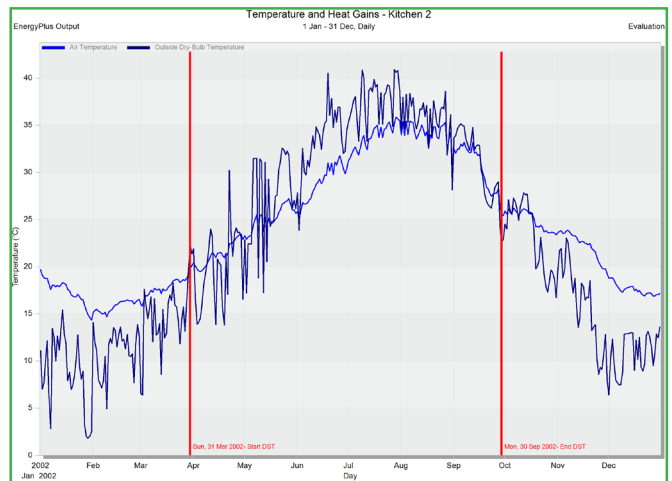
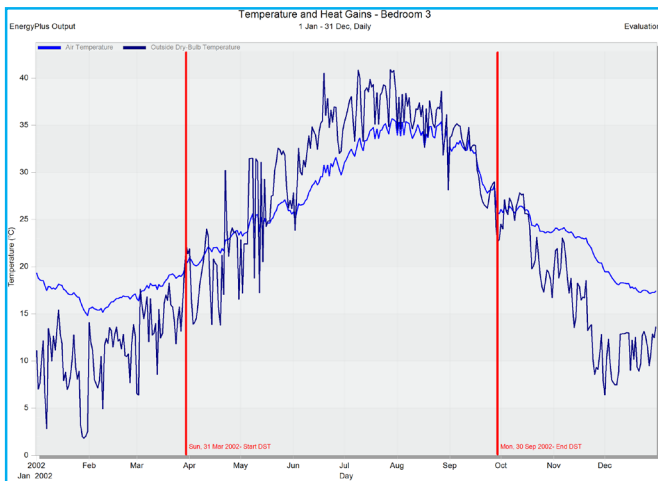
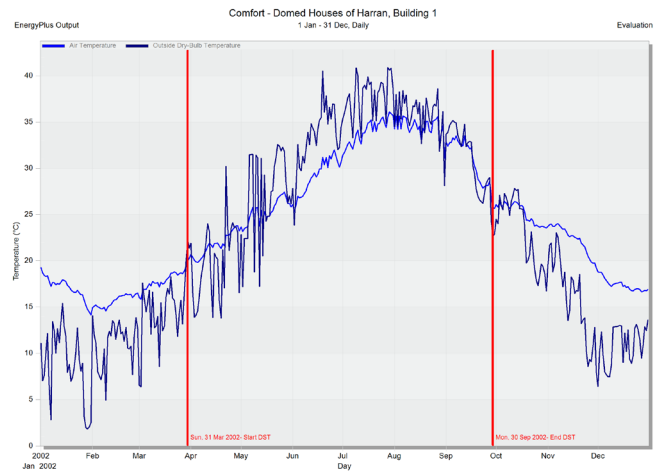
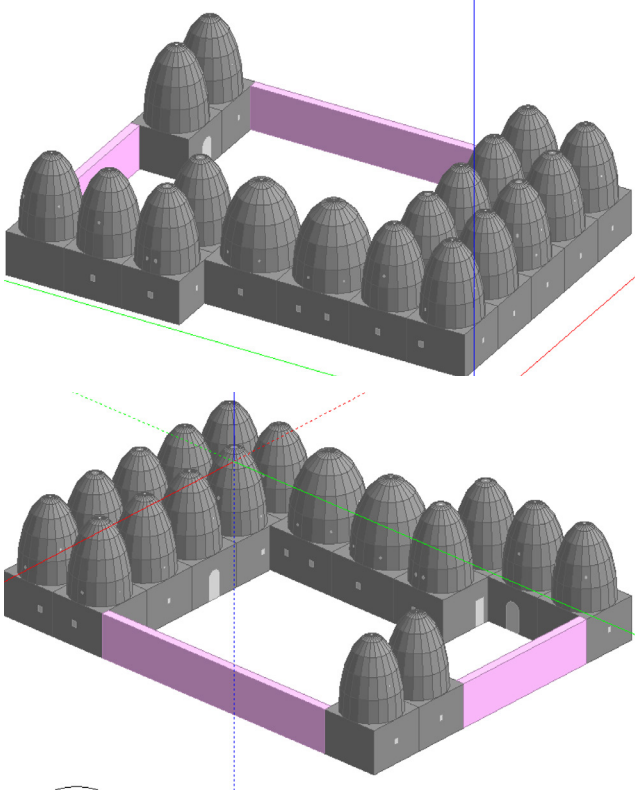
4.1 3m dome height inputs and outputs



4.2 4m dome height inputs and outputs

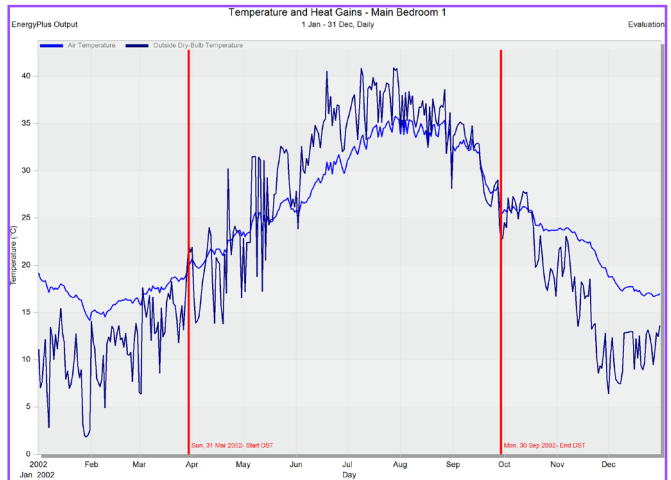
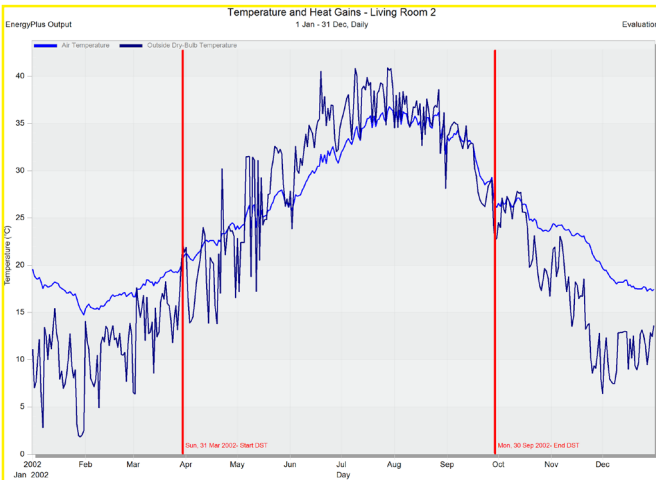
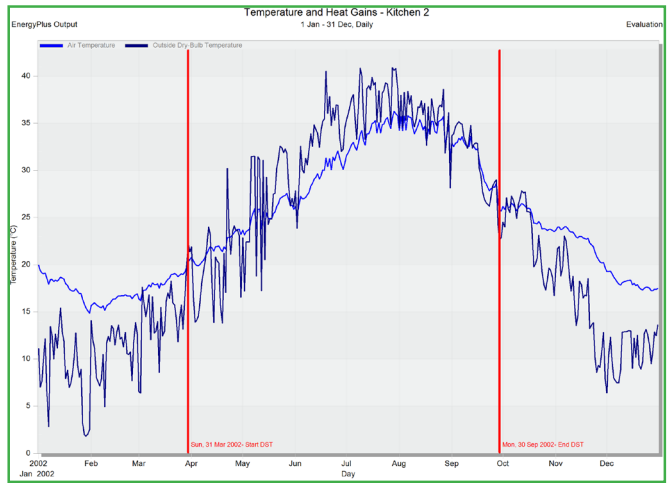
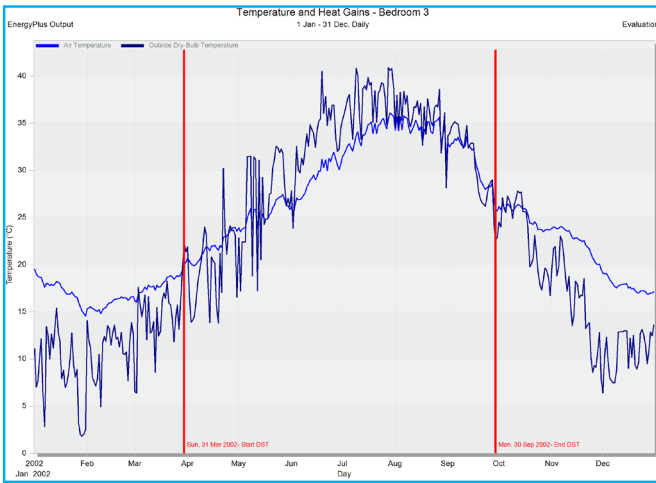
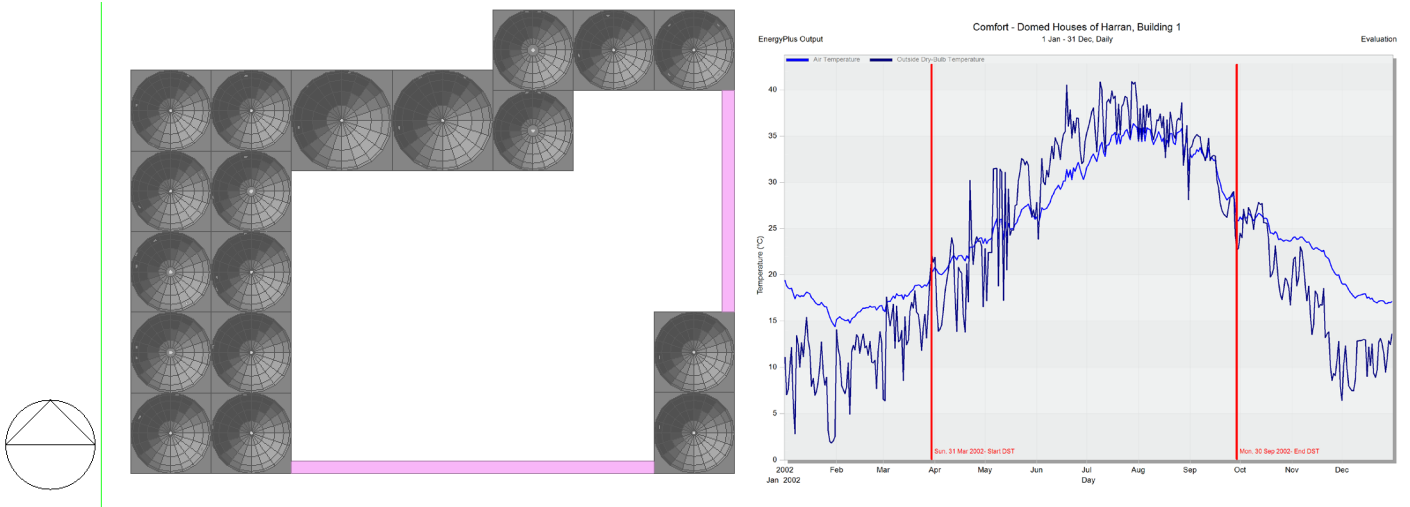


4.3 5m dome height inputs and outputs

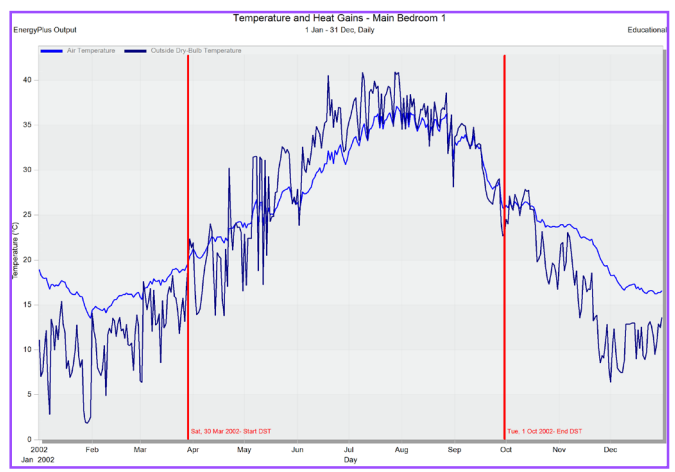
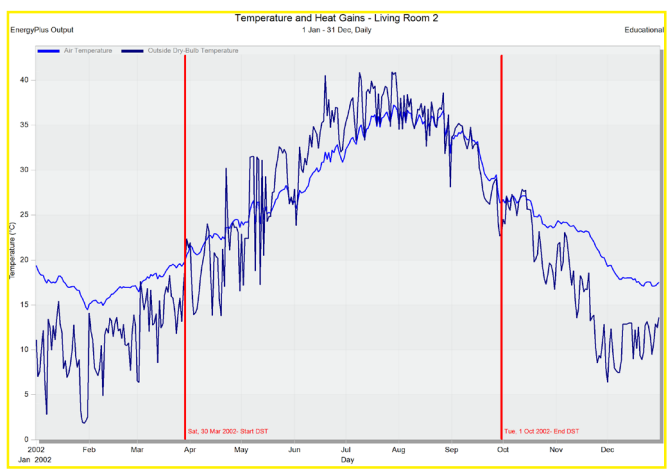
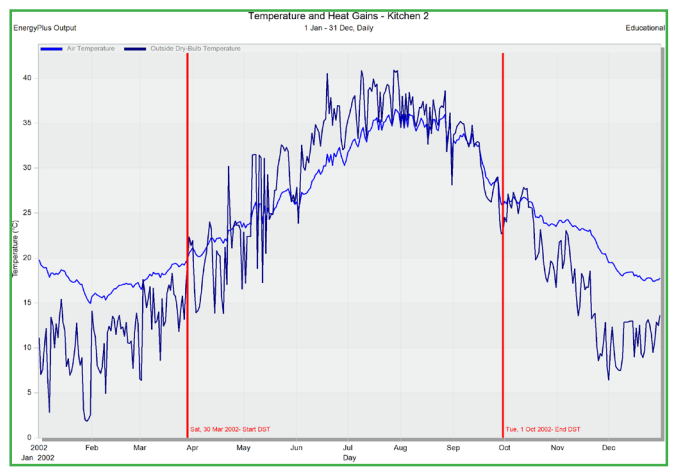
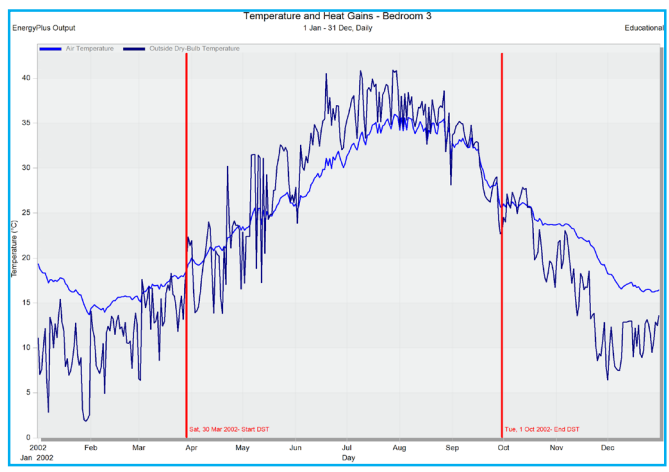
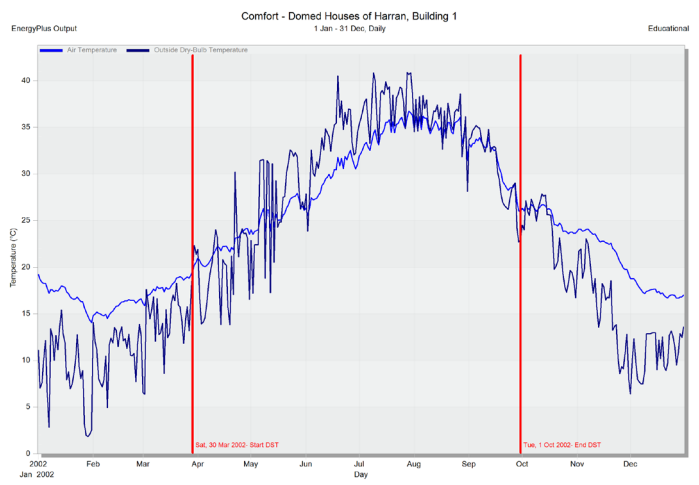
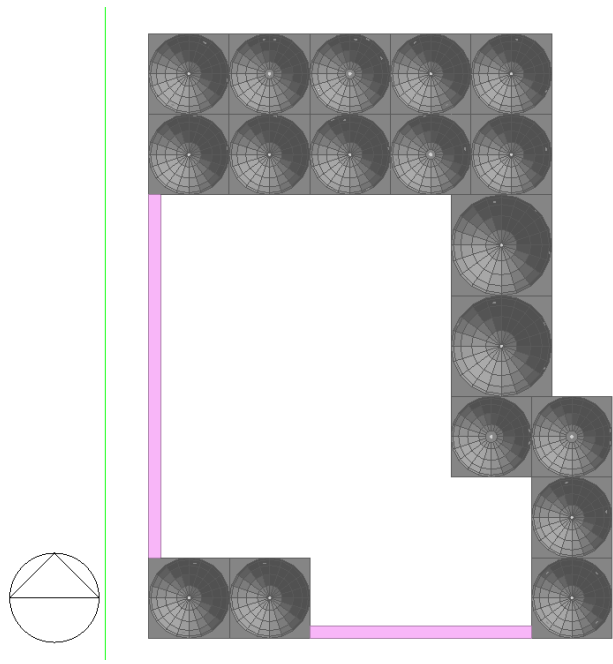


Appendix 5: Building orientation changes

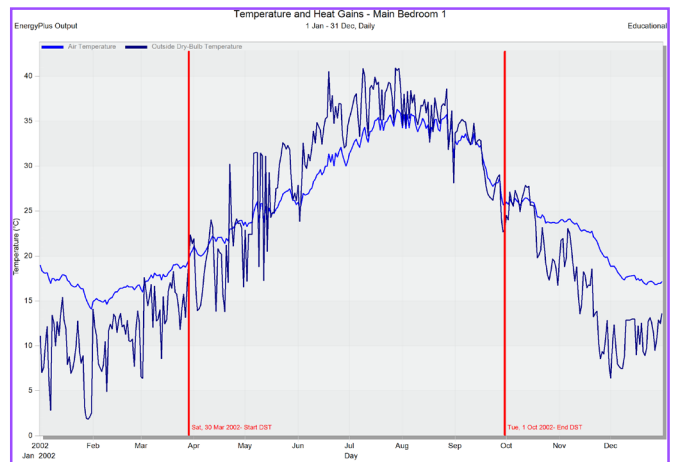
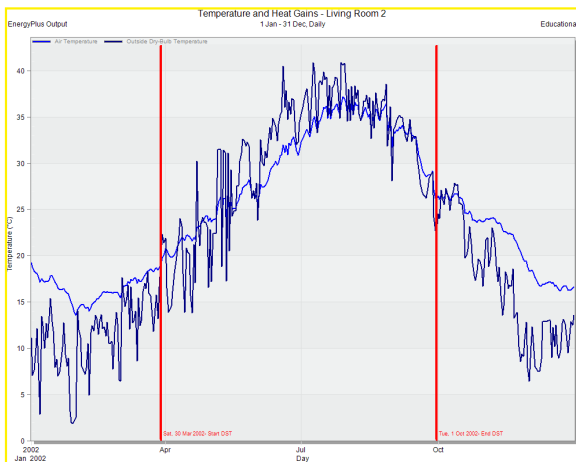
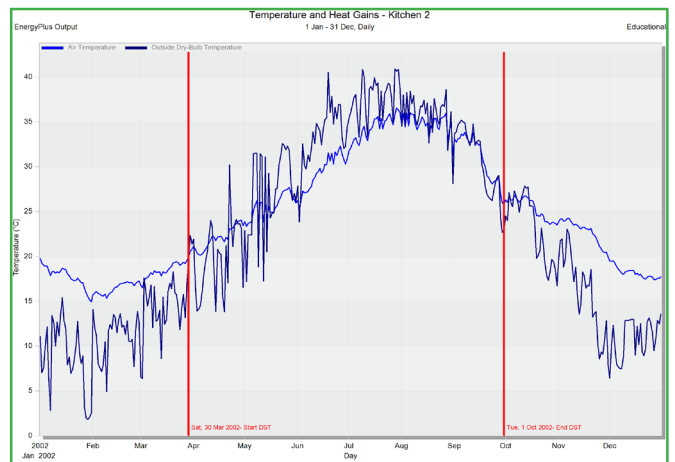
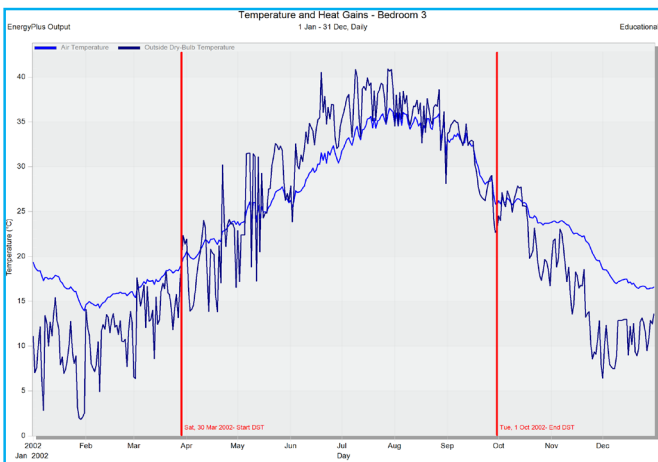
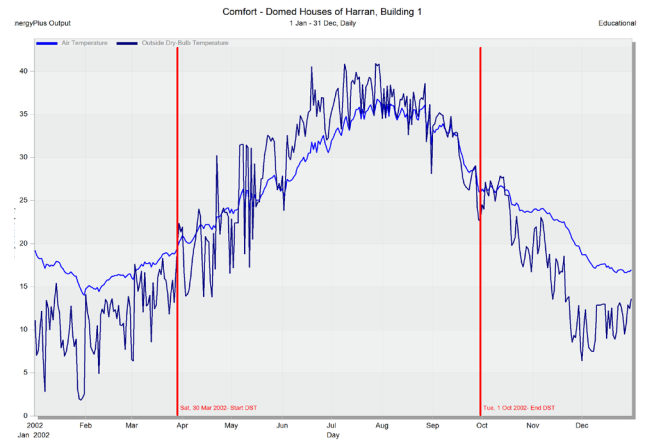
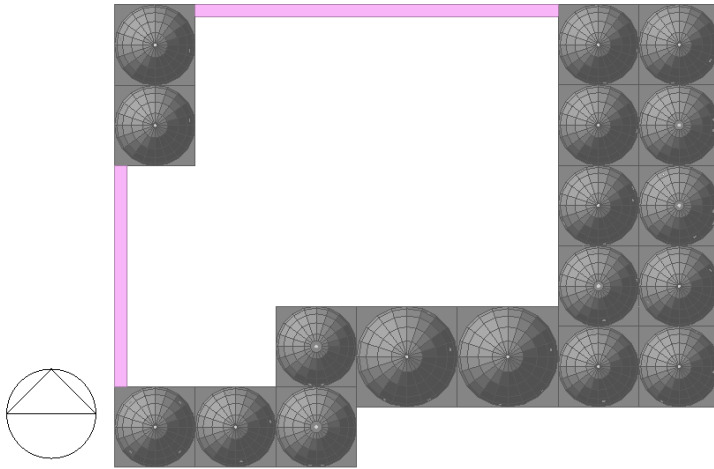
5.1 90° orientation change inputs and outputs



5.2 180° orientation change inputs and outputs

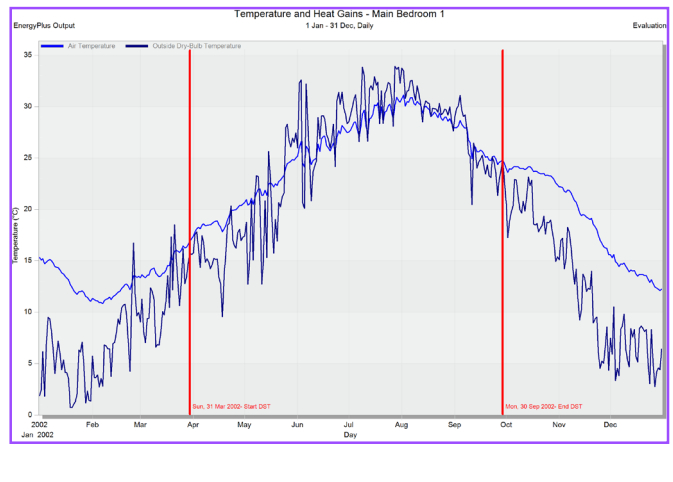
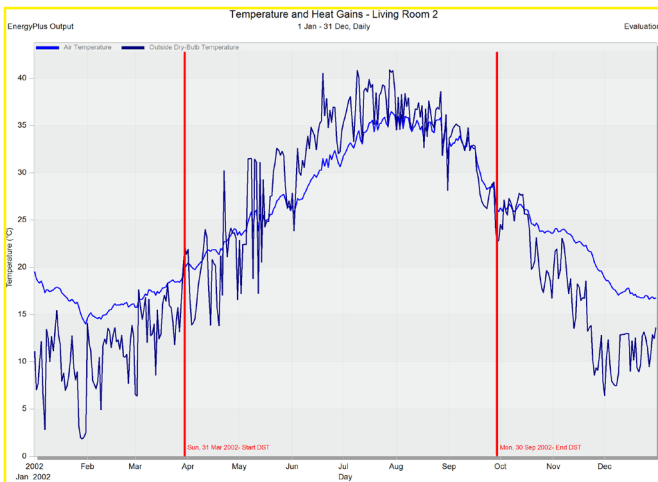
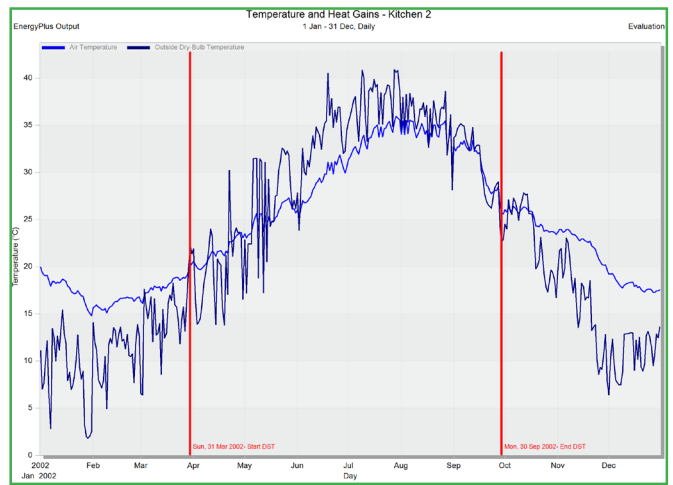
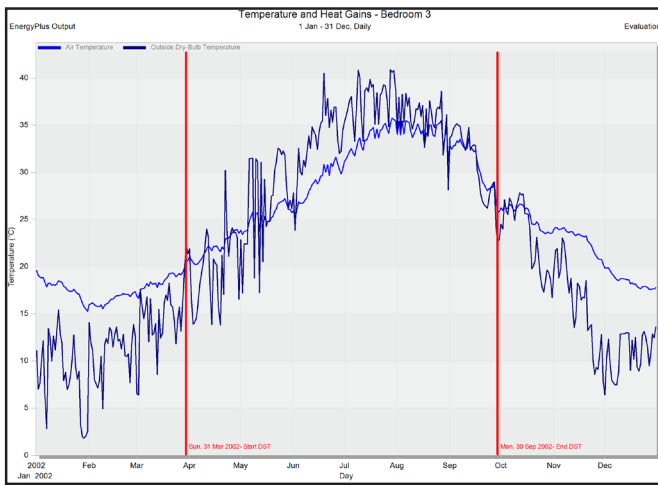
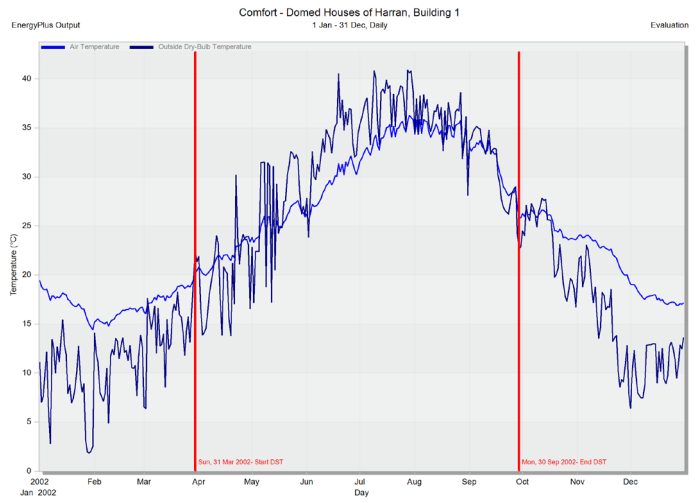
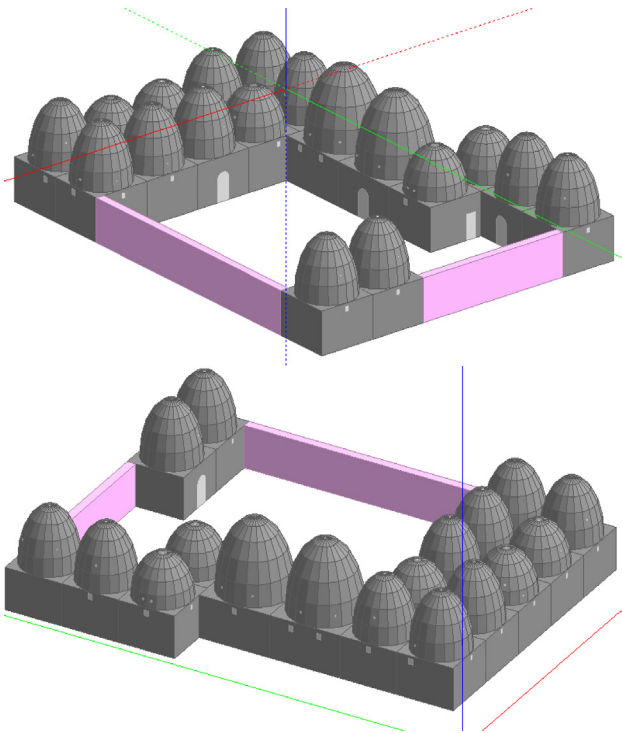


5.3 270° orientation change inputs and outputs

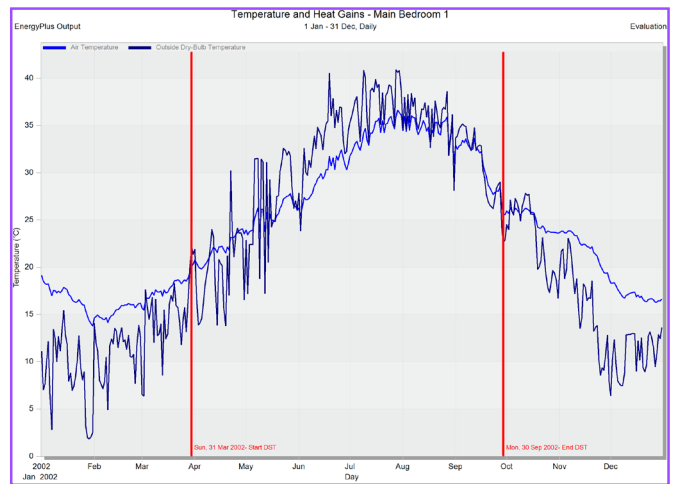
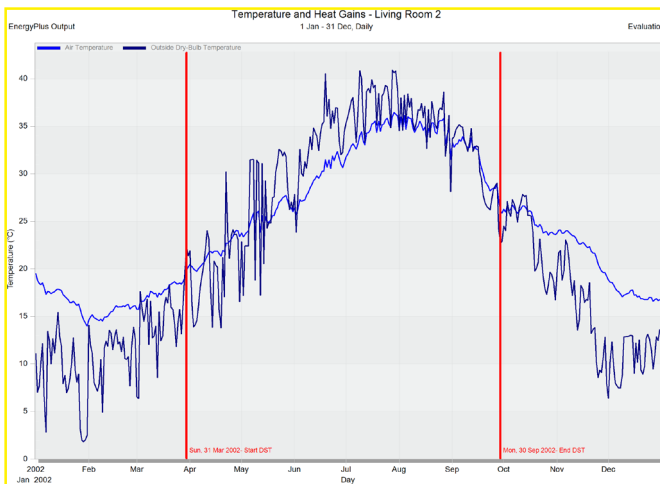
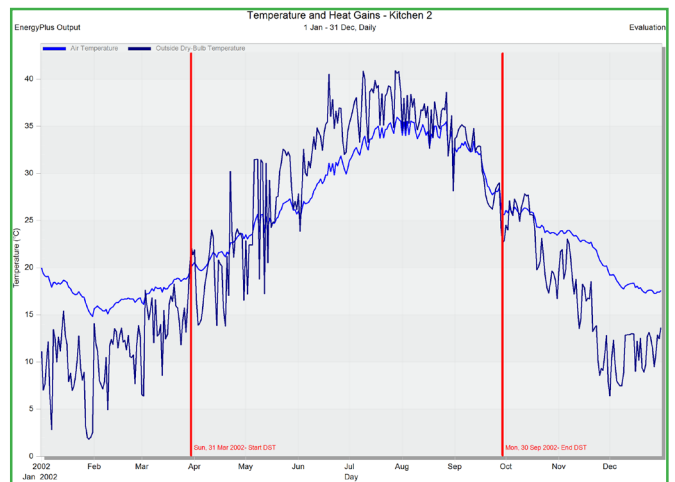
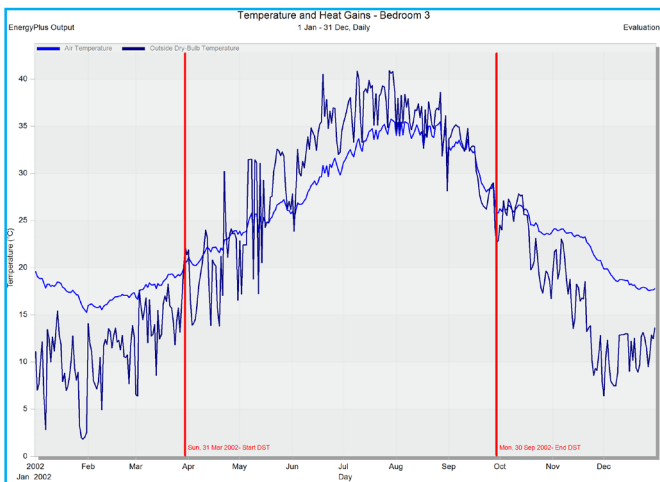
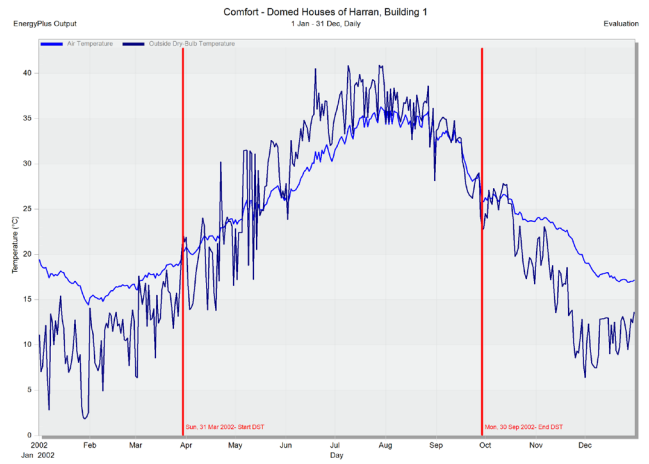
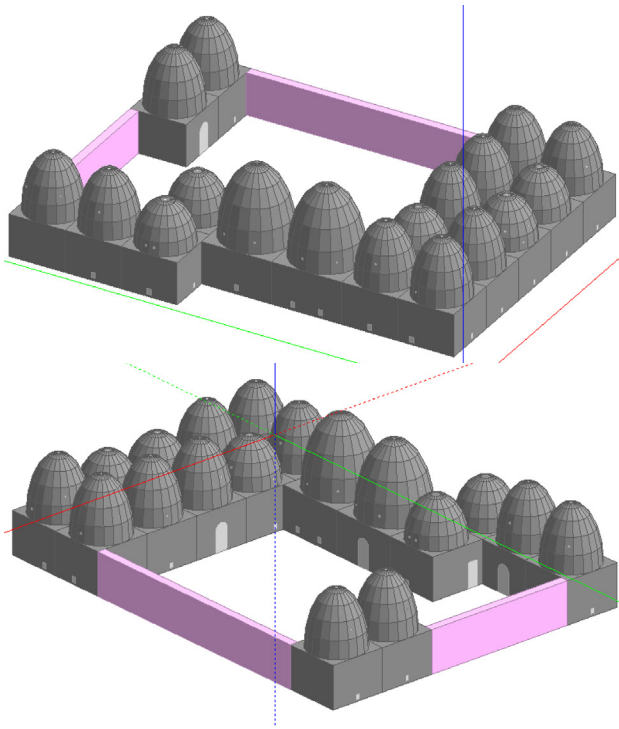


Appendix 6: Window height changes

6.1 Windows up 800mm inputs and outputs

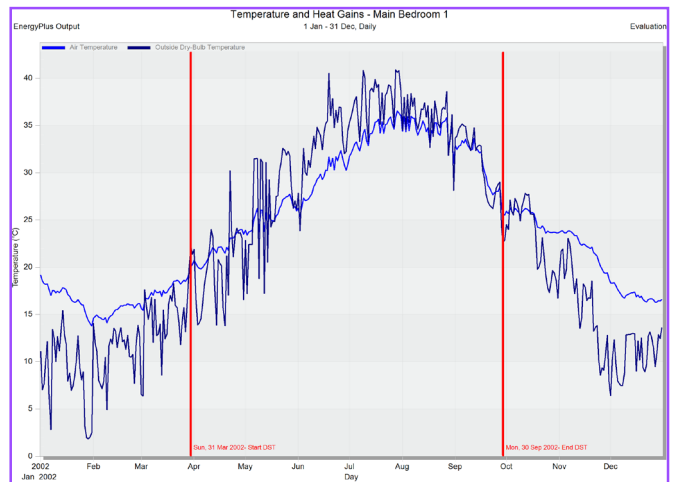
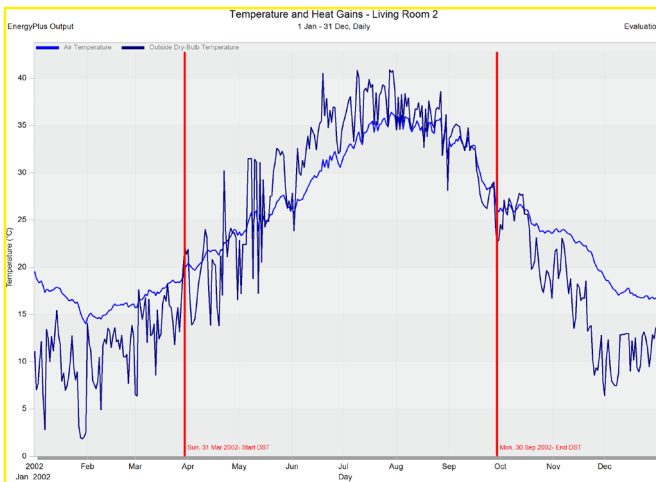
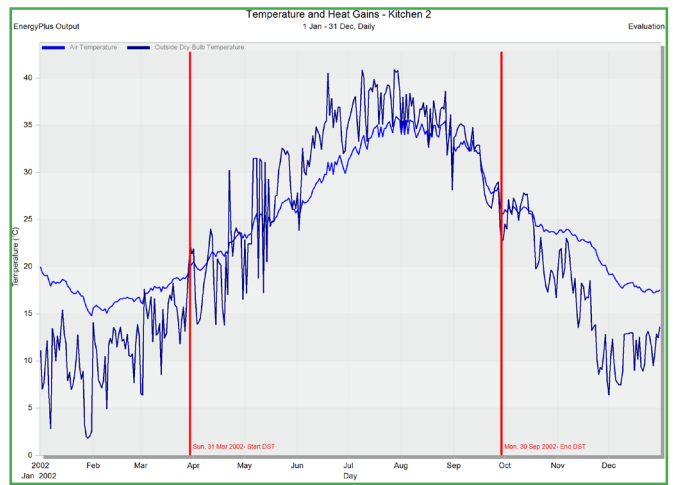
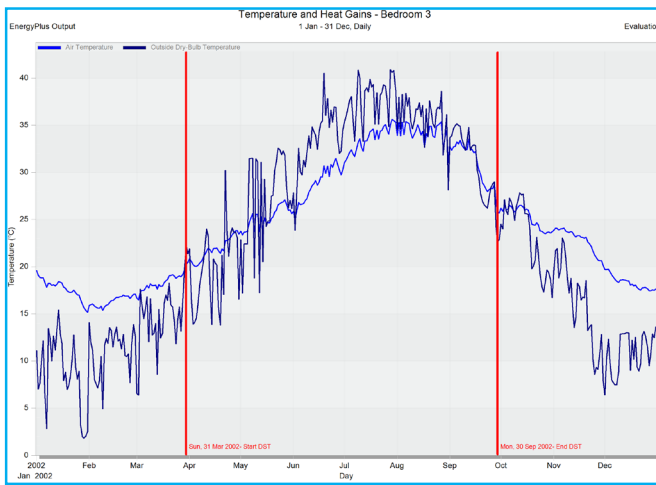
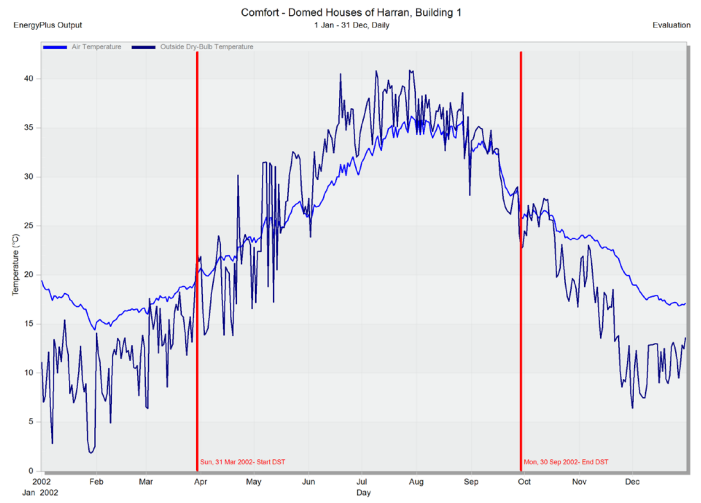
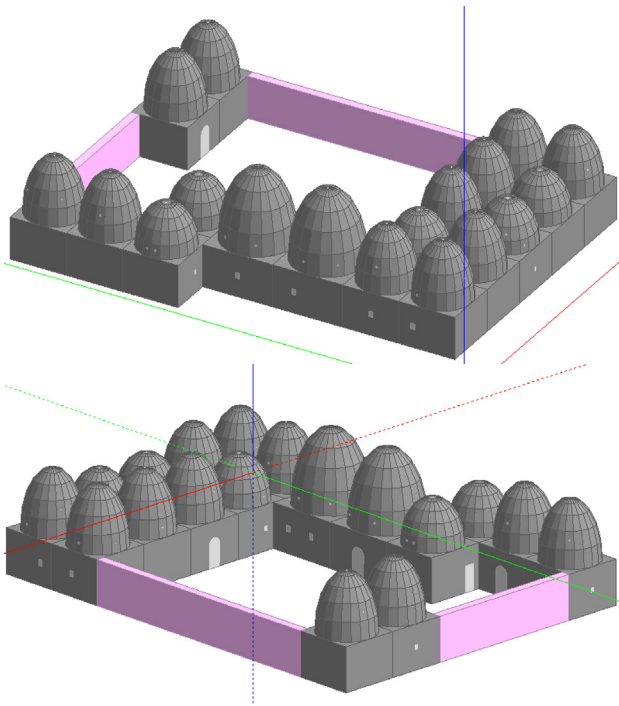


6.2 Windows down 800mm inputs and outputs

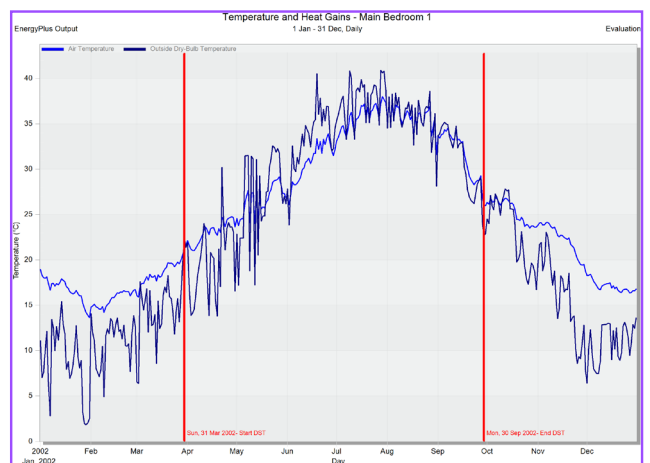
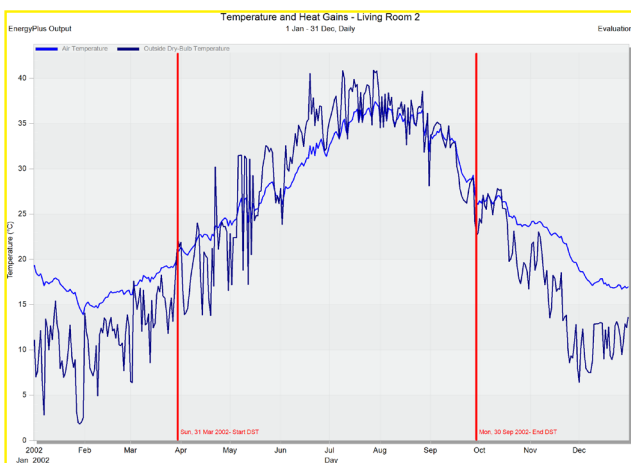
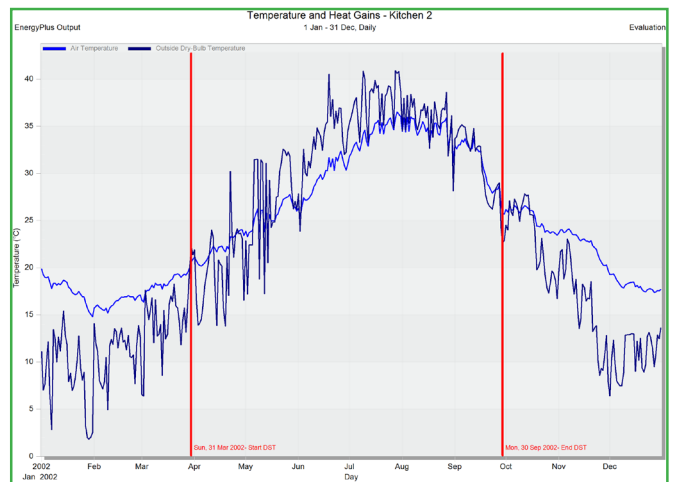
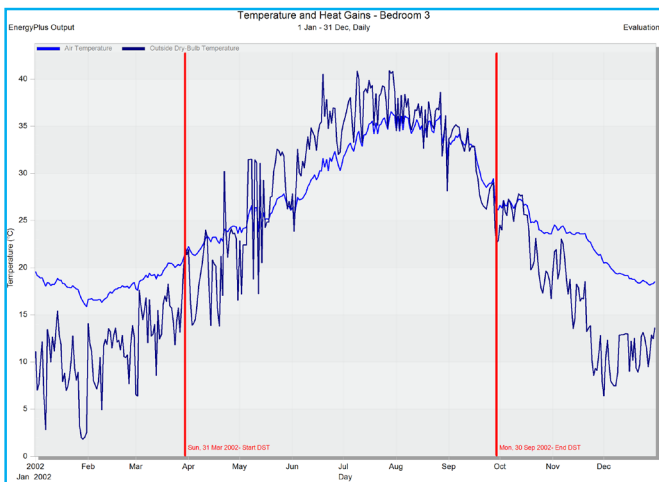
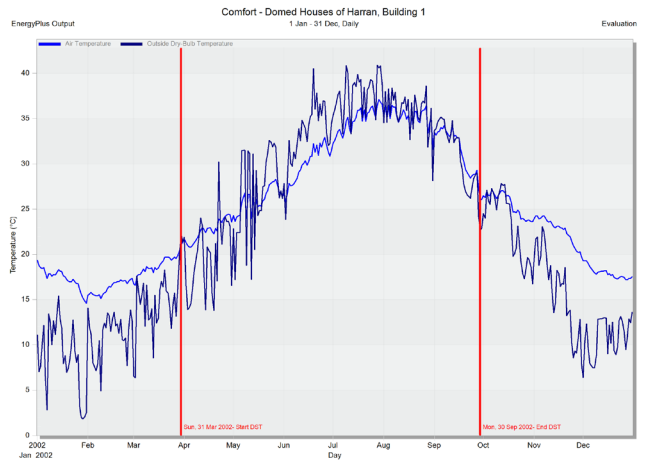
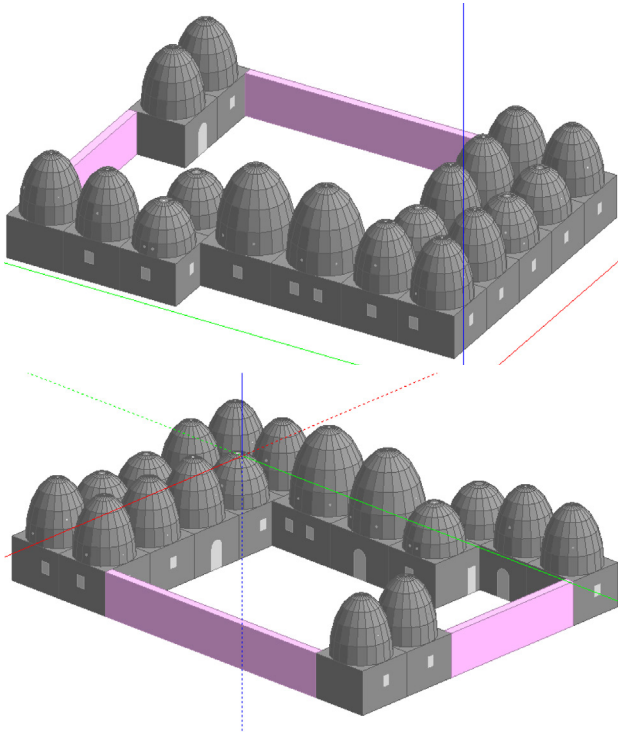


Appendix 7: WWR changes

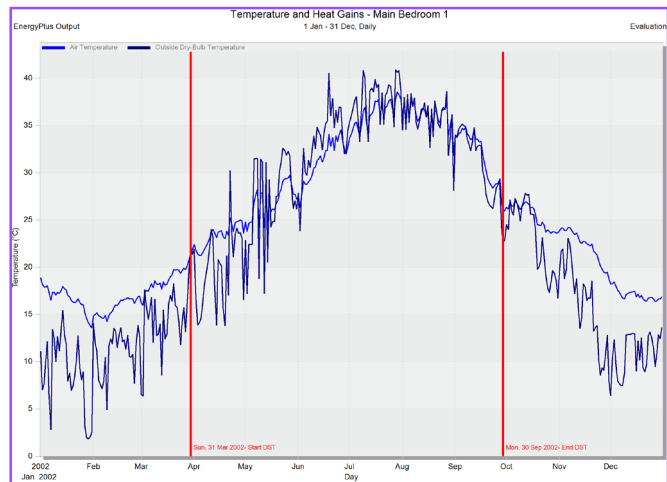
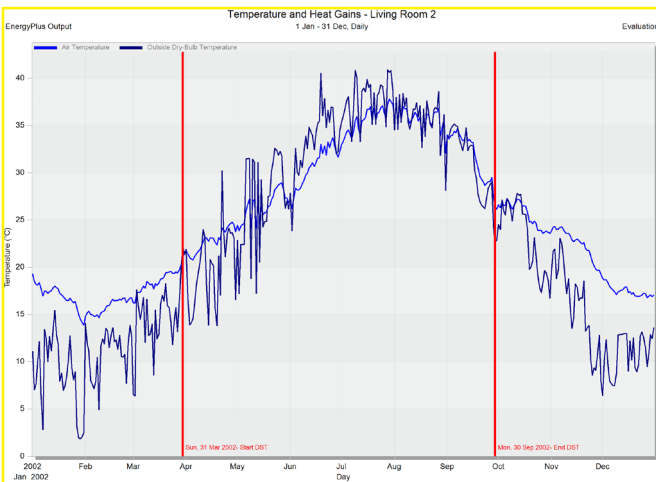
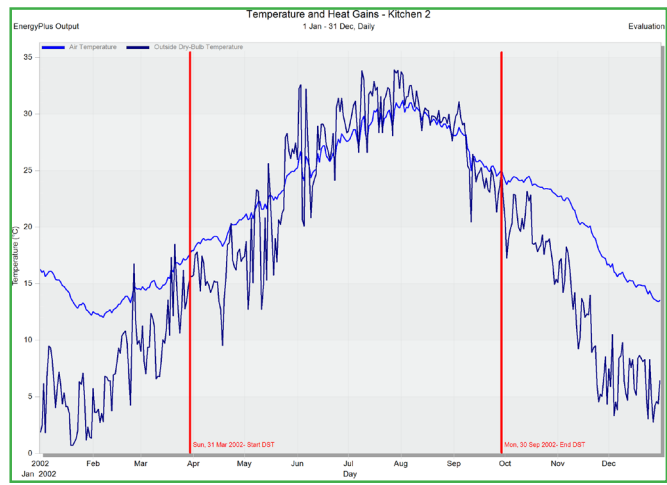
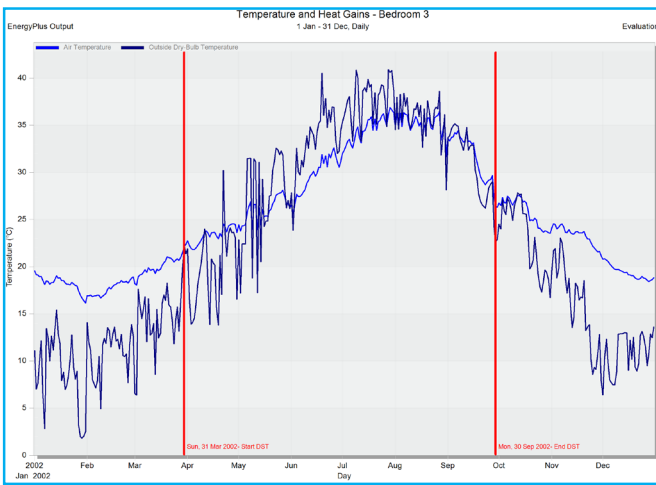
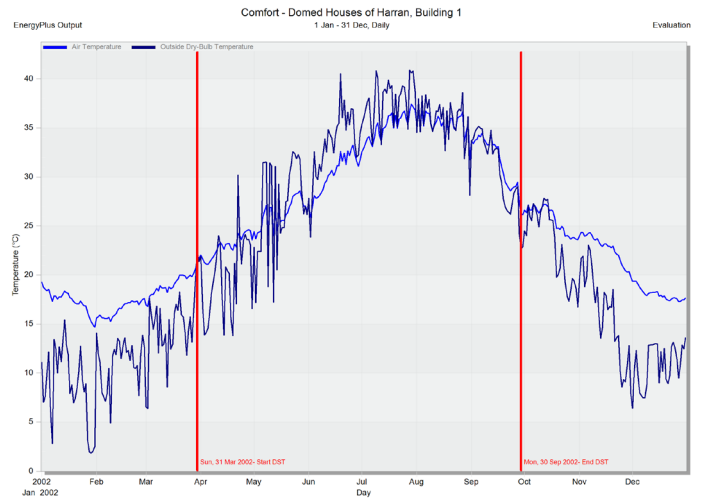
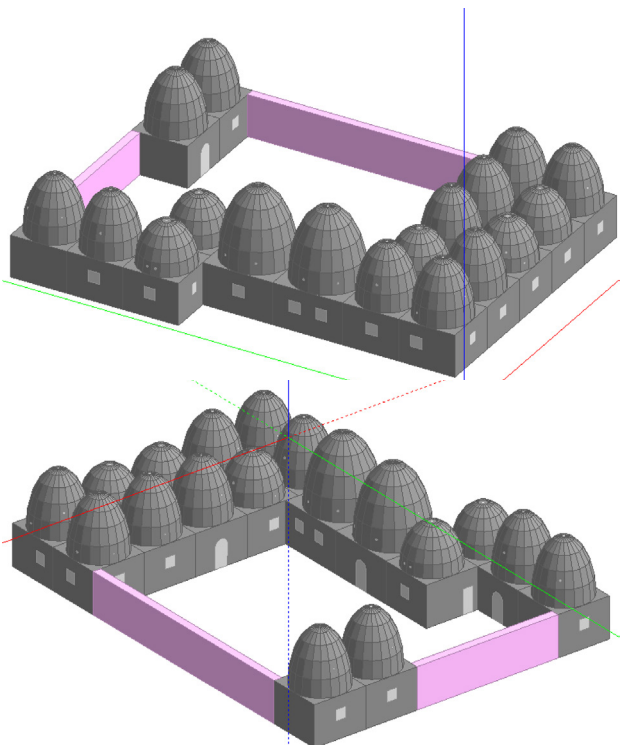
7.1 0.4% WWR inputs and outputs



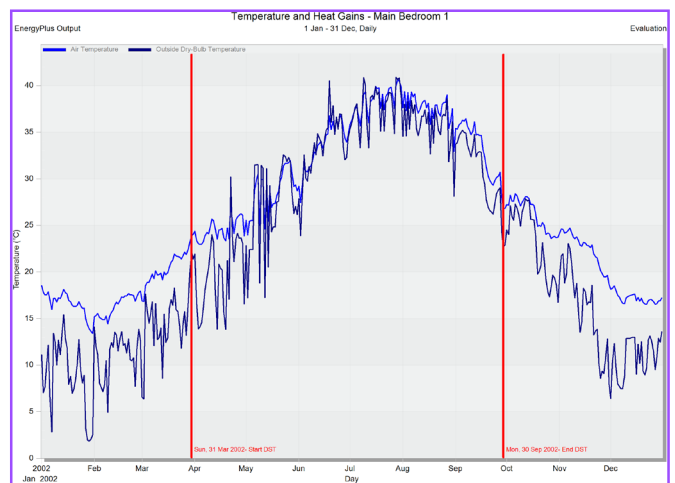
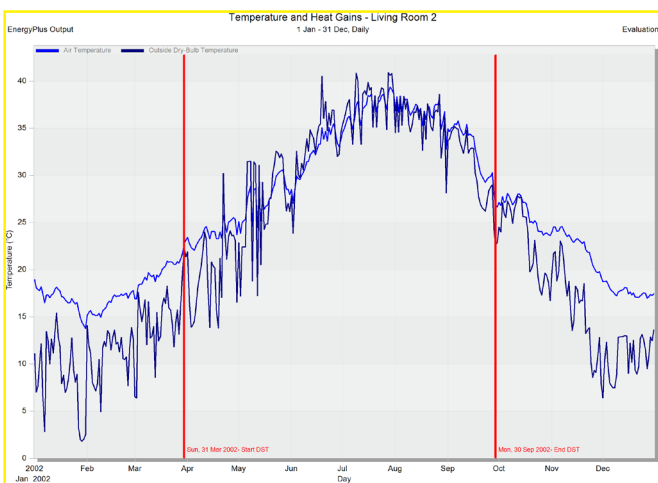
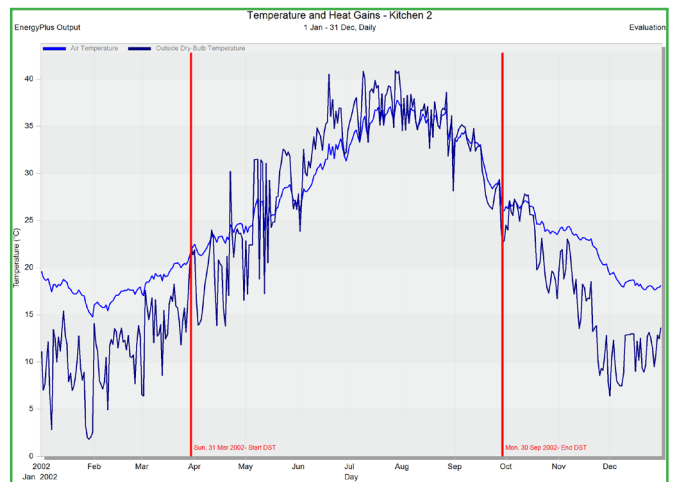
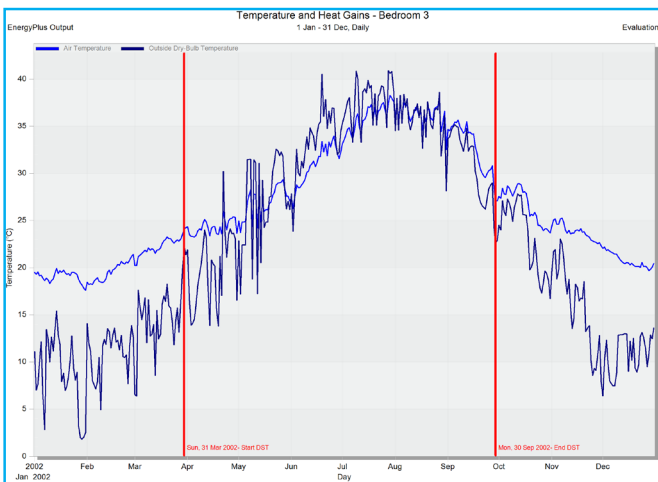
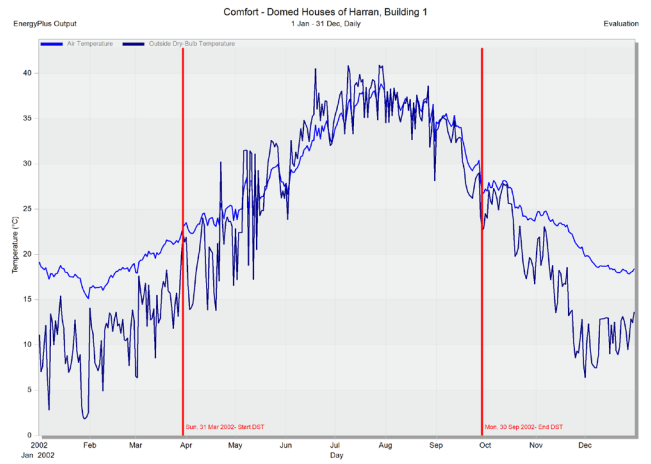
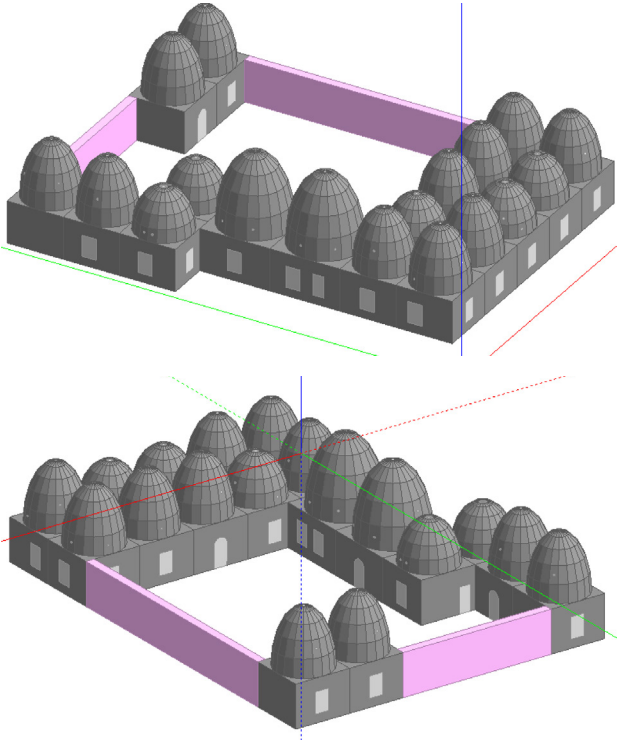
7.2 2.5% WWR inputs and outputs



7.3 5% WWR inputs and outputs



7.4 10% WWR inputs and outputs



Appendix 8: Openable window percentage change

8.1 15% Openable windows inputs and outputs

Glazing Template

Template: **No windows**

External Windows

Glazing type: **Sgl Clr 3mm**

Layout: **Preferred height 1.5m, 30% glazed**

Dimensions

Type: **3-Preferred height**

Window to wall %: **30.00**

Window height (m): **1.50**

Window spacing (m): **5.00**

Sill height (m): **0.80**

Outside reveal depth (m): **0.000**

Frame and Dividers

Shading

Airflow Control Windows

Free Aperture

Opening position: **1-Top**

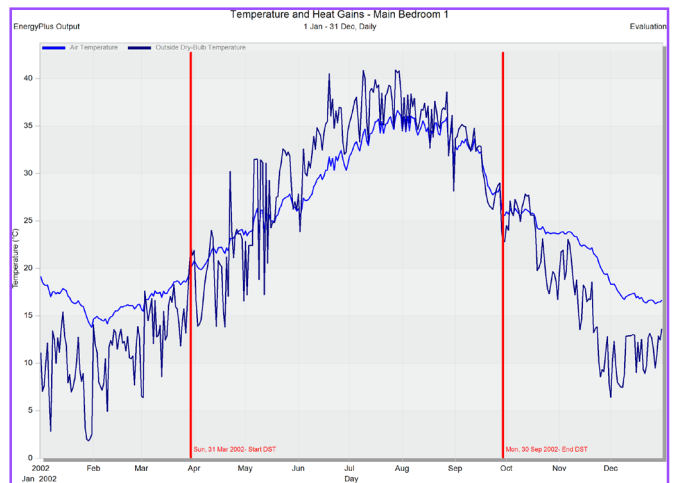
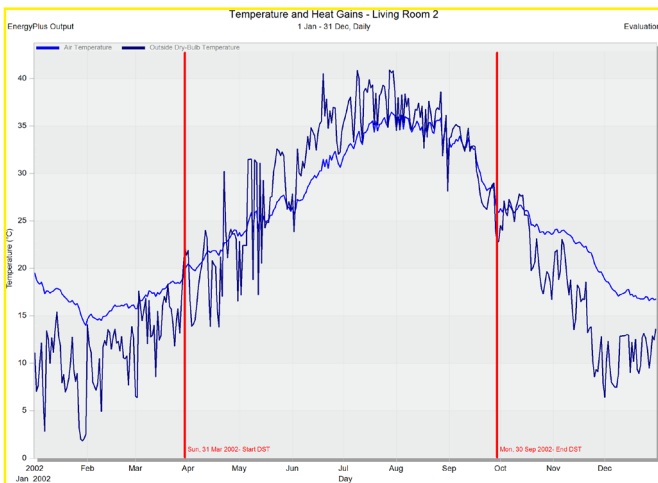
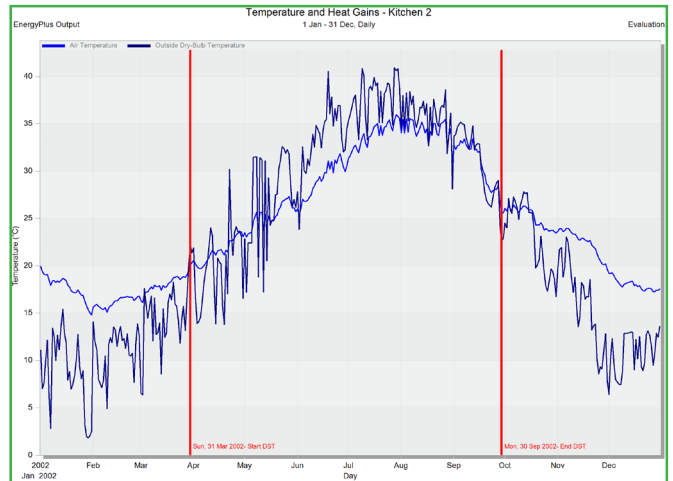
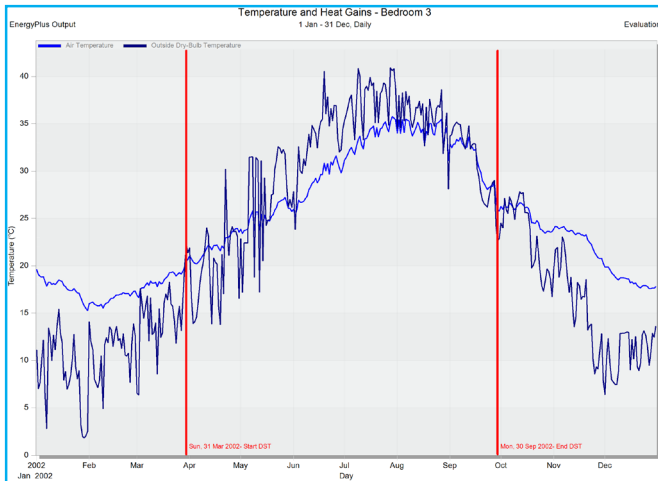
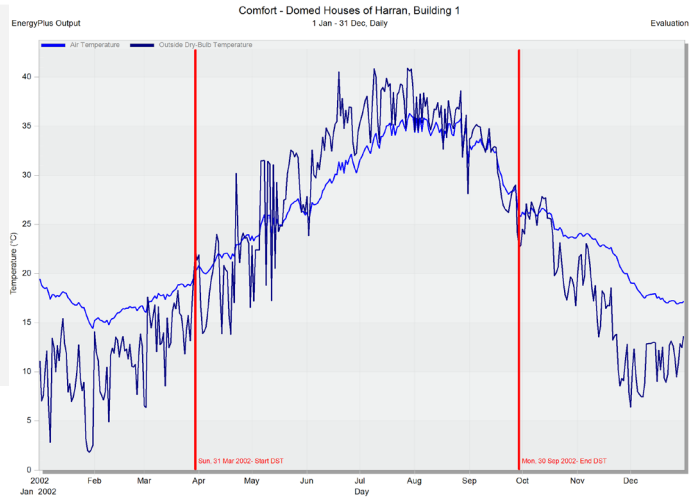
% Glazing area opens: **15**

Internal Windows

Sloped Roof Windows/Skylights

Doors

Vents



8.2 35% Openable windows inputs and outputs

Glazing Template

Template No windows

External Windows

Glazing type Sgl Clr 3mm

Layout Preferred height 1.5m, 30% glazed

Dimensions

Type 3-Preferred height

Window to wall % 30.00

Window height (m) 1.50

Window spacing (m) 5.00

Sill height (m) 0.80

Outside reveal depth (m) 0.000

Frame and Dividers

Shading

Airflow Control Windows

Free Aperture

Opening position 1-Top

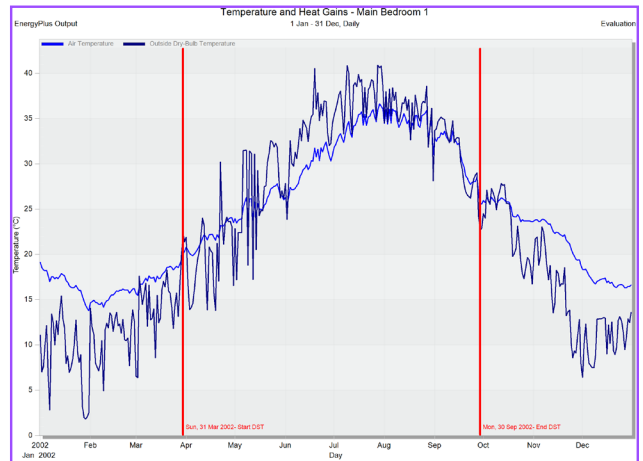
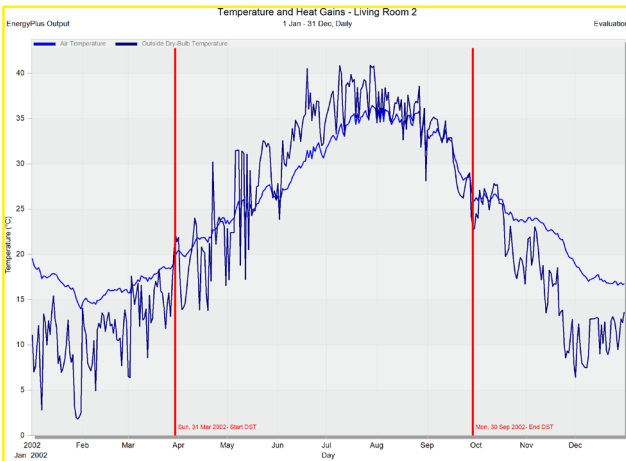
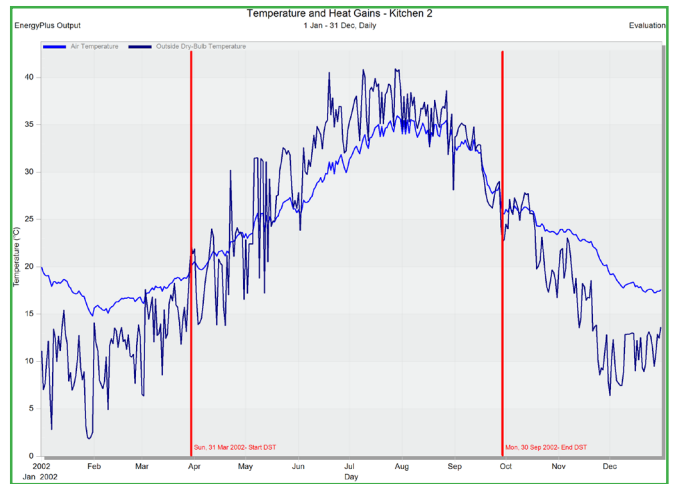
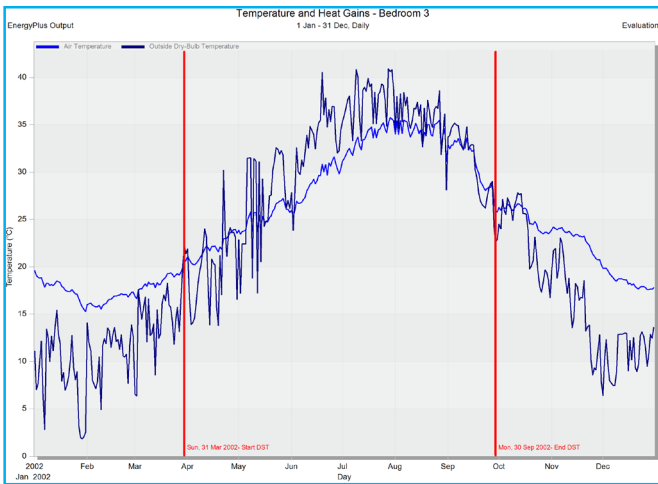
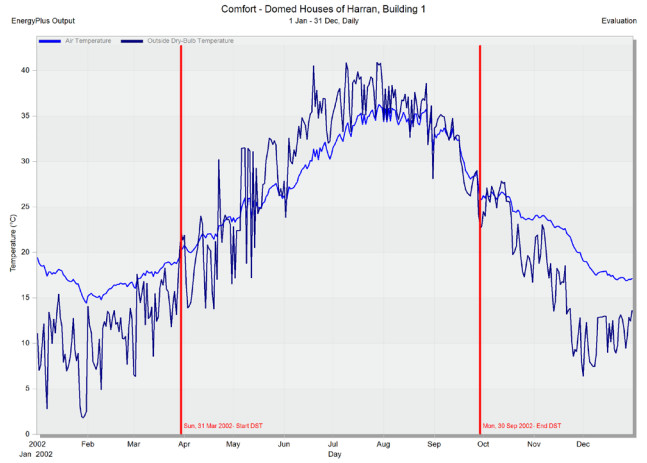
% Glazing area opens 35

Internal Windows

Sloped Roof Windows/Skylights

Doors

Vents



8.3 55% Openable windows inputs and outputs

Glazing Template

Template No windows

External Windows

Glazing type Sgl Clr 3mm

Layout Preferred height 1.5m, 30% glazed

Dimensions

Type 3-Preferred height

Window to wall % 30.00

Window height (m) 1.50

Window spacing (m) 5.00

Sill height (m) 0.80

Outside reveal depth (m) 0.000

Frame and Dividers

Shading

Airflow Control Windows

Free Aperture

Opening position 1-Top

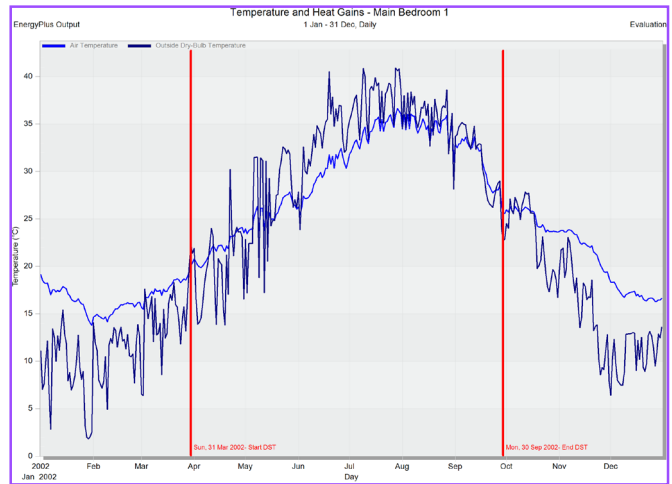
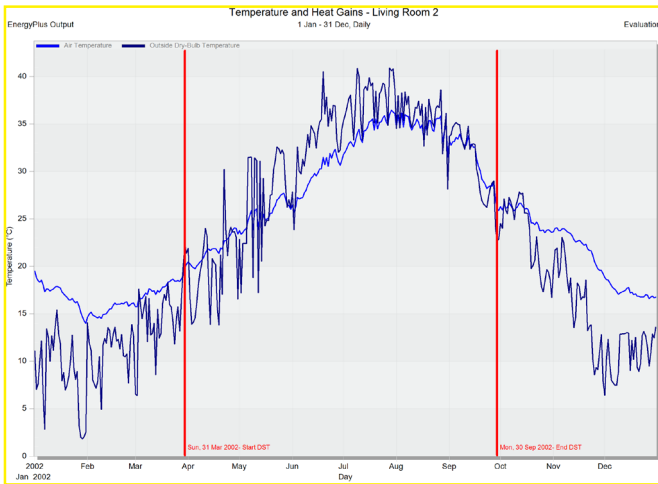
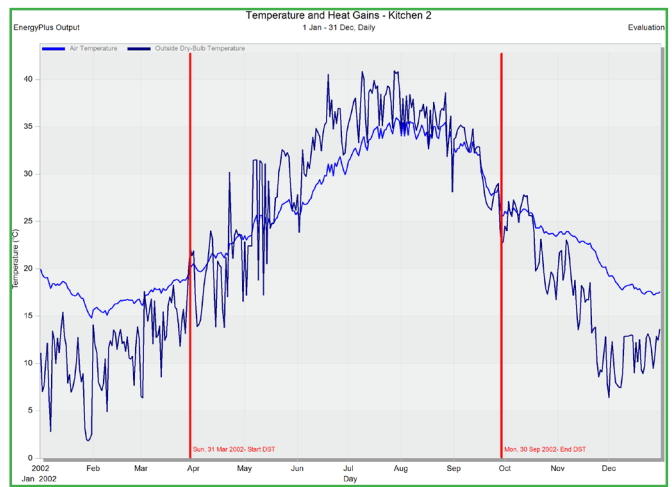
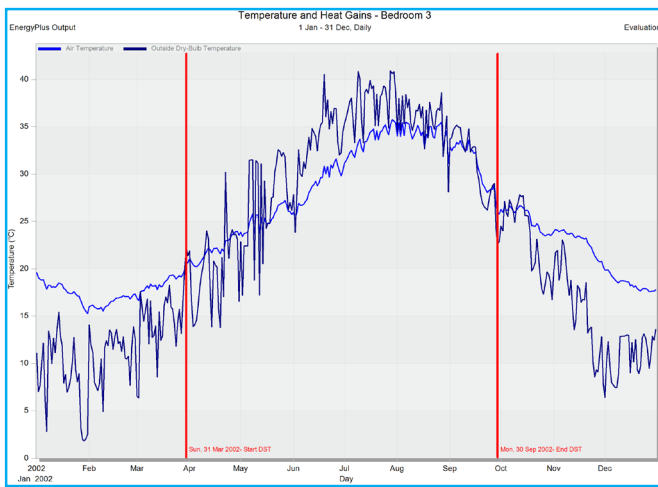
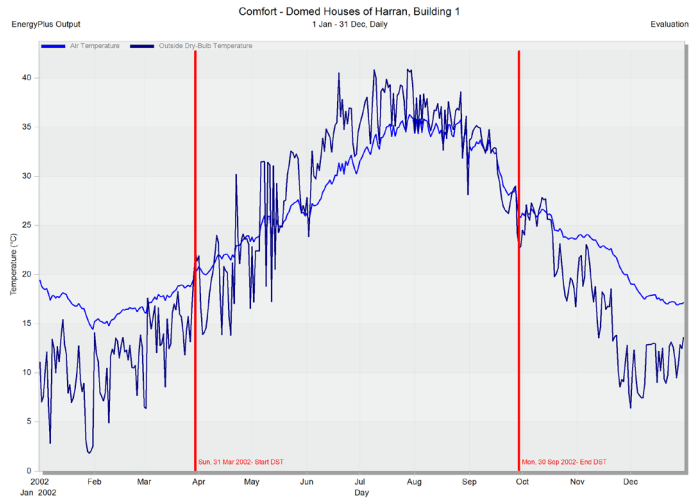
% Glazing area opens 55

Internal Windows

Sloped Roof Windows/Skylights

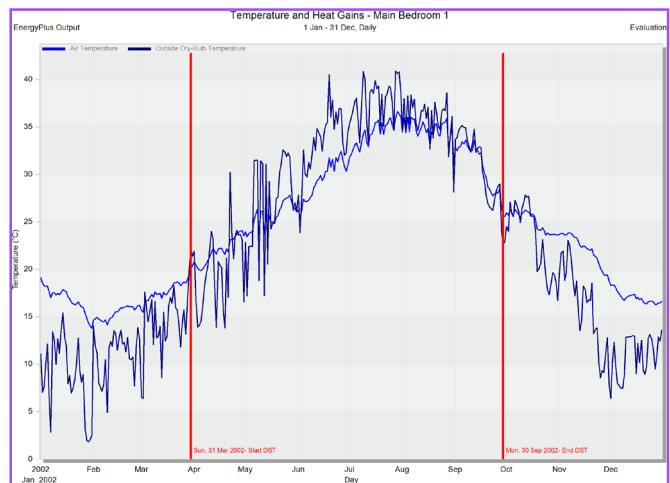
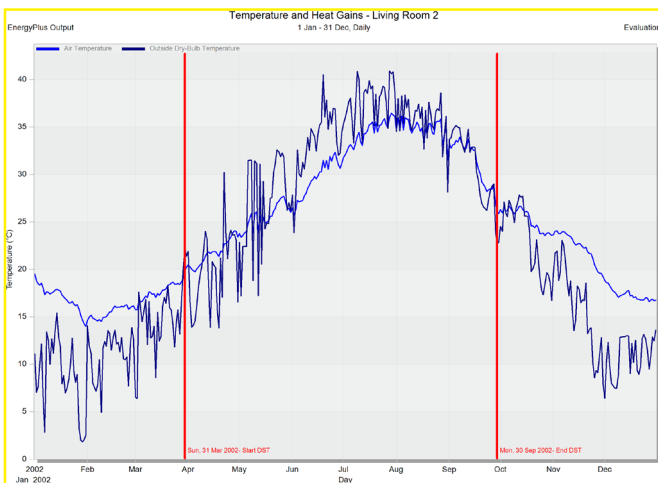
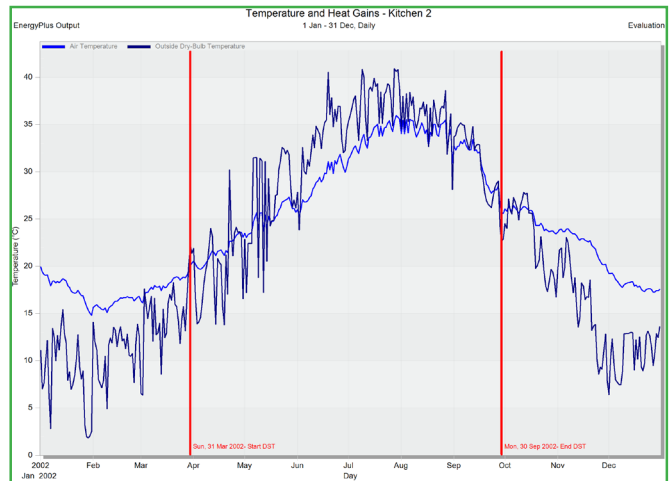
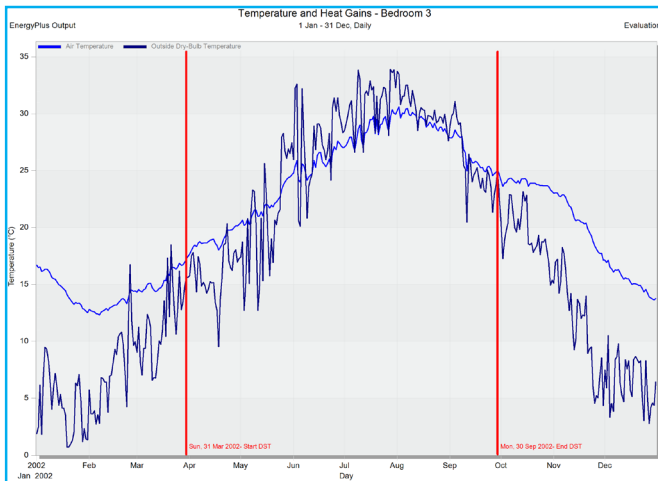
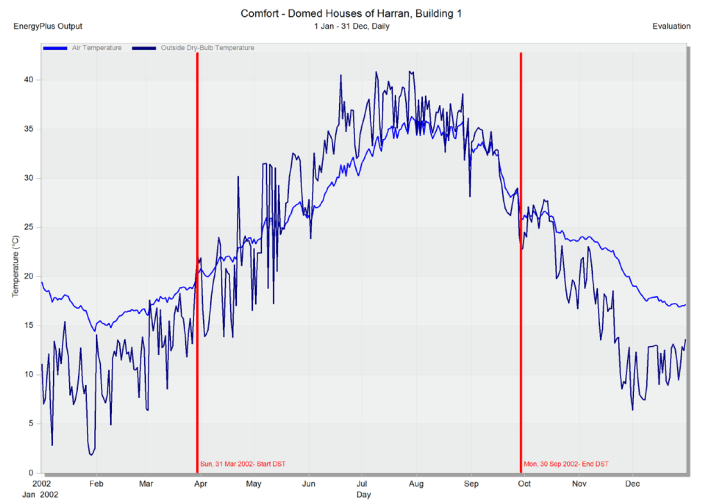
Doors

Vents



8.4 75% Openable windows inputs and outputs

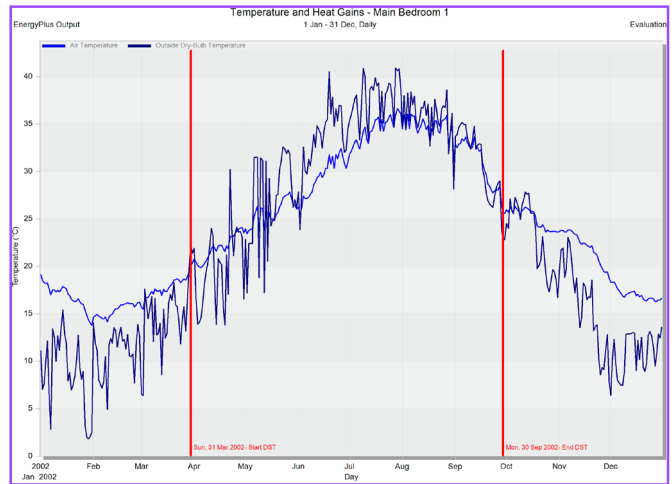
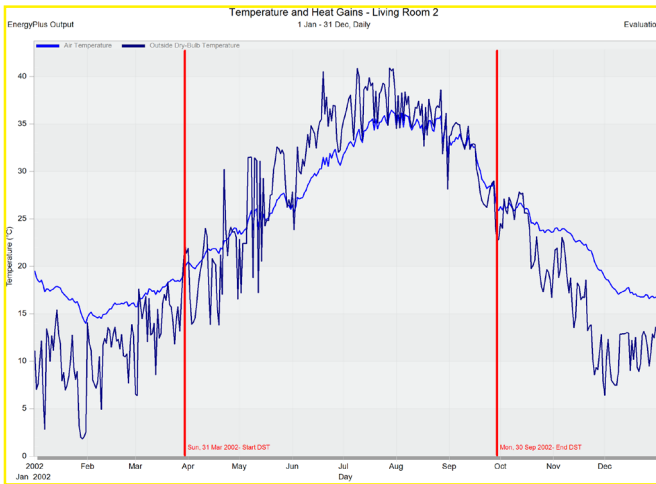
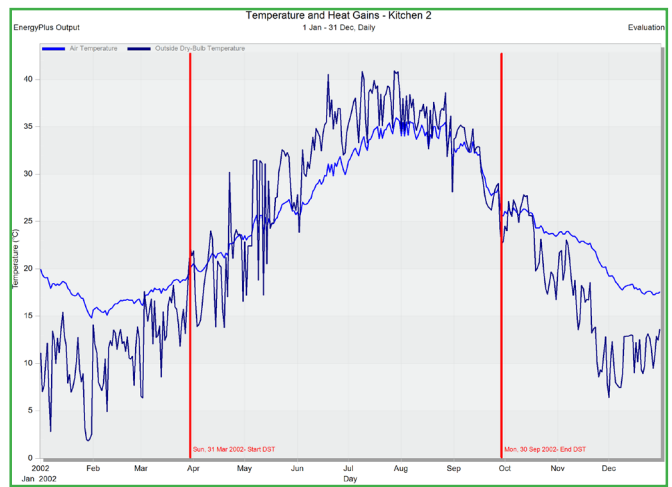
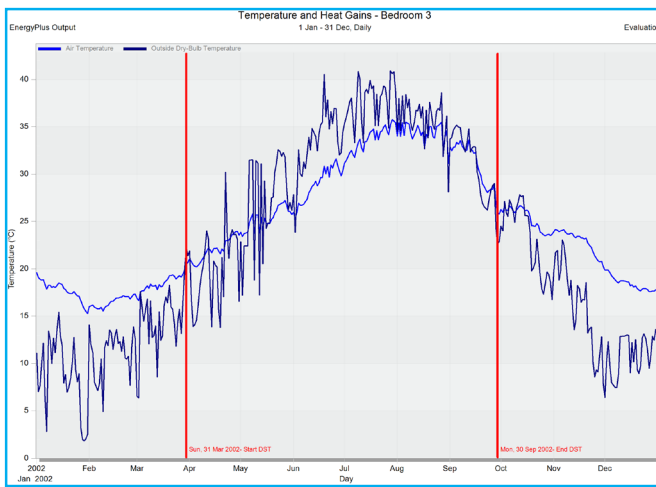
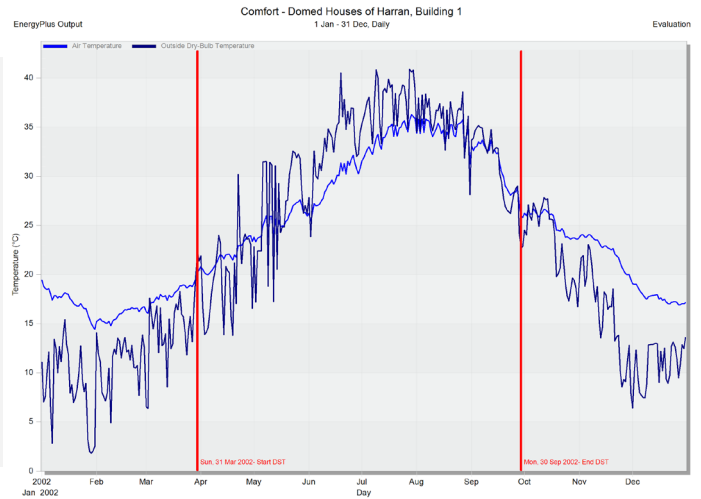
Glazing Template	
Template	No windows
External Windows	
Glazing type	Sgl Clr 3mm
Layout	Preferred height 1.5m, 30% glazed
Dimensions	
Type	3-Preferred height
Window to wall %	30.00
Window height (m)	1.50
Window spacing (m)	5.00
Sill height (m)	0.80
Outside reveal depth (m)	0.000
Frame and Dividers	
Shading	
Airflow Control Windows	
Free Aperture	
Opening position	1-Top
% Glazing area opens	75
Internal Windows	
Sloped Roof Windows/Skylights	
Doors	
Vents	



8.5 95% Openable windows inputs and outputs

Glazing Template

- Template**: No windows
- External Windows**
 - Glazing type**: Sgl Clr 3mm
 - Layout**: Preferred height 1.5m, 30% glazed
 - Dimensions**
 - Type: 3-Preferred height
 - Window to wall %: 30.00
 - Window height (m): 1.50
 - Window spacing (m): 5.00
 - Sill height (m): 0.80
 - Outside reveal depth (m): 0.000
 - Frame and Dividers**
 - Shading**
 - Airflow Control Windows**
 - Free Aperture**
 - Opening position: 1-Top
 - % Glazing area opens: 95
- Internal Windows**
- Sloped Roof Windows/Skylights**
- Doors**
- Vents**



Appendix 9: Glazing system changes

9.1 Single glazing inputs and outputs

Glazing templates >>
Data Report (Not Editable) >>

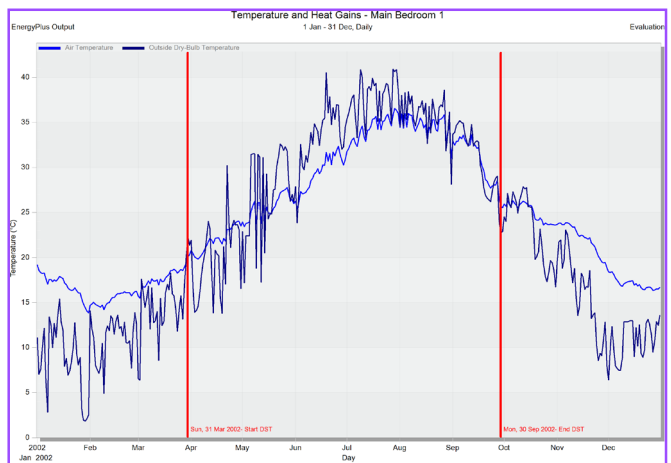
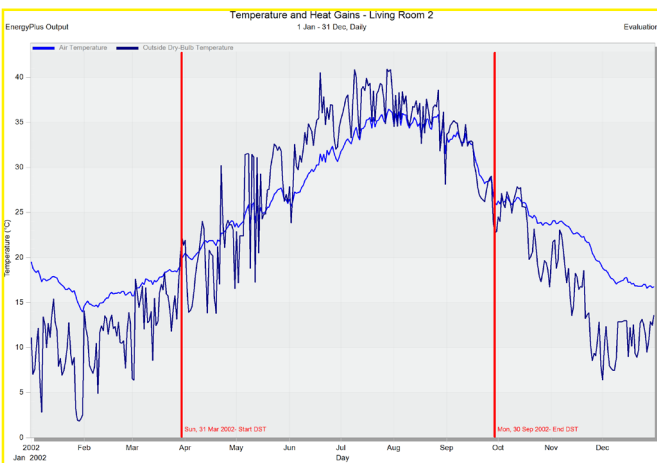
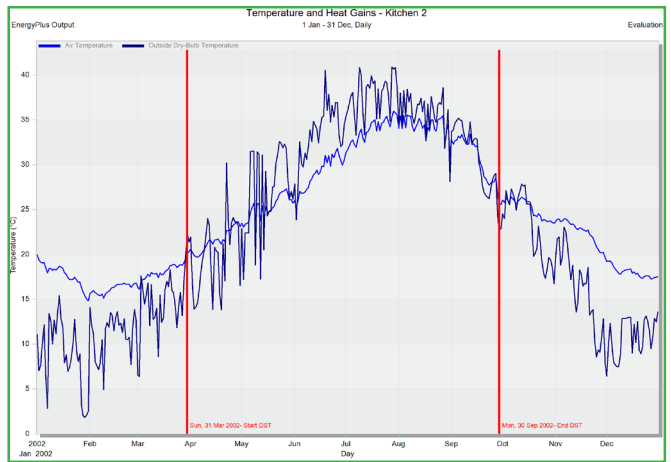
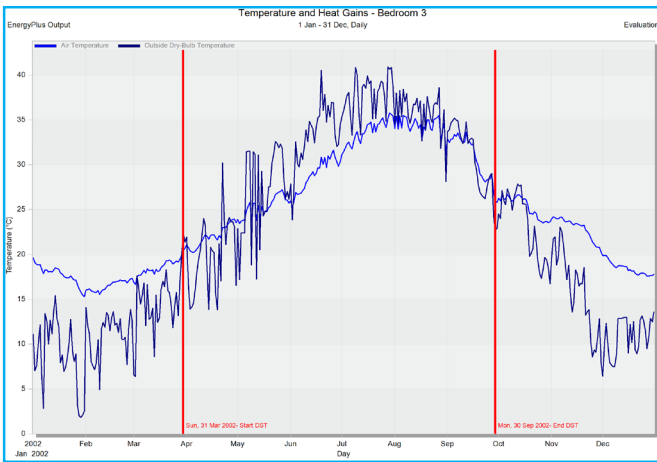
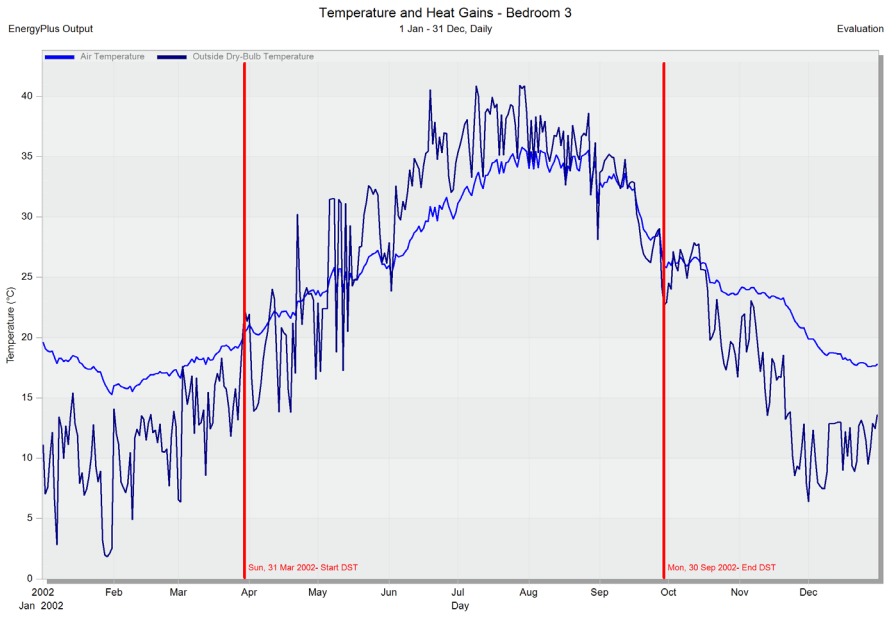
General
Single glazing, clear, no shading
 Category: Single glazing
 Region: General

External Glazing
 Glazing: Sgl Ctr 6mm
 Frame construction: Painted Wooden win
 % Glazing area opens: 5

Internal Glazing
 Glazing: Sgl Ctr 6mm
 Frame construction: Painted Wooden win
 % Glazing area opens: 0

Roof Glazing
 Glazing: Sgl Ctr 6mm
 Frame construction: Painted Wooden win
 % Glazing area opens: 20

External Shading
Detailed Shading Data
 Window shading: No
 Roof window shading: No
 Local shading: No



9.2 Double reflective glazing inputs and outputs

Data Report (Not Editable)

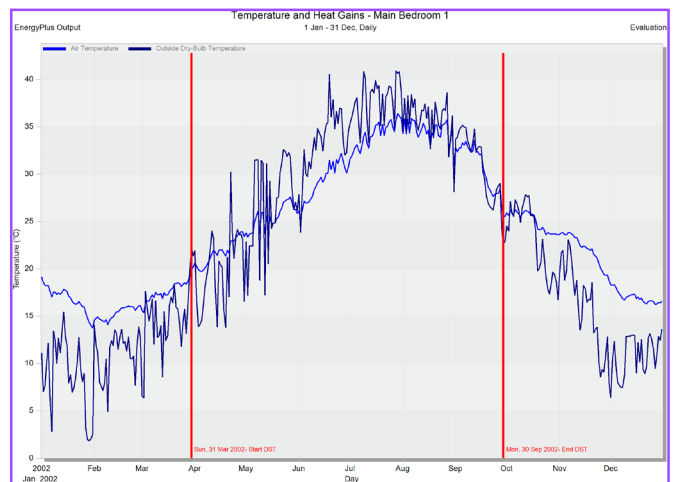
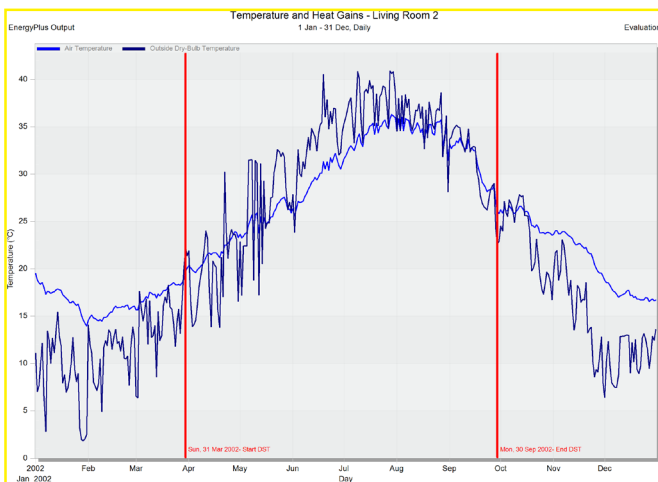
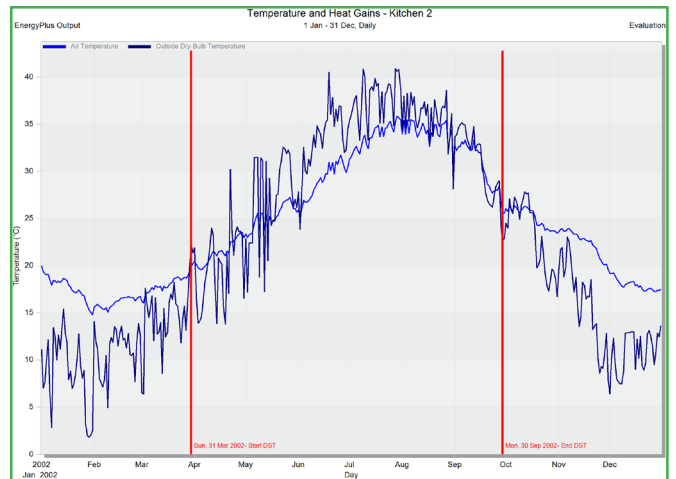
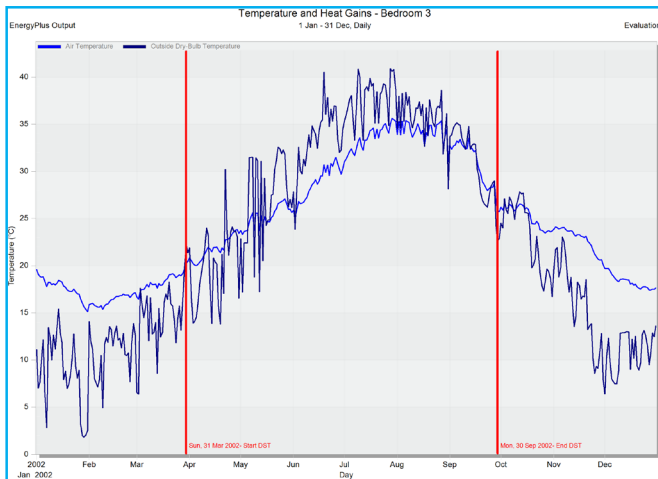
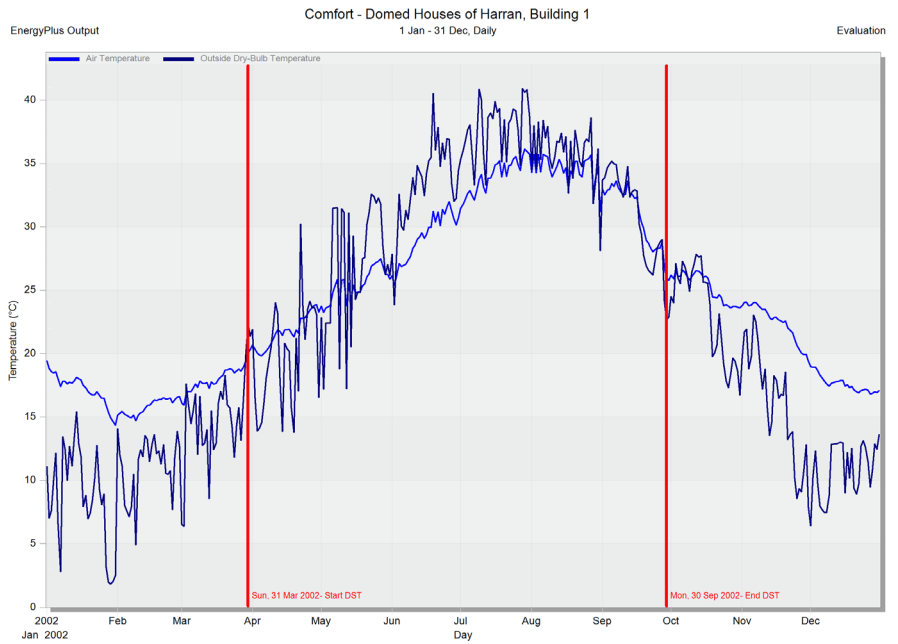
General
Double glazing, reflective, clear, no shading
 Category: Double glazing
 Region: General

External Glazing
 Glazing: Dbl Ref-A-L Clr 6mm/
 Frame construction: Painted Wooden win
 % Glazing area opens: 5

Internal Glazing
 Glazing: Sgl Clr 3mm
 Frame construction: Painted Wooden win
 % Glazing area opens: 0

Roof Glazing
 Glazing: Sgl Clr 3mm
 Frame construction: Painted Wooden win
 % Glazing area opens: 0

External Shading
Detailed Shading Data
 Window shading: No
 Roof window shading: No
 Local shading: No



9.3 Double electrochromic glazing inputs and outputs

Data Report (Not Editable)

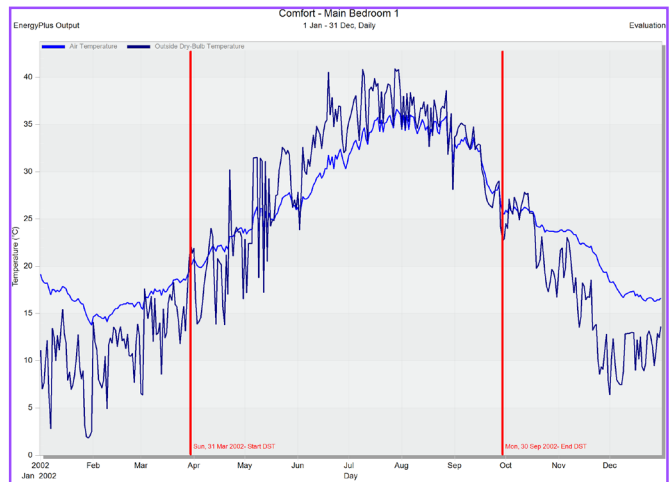
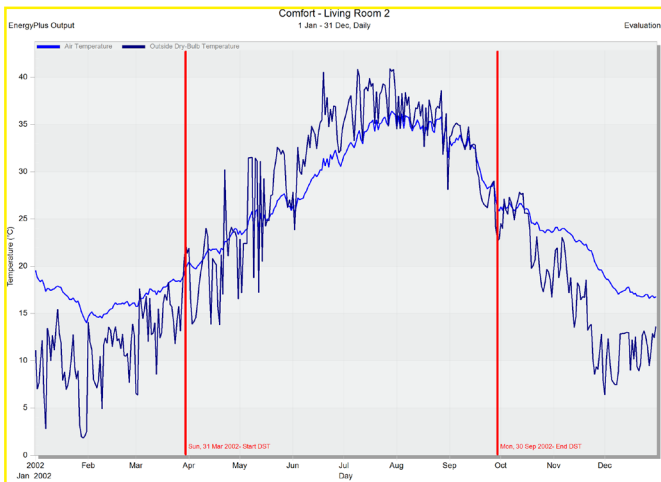
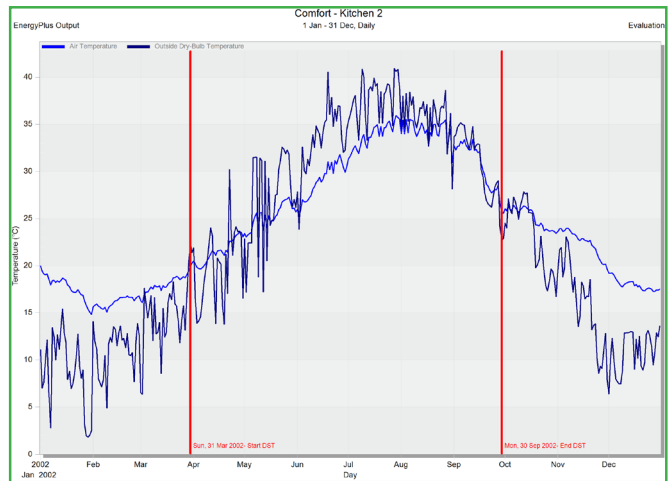
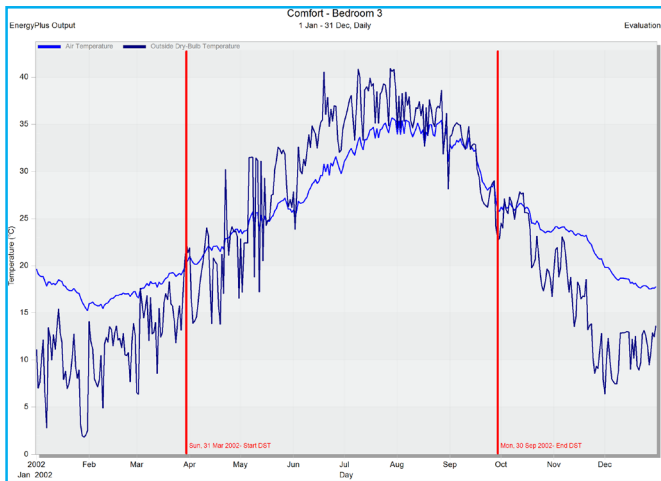
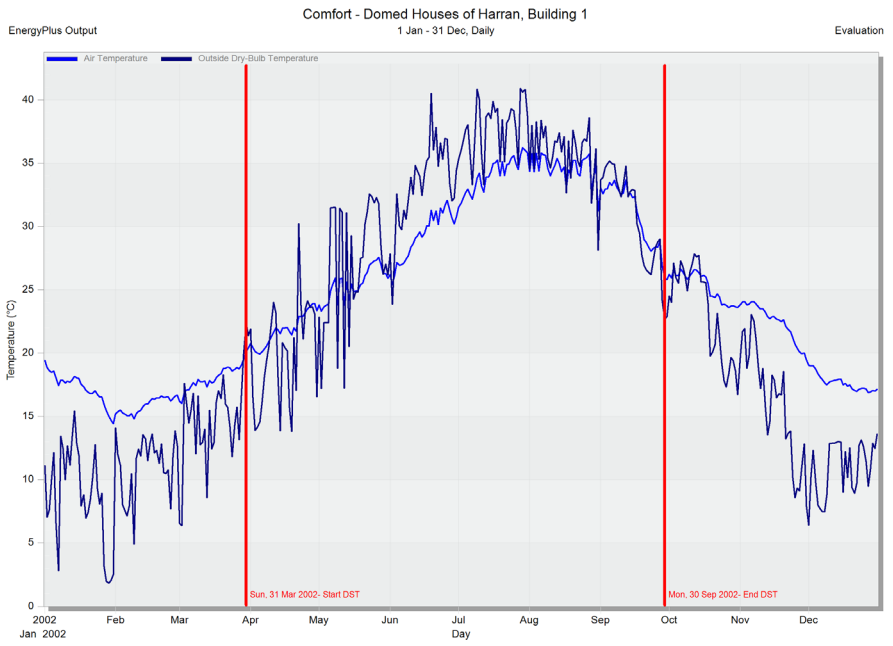
General
Double glazing, clear, electrochromic (reflective) sw
 Category: Double glazing
 Region: General

External Glazing
 Glazing: Dbl Elec Ref Bleache
 Frame construction: Painted Wooden win
 % Glazing area opens: 5

Internal Glazing
 Glazing: Sgl Clr 3mm
 Frame construction: Painted Wooden win
 % Glazing area opens: 0

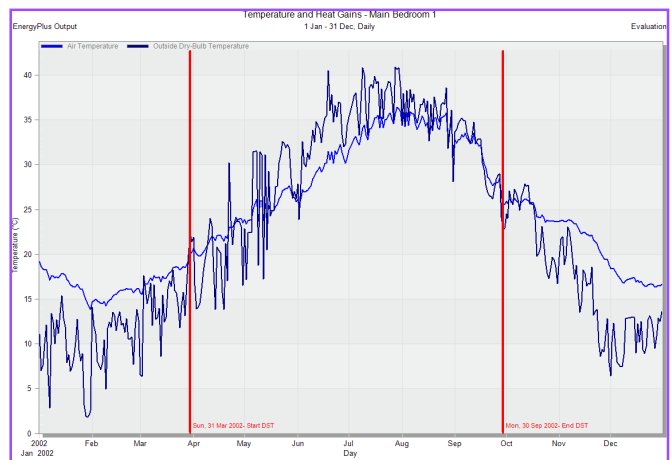
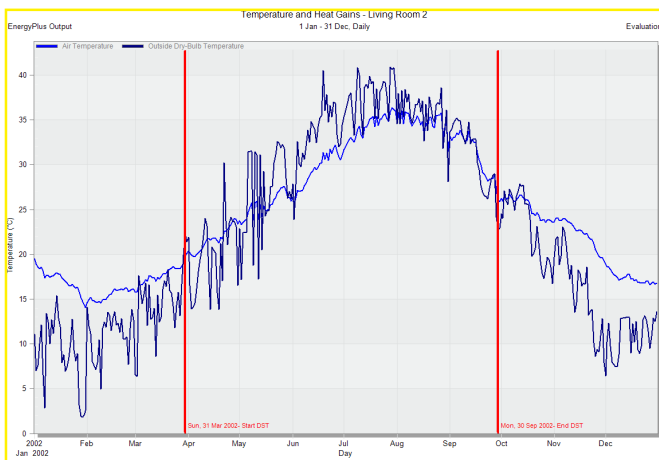
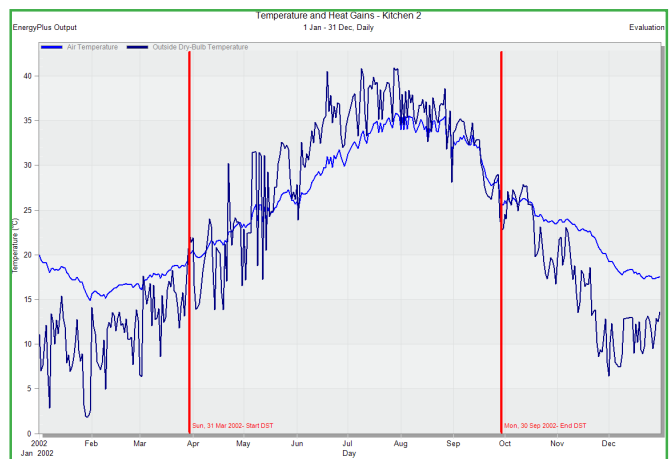
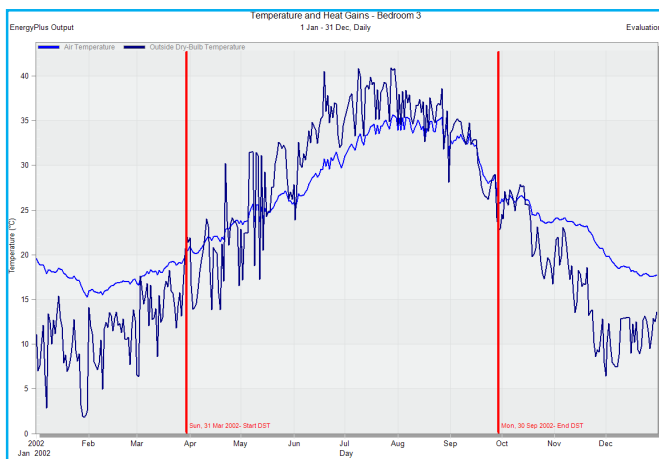
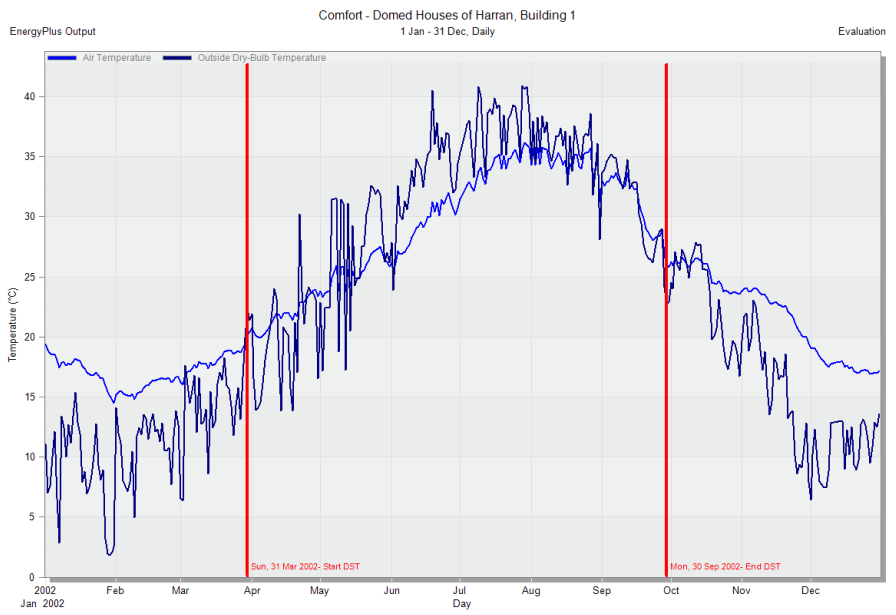
Roof Glazing
 Glazing: Sgl Clr 3mm
 Frame construction: Painted Wooden win
 % Glazing area opens: 0

External Shading
Detailed Shading Data
 Window shading: Yes
 Type: Electrochromic reflect
 Position: 4-Switchable
 Control type: 4-Solar
 Glare override: No
 Heating/cooling override only op...: No
 Solar setpoint (W/m2): 120
 Outside air temperature setpoint (...): 24.00
 Inside air temperature setpoint (°C): 24.00
 Schedule definition: 1-Follow occupancy
 Roof window shading: No
 Local shading: No



9.4 Triple Low-E glazing inputs and outputs

General	
Triple glazing, clear, LoE, argon-filled	
Category	Triple glazing
Region	General
External Glazing	
Glazing	Trp LoE (e2=e5=1) C
Frame construction	Painted Wooden win
% Glazing area opens	5
Internal Glazing	
Glazing	Dbl Clr 6mm/6mm Air
Frame construction	Painted Wooden win
% Glazing area opens	0
Roof Glazing	
Glazing	Trp Clr 3mm/6mm Air
Frame construction	Painted Wooden win
% Glazing area opens	20
External Shading	
Detailed Shading Data	
Window shading	Yes
Type	Blind with medium re
Position	1-Inside
Control type	3-Schedule
Glare override	No
Heating/cooling override only op...	No
Solar setpoint (W/m2)	120
Outside air temperature setpoint (...)	24.00
Inside air temperature setpoint (°C)	24.00
Schedule definition	1-Follow occupancy
Roof window shading	No
Local shading	No



10.2 WWR 2.5% and double reflective glazing inputs and outputs

Data Report (Not Editable)

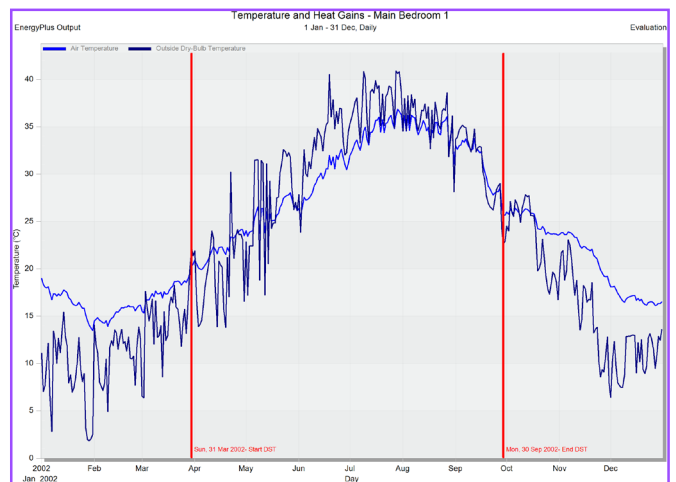
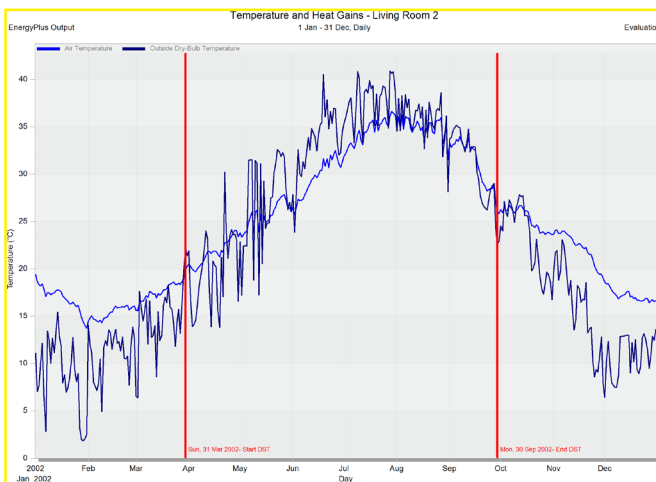
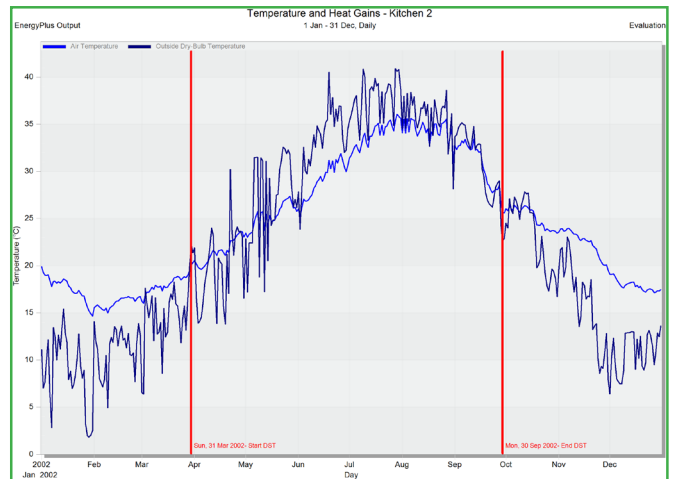
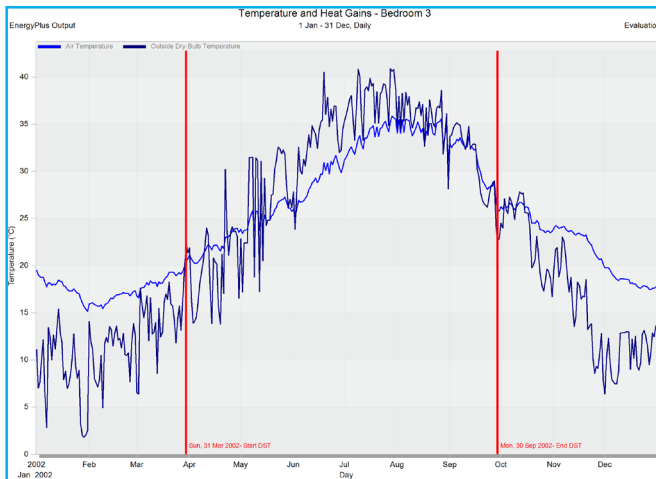
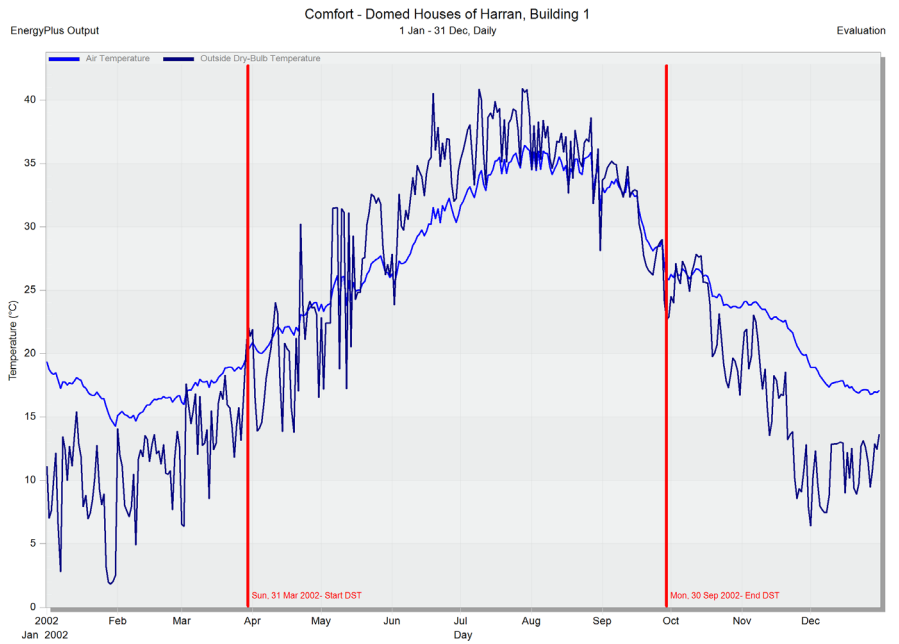
General
Double glazing, reflective, clear, no shading
 Category: Double glazing
 Region: General

External Glazing
 Glazing: Dbl Ref-A-L Clr 6mm/
 Frame construction: Painted Wooden win
 % Glazing area opens: 5

Internal Glazing
 Glazing: Sgl Clr 3mm
 Frame construction: Painted Wooden win
 % Glazing area opens: 0

Roof Glazing
 Glazing: Sgl Clr 3mm
 Frame construction: Painted Wooden win
 % Glazing area opens: 0

External Shading
Detailed Shading Data
 Window shading: No
 Roof window shading: No
 Local shading: No



10.3 WWR 2.5% and double electrochromic glazing inputs and outputs

Data Report (Not Editable)

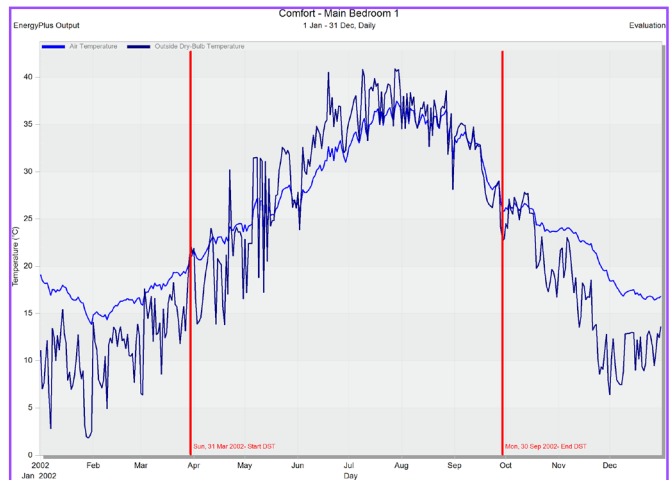
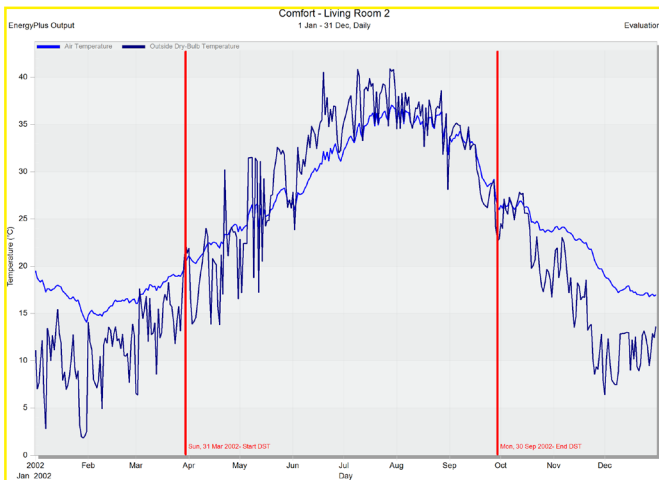
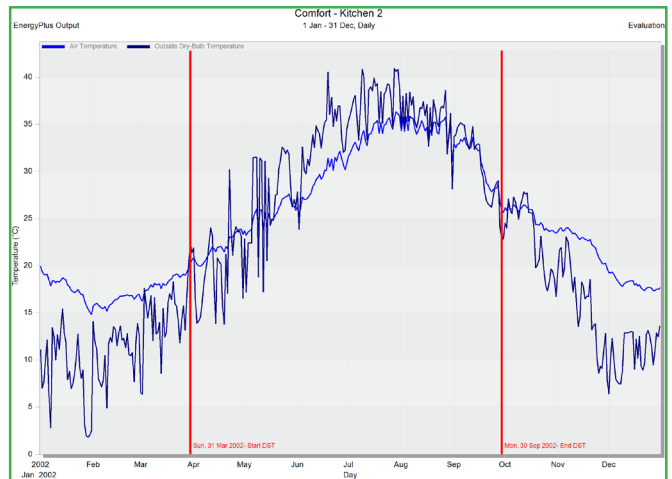
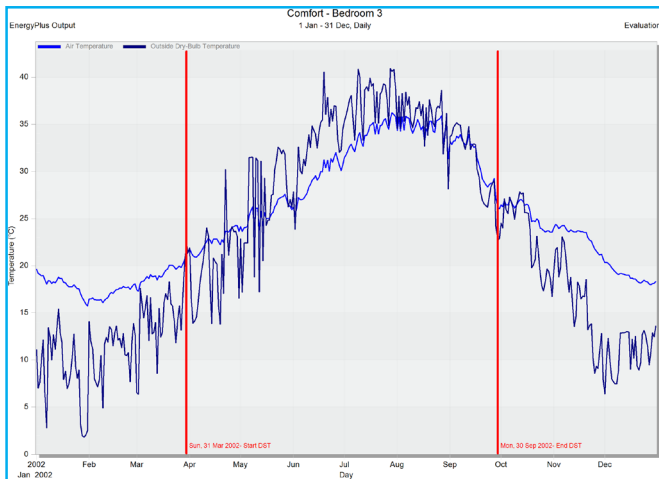
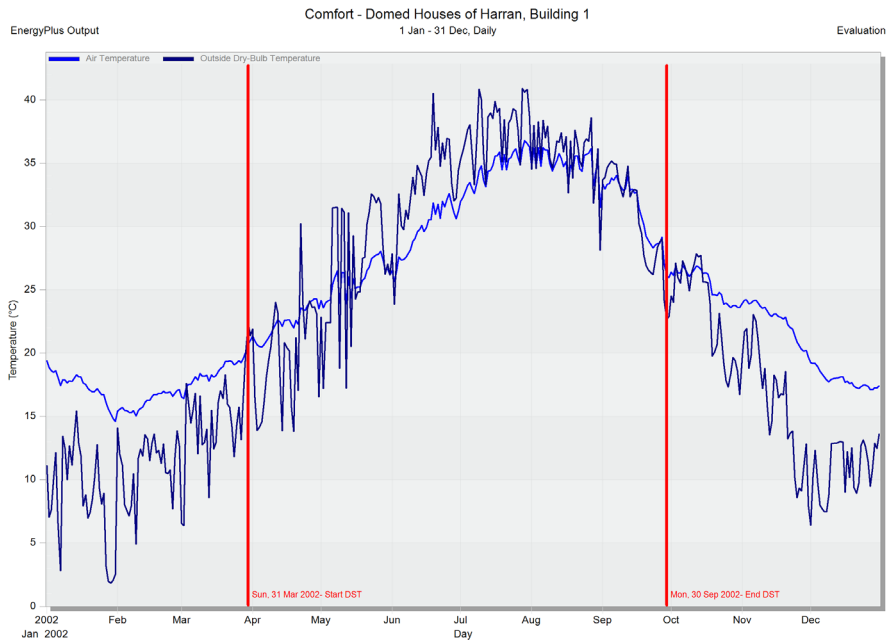
General
Double glazing, clear, electrochromic (reflective) sw
 Category: Double glazing
 Region: General

External Glazing
 Glazing: Dbl Elec Ref Bleache
 Frame construction: Painted Wooden win
 % Glazing area opens: 5

Internal Glazing
 Glazing: Sgl Clr 3mm
 Frame construction: Painted Wooden win
 % Glazing area opens: 0

Roof Glazing
 Glazing: Sgl Clr 3mm
 Frame construction: Painted Wooden win
 % Glazing area opens: 0

External Shading
Detailed Shading Data
 Window shading: Yes
 Type: Electrochromic reflect
 Position: 4-Switchable
 Control type: 4-Solar
 Glare override: No
 Heating/cooling override only op...: No
 Solar setpoint (W/m2): 120
 Outside air temperature setpoint (...): 24.00
 Inside air temperature setpoint (°C): 24.00
 Schedule definition: 1-Follow occupancy
 Roof window shading: No
 Local shading: No



10.4 WWR 2.5% and triple low-e glazing inputs and outputs

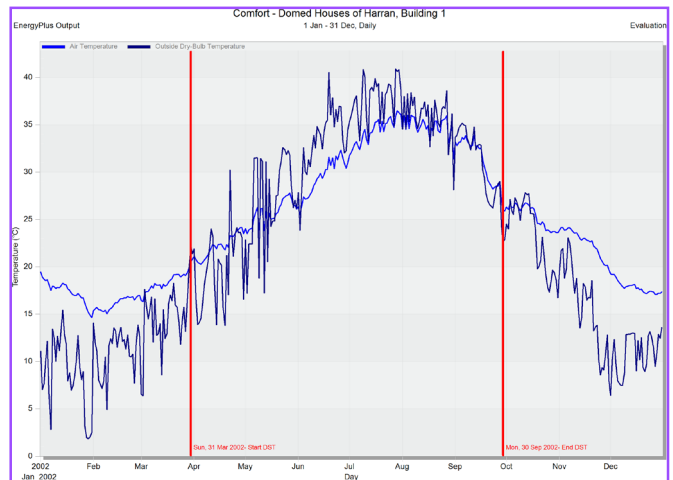
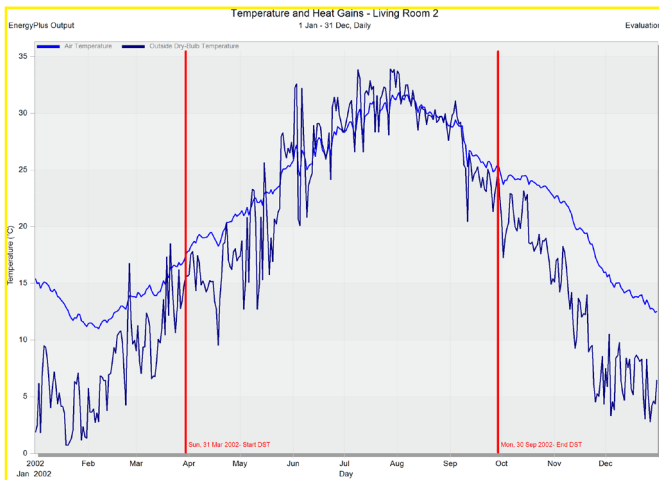
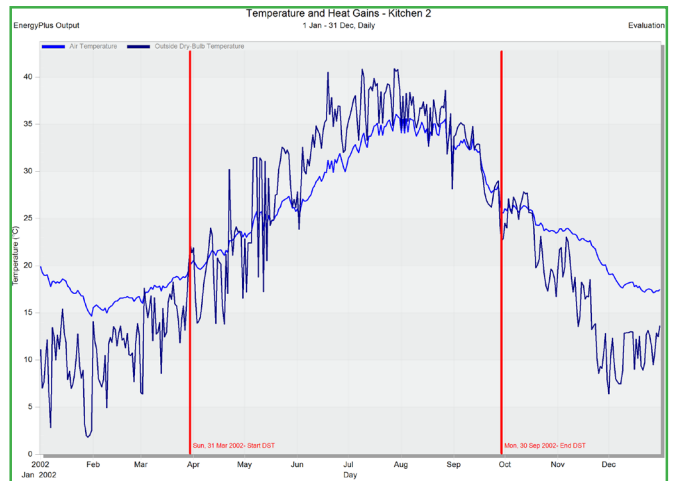
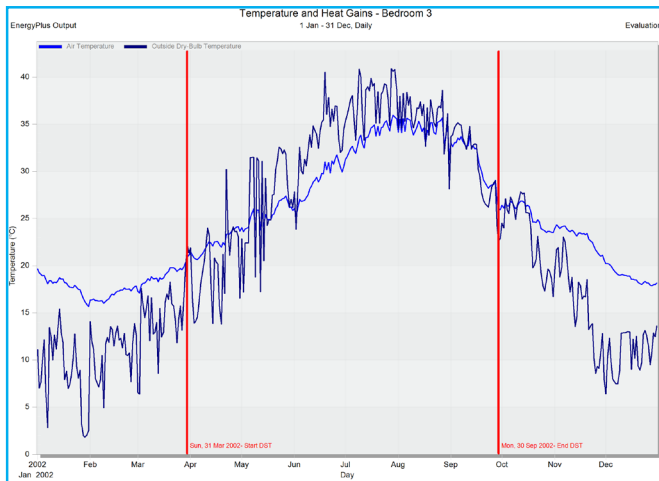
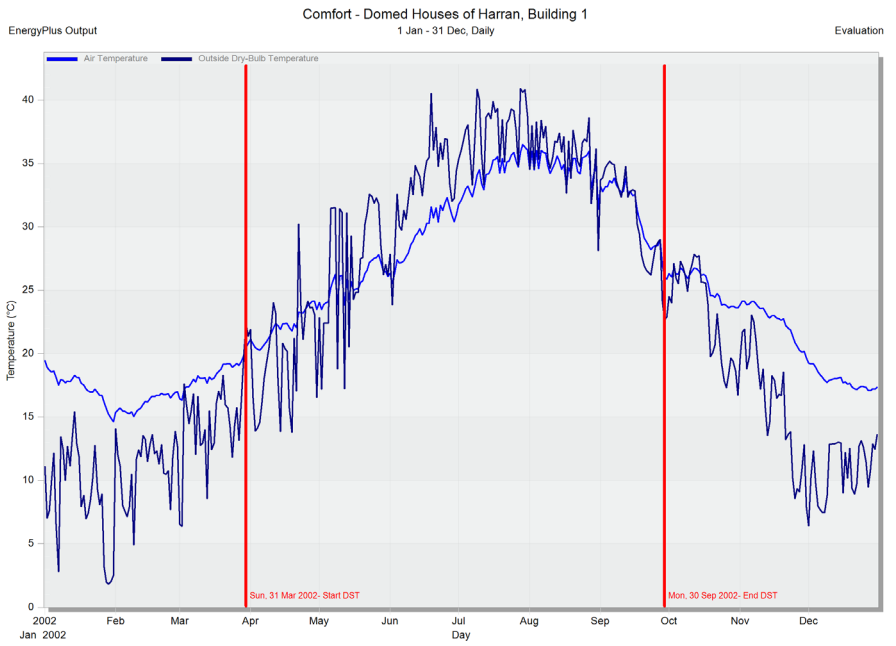
General
Triple glazing, clear, LoE, argon-filled
 Category Triple glazing
 Region General

External Glazing
 Glazing Trp LoE (e2=e5=1) C
 Frame construction Painted Wooden win
 % Glazing area opens 5

Internal Glazing
 Glazing Dbl Clr 6mm/6mm Air
 Frame construction Painted Wooden win
 % Glazing area opens 0

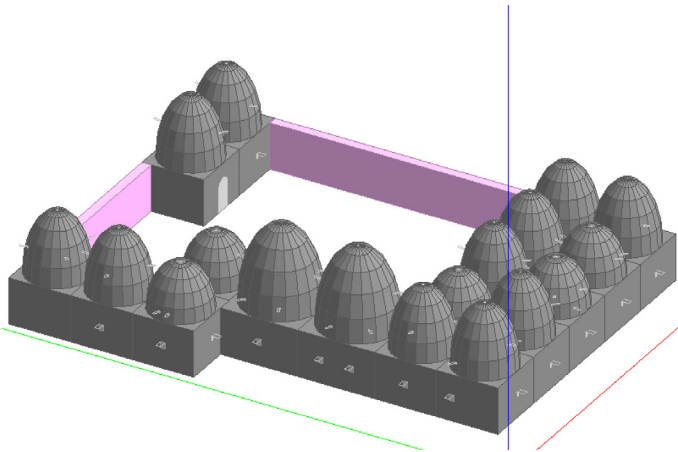
Roof Glazing
 Glazing Trp Clr 3mm/6mm Air
 Frame construction Painted Wooden win
 % Glazing area opens 20

External Shading
Detailed Shading Data
 Window shading Yes
 Type Blind with medium re
 Position 1-Inside
 Control type 3-Schedule
 Glare override No
 Heating/cooling override only op... No
 Solar setpoint (W/m2) 120
 Outside air temperature setpoint (...) 24.00
 Inside air temperature setpoint (°C) 24.00
 Schedule definition 1-Follow occupancy
 Roof window shading No
 Local shading No

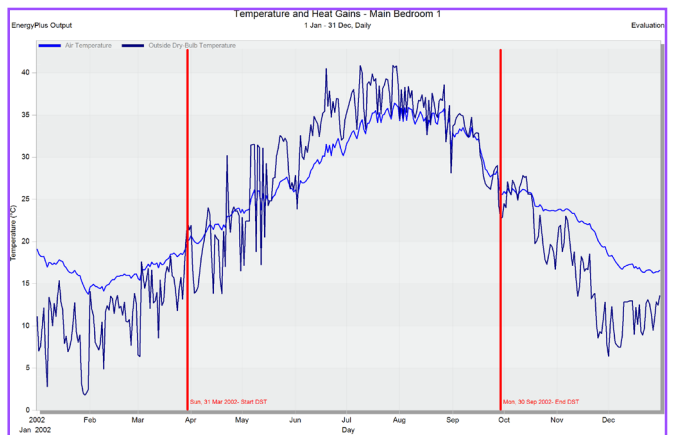
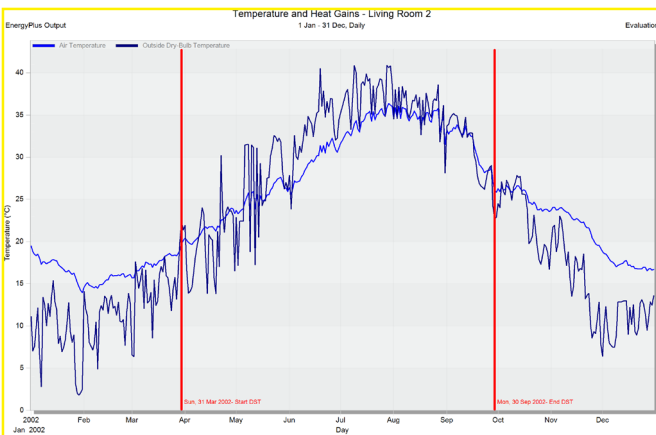
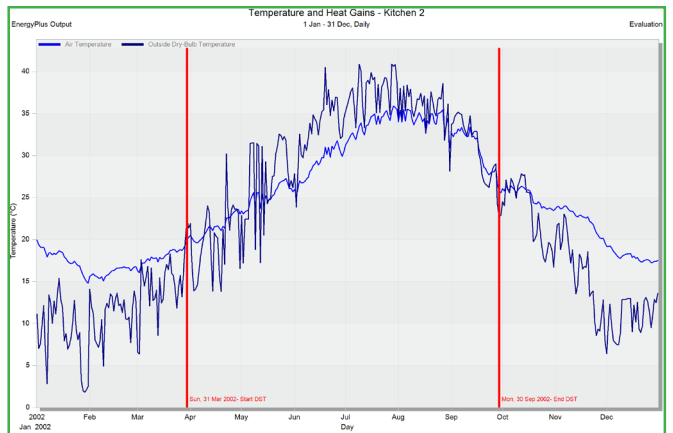
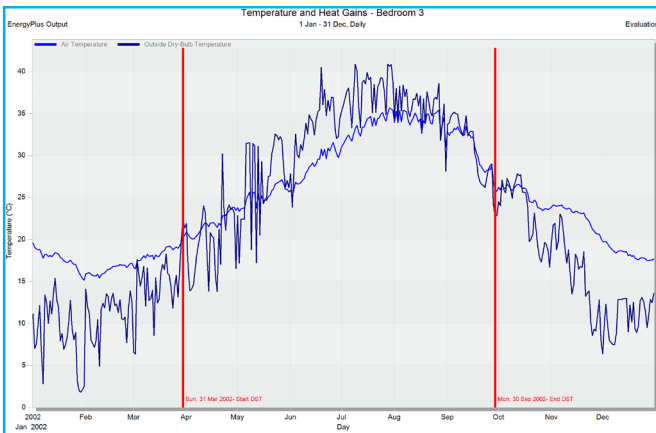
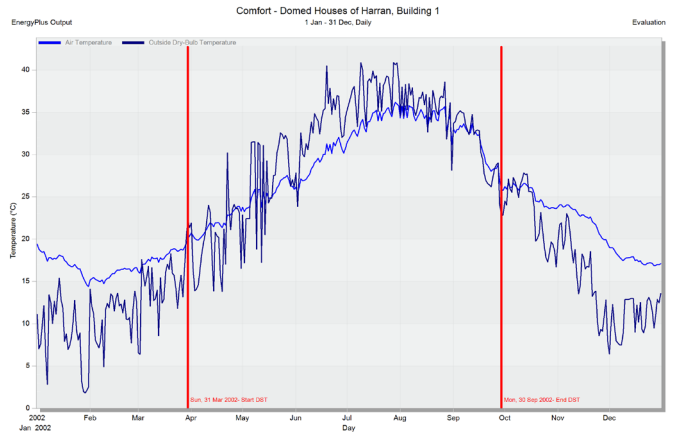


Appendix 11: Shading device changes

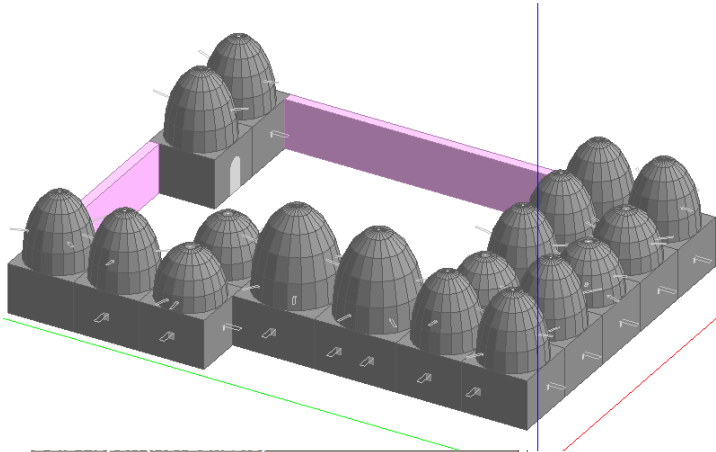
11.1 0.5m local shading inputs and outputs



General	
0.5m Overhang	
Category	Overhangs
Blade material	Steel
Louvre Blade Geometry	
Louvres	No
Sidefin Geometry	
Left sidefin	No
Right sidefin	No
Overhang Geometry	
Overhangs	Yes
Vertical offset from window top (m)	0.000
Projection (m)	0.500
Horizontal window overlap (m)	0.000
Cost	
Cost per window area (GBP/m2)	50.00
Carbon	
CO2 (kgCO2/m2)	50.00
Equivalent CO2 (kgCO2/m2)	50.00



11.2 1m local shading inputs and outputs



General

1.0m Overhang

Category Overhangs

Blade material Steel

Louvre Blade Geometry

Louvres No

Sidefin Geometry

Left sidefin No

Right sidefin No

Overhang Geometry

Overhangs Yes

Vertical offset from window top (m) 0.000

Projection (m) 1.000

Horizontal window overlap (m) 0.000

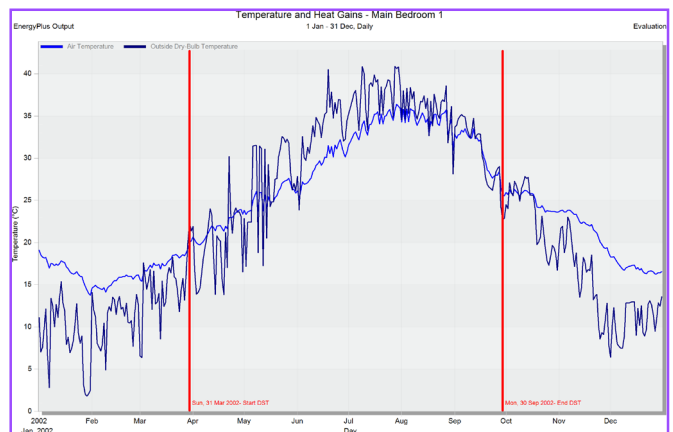
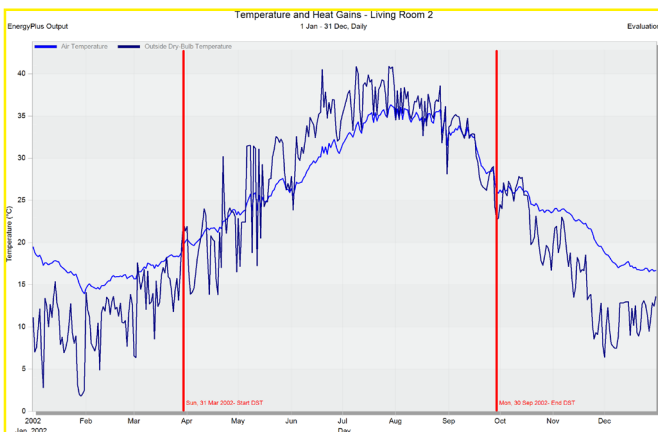
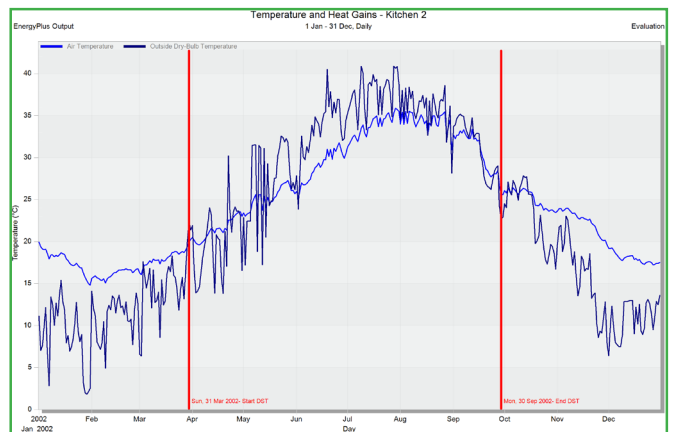
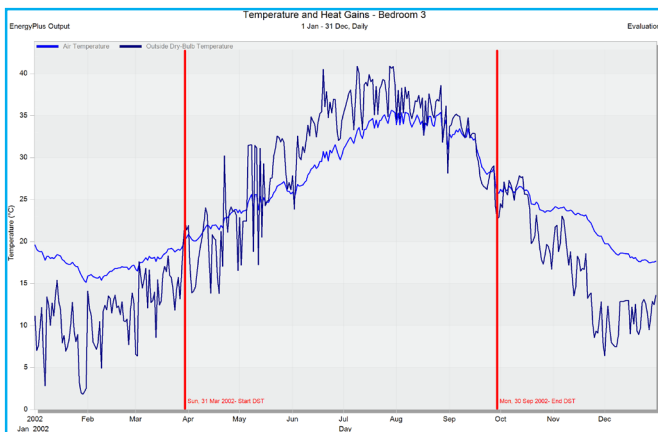
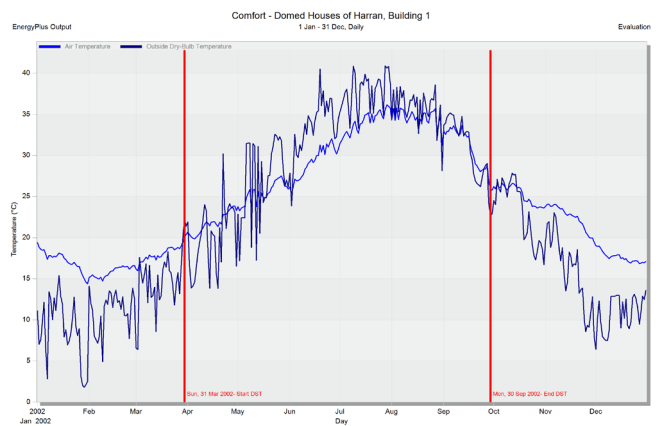
Cost

Cost per window area (GBP/m²) 60.00

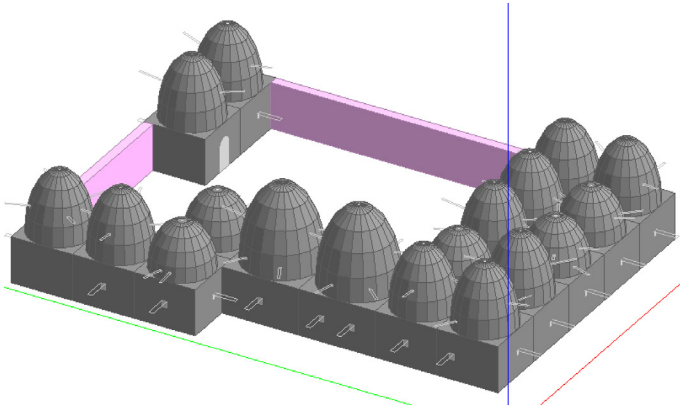
Carbon

CO₂ (kgCO₂/m²) 50.00

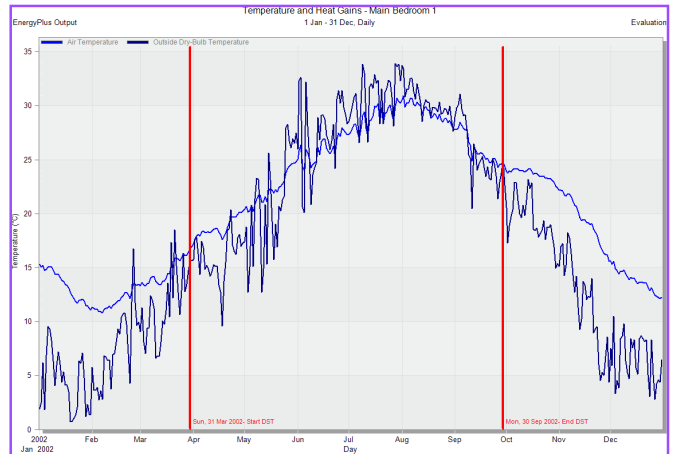
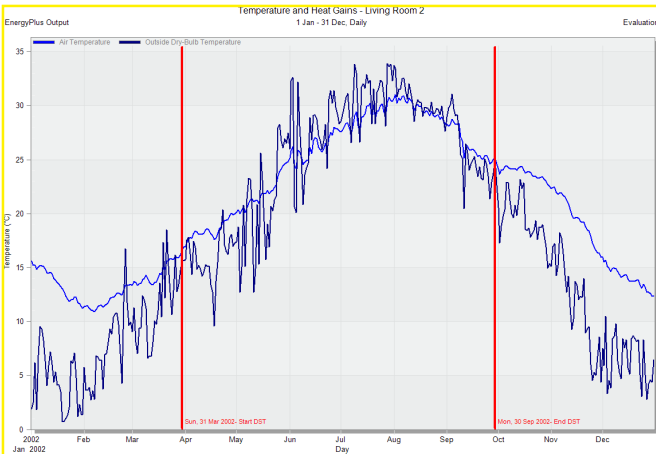
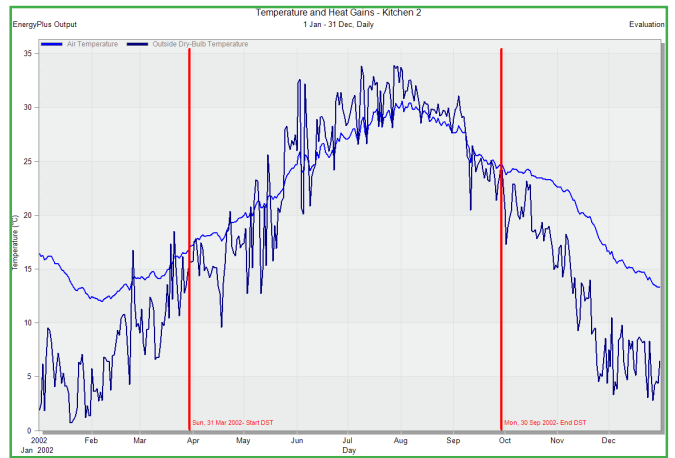
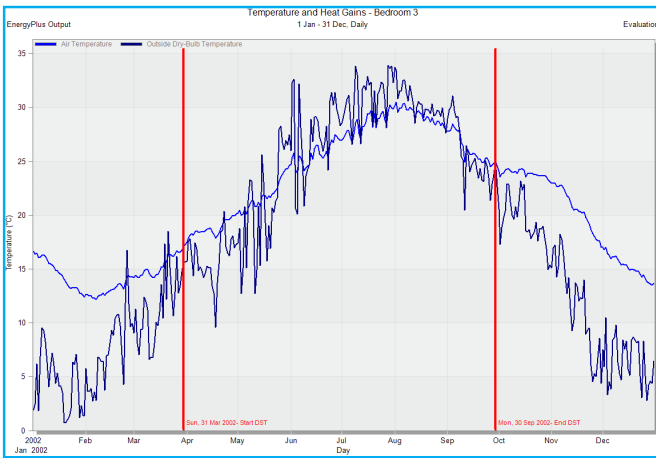
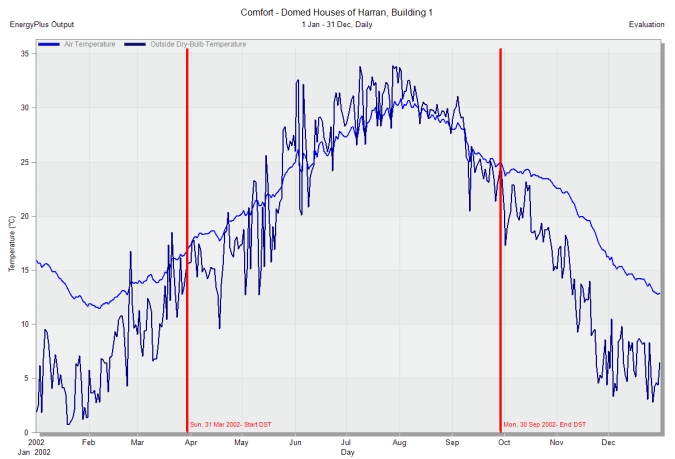
Equivalent CO₂ (kgCO₂/m²) 50.00



11.3 1.5m local shading inputs and outputs



General	
1.5m Overhang	
Category	Overhangs
Blade material	Steel
Louvre Blade Geometry	
Louvres	No
Sidefin Geometry	
Left sidefin	No
Right sidefin	No
Overhang Geometry	
Overhangs	Yes
Vertical offset from window top (m)	0.000
Projection (m)	1.500
Horizontal window overlap (m)	0.000
Cost	
Cost per window area (GBP/m ²)	70.00
Carbon	
CO ₂ (kgCO ₂ /m ²)	50.00
Equivalent CO ₂ (kgCO ₂ /m ²)	50.00



11.4 Blinds with highly reflective slats inputs and outputs

General

Blind with high reflectivity slats

Category Slatted blinds
Source E+

Slat Properties

Blind-to-glass distance (m) 0.0150
Slat orientation Horizontal
Slat width (m) 0.02500
Slat separation (m) 0.01875
Slat thickness (m) 0.00100
Slat conductivity (W/m-K) 0.900
Slat angle (°) 45.0
Minimum slat angle (°) 0
Maximum slat angle (°) 180

Slat Solar Properties

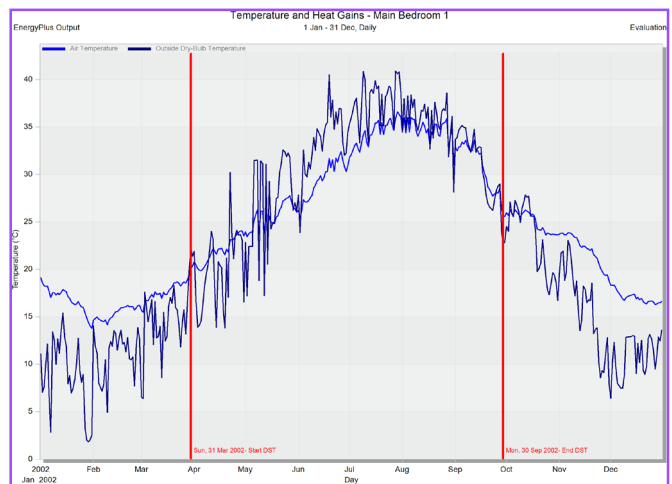
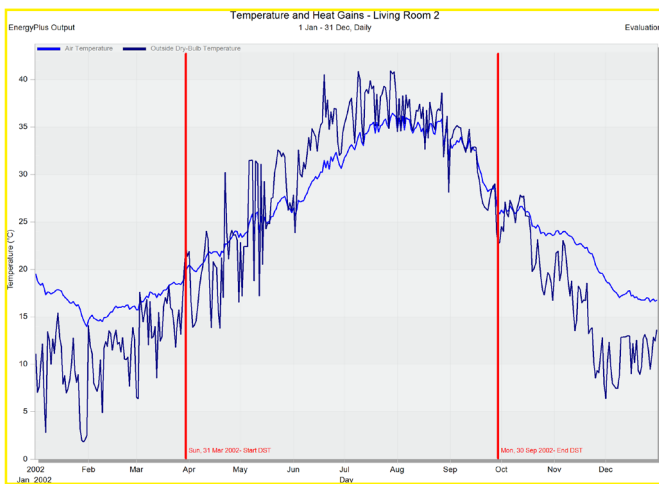
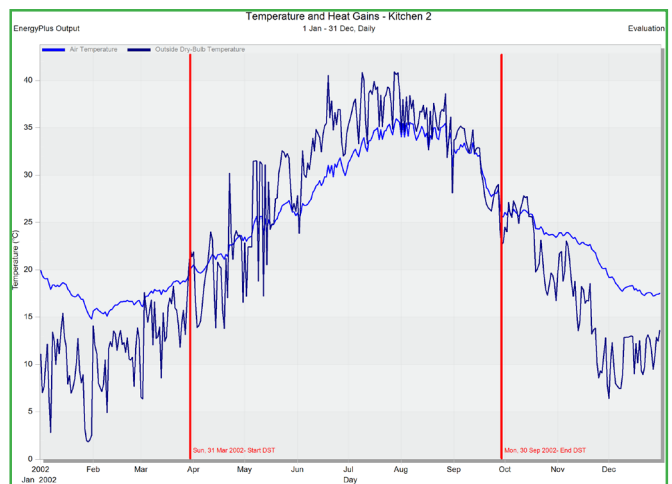
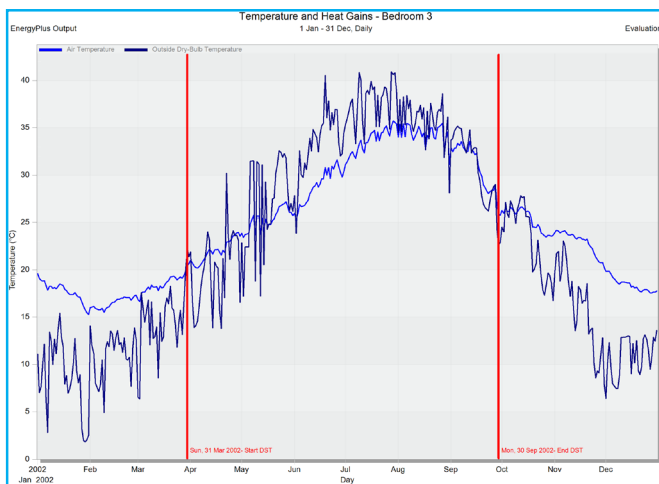
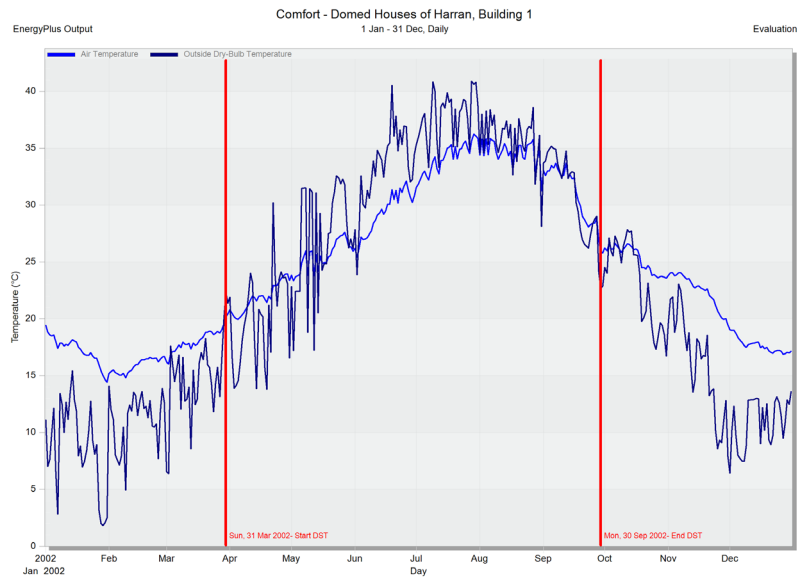
Slat solar transmittance 0.000
Slat solar reflectance, front side 0.800
Slat solar reflectance, back side 0.800

Slat Visible Properties

Slat visible transmittance 0.000
Slat visible reflectance, front side 0.800
Slat visible reflectance, back side 0.800

Slat IR (Thermal) Properties

Slat hemispherical transmittance 0.000
Slat hemispherical emissivity, front si... 0.900
Slat hemispherical emissivity, back s... 0.900



11.5 Venetian blinds inputs and outputs

General

Venetian blinds - medium (modelled as diffusing)

Category: Diffusing shades
Source: BLAST

Shade Properties

Thickness (m): 0.0030
Conductivity (W/m-K): 0.10000
Solar transmittance: 0.600
Solar reflectance: 0.120
Visible transmittance: 0.600
Visible reflectance: 0.120
Long-wave emissivity: 0.900
Long-wave transmittance: 0.000

Openings

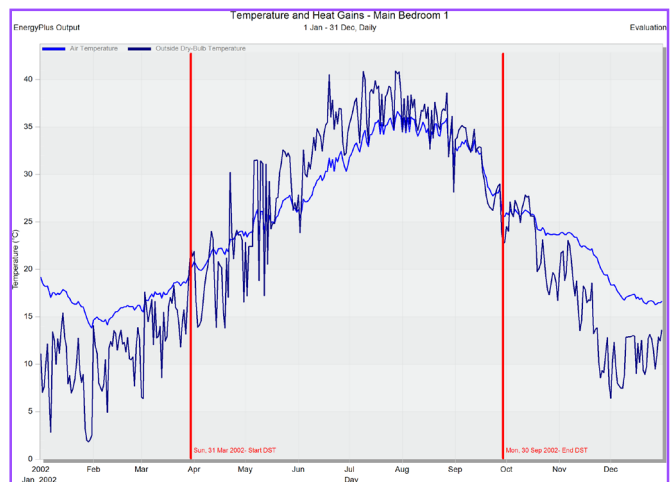
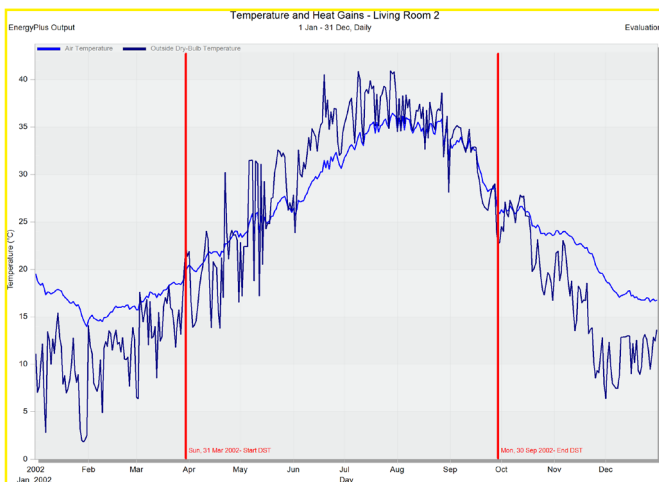
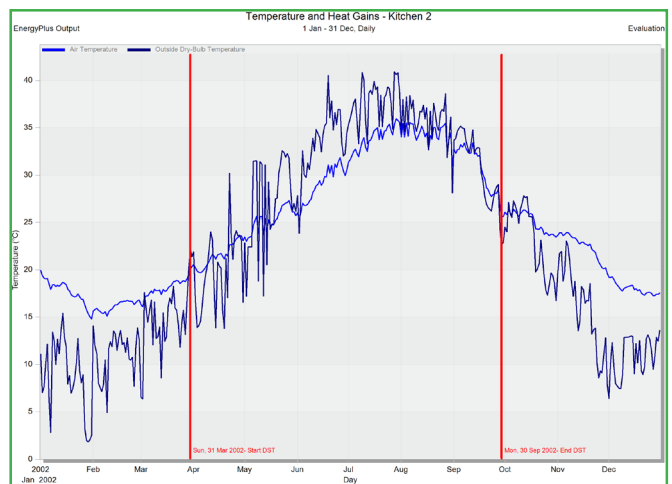
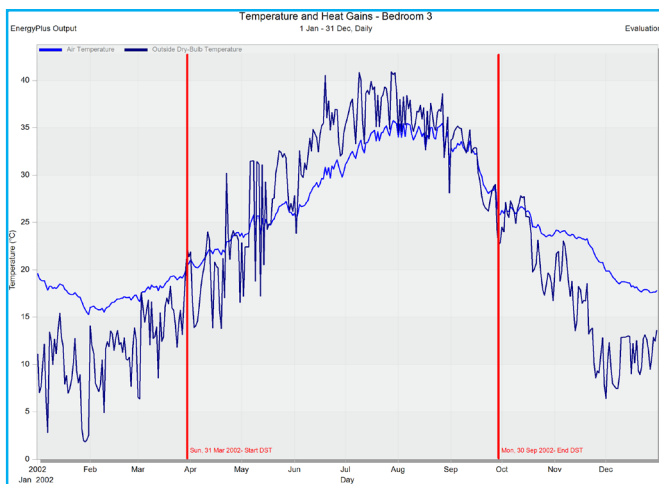
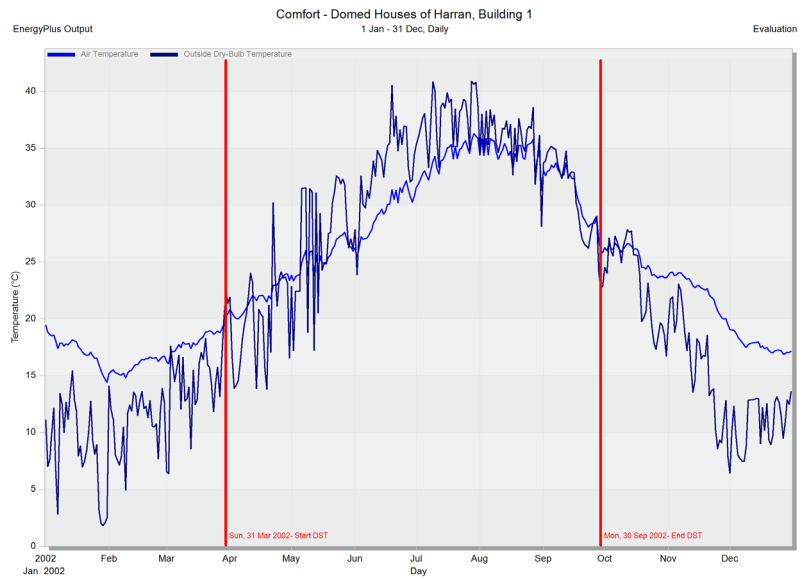
Shade-to-glass distance (m): 0.050
Shade top opening multiplier: 1.000
Shade bottom opening multiplier: 1.000
Shade left-side opening multiplier: 0.000
Shade right-side opening multiplier: 0.000
Shade airflow permeability: 0.000

Cost

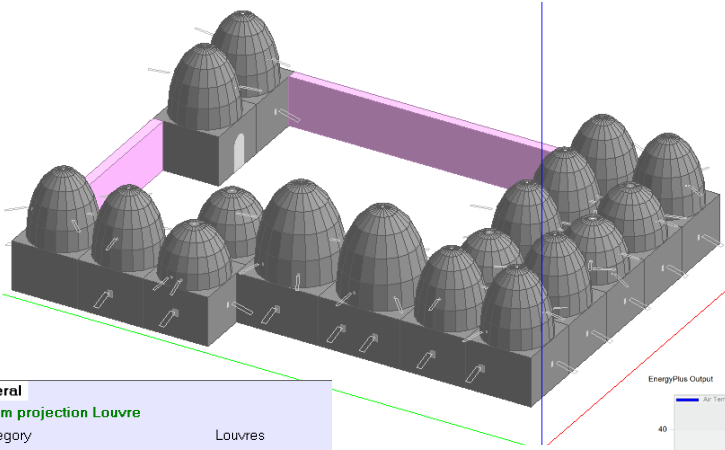
Cost per window area (GBP/m²): 50.00

Carbon

CO₂ (kgCO₂/kg): 50.00
Equivalent CO₂ (kgCO₂/kg): 50.00



11.6 1.5m louvres inputs and outputs



General

1.5 m projection Louvre

Category Louvres

Blade material Steel

Louvre Blade Geometry

Louvres Yes
 Number of blades 4
 Vertical spacing (m) 0.300
 Angle (°) 15.000
 Distance from window (m) 0.300
 Blade depth (m) 1.200
 Vertical offset from window top (m) 0.000
 Horizontal window overlap (m) 0.000

Sidfin Geometry

Left sidfin No

Right sidfin No

Overhang Geometry

Overhangs No

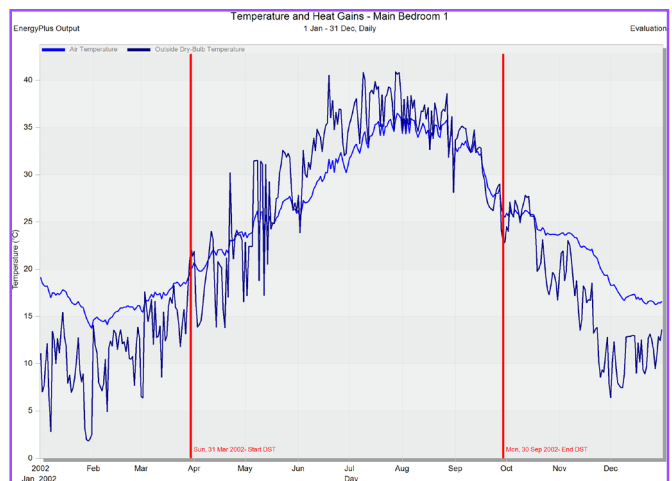
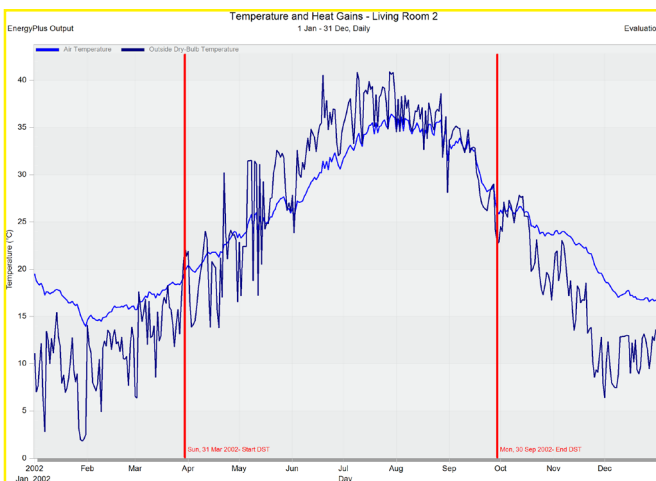
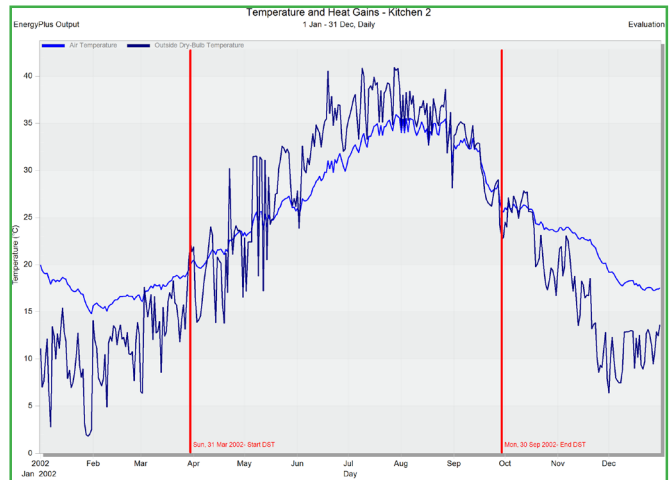
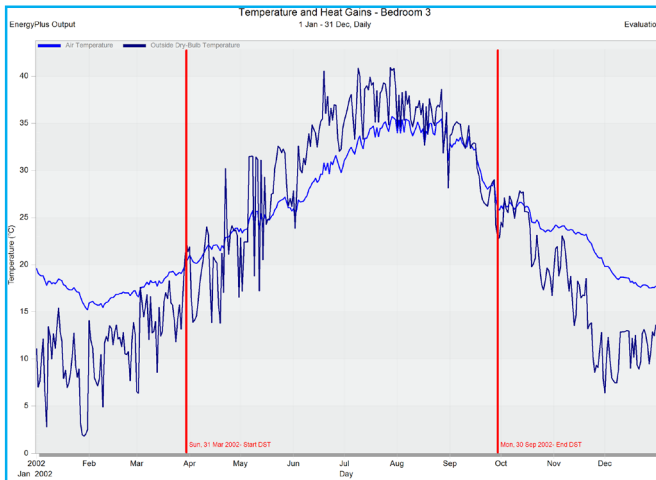
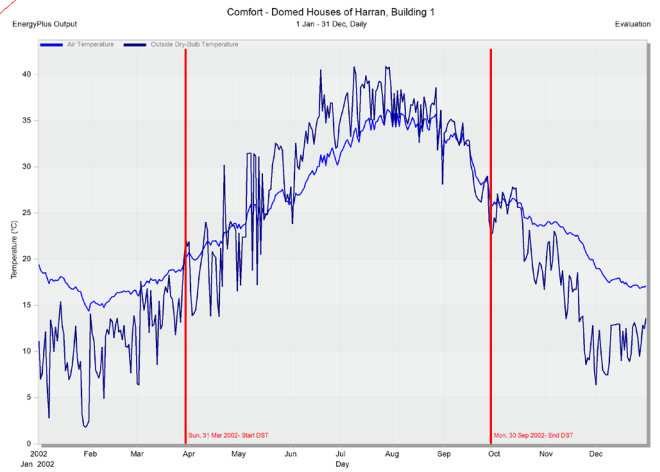
Cost

Cost per window area (GBP/m²) 80.00

Carbon

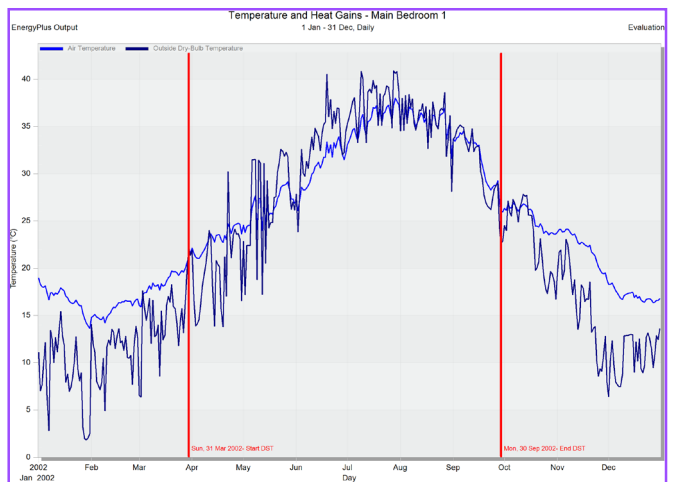
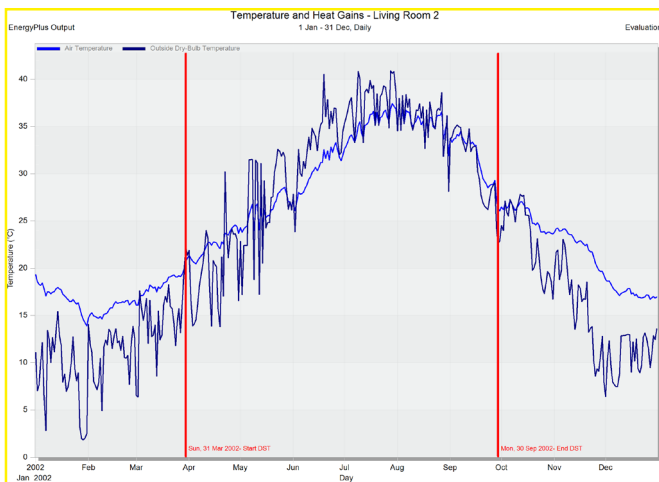
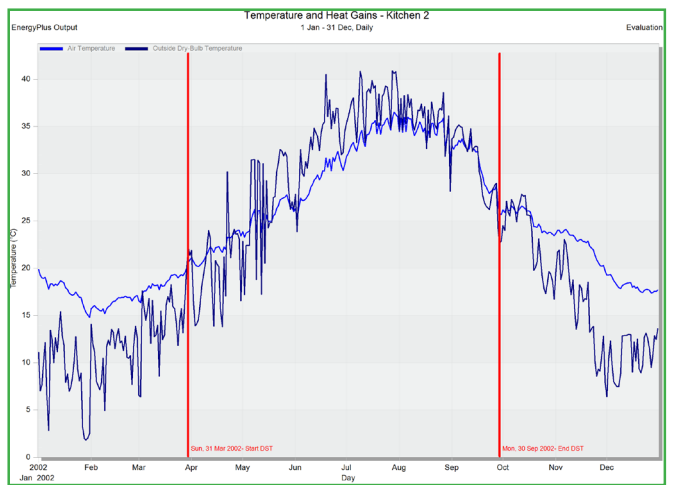
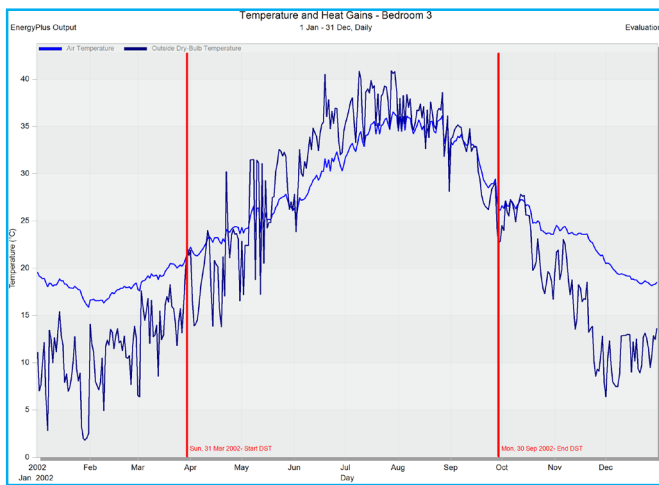
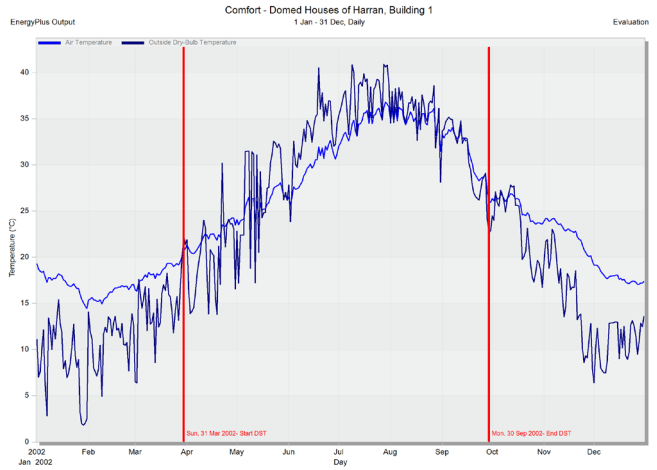
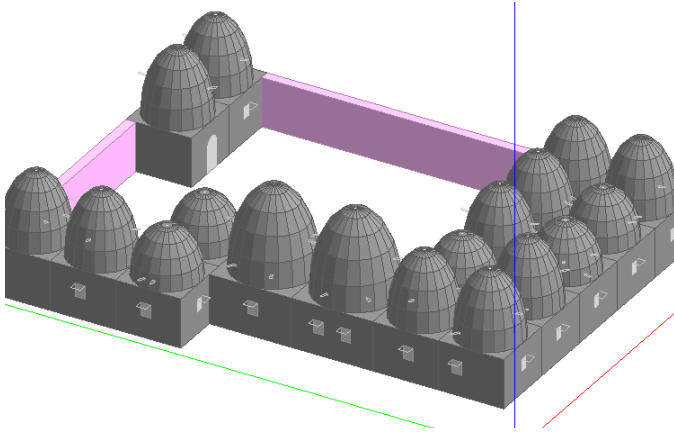
CO₂ (kgCO₂/m²) 50.00

Equivalent CO₂ (kgCO₂/m²) 50.00

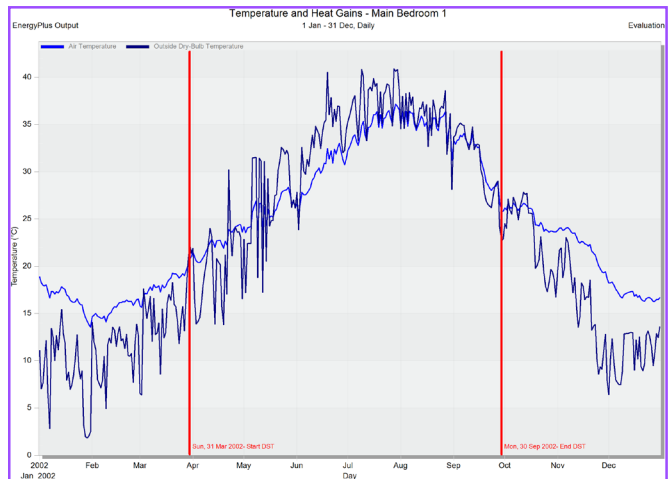
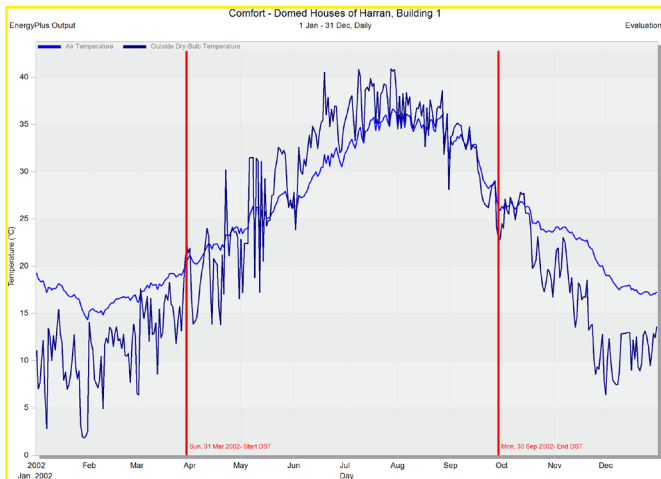
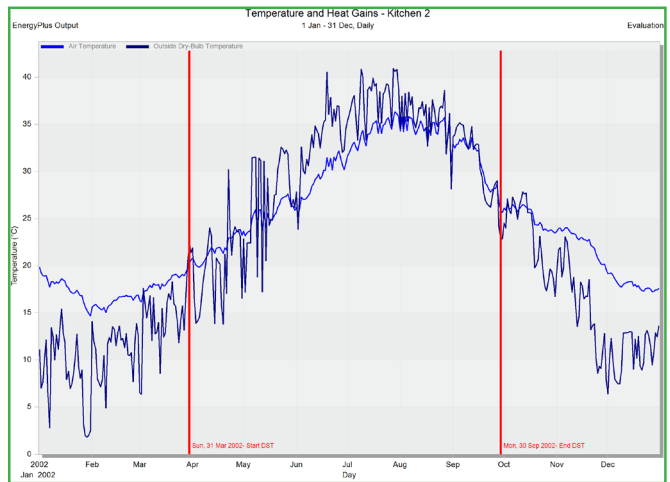
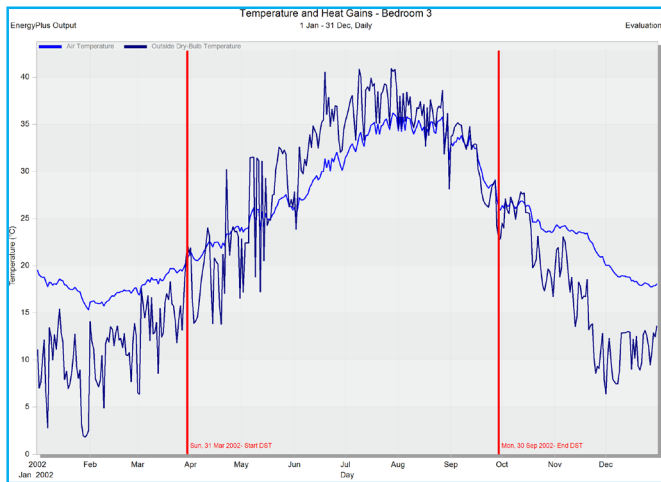
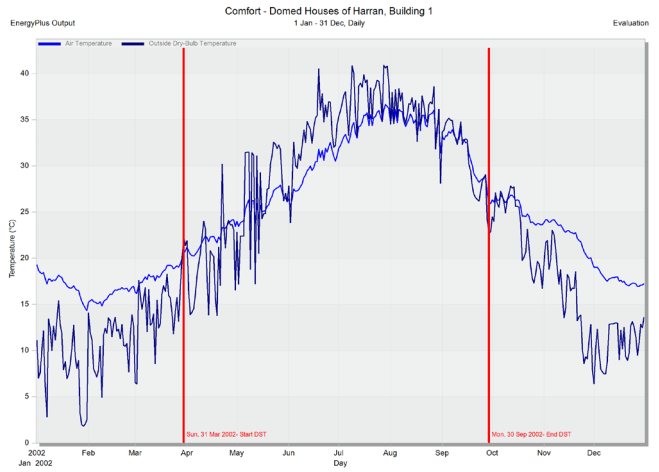
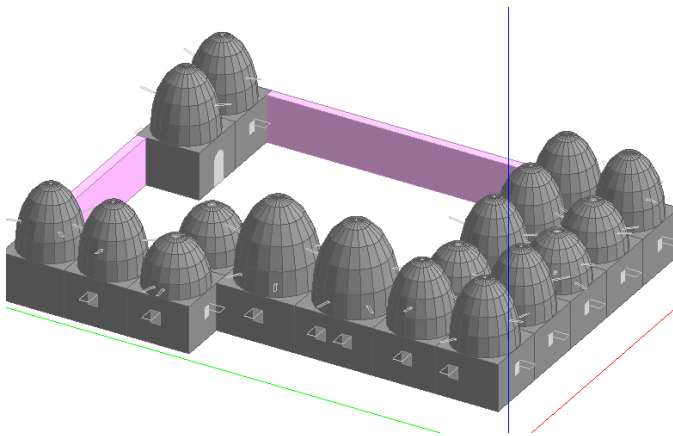


Appendix 12: Shading device changes on a WWR of 2.5%

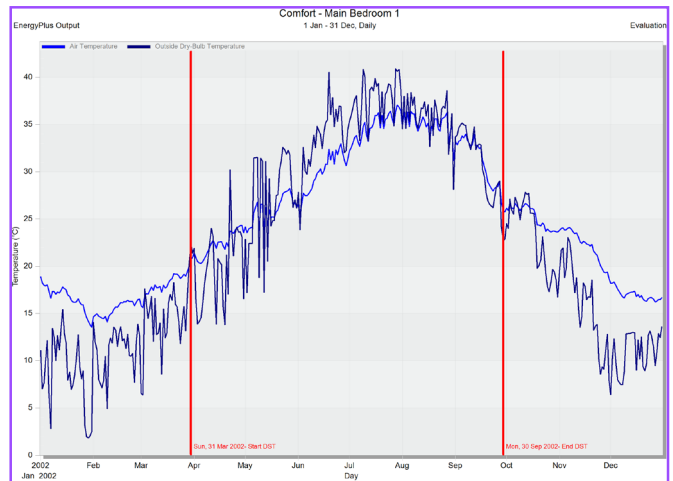
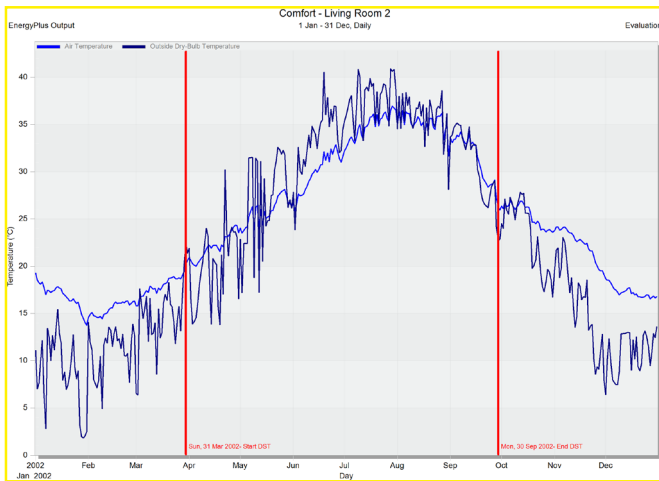
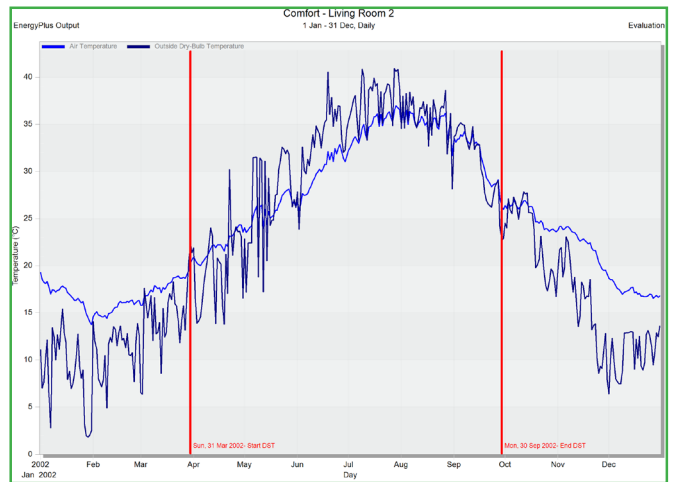
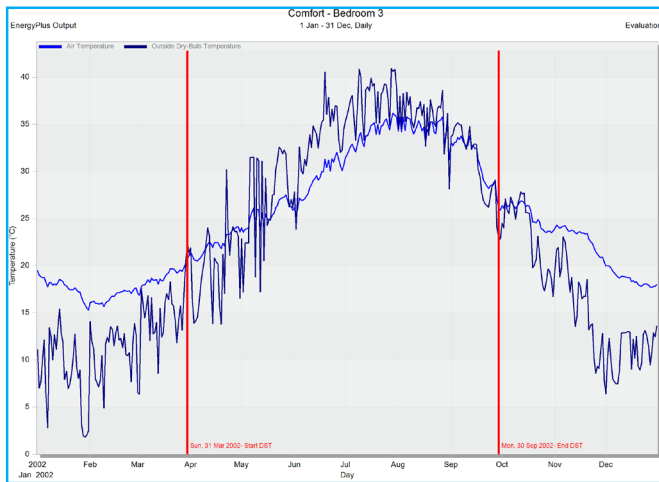
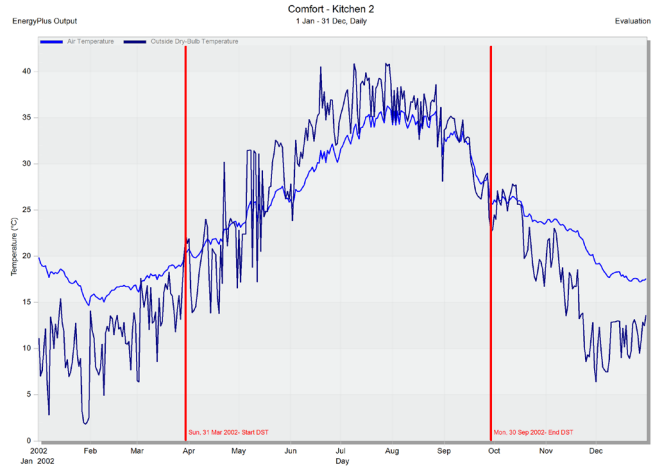
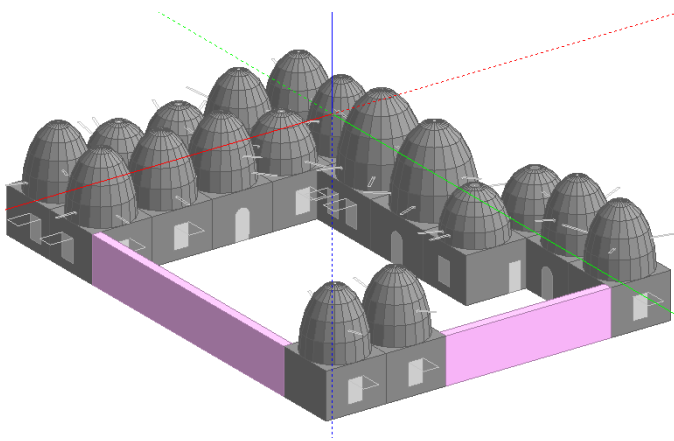
12.1 WWR 2.5% and 0.5m local shading inputs and outputs



12.2 WWR 2.5% and 1m local shading inputs and outputs



12.3 WWR 2.5% and 1.5m local shading inputs and outputs



12.4 WWR 2.5% and blinds with highly reflective slats inputs and outputs

General

Blind with high reflectivity slats

Category Slatted blinds
Source E+

Slat Properties

Blind-to-glass distance (m) 0.0150
Slat orientation Horizontal
Slat width (m) 0.02500
Slat separation (m) 0.01875
Slat thickness (m) 0.00100
Slat conductivity (W/m-K) 0.900
Slat angle (°) 45.0
Minimum slat angle (°) 0
Maximum slat angle (°) 180

Slat Solar Properties

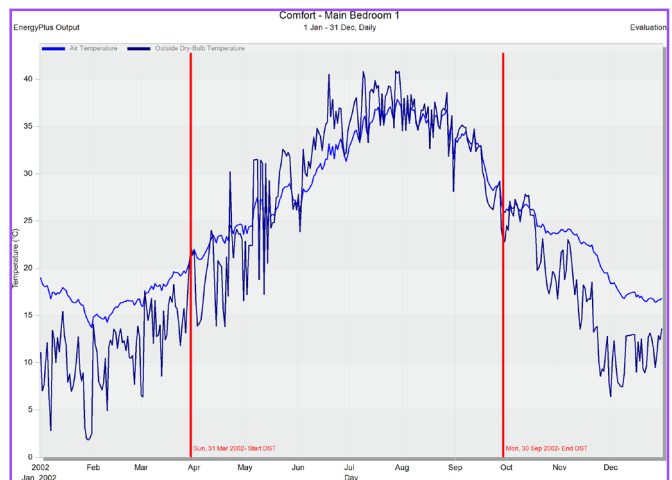
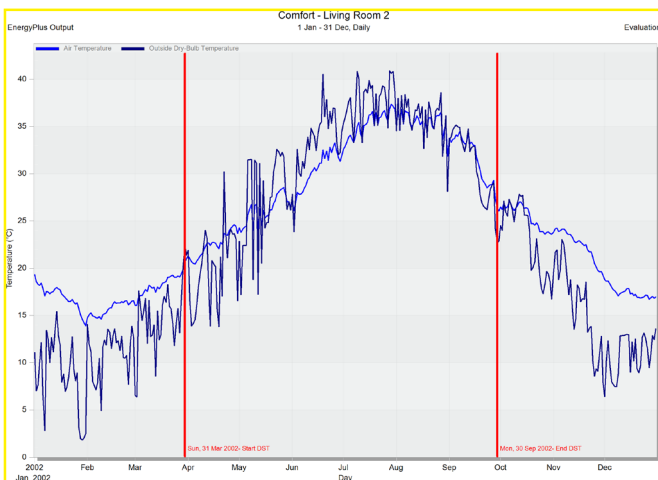
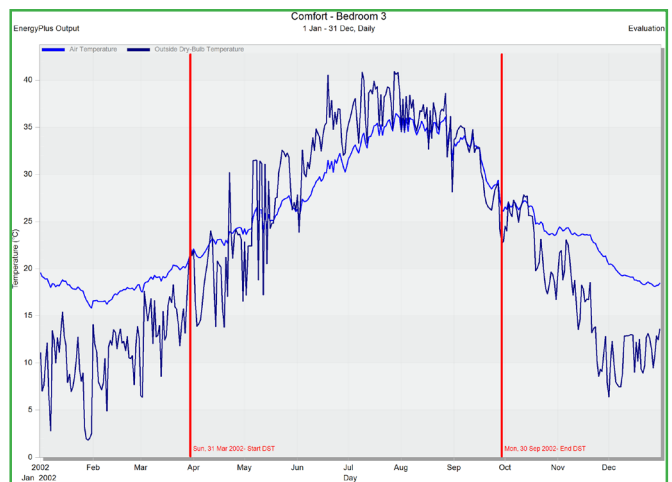
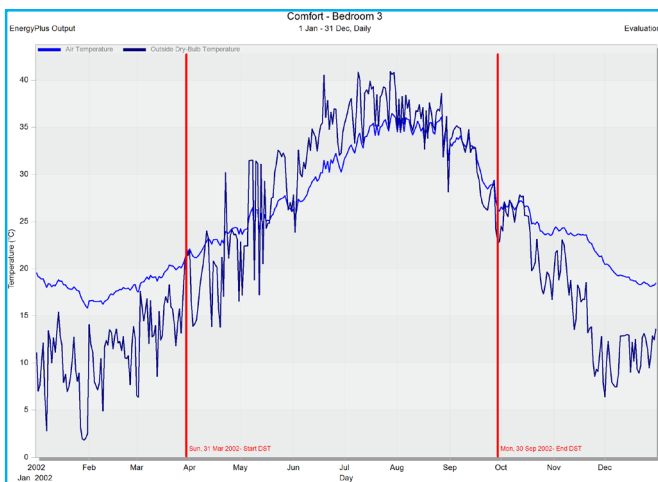
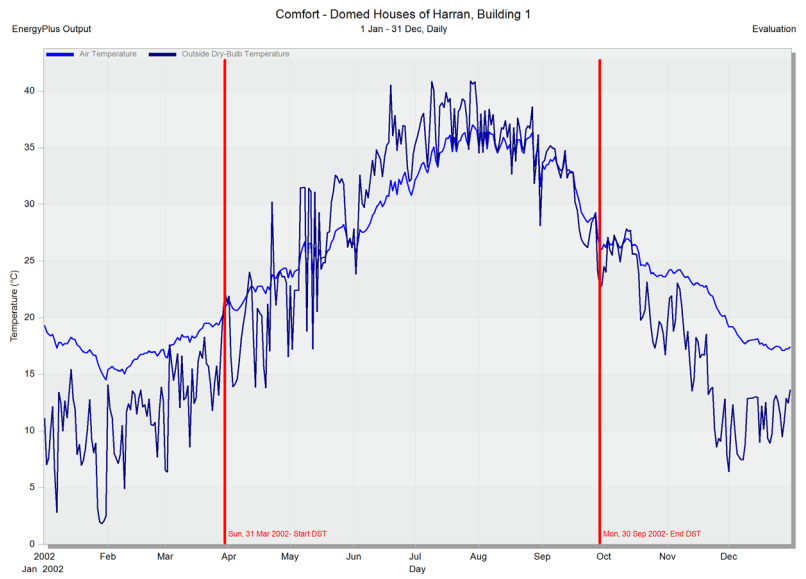
Slat solar transmittance 0.000
Slat solar reflectance, front side 0.800
Slat solar reflectance, back side 0.800

Slat Visible Properties

Slat visible transmittance 0.000
Slat visible reflectance, front side 0.800
Slat visible reflectance, back side 0.800

Slat IR (Thermal) Properties

Slat hemispherical transmittance 0.000
Slat hemispherical emissivity, front si... 0.900
Slat hemispherical emissivity, back s... 0.900



12.5 WWR 2.5% and venetian blinds inputs and outputs

General

Venetian blinds - medium (modelled as diffusing)

Category Diffusing shades
Source BLAST

Shade Properties

Thickness (m) 0.0030
Conductivity (W/m-K) 0.10000
Solar transmittance 0.600
Solar reflectance 0.120
Visible transmittance 0.600
Visible reflectance 0.120
Long-wave emissivity 0.900
Long-wave transmittance 0.000

Openings

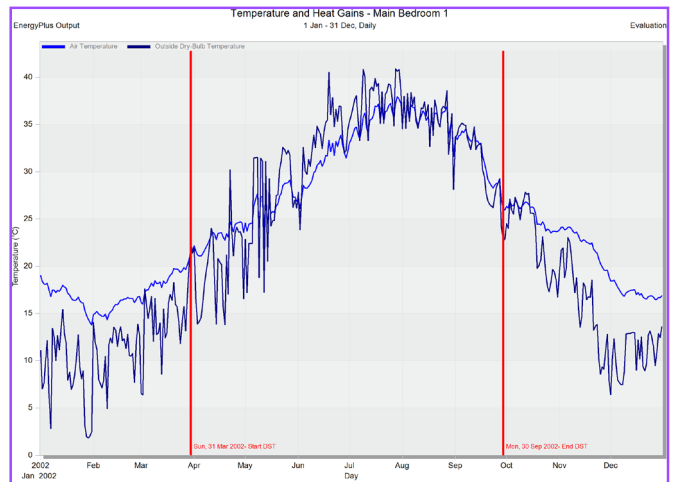
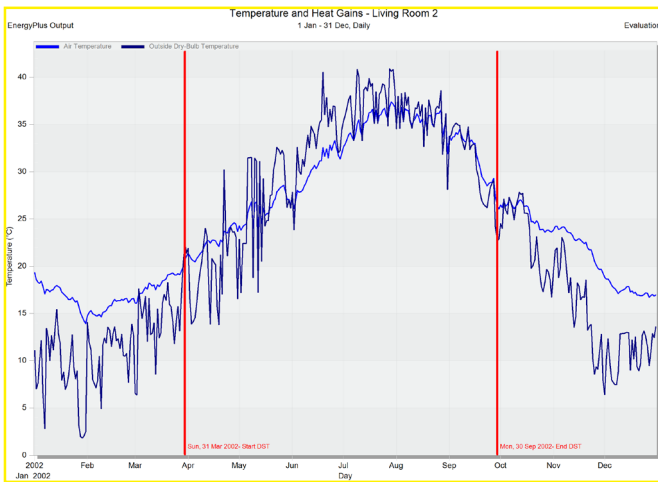
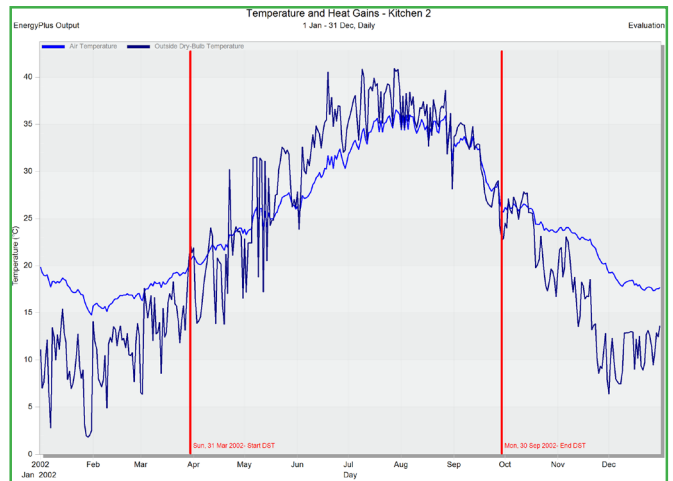
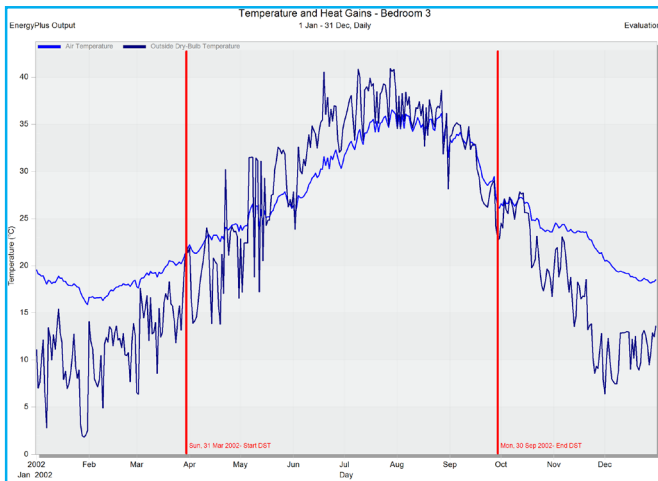
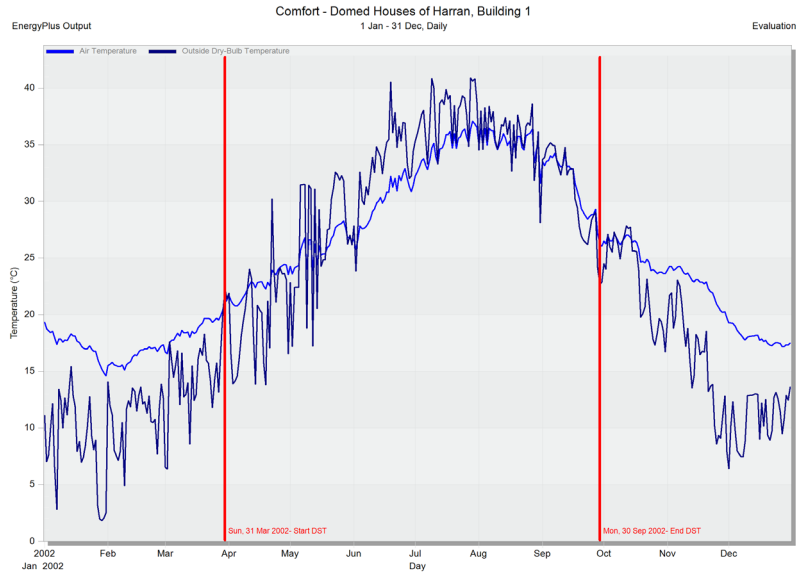
Shade-to-glass distance (m) 0.050
Shade top opening multiplier 1.000
Shade bottom opening multiplier 1.000
Shade left-side opening multiplier 0.000
Shade right-side opening multiplier 0.000
Shade airflow permeability 0.000

Cost

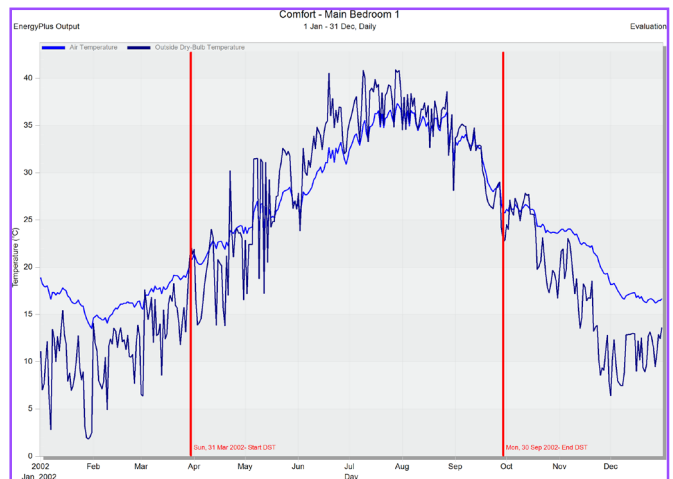
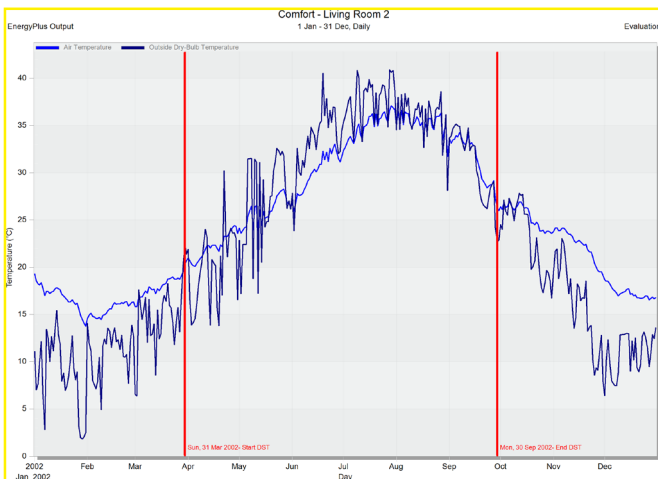
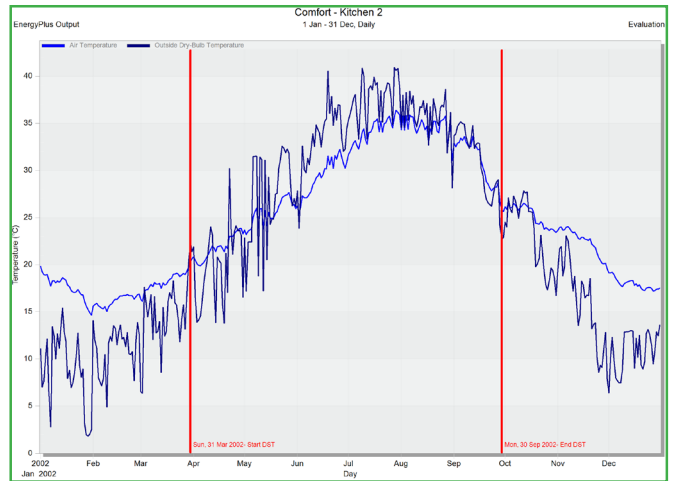
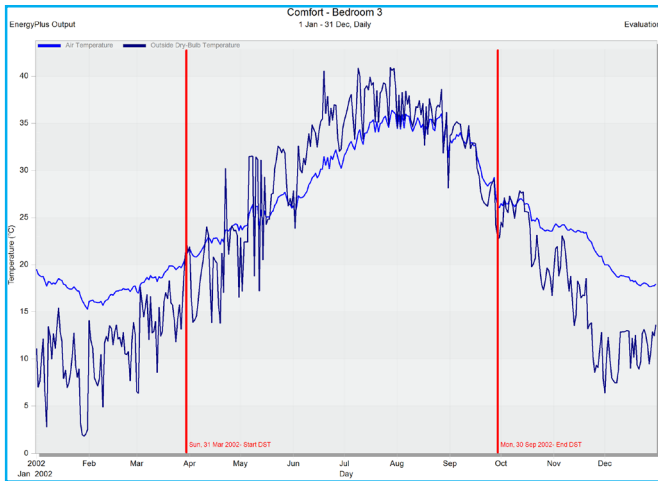
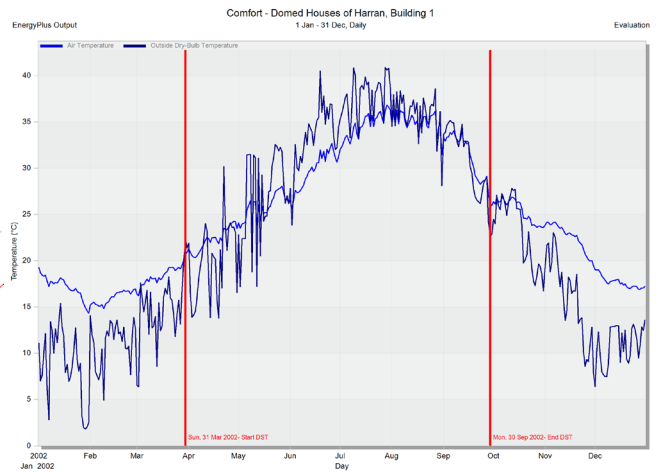
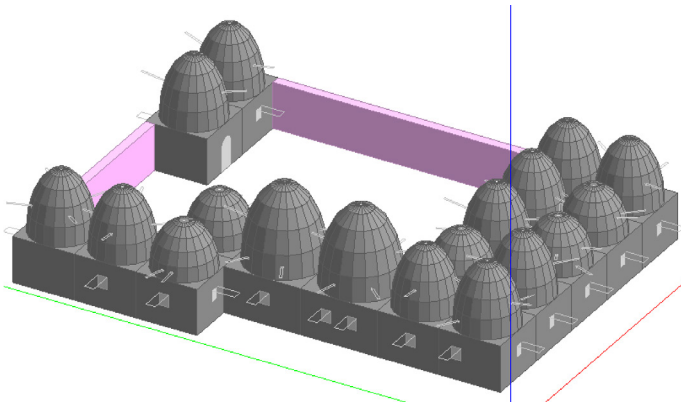
Cost per window area (GBP/m²) 50.00

Carbon

CO₂ (kgCO₂/kg) 50.00
Equivalent CO₂ (kgCO₂/kg) 50.00

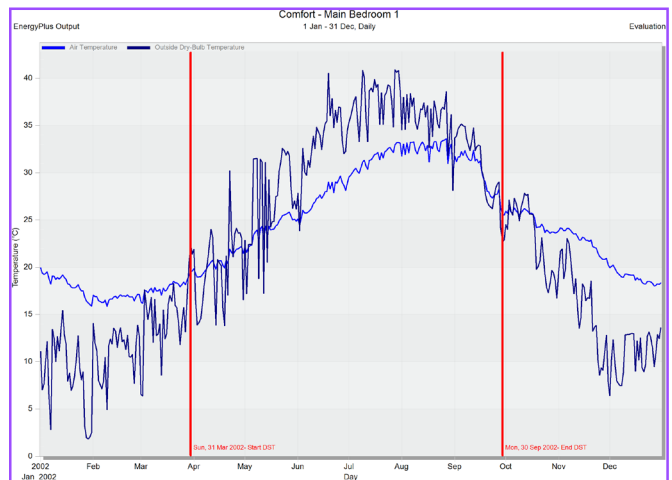
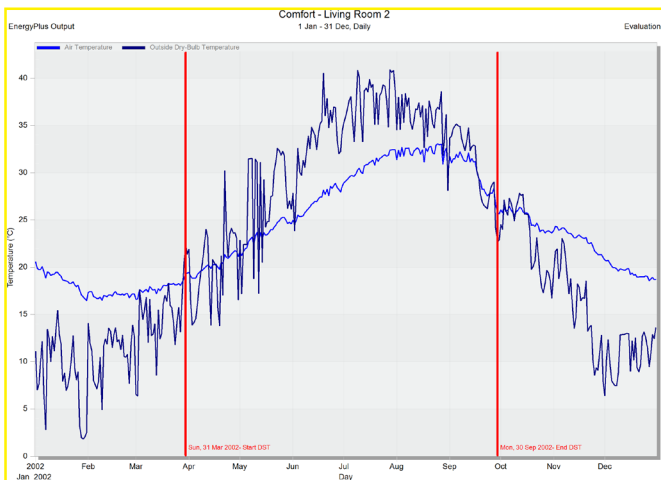
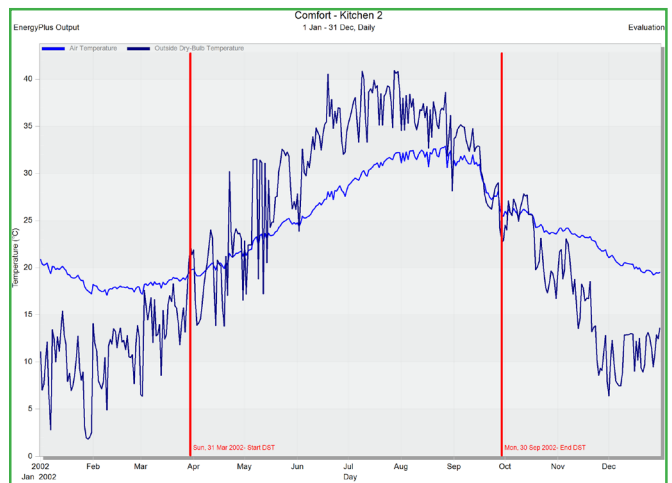
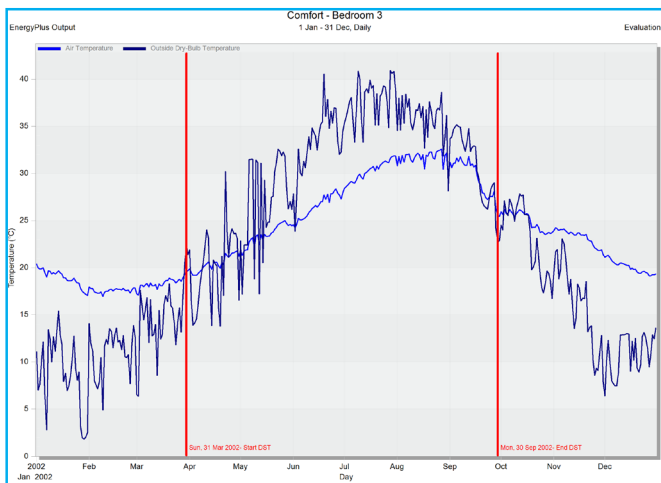
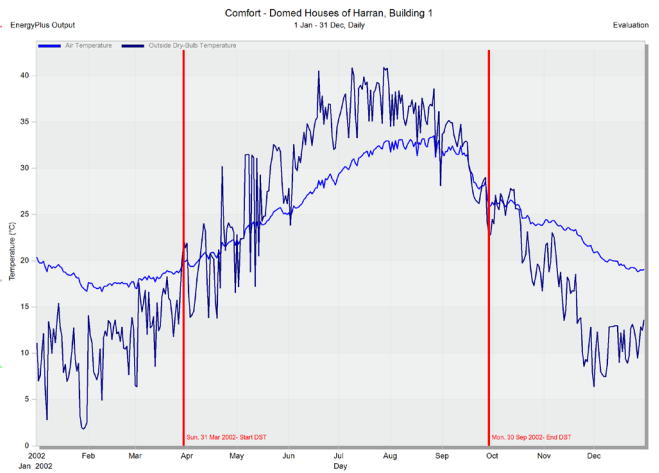
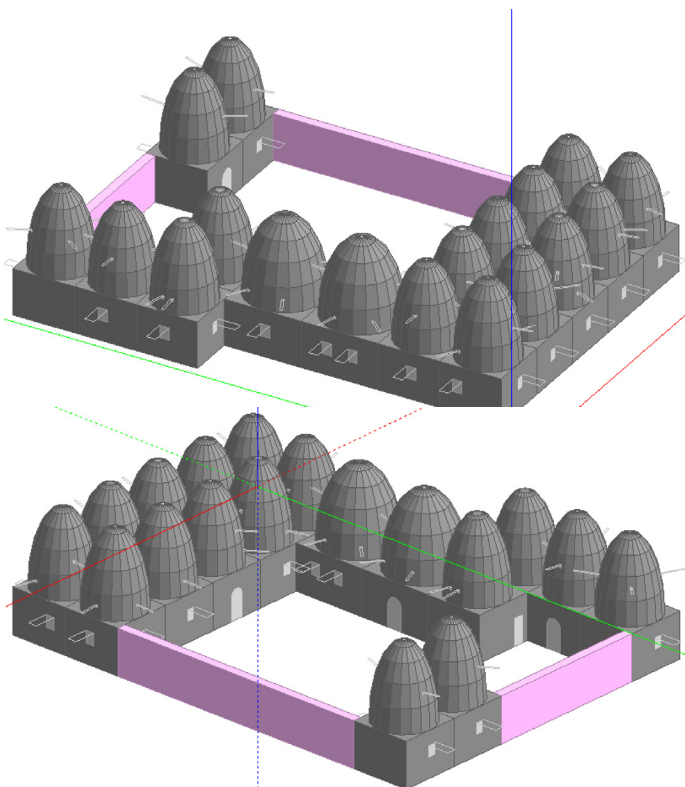


12.6 WWR 2.5% and 1.5m louvres inputs and outputs



Appendix 13: Shading device changes on a WWR of 2.5%

13.1 Optimal model 1 and outputs



13.2 Optimal model 2 and outputs

